

Some pages of this thesis may have been removed for copyright restrictions.

If you have discovered material in AURA which is unlawful e.g. breaches copyright, (either yours or that of a third party) or any other law, including but not limited to those relating to patent, trademark, confidentiality, data protection, obscenity, defamation, libel, then please read our [Takedown Policy](#) and [contact the service](#) immediately

USE OF ULTRASONIC AGITATION IN IRON
GROUP ALLOY ELECTRODEPOSITIONS

by

TARIQ RAFIQ MAHMOOD
MSc., M.I.M.F

A thesis submitted for the degree of Doctor
of Philosophy of the University of Aston in
Birmingham

April 1983

THE UNIVERSITY OF ASTON IN BIRMINGHAM

TITLE: USE OF ULTRASONIC AGITATION IN IRON
GROUP ALLOY ELECTRODEPOSITION

AUTHOR'S NAME: TARIQ RAFIQ MAHMOOD

DEGREE: Ph.D. 1983

SUMMARY

The effects of ultrasonic agitation on deposition from two iron group alloy plating solutions, nickel-cobalt and bright nickel-iron, have been studied. Comparison has been made with deposits plated from the same solutions using controlled air agitation. The ultrasonic equipment employed had a fixed frequency of 13 KHz but the power output from each transducer was variable up to a maximum of 350 watts.

The effects of air and ultrasonic agitation on hardness, ductility, tensile strength, composition, structure, surface topography, limiting current density, cathode current efficiency and macro-throwing power were determined. Transmission and scanning electron microscopy, electron-probe microanalysis and atomic absorption spectrophotometry have been employed to study the nickel alloy deposits produced.

The results obtained show that the use of ultrasonics increased significantly the hardness of both alloy deposits and altered their composition by decreasing the cobalt and iron contents from nickel-cobalt and nickel-iron solutions respectively. The ductility of coatings improved but the tensile strength did not change very much.

Ultrasonic agitation gave larger grained deposits than air and they seemed to have a lower stress. Dull cobalt-nickel deposits had a similar pyramidal surface topography regardless of the type of agitation but the bright appearance of the nickel-iron was destroyed by ultrasonic agitation; an unusual ribbed pattern was produced.

The use of ultrasonic agitation permitted approximately a twofold increase in the plating current density at which sound deposits could be achieved but there was only a slight increase in cathode current efficiency. Macro-throwing power of the solutions was increased slightly by the use of ultrasonic agitation.

Ultrasonic agitation is an expensive means of agitating plating solutions and would be worthwhile only if significant improvements in properties could be achieved. The simultaneous improvement in hardness and ductility is a novel feature that should have useful engineering applications.

KEY WORDS: Ultrasonics, Electrodeposition, Agitation, Nickel alloys, Hardness.

List of Contents

	CHAPTER ONE	Page
1	INTRODUCTION	1
	CHAPTER TWO	
2	LITERATURE REVIEW OF ULTRASONIC AGITATION IN ELECTRODEPOSITING	4
2.1	Production of Ultrasonics	4
2.2	The Application of Ultrasonic Agitation	6
2.3	Effect of Ultrasonics on Electrodeposition	6
2.3.1	The Effect of Ultrasonic Agitation on the Current Efficiency	11
2.3.2	The Effect of Ultrasonic Agitation on Hardness	13
2.3.3	The Effect of Ultrasonic Agitation on Current Density	15
2.3.4	The Effect of Ultrasonic Agitation on Macrothrowing Power	17
	CHAPTER THREE	
3	ELECTRODEPOSITION OF IRON GROUP METALS	18
3.1	Nickel Electrodeposition	18
3.1.1	Type of Iron Plating Baths	19

	Page
3.1.1.1 The Watts Bath	19
3.1.1.1.1 Effect of Variables	21
3.1.1.1.2 Variations on the Watts Bath	24
3.1.1.2 Hard Nickel Baths	25
3.1.1.3 Chloride Baths	26
3.1.1.4 Chloride-Sulphate and the Chloride-Acetate Bath	27
3.1.1.5 Nickel-Fluoborate Baths	28
3.1.1.6 Nickel-Sulphamate Baths	29
3.1.2 Properties of Electrodeposited Nickel	30
3.2 Cobalt Electrodeposition	31
3.2.1 Properties of Electrodeposited Cobalt	33
3.2.1.1 Hardness	33
3.2.1.2 Strength and Ductility	35
3.2.1.3 Internal Stress	35
3.2.2 Structure	36
3.3 Iron Electrodeposition	38
3.3.1 Types of Iron Plating Baths	39
3.3.1.1 The Ferrous Sulphate Bath	39
3.3.1.2 The Ferrous Chloride Bath	42
3.3.1.3 The Ferrous Sulphate-Ferrous Chloride Bath	45
3.3.2 Properties of Electrodeposited Iron	46
3.3.2.1 Hardness	47
3.3.2.2 Tensile Strength and Ductility	48
3.3.3 Structure	50

CHAPTER FOUR		Page
4	ALLOY ELECTRODEPOSITION	52
4.1	Electrochemical Aspects of Electrodeposition	56
CHAPTER FIVE		
5	NICKEL-COBALT ALLOY ELECTRODEPOSITION	61
5.1	Bath Formulation for the Electrodeposition of Nickel-Cobalt Alloys	61
5.1.1	Nickel-Cobalt Sulphate Bath	62
5.1.2	Nickel-Cobalt Sulphamate Bath	63
5.2	The Effects of Plating Variables on Nickel-Cobalt Deposition	65
5.2.1	Effect of Current Density on the Composition of the Deposit	65
5.2.2	Effect of Bath Temperature on the Composition of the Deposit	66
5.2.3	Effect of the Metal Ratio of the Bath on Deposit Composition	66
5.2.4	Effect of the Total Metal Content of the Bath on Deposit Composition	67
5.2.5	Effect of pH	68
5.2.6	Effect of Agitation on the Deposit	68
5.2.7	Effect of Complexing Agents	69
5.3	Properties of Nickel-Cobalt Alloy Electrodeposits	70

	Page
5.3.1 Hardness	71
5.3.2 Tensile Strength and Ductility	73
5.3.3 Macrothrowing Power	77
5.4. Structure	79
5.5 The Magnetic Properties of Alloys	81
5.5.1 Properties of the Magnetic Materials	82

CHAPTER SIX

6 NICKEL-IRON ALLOY ELECTRODEPOSITION	84
6.1 The Decorative Bright Nickel-Iron Process	87
6.2 Development of Nickel-Iron Plating Solutions	88
6.3 Corrosion Behaviour of Nickel-Iron Electrodeposition	89
6.4 Plating Baths	91
6.4.1 Solution Composition	91
6.4.2 Oxidation States of Iron in Plating Baths	92
6.4.3 Addition Agents	93
6.4.4 Operating Parameters	94
6.4.5 Properties of the Bath	95
6.4.6 Structure	96
6.4.7 Properties of Electrodeposited Nickel-Iron	96

CHAPTER SEVEN	Page
7 EXPERIMENTAL PROCEDURE	99
7.1 Equipment	99
7.2 Electroplating Procedure	102
7.2.1 Plating of Hounsfield Test Pieces	103
7.2.2 Nickel Solution	104
7.2.3 Cobalt Solution	105
7.2.4 Nickel-Cobalt Sulphate / Chloride Bath	106
7.2.5 Nickel-Iron Solution	107
7.2.5.1 Plating Conditions	108
7.2.5.1.1 pH Value	108
7.2.5.1.2 Temperature	109
7.2.5.1.3 Cathode Current Density	109
7.2.5.1.4 Density	109
7.2.5.2 Maintenance of the Bath	110
7.2.5.2.1 Brightener Additions	110
7.2.5.2.2 Anti-pit Agents (Wetting Agents)	111
7.2.5.3 Anodes	111
7.2.6 Evaluation of Plating Deposits	111
7.2.6.1 Hardness	112
7.2.6.2 Tensile Tests	112
7.2.6.3 Structure and Surface Topography	113
7.2.6.3.1 Transmission Electron Microscopy (T.E.M)	113
7.2.6.3.2 Scanning Electron Microscopy (S.E.M)	116
7.2.6.3.3 X-Ray Diffractometer	116
7.2.6.3.4 X-Ray Texture Goniometer	116
7.2.6.3.5 Progressive Growth of Nickel-Cobalt Alloys	118

	Page
7.2.6.4 Analysis	120
7.2.6.4.1 Electron Probe Microanalysis	121
7.2.6.4.2 Atomic Absorption Spectrophotometry	121
7.2.6.4.2.1 Nickel-Cobalt Plating Solution	121
7.2.6.4.2.2 Nickel-Iron Plating Solution	123
7.2.6.4.3 Wet Chemical Analysis	124
7.2.6.4.3.1 Nickel-Cobalt Plating Solution	124
7.2.6.4.3.2 Nickel-Iron Plating Solution	125
7.2.6.5 Cathode Current Efficiency	126
7.2.6.6 Limiting Current Density	127
7.2.6.7 Macrothrowing Power	128

CHAPTER EIGHT

8 RESULTS	129
8.1 HARDNESS AND DEPOSIT COMPOSITION	129
8.1.1 Nickel-Cobalt Deposits	129
8.1.1.1 Effect of Change in Solution Composition	135
8.1.2 Nickel-Cobalt Solution Containing 110 g/l of Cobalt Sulphate	138
8.1.3 Nickel Deposits	139
8.1.4 Cobalt Deposits	144
8.1.5 Nickel-Iron Deposits	146
8.1.5.1 Effect of Different Types of Agitation on Composition	148
8.2 Tensile Strength and Ductility	151
8.2.1 Nickel-Cobalt	151
8.2.2 Nickel-Iron	161
8.3 Structure	166

	Page
8.3.1 Nickel-Cobalt	166
8.3.1.1 Nickel-Cobalt Alloy Plating Solution Containing 110 g/l Cobaltous Sulphate	167
8.3.2 Structure of Cobalt Electrodeposit	168
8.3.3 Structure of Nickel-Iron Deposits	169
8.3.4 Determination of the Structure of Nickel- Iron Alloy Plated Deposits using X-Ray Techniques	170
8.3.4.1 Plane Orientation of the Nickel-Iron Structure	171
8.4 Surface Topography	208
8.4.1 Nickel-Cobalt Deposits	208
8.4.2 Nickel-Iron Deposits	209
8.4.2.1 The Effect of Ultrasonic Agitation on the Brightness of the Nickel-Iron Deposits	210
8.5 Progressive Growth of Deposits	226
8.5.1 Nickel-Cobalt Deposits	226
8.6 Limiting Current Density	236
8.6.1 Nickel-Cobalt	236
8.6.1.1 Hardness and Composition of Deposits Obtained Using Air Agitation	236
8.6.1.2 Hardness and Composition Obtained Using Ultrasonic Agitation, 350 Watts	243
8.6.2 Nickel-Iron	246
8.6.2.1 Hardness and Composition of Deposits Obtained Using Air Agitation	254

	Page
8.6.2.2 Hardness and Composition of Deposits Obtained Using Ultrasonic Agitation	256
8.7 Cathode Current Efficiency	261
8.7.1 Nickel-Cobalt	261
8.7.1.1 Air Agitation	261
8.7.1.2 Ultrasonic Agitation	262
8.7.2 Nickel-Iron	263
8.7.2.1 Air Agitation	263
8.7.2.2 Ultrasonic Agitation	264
8.8 Macrothrowing Power	266
8.8.1 Nickel-Cobalt Deposits	266
8.8.1.1 Macrothrowing Power Air Agitated	266
8.8.1.2 Macrothrowing Power Using Ultrasonic Agitation Power, 350 Watts	268
8.8.2 Nickel-Iron Deposits	275

CHAPTER NINE

9 DISCUSSION	277
9.1 Electrolyte Agitation	277
9.2 Ultrasonic Agitation	280
9.2.1 Introduction of Ultrasonic Energy to the Cell	280
9.2.2 Operating Cell Voltage and Possible Power Saving	280
9.3 Efficiency of Ultrasonic Equipment	282

	Page
9.4 Hardness	283
9.4.1 Statistical Analysis of Hardness Results	283
9.4.2 Effect of Cobalt Content on Hardness of Nickel-Cobalt Alloys	288
9.4.3 Dependence of Hardness on Grain Size	291
9.4.3.1 Conflicting Factors Involved in Grain Size	295
9.4.4 Dependence of Hardness on Work Hardening Effect	295
9.4.5 Dependence of Hardness on Dislocation Density	296
9.4.6 Dependence of Hardness on Internal Stress	297
9.4.7 Significance of Factors Affecting Hardness	298
9.5 Composition	300
9.6 Tensile Strength and Ductility	302
9.6.1 Nickel-Cobalt	308
9.6.2 Nickel-Iron	312
9.7 Surface Topography and Progressive Growth	314
9.7.1 Comparison of Results Obtained Using SEM and Replica Techniques	316
9.8 Cathode Current Efficiency	317
9.9 Limiting Current Density	321
9.9.1 Analysis of Results Using Regression Analysis	327
9.10 Macrothrowing Power	340
10 CONCLUSIONS	344
11 SUGGESTIONS FOR FUTURE WORK	346
12 ACKNOWLEDGEMENTS	347

List of Figures

	Page
Fig.(1) Cavitation threshold	12
a) aerated water; b) degassed water	
Fig.(2) Effect of concentration polarisation	58
Fig.(3) Relationship between the concentration of cobaltous sulphate in solution and the percentage cobalt in the deposit	64
Fig.(4) The power unit and ultrasonic tank	101
Fig.(5) The electroplating plant	101
Fig.(6) High resolution Transmission Electron Microscope Model Jem 100B	114
Fig.(7) Scanning Electron Microscope Model Cambridge-150	115
Fig.(8) Struers Polipower Jet-polisher	115
Fig.(9) Philips X-Ray diffractometer	117
Fig.(10)a,b,c,d The Texture Goniometer and schematic diagram which explains the geometrical arrangement of the goniometer	119
Fig.(11) Electron Probe Microanalyser Model Cambridge Microscan V	122
Fig.(12) Perkin-Elmer Atomic Absorption Spectrophotometer Model 560	122

	Page
Fig.(13) Variation in hardness of nickel-cobalt alloys with degree of ultrasonic agitation. (Plating solution containing 10 g/l cobaltous sulphate)	132
Fig.(14) Variation in nickel-cobalt alloy composition with degree of ultrasonic agitation (Plating solution containing 10 g/l cobaltous sulphate)	133
Fig.(15) Relation between cobalt sulphate concentration in solution and cobalt content deposit, using air and ultrasonic agitation, pH 4, temp. 55°C and C.D.4 A/dm ²	137
Fig.(16) Variation in hardness of nickel-cobalt alloys with degree of ultrasonic agitation (Plating solutions containing 10 g/l and 110 g/l cobalt sulphate).	140
Fig.(17) Variation in nickel-cobalt alloy composition with degree of ultrasonic agitation. (Plating solution containing 110 g/l cobalt sulphate)	141
Fig.(18) Variation in hardness of dull nickel alloys with degree of ultrasonic agitation	142
Fig.(19) Variation in hardness of cobalt with degree of ultrasonic agitation	145

	Page
Fig.(20) Variation in hardness of nickel-iron alloys with degree of ultrasonic agitation	147
Fig.(21) Variation in nickel-iron alloy composition with degree of ultrasonic agitation. Results determined by Electron Probe Microanalysis and Atomic Absorption Spectrophotometry	150
Fig.(22) Load-Extension curves for brass, and for a nickel-cobalt plated brass specimen	152
Fig.(23) T.E.M. micrographs of nickel-cobalt alloy deposit plated from solution containing 10 g/l $\text{CoSO}_4 \cdot 7\text{H}_2\text{O}$ at 4 A/dm ² , 55°C and pH 4. Air agitated	174
Fig.(24) Conditions as in Fig.(23) but ultrasonically agitated 20 watts	176
Fig.(25) Conditions as in Fig.(23) but ultrasonically agitated 100 watts	178
Fig.(26) Conditions as in Fig.(23) but ultrasonically agitated 200 watts	179
Fig.(27) Conditions as in Fig.(23) but ultrasonically agitated 350 watts	181
Fig.(28) Transmission electron micrograph of Ni-Co alloy deposit plated from solution containing 110 g/l $\text{CoSO}_4 \cdot 7\text{H}_2\text{O}$ at 4 A/dm ² , 55°C and pH 4. Air agitated	183

	Page
Fig.(29) Conditions as in Fig.(28) but C.D. used 8 A/dm ² , air agitated	185
Fig.(30) Conditions as in Fig.(28) but ultra- sonically agitated 20 watts	187
Fig.(31) Conditions as in Fig.(28) but ultra- sonically agitated 40 watts	189
Fig.(32) Conditions as in Fig.(28) but ultra- sonically agitated 200 watts	191
Fig.(33) Conditions as in Fig.(28) but ultra- sonically agitated 350 watts	193
Fig.(34) T.E.M. micrograph of cobalt deposit plated at 4 A/dm ² , 55°C and pH 4, air agitated	195
Fig.(35) Conditions as in Fig.(34) but plated at 8 A/dm ²	196
Fig.(36) Conditions as in Fig.(34) but ultra- sonically agitated 20 watts	197
Fig.(37) Conditions as in Fig.(34) but ultra- sonically agitated 100 watts	198
Fig.(38) Conditions as in Fig.(34) but ultra- sonically agitated 200 watts	199
Fig.(39) T.E.M. micrograph of nickel-iron alloy deposit plated at 4 A/dm ² , 68°C and pH 4, air agitated	200

	Page
Fig.(40) Conditions as in Fig.(39) but deposit plated at 8 A/dm ²	201
Fig.(41) Conditions as in Fig.(39) but ultra-sonically agitated 20 watts	202
Fig.(42) Conditions as in Fig.(39) but ultra-sonically agitated 40 watts	203
Fig.(43) Conditions as in Fig.(39) but ultra-sonically agitated 100 watts	204
Fig.(44) Conditions as in Fig.(39) but ultra-sonically agitated 200 watts	205
Fig.(45) Conditions as in Fig.(39) but ultra-sonically agitated 350 watts	206
Fig.(46) Pole figure of nickel-iron electro-deposit	207
Fig.(47) Surface topography of nickel-cobalt deposit plated at 4 A/dm ² from a solution containing 10 g/l cobaltous sulphate. Air agitation	211
Fig.(48) Conditions as in Fig.(47) but ultra-sonically agitated 350 watts	212
Fig.(49) Surface topography of nickel-cobalt deposit plated at 4 A/dm ² from a solution containing 35 g/l cobaltous sulphate. Air agitation	213

Fig.(50)	Conditions as in Fig.(49) but ultra-sonically agitated 350 watts	Page 214
Fig.(51)	Surface topography of nickel-cobalt deposit plated at 4 A/dm^2 from a solution containing 60 g/l cobaltous sulphate. Air agitation	215
Fig.(52)	Conditions as in Fig.(51) but ultra-sonically agitated 350 watts	216
Fig.(53)	Surface topography of nickel-cobalt deposit plated at 4 A/dm^2 from a solution containing 85 g/l cobaltous sulphate. Air agitation	217
Fig.(54)	Conditions as in Fig.(53) but ultra-sonically agitated 350 watts	218
Fig.(55)	Surface topography of nickel-cobalt deposit plated at 4 A/dm^2 from a solution containing 110 g/l cobaltous sulphate. Air agitation	219
Fig.(56)	Conditions as in Fig.(55) but ultra-sonically agitated 100 watts	220
Fig.(57)	Conditions as in Fig.(55) but ultra-sonically agitated 350 watts	221
Fig.(58)	Scanning Electron photomicrograph of nickel-iron alloy deposit plated at 4 A/dm^2 , 68°C and pH 4, air agitated	222

	Page
Fig.(59) Conditions as in Fig.(58) but ultra- sonically agitated, 100 watts	223
Fig.(60) Conditions as in Fig.(58) but ultra- sonically agitated, 200 watts	224
Fig.(61) Conditions as in Fig.(58) but ultra- sonically agitated, 350 watts	225
Fig.(62) Surface topography X 8.4K for 1 minute deposit using air agitation	228
Fig.(63) Surface topography X 8.4K for 5 minutes deposit using air agitation	228
Fig.(64) Surface topography X 8.4K for 10 minutes deposit using air agitation	229
Fig.(65) Surface topography X 8.4K for 15 minutes deposit using air agitation	229
Fig.(66) Surface topography X 8.4K for 1 minute deposit using ultrasonic agitation 350 watts	230
Fig.(67) Surface topography X 8.4K for 5 minutes deposit using ultrasonic agitation 350 watts	230
Fig.(68) Surface topography X 8.4K for 10 minutes deposit using ultrasonic agitation 350 watts	231
Fig.(69) Surface topography X 8.4K for 15 minutes deposit using ultrasonic agitation 350 watts	231

	Page
Fig.(70) Surface topography X 8.4K for 1 minute deposit using air agitation, solution containing 110 g/l $\text{CoSO}_4 \cdot 7\text{H}_2\text{O}$	232
Fig.(71) Surface topography X 8.4K for 5 minutes deposit using air agitation, solution containing 110 g/l $\text{CoSO}_4 \cdot 7\text{H}_2\text{O}$	232
Fig.(72) Surface topography X 8.4K for 10 minutes deposit using air agitation, solution containing 110 g/l $\text{CoSO}_4 \cdot 7\text{H}_2\text{O}$	233
Fig.(73) Surface topography X 8.4K for 15 minutes deposit using ultrasonic agitation 350 watts, solution containing 110 g/l $\text{CoSO}_4 \cdot 7\text{H}_2\text{O}$	233
Fig.(74) Surface topography X 8.4K for 1 minute deposit using ultrasonic agitation 350 watts, solution containing 110 g/l $\text{CoSO}_4 \cdot 7\text{H}_2\text{O}$	234
Fig.(75) Surface topography X 8.4K for 5 minutes deposit using ultrasonic agitation 350 watts, solution containing 110 g/l $\text{CoSO}_4 \cdot 7\text{H}_2\text{O}$	234
Fig.(76) Surface topography X 8.4K for 10 minutes deposit using ultrasonic agitation 350 watts, solution containing 110 g/l $\text{CoSO}_4 \cdot 7\text{H}_2\text{O}$	235

	Page
Fig.(77) Surface topography X 8.4K for 15 minutes deposit using ultrasonic agitation 350 watts, solution containing 110 g/l $\text{CoSO}_4 \cdot 7\text{H}_2\text{O}$	235
Fig.(78) Effect of variation of current density on the hardness of nickel-cobalt alloy deposit plated using air agitation	241
Fig.(79) Effect of variation of current density on the cobalt content of nickel-cobalt alloy deposit plated using air agitation	242
Fig.(80) Effect of variation of current density on the hardness of nickel-cobalt alloy deposit plated using ultrasonic agitation 350 watts	244
Fig.(81) Effect of variation of current density on the cobalt content of nickel-cobalt alloy deposit plated using ultrasonic agitation 350 watts	245
Fig.(82) Appearance of nickel-iron deposits plated at current densities ranging from 10 to 80 A/dm^2 using air agitation, pH 4, temperature 68°C	247
Fig.(83) Appearance of nickel-iron deposits plated at current densities ranging from 10 to 80 A/dm^2 using ultrasonic agitation 350 watts, pH 4, Temp. 68°C	247

	Page
Fig.(84) Effect of variation of current density on the hardness of nickel-iron alloy deposit plated using air agitation	253
Fig.(85) Effect of variation of current density on the content of nickel-iron alloy deposit plated using air agitation	254
Fig.(86) Effect of variation of current density on the hardness of nickel-iron alloy deposit plated using ultrasonic agitation 200 watts	257
Fig.(87) Effect of variation of current density on the iron content of nickel-iron alloy deposit plated using ultrasonic agitation 200 watts	258
Fig.(88) Effect of variation of current density on the hardness of nickel-iron alloy deposit plated using ultrasonic agitation 350 watts	259
Fig.(89) Effect of variation of current density on the iron content of nickel-iron alloy deposit plated using ultrasonic agitation 350 watts	260
Fig.(90) Average deposits thickness of nickel-cobalt alloy (10 g/l cobaltous sulphate)/ Distance in (cm) from high current density end of the cathode panel	267

	Page
Fig.(91) Average deposits thickness of nickel-	272
cobalt alloy (110 g/l cobaltous sulphate)	
/ Distance in (cm) from high current	
density end of the cathode panel	
Fig.(92) Average deposits thickness of nickel-	276
iron alloy / Distance in (cm) from	
high current density end of the cathode	
panel	

List of Tables

	Page
Table I The watts nickel bath	21
Table II Nickel baths for electroplating	22
Table III Mechanical properties of nickel electrodeposits	23
Table IV Composition and operating conditions of cobalt plating baths	32
Table V Tensile strength and ductility of cobalt electrodeposits	35
Table VI Composition and operating conditions for iron plating baths	40
Table VII Mechanical properties of electrolytic iron	49
Table VIII Hardness and cobalt content of Ni-Co alloys deposited using air or ultra- sonic agitation. Cobalt sulphate content of solution 10 g/l; temperature 55°C.; pH 4	130
Table IX The effect of the concentration of cobalt sulphate in solution on hardness and on the percentage cobalt obtained in the deposit, using either air or ultrasonic agitation. pH4; 55°C	136

		Page
Table X	Hardness and composition of nickel-cobalt alloy deposits obtained using air or ultrasonic agitation and pH 4, temp. 55°C (Plating solution containing 110 g/l cobalt sulphate)	138
Table XI	Hardness and composition of nickel electrodeposits obtained using air or ultrasonic agitation. pH 4, temp. 55°C and current density 4 A/dm ² unless otherwise stated	143
Table XII	Hardness of cobalt electrodeposits obtained using air or ultrasonic agitation. pH 4; temperature 55°C.	144
Table XIII	Variation in nickel-iron contents with agitation using air, ultrasonic, both air and ultrasonic together, and with no agitation. Both electron probe microanalysis and atomic absorption spectrophotometry were used. Plating condition pH 4, temperature 65°C and current density 4 A/dm ² unless otherwise stated.	149
Table XIV	Tensile strength and ductility of plated nickel-cobalt coatings obtained from solution containing 10 g/l CoSO ₄ .7H ₂ O determined in situ on brass substrates	155

		Page
Table XV	Tensile strength and ductility of test pieces plated with nickel-cobalt coating obtained from solution containing 10 g/l $\text{CoSO}_4 \cdot 7\text{H}_2\text{O}$, and uncoated brass	156
Table XVI	Average tensile strength and ductility of plated nickel-cobalt coatings obtained from solution containing 10 g/l $\text{CoSO}_4 \cdot 7\text{H}_2\text{O}$, determined in situ on brass substrates	157
Table XVII	Average tensile strength and ductility of test pieces plated with nickel-cobalt coating obtained from solution containing 10 g/l $\text{CoSO}_4 \cdot 7\text{H}_2\text{O}$, and uncoated brass	158
Table XVIII	Tensile strength and ductility of test pieces plated with nickel-cobalt coating obtained from solution containing 110 g/l $\text{CoSO}_4 \cdot 7\text{H}_2\text{O}$	159
Table XIX	Average tensile strength and ductility of test pieces plated with nickel-cobalt coating obtained from solution containing 110 g/l $\text{CoSO}_4 \cdot 7\text{H}_2\text{O}$	160
Table XX	Tensile strength and ductility of plated nickel-iron coatings determined in situ on brass substrates	162

	Page
Table XXI Tensile strength and ductility of test pieces plated with nickel-iron coatings	163
Table XXII Average tensile strength and ductility of plated nickel-iron coatings determined in situ on brass substrate	164
Table XXIII Average tensile strength and ductility of test pieces plated with nickel-iron coating	165
Table XXIV Results obtained from X-ray diffraction of nickel-iron deposits, using either air or ultrasonic agitation	173
Table XXV Limiting current density results using air agitation pH4; 55°C.	237
Table XXVI Limiting current density results using ultrasonic agitation 100 watts; pH 4; 55°C	238
Table XXVII Limiting current density results using ultrasonic agitation 350 watts; pH 4; 55°C	239
Table XXVIII Variation in hardness and composition of nickel-cobalt alloy deposits with changes in current density using air agitation pH 4; 55°C	240

	Page
Table XXIX Variation in hardness and composition of nickel-cobalt alloy deposits with changes in current density using ultrasonic agitation 350 watts; pH 4; 55°C	243
Table XXX Limiting current density results using air agitation, pH 4, 68°C	248
Table XXXI Limiting current density results using ultrasonic agitation 200 watts; pH 4; 68°C	249
Table XXXII Limiting current density results using ultrasonic agitation 350 watts; pH 4; 68°C	250
Table XXXIII Variation in hardness and composition of nickel-iron alloy deposits with changes in current density using air agitation, pH4, 68°C	252
Table XXXIV Variation in hardness and composition of nickel-iron alloy deposits with changes in current density using ultrasonic agitation 200 watts, pH 4, 68°C.	255
Table XXXV Variation in hardness and composition of nickel-iron alloy deposits with changes in current density using ultrasonic agitation 350 watts, pH 4, 68°C.	256

		Page
Table XXXVI	Relation between power of ultra-sonic agitation and cathode current efficiency for nickel-cobalt solution containing 10 g/l $\text{CoSO}_4 \cdot 7\text{H}_2\text{O}$	262
Table XXXVII	Relation between power of ultra-sonic agitation and cathode current efficiency for nickel-iron solution	264
Table XXXVIII	Effect of agitation on macro-throwing power, using nickel-cobalt solution containing 10 g/l $\text{CoSO}_4 \cdot 7\text{H}_2\text{O}$	273
Table XXXIX	Effect of agitation on macro-throwing power, using nickel-cobalt solution containing 110 g/l cobaltous sulphate ($\text{CoSO}_4 \cdot 7\text{H}_2\text{O}$)	274
Table XXXX	Effect of agitation on macro-throwing power using nickel-iron solution.	275
Table XXXXI	The relations between total power (watts) generated by two transducers at 100% efficiency and total power received (watts) into the bath.	282
Table XXXXII	Hardness measurements with 260 subtracted from all results of case I.	284

Table XXXXIII	Analysis of Variance (case I)	Page 285
Table XXXXIV	Hardness measurements with 254 subtracted from all results of (case II)	286
Table XXXXV	Analysis of Variance (case II)	287
Table XXXXVI	Increase in average hardness using 350 watts ultrasonic agitation, plating conditions pH 4, C.D. 4 A/dm ² and temp. 55°C for all solutions except 68°C for Ni-Fe	288
Table XXXXVII	Variation in hardness and cobalt content using either air or ultra- sonic agitation in nickel-cobalt solutions containing different cobalt sulphate contents (Plating conditions pH 4, current density 4 A/dm ² , 55°C).	291
Table XXXXVIII	The effect of plating variation on tensile strength and ductility using ferrous fluoborate-ferrous chloride solution.	303
Table XXXXIX	The effect of heat treatment variation on tensile strength and ductility. Obtained from concentrated sulphamate solution pH 4, temp. 60°C.	305

		Page
Table XXXXX	The effect of current density variation on cobalt content, tensile strength and ductility pH 4 at room temperature.	306
Table XXXXI	The effect of plating variables on the U.T.S. and ductility.	307
Table XXXXII	The effect of compositon variation on tensile strength and ductility obtained from different nickel- cobalt solutions.	308
Table XXXXIII	Average tensile strength and ductility of plated nickel-cobalt and nickel-iron coatings	309
Table XXXXIV	Variance of regression equations	338

CHAPTER ONE

1. INTRODUCTION.

The use of ultrasonic agitation has received much attention in recent years in its application to industrial processing. Attempts have been made to use ultrasonics as means of agitation in electroplating and so far, most attention has been paid to single metal deposits and there appears to be very little information on the behaviour of alloy plating solutions and deposits.

The application of ultrasonic agitation to electroplating was the subject of many exaggerated claims in the fifties. The electrodeposition of single metals from solutions has shown that in many electrolytic processes high frequency sound increases anode and cathode metal current efficiencies, decreases cell voltages, influences the grain size and crystal orientation of deposits, results in depolarization effects at the anode and cathode and increases the limiting current density, as reported by Kenahan et al⁽¹⁾.

It has however been demonstrated that some definite advantages may be gained by using high frequency sound during the electrodeposition of alloys, these include improved deposition at higher than normal current densities thus resulting in decreased plating times, improvement of physical properties,⁽²⁾ increased bright-

ness and hardness, better adhesion to the substrate, finer grain size, reduced internal stresses and lower porosity. At higher current densities than normal good quality deposits can be obtained which decrease the deposition time required to produce a certain thickness of deposit.

At the present time, ultrasonics are used extensively in cleaning, degreasing, and testing operations. There have been many suggestions for using ultrasonics in chemical, electrolytic, and metallurgical processes. For several years many researchers have been engaged in research designed to evaluate the effect of high-frequency sound waves on the electrodeposition of certain metals from aqueous solutions.

It has been found that ultrasonic fields can increase the rate of metal ion transfer within the electrolyte solution and modify the properties of the deposit. Sound^(3,4) can interact with an electrodeposit and the frequency, intensity and distribution of the sound field within a plating cell can play an important role in determining the type of effects observed.

The literature pertinent to the subject is of multinational origin and contains many conflicting results. The reason for this is that standard equipment and conditions have not been used. This results in cells of different geometry and the methods by which ultrasonic

agitation is applied to the systems varies as well. Also different workers have used ultrasonics of different frequencies and intensities. All of this makes comparisons of results somewhat difficult. An excellent review of the effects of ultrasonics on grain size, hardness, internal stresses, brightness and porosity of electrodeposits has been published by G.T.Walker and R.Walker⁽⁵⁾.

It is the aim of this work to investigate the effects of ultrasonic agitation during electrodeposition on nickel-cobalt and nickel-iron alloy plating systems.

The following properties and characteristics will be investigated :-

Hardness, tensile strength and ductility, structure and surface topography, composition, cathode current efficiency, limiting current density and macrothrowing power.

2. LITERATURE REVIEW OF ULTRASONIC AGITATION IN ELECTROPLATING.

2.1 Production of Ultrasonics.

Ultrasonics is the branch of acoustics which deals with the production, transmission and effects of vibratory waves at frequencies above the audibility range of the average human ear. The ultrasonic frequency range has been defined as extending from 10 kHz to several thousand kHz, usually ultrasonic frequencies are produced by transducers which convert energy from one form to another.

The transducers used for generating ultrasonic vibrations are piezoelectric, magnetostrictive, electromagnetic, pneumatic and mechanical devices⁽⁶⁾. Piezoelectric, magnetostrictive and electromagnetic transducers convert electrical energy to ultrasonic energy. Ultrasonic waves are mechanical and in order for wave motion to occur it is necessary to have a source (a transducer) that produces a displacement or disturbance of some kind in an elastic medium through which the disturbance can be transmitted. In this respect, ultrasonic waves differ from light and other forms of electromagnetic energy which travel freely through a vacuum.

It is evident that ultrasonic wave propagation depends

on the physical properties and in particular, the elastic property of the transmitting medium.

The applications of ultrasonics have been divided into two categories, that is low-intensity and high-intensity⁽⁶⁾. The low-intensity is defined as energy transmitted through a medium without changing the state of the medium. The high-intensity is defined as energy producing waves which have some effect on the medium or its contents. Typical applications of this type are metal cleaning, machining, metal bonding and metal deposition.

The effects of ultrasonic agitation on the plating process can be related to the phenomenon known as cavitation⁽⁷⁾. This term is used to describe the formation and collapse of cavities in solution media, and tends to dominate at frequencies (10 - 50 kHz). Bubbles develop the vapor pressure of the liquid in which cavitation is occurring, finally collapsing and in doing so releasing localised energy. This energy is sufficient to break chemical bonds forming free radicals, accelerate isomeric conversions and remove gas films. It has also been proposed^(8,9) that cavitation phenomena can lead to surface work hardening, brightening and grain refinement in electrodeposited metallic films and a general increase in metal ion transport.^(10,11)

2.2 The Application of Ultrasonic Agitation.

The application of ultrasonic agitation in electroplating has received much attention in recent years because of its advantages such as its effects on grain size, hardness, internal stress, brightness, porosity, acceleration of certain chemical reactions⁽¹²⁾ and reduction in plating time. Relevant literature and references in this field give many conflicting results probably because of the methods by which ultrasonics are applied and due to the different frequencies and intensities which makes the comparison of results somewhat difficult.

2.3 Effects of Ultrasonics on Electrodeposition.

When a solution is ultrasonically agitated during the electrodeposition process ultrasonic waves are transmitted through the solution and strike the barrier layer with high velocity. This phenomena according to Ashley is termed the acoustic micro-streaming effect⁽¹³⁾ causing the break-up of boundary layers and assisting diffusion processes. For this reason ultrasonic waves are used in an attempt to increase the rate of diffusion to the electrode by reducing the boundary layer thickness.

Drake⁽¹⁴⁾ has observed in experiments that ultrasonic agitation at frequencies around 1 MHz had a great effect on the diffusion layer thickness and diffusion constant for copper deposition from an acid copper sulphate

solution where the diffusion layer thickness, δ , was 34 μm for irradiation normal to the surface and 22 μm for irradiation at an inclined angle of 45° . For comparison, with no agitation of any kind δ equals about 200 μm . The difference between normally incident and inclined incident ultrasonics may be due to the greater bulk streaming of the electrolyte in the latter case. Normally incident sound produces a standing wave field at the surface of the electrode which suppresses fluid streaming. The radiation pressure of the ultrasonics can also influence a diffusion process by exerting a mechanical force on the diffusion layer. Irradiation of the electrode with sound above the cavitation threshold at 20 kHz produces a far greater effect on mass transport than the high frequency ultrasonics.

As the ultrasonic vibrations are increased solutions become incapable of stable transmission of sound energy and cavitation occurs. This causes the formation of vapour bubbles during the tension phase of the sound pressure wave, These bubbles collapse violently during the compression phase due to the combined effects of the atmospheric pressure, surface tension and induced pressure wave. It is this cavitation effect which is most effective in collapsing the boundary layers. The effect is much more intense at frequencies from 10 - 50 kHz since displacement is greater and cavities therefore larger.

Eggelt et al⁽¹⁵⁾ recommend the frequencies giving best

results are from 10 to 50 kHz where standing waves can be prevented and which agrees well with other researchers.

Kozan⁽¹⁶⁾ claimed that when ultrasonic agitation was applied to a nickel plating electrolyte it was possible to increase the current density twofold. Other researchers, Walker and Benn^(17,18) and Vrobel⁽¹⁹⁾, found that an increase in plating current density and limiting current density were possible due to the use of ultrasonic agitation. Rich⁽⁷⁾ claimed that ultrasonic agitation of 20 kHz permitted plating at up to thirty times normal speed and he also stated that deposits with good adhesion to the substrate could be produced when using ultrasonic agitation. Many workers in this field have agreed that ultrasonic agitation increases hardness. With a few exceptions, the micro-hardness of most electrodeposited metals is increased but the hardness of electrodeposited alloys depends on frequency in most cases.

Recent theory published by R.Walker and C.T.Walker⁽⁹⁾ related the increase in hardness to the effect of cavitation which caused indentations in the surface. The area around the indentations was embrittled and hardened by the shock wave from the implosion of the cavities. This theory also accounted for the restriction of growth of crystal structure and may also account for the increase in brightness of deposits. Kochegin and Vyaseleva⁽⁴⁾ recently published a theory relating the increase of deposit hardness to the grain size, the

harder deposits having the finer grain.

Cavitation is responsible for all ultrasonic effects relevant in electrodeposition so consequently only sufficient sound intensity to achieve cavitation is required. Wolfe, Chessin, Yeager and Hovorka⁽²⁰⁾ used ultrasonic agitation at frequencies of 200 and 1000 kHz, mostly of the latter. A reflector was placed at an oblique angle in the plating cell at the end opposite to the transducer which prevented the formation of standing waves and reduced complications associated with reflections from the back of the cell. The cathode surface was oriented approximately at 15° to prevent the formation of standing waves. Their conclusions were as follows:-

1. The depolarising action of ultrasonics was primarily associated with the interaction of acoustic waves with concentration gradients at the cathode surface.
2. Ultrasonic waves at cavitation level were more effective than conventional agitation in breaking up the concentration gradients.

The effect of cavitation on metal electrodeposition was still slightly confused, but certain trends keep recurring. Almost all researchers have found that ultrasonic agitation reduced cathodic polarisation producing harder and brighter deposits than those obtained by

conventional agitation. However, certain anomalies have occurred, for example a deposit of nickel with less than half the amount of hydrogen than that obtained with conventional plating procedures has been deposited although the hardness was found to increase. This phenomena could be explained by the fact that the accelerated removal of hydrogen allowed uniform deposition to occur and prevented the formation of pores in the coating thereby increasing the hardness.

The conclusions of Wolf et al⁽²⁰⁾ were that :

1. The grain size of the deposit could be coarser or finer, depending on whether ultrasonics caused depolarisation or passivation of the cathode.
2. Changes in grain size had a significant effect on properties.
3. Electrodeposits produced using ultrasonic agitation were generally harder and brighter than those produced by conventional means.
4. Results of ultrasonic agitation on the internal stress of deposits were often contradictory.

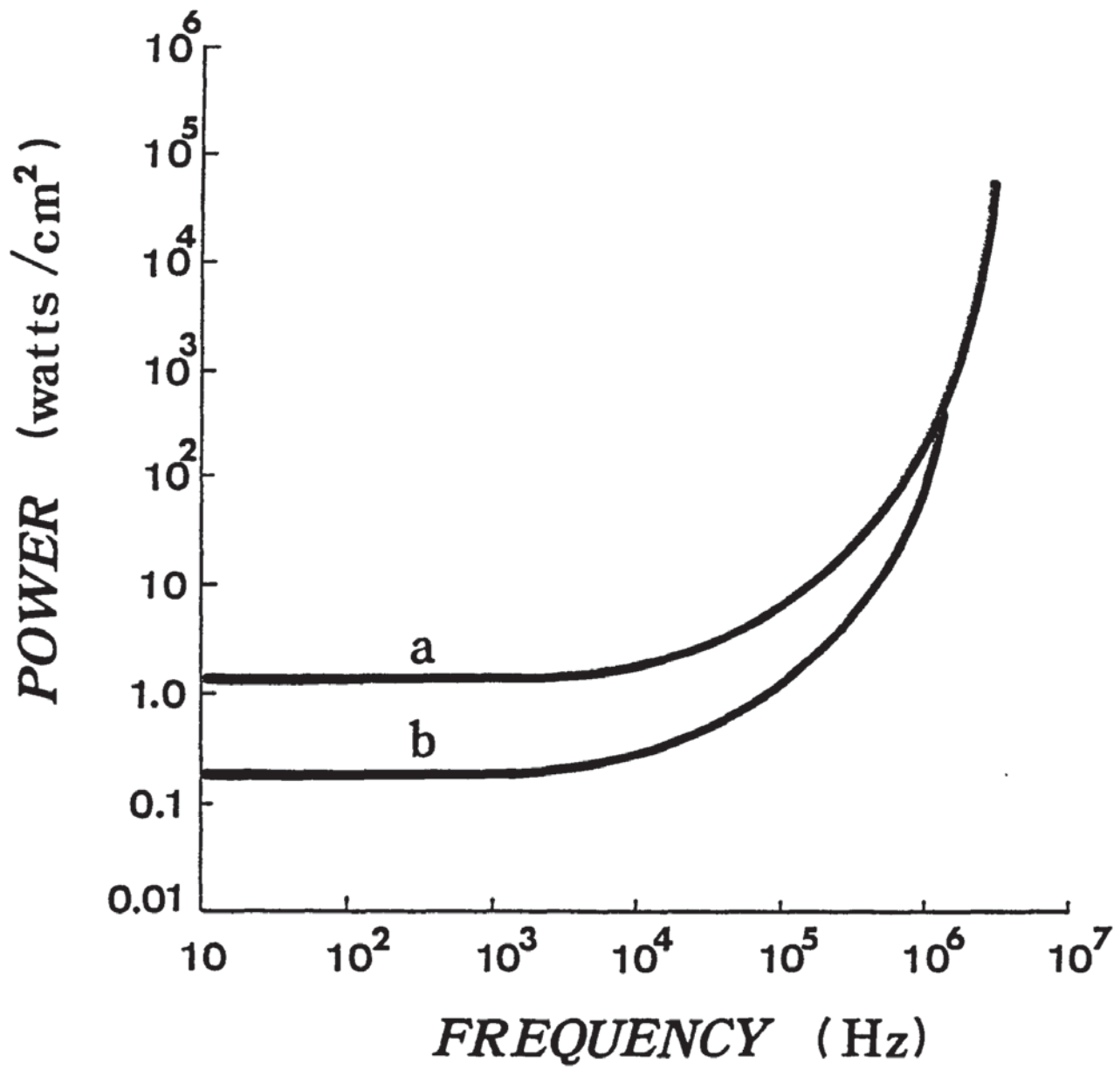
There are many mechanisms⁽³⁾⁽⁴⁾ by which sound can interact with an electrodeposition system, and the frequency, intensity and distribution of the sound field within a plating cell can play an important role

in determining the type of effect observed. At low frequencies (10 - 50 kHz) cavitation phenomena tended to dominate. The shock waves generated by the collapse of vapor cavities can cause severe erosion of the electrode surface and remove absorbed impurities and gas films. Where very intense cavitation was present the electrodeposit could be completely removed as fine particles⁽²⁰⁾.

Fig.(1) shows how the cavitation threshold of water varies with frequency.⁽²¹⁾ It can be seen that above 500 kHz cavitation conditions require extremely high ultrasonic intensities. Many phenomena have been observed at frequencies and intensities where cavitation must be ruled out. Striped or undulating deposits have been obtained in standing wave fields in the 500 - 10000 kHz range and a general increase in mass transport has been observed⁽¹⁰⁾⁽¹¹⁾.

2.3.1 The Effect of Ultrasonic Agitation on the Current Efficiency.

In practical electroplating a metal is hardly ever deposited at 100% current efficiency, some hydrogen is nearly always evolved. After combining into molecules, the hydrogen accumulates at the cathode surface in small visible bubbles. These bubbles may adhere for a while to the surface or they may keep growing and finally detach themselves from the surface. Such bubbles



Fig(1) Cavitation threshold, a) aerated water;
b) degassed water.

are immediately disturbed in an ultrasonic agitation field and are driven off by the pressure of the sound beam.

When a cathode in an ultrasonic field of a few tenths of a W/cm^2 intensity was inspected visually under conditions of moderate hydrogen development, it always appeared bright, whereas it was immediately covered with a film of hydrogen bubbles as soon as the ultrasonic oscillations were stopped.

Kenahan and Schlain⁽¹⁾ have reported that the application of ultrasonic agitation at a frequency of 18.5 kHz and an average acoustic intensity of 0.5 W/cm^2 to the electrodeposition of brass from a cyanide bath resulted in increased anode and cathode current efficiencies, and decreased cell voltage.

2.3.2 The Effect of Ultrasonic Agitation on Hardness.

Many theories have been proposed to explain the phenomena of increasing the hardness of an electrodeposit produced by ultrasonic agitation including the production of a deposit with a smaller grain size and/or the incorporation in the deposit of foreign particles. It may also be associated with the presence of a high internal stress in the coating, but this cannot be the explanation when stress is reduced by ultrasonics. Kochergin and Vyaseleva indicate in their paper⁽⁴⁾ that the harder deposits had

a smaller grain size and packing density which played a major role in the variation of hardness. It is widely accepted that ultrasonic agitation increases the hardness of electrodeposited metals, although there exists some divergence of views regarding the magnitude of the increase obtained and the factors responsible. For example, Muller and Kuss⁽²⁾ found that the hardness of chromium deposits produced on a vibrating cathode at a frequency of 16 kHz increased by an average of 40%, whereas the hardness of copper, nickel and chromium deposits obtained in an ultrasonic field at a frequency of 320 kHz increased by only 15 to 20%. In all cases the hardness of the deposits formed under ultrasonic conditions exceeded that of deposits from an electrolyte subjected to air agitation. Lanyi et al⁽²²⁾ also observed that electrodeposits produced in an ultrasonic field were harder than deposits obtained by conventional practice, silver was only 15% harder, copper 48%, whereas the increase was much higher for cadmium, 160% and zinc, 106%. Similarly Kochergin and Vyaseleva⁽⁴⁾ reported that the hardness of nickel deposits formed in an ultrasonic field at a frequency of 23 kHz and an intensity of $2 \times 10^4 \text{ W/m}^2$ were 60% harder than those produced under ordinary conditions. Walker and co-workers^(23,24,18) found that hardness increased with the application of ultrasonics at a frequency of 30 kHz in the case of several metal deposits. Copper deposits from an acid sulphate bath became harder compared with the still bath, 75 to 111 Hv and 86 to 105 Hv⁽²⁴⁾ depending upon

the conditions, while those from the cyanide bath changed from 146 to 185 Hv⁽²⁴⁾.

The hardness of nickel deposits from the Watts bath increased⁽²⁴⁾ from 241 to 310 Hv but the change in zinc was negligible (46 to 49 Hv). It was observed by Walker et al⁽¹⁸⁾ that the hardness of copper deposits from a sulphate bath, both with and without the addition of a brightening agent, benzotriazole, increases with a rise in the current density from 0.5 to 6.50 A/dm². The effect of ultrasonics was larger at the higher current density.

2.3.3 The Effect of Ultrasonic Agitation on Current Density.

In a paper by Domnikov⁽²⁵⁾ reporting on the effect of ultrasonic agitation at a frequency of 15 to 16 kHz applied to nickel plating baths consisting of 200 - 250 g/l and 500 g/l nickel sulphate she showed that the maximum current density under the action of ultrasonics may be increased three to five fold for both solutions. In the case of the concentrated solution the effect of ultrasonics was most pronounced at higher temperatures. Using ultrasonic agitation, the current efficiency of both baths over the current density range 5 - 15 A/dm² was between 96% to 98%. The positive effect of the use of ultrasonics was the ability to increase the operating current density. However the edge effect, that is the build up of heavier deposits at sharp edges on the cathode,

was more pronounced. Consequently the operating current density for such parts with the use of ultrasonics was somewhat lower than the maximum allowable on cylindrical cathodes. In a comprehensive review, Kochergin and Vyaseleva⁽⁴⁾ concluded that in an ultrasonic field, the electrodeposition of metal could be considerably accelerated by allowing higher current densities to be used. It was also shown that the physicommechanical properties of the deposit were improved, the hardness and elasticity being increased and the porosity diminished. These general conclusions were supported by considerable experimental evidence produced mainly in the USA and USSR. Adherent and well consolidated copper deposits were electrowon from acid sulphate solutions at 50°C using current densities of up to 33 A/dm², Kenahan and Schlain⁽²⁶⁾. Current densities as high as 110 A/dm² have been reported by Kochergin and Vyaseleva⁽⁴⁾. Muller⁽²⁾ reported that ultrasonic agitation raised the lowest current density at which bright deposits were produced from an organic bright nickel and extended the current density range over which lustrous nickel coatings were formed from Watts nickel solution. Roll⁽¹⁰⁾ found that ultrasonic agitation of a low metal content solution moved the current density range for bright nickel deposition to higher values. In a quiescent electrolyte the brightest coatings were obtained at a current density of 0.27 A/dm² whereas the same degree of brightness was achieved at the very much higher value of 4 A/dm² in an ultrasonic field of frequency 34 kHz and intensity 3×10^3 W/m².

2.3.4 The Effect of Ultrasonic Agitation on Macrothrowing Power.

Kozan⁽¹⁶⁾ noted that there was a definite decrease in macrothrowing power when ultrasonic agitation was applied to a nickel plating electrolyte, because of a reduction in concentration polarization.

The throwing powers of nickel baths containing 150 - 200 g/l and 500 g/l nickel sulphate were tested at a current density of 5 A/dm² with and without ultrasonics, and at 15 A/dm² only with ultrasonics, since at this current density it was impossible to produce good quality nickel coatings without ultrasonic agitation. It was found that ultrasonic agitation has no appreciable effect on the throwing power of the nickel plating solution as reported by Domnikov⁽²⁵⁾.

3. ELECTRODEPOSITION OF IRON GROUP METALS.

3.1 Nickel Electrodeposition.

Nickel is one of the most important metals applied by electrodeposition. The plate is used principally as a bright coating underneath a much thinner chromium electroplate to provide a highly lustrous and corrosion resistant finish for articles of steel, brass, zinc die castings, chemically metalized plastics and to a much smaller extent for coatings on aluminium and magnesium alloys. The protection of the underlying metal depends primarily on the nickel plate, but the chromium overlay can be modified to give improved corrosion performance. To a far lesser extent, and only for mild exposures, thin gold or brass electroplate with a clear lacquer finish is used as a decorative coating on thin bright nickel deposits. Nickel coatings alone are also used industrially to afford corrosion protection to prevent contamination of a product. Safranek⁽²⁷⁾ has reported that because of favourable mechanical properties nickel electrodeposits are used for electroforming of printing plates, phonograph record stampers, foil, tubes, screens and many other articles.

The bath chosen and the conditions of operation will depend on the use to be made of the deposit, whether

for engineering applications where physical properties and thickness are paramount or for purely decorative applications on inexpensive articles where the principal aim is to achieve a bright deposit at the minimum thickness (therefore minimum cost) or for such uses as automotive brightwork, where both appearance and protective value must be balanced against cost. To serve these many markets many different electrolytes are available and within any given bath formulation minor variations in additives and operating conditions offer further possibilities for choice.

Nickel plating evolved slowly to its present state. The first 'sound' nickel deposits were reported by Bottger in 1842, Adams, often called the father of nickel plating, developed the first commercially successful process in about 1870. The use of boric acid was introduced a little later and that of chlorides to prevent anode passivity in about 1906. The present Watts bath, named after its inventor, was announced in 1916. It has remained with some improvement the basis of most nickel-plating operations up to the present time.

3.1.1 Type of Nickel Plating Baths.

3.1.1.1 The Watts Bath.

The typical formulation of the Watts bath is shown in Table No.(I)⁽²⁸⁾. The functions of the constituents may be summarised as follows:-

Nickel sulphate provides most of the nickel-ion content. It is the cheapest available nickel salt with a stable anion that is neither reduced at the cathode nor oxidised at the anode and that is nonvolatile. One of the few changes made in the original Watts formula was to increase the nickel sulphate concentration thus allowing the use of higher current densities and better plate distribution.

Nickel chloride is used as the source of chloride ion required to prevent anode passivity. Although other chlorides would serve this function they would introduce extraneous cations. Some of these such as sodium, potassium, and ammonium would result in unsatisfactory nickel deposits. Chloride ion also increases the conductivity of the bath and improves throwing power.

Boric acid serves as a buffer, controlling the pH of the cathode film. Although good deposits can be produced without it, it tends to produce whiter deposits and it is compatible with the many additives that have been developed for the Watts bath. It is obtainable in very pure form and is relatively inexpensive, stable, and nonvolatile.

Anti-pitting agents are necessary because the cathode efficiency of the Watts bath is not 100 percent, it averages about 97 percent. Thus sufficient hydrogen is discharged to produce pits caused by slowly forming

hydrogen gas bubbles clinging to the cathode surface. To promote release of this hydrogen, hydrogen peroxide was used as an anti-pitter before the development of the organic bright nickels, and it is still used occasionally. It functions by depolarisation of the cathode for hydrogen evolution and by oxidation of traces of organic contaminants in the bath.

Table No. (1)⁽²⁸⁾

The Watts Nickel Bath.

Composition	Range g/l	Usual g/l
Nickel sulphate, $\text{NiSO}_4 \cdot 7\text{H}_2\text{O}$	225-375	330
Nickel chloride, $\text{NiCl}_2 \cdot 6\text{H}_2\text{O}$	30-60	45
Boric acid, H_3BO_3	30-40	35
Temperature, $^{\circ}\text{C}$.	45-65	60
pH	1.5-4.5	3-4
Current density, A/dm^2	2.5-10.0	5

3.1.1.1.1 Effect of Variables.

The composition of the Watts bath can be varied over fairly wide ranges, as shown in Table(1). The average formula is suitable for average current densities of 5 A/dm^2 at about 50°C , although current densities from one-half to twice this value will still yield good deposits. At lower current densities, about 2 A/dm^2 , the nickel sulphate and nickel chloride concentrations may be halved. For higher current densities, their concent-

Table (11) Nickel Baths for Electroplating (28).

Baths Type	Composition	Concentration g/l	pH	Temperature $^{\circ}\text{C}$	Cathode Current Density A/dm ²
Watts	Nickel sulphate $\text{NiSO}_4 \cdot 7\text{H}_2\text{O}$	300	1.5-4.5	45-65	2.5-10
	Nickel chloride $\text{NiCl}_2 \cdot 6\text{H}_2\text{O}$	45			
	Boric acid H_3BO_3	38			
Hard Nickel Baths	Nickel sulphate $\text{NiSO}_4 \cdot 7\text{H}_2\text{O}$	180	5.6-5.9	43.-60	2-10
	Ammonium chloride NH_4Cl	25			
	Boric acid, H_3BO_3	30			
Chloride	Nickel chloride $\text{NiCl}_2 \cdot 6\text{H}_2\text{O}$	300	2.0	50-70	2.5-10
	Boric acid H_3BO_3	38			
Chloride-sulphate	Nickel sulphate $\text{NiSO}_4 \cdot 7\text{H}_2\text{O}$	200	1.5-2.0	45	2.5-10
	Nickel chloride $\text{NiCl}_2 \cdot 6\text{H}_2\text{O}$	175			
	Boric acid H_3BO_3	40			
Chloride-Acetate	Nickel chloride $\text{NiCl}_2 \cdot 6\text{H}_2\text{O}$	135	4.5-4.9	30-50	2-10
	Nickel acetate $\text{Ni}(\text{C}_2\text{H}_3\text{O}_2)_2 \cdot 4\text{H}_2\text{O}$	105			
Fluoborate	Nickel (as fluoborate)	75	2.0-3.5	40-80	4-10
	Free Fluoboric acid, HBF_4	3.7-37.5			
	Free boric acid, H_3BO_3	30			
Sulfamate	Nickel sulfamate $\text{Ni}(\text{NH}_2\text{SO}_3)_2$	450	3.0-5.0	40-60	2-30
	Boric acid H_3BO_3	30			
Sulfamate-Chloride	Nickel sulfamate $\text{Ni}(\text{NH}_2\text{SO}_3)_2$	300	3.5-4.2	28-60	2-25
	Nickel chloride $\text{NiCl}_2 \cdot 6\text{H}_2\text{O}$	6			
	Boric acid H_3BO_3	30			

Table (III) Mechanical Properties of
Nickel Electrodeposits.

Baths Type	Properties		
	Hardness (Hv)	Tensile strength KN/cm ²	Elongation %
Watts	140-160	37.74	30
Hard Nickel Baths	350-500	102.9	5-8
Chloride	230-260	68.6	20
Chloride- Acetate	350	137.25	10
Fluoborate	183	51.47	15-30
Sulfamate	250-350	61.76	20-30
Sulfamate- Chloride	190	74.1	15-20

rations may be increased somewhat, but limits are set by excessive drag-out and possible crystallization of salts. Current densities above 10 A/dm^2 can be achieved more satisfactorily by increasing the agitation, temperature, and ratio of chloride to sulphate.

All operating conditions are interrelated: current density, pH, temperature, agitation and bath composition. Low pH allows a greater range of current densities, but current efficiency and throwing power suffer. The usual pH range is 3.5 to 4.5: a pH as low as 1.5 to 2 is sometimes used for a flash coat on steel to be followed by plating under the more usual conditions.

3.1.1.1.2 Variations on the Watts Bath.

Many variations on the basic Watts formulation are used in special applications. An all-chloride bath, included in Table (II), has better conductivity and throwing power than the Watts bath, and yields harder and finer-grained deposits but it is not as amenable to modification by brighteners and other addition agents. A high-chloride, or chloride-sulphate bath, is intermediate in properties between the Watts and the all-chloride, as might be expected. An all-sulphate bath, with no nickel chloride, is used in special situations where insoluble lead anodes must be used, such as in plating the inside of small-diameter tubes. Platinum or platinized anodes may be used with conventional baths for similar purposes.

All these solutions can produce nickel deposits with no limit on the thickness obtainable. Under average conditions, 5 A/dm², pH 3 to 4, and 60°C, the Watts bath produces satiny, matt deposits. These deposits are satisfactory as plated for many engineering applications and for many years, before the development of the modern bright nickel bath, they were buffed to a high lustre before application of the thin chromium deposit. The buffing operation not only brightened the plate, making it suitable for decorative applications, but undoubtedly improved its corrosion resistance by filling in or bridging over pores or discontinuities.

3.1.1.2 Hard Nickel Baths.

A bath recommended by Wesley and Roehl⁽²⁹⁾⁽³⁰⁾ for producing hard nickel deposits has been used for applying nickel on the surfaces of rolls, the salvaging of worn or mismachined parts and coating machine parts for abrasion resistance. Close control of pH, temperature, and current density is necessary to maintain the desired hardness values. The tensile strength increases and ductility decreases with an increase of pH and a decrease in temperature. The deposit has a rather low annealing temperature and will not retain full hardness above about 232°C. Disadvantages of this hard nickel bath are a greater tendency to form nodules and trees than the chloride or Watts bath and a high internal stress in the deposits which can cause sporadic cracking.

In almost all cases, it is much better and much simpler to use the organic stress reducers, in Watts or sulphamate baths to obtain the desired hardness without tensile stress. The stress reducers such as saccharin, p-toluene sulphonamide, sodium m-benzene disulfonate, sodium 1,3,5-naphthalene trisulfonate, 0-sulfobenzaldehyde (0-formyl benzene sulfonate), which introduce about 0.03% sulphur as sulphide in the plate, are most generally used. In no case does the stress reducer endow the plate from a Watts solution with a compressive stress of the same order of magnitude as the original tensile stress. Carr⁽³¹⁾ found that the 0-formylbenzene sulfonate produced deposits with a hardness of 440 to 710 HV and a compressive stress of 0.017 KN/mm^2 to 0.036 KN/mm^2 . Such deposits have been used successfully on steel airplane propellers where hard, abrasion-resistant, ductile and compressively stressed coatings must be employed.

3.1.1.3 Chloride Baths.

Blum and Kasper⁽³²⁾ worked with an all-chloride bath operated at the boiling point. Later, Wesley and Carey⁽³³⁾ made a comprehensive study of the chloride-boric acid electrolyte and the properties of the deposits produced. Deposits are smoother, fine grained, harder and stronger than those from a Watts bath and are more highly stressed. Although it is possible to operate this bath under conditions giving hardnesses over 380 Hv, such deposits are so highly stressed that they may crack spontaneously.

Kendrick⁽³⁴⁾ found that high-frequency periodic current reversal with relatively large amounts of deplating during each cycle resulted in soft ductile deposits with greatly reduced stress. High conductivity of the all-chloride bath permits operation at lower voltages thus saving power costs. When high current densities are employed anode and cathode efficiencies are high and deposits have less tendency to form pits, nodules and trees.

3.1.1.4 Chloride-Sulphate and the Chloride Acetate Bath.

Chloride-sulphate and the chloride-acetate baths are other high-chloride electrolytes. Pinner and Kinnaman⁽³⁵⁾ described a sulphate-chloride bath which overcame some of the disadvantages of the all-chloride bath but retained many of the advantages. Aside from decorative plating with suitable organic addition agents it has found some use in resizing worn parts.

The chloride-acetate bath⁽³⁶⁾ has low resistivity and produces deposits of moderate hardness and high tensile strength. It has found use in plating stereotypes and electrotypes, building up worn parts and plating steel billets as a bonding layer before cladding and rolling.

3.1.1.5 Nickel-Fluoborate Baths.

Nickel-fluoborate baths have some unique qualities which make them applicable for a number of uses despite the higher initial cost of the electrolyte⁽³⁷⁾. Control of the fluoborate bath is very simple, it usually involves only a specific gravity reading and a pH determination. The bath is buffered more highly than the conventional sulphate or chloride baths and as a result changes in pH during operation are not as rapid. Nickel fluoborate has high solubility allowing the use of nickel concentrations far above those possible in chloride-sulphate solutions. This characteristic, along with high conductivity and excellent anode corrosion over wide variations in conditions, permits high current densities to be employed at reasonable voltages. Other favourable characteristics are freedom from sludge formation and higher tolerance to metallic impurities. The deposits are light in colour, ductile, and smooth and do not tend to tree or show nodule formation at higher current density areas. Their internal stress is even lower than that of deposits from the Watts bath. Nickel-fluoborate baths are used for facing stereotypes⁽³⁸⁾. Other applications are for the production of electrotypes, electroforming, barrel plating, and the drawing of nickel-plated copper wire.

3.1.1.6 Nickel Sulphamate Baths.

Cambi and Piontelli⁽³⁹⁾ suggested the use of nickel sulphamate baths in 1938. Commercial use of this type of bath did not start until 1949 however when it was first introduced by Barrett⁽⁴⁰⁾ and employed for producing electrotypes.

Because nickel sulphamate baths are usually employed to produce deposits for engineering purposes the control of mechanical properties, particularly stress, ductility and hardness is important. The stress in nickel deposits plated from a sulphamate bath is the lowest achieved for any commonly used nickel electrolyte. Low stress can only be obtained from baths which have been thoroughly treated to remove inorganic and organic impurities. Nickel sulphamate is much more soluble than the sulphate, and the use of a concentrated nickel sulphamate solution (600 g/l) makes possible very high rates of deposition with the possibility of obtaining consistently low internal stress if continuous conditioning⁽⁴¹⁾ is used. These advantages are particularly valuable in electroforming simple shapes and in electrotyping. Highly polarized anodes or the use of insoluble anodes in sulphamate baths causes the formation of azo-disulphonate⁽⁴²⁾ which introduces sulphur into the nickel plate and can change a low tensile stressed columnar structured deposit to a bright laminar deposit with compressive stress.⁽⁴¹⁾⁽⁴²⁾ Conditioning referred to above is carried out by plating in a by-pass tank using non-active anodes to produce a

controlled concentration of an unspecified organic compound⁽⁷⁵⁾.

Conventional soluble anodes are used in the main plating vat so that undesirable high concentrations of the compound are not produced. Low stressed deposits can then be produced which have adequate ductility and which can be heated without serious deterioration of properties.

Kendrick⁽⁴¹⁾ reported that the sulphamic acid is not as stable as sulphuric acid, and the sulphamate baths require more careful control than Watts bath. Low pH, below 3, and temperatures above 60°C causes marked hydrolysis to ammonium sulphate. The concentrated bath can tolerate slightly higher temperatures⁽⁴¹⁾.

Deposits from nickel sulphamate solutions, either with or without stress-reducing agents, are extensively used for electroforming complicated shapes, salvage of worn or mismachined parts, production of phonograph record stampers, manufacture of electrotypes, and chemical vessels as well as the plating of typewriter parts in barrel plating equipment.

3.1.2 Properties of Electrodeposited Nickel.

The properties of nickel have been studied extensively and results published by many authors.^{(47),(76),(88),(98)} Consequently this information will not be reproduced here.

3.2 Cobalt Electrodeposition.

Electrodeposited cobalt and nickel are similar in many respects. Applications of cobalt and cobalt alloy plating has been centred on electronic gear such as recording tapes, discs and drums. Thus considerable data have been obtained on magnetic properties. Such properties are critically dependent on solution formulation and operating conditions.

Conflicting information has been published regarding the optimum operating condition for cobalt deposition. Dennis et al⁽⁴³⁾ have stated that cobalt has been successfully deposited from chloride, sulphate, mixed chloride/sulphate and sulphamate baths at relatively low pH and from solutions having a lower metal ion concentration than normally employed in nickel plating baths.

Nakahara et al⁽⁴⁴⁾ have reported that the plating characteristics in low and high pH sulphate solutions, 300 g/l $\text{CoSO}_4 \cdot 7\text{H}_2\text{O}$, 3 g/l NaCl and 6 g/l boric acid, were quite different. In the low pH (1.6) solution, plating was accompanied by the evolution of a large amount of hydrogen gas and, consequently, the current efficiency for the metal deposition was low. The composition and operating conditions of the major plating solutions that have been used are given in Table (IV). It was apparent that both cobalt and hydrogen are depositing simultaneously at the cathode. In the high pH (5.7) solution, on the

Table IV

Composition and Operating Conditions for Cobalt Plating Baths

Type of solution	Component salts	Concentration g/l	Temperature C°	pH	Cathode Current Density A/dm ²
1. Sulphate	CoSO ₄ ·7H ₂ O CoCl ₂ ·6H ₂ O	330-565	35-38	3-5	2.15-5
2. Double sulphate (Ammonium sulphate solution)	Co(NH ₄) ₂ (SO ₄) ₂ ·6H ₂ O	175-200	25	5-5.2	1-3
3. Sulphamate	Co(SO ₃ NH ₂) ₂ Formamide HCONH ₂ Wetting agent	450 30 0.3-0.5	20-50		1.6-4.8
4. Chloride	CoCl ₂ ·6H ₂ O	90-105	49-54	2.5-3.5	3-4

other hand, only a small amount of hydrogen gas was seen to evolve at the cathode and the current efficiency for the metal deposition was nearly 100%.

Cassel et al⁽⁴⁵⁾ reported that the cathode efficiency decreased with decreasing pH when electrodepositing from relatively dilute solutions operated at room temperature and this effect was greater for cobalt than for nickel. For example, a reduction in pH from 6.0 to 4.0 in a cobalt sulphate-boric acid-sodium fluoride bath resulted in a decrease in the cathode efficiency from 98 to 82% for a cathode current density of 2.6 A/dm^2 and from 98 to 91% for a current density of 4.3 A/dm^2 . However, Shelton et al⁽⁴⁶⁾ reported that increasing the temperature of the cobalt concentration raised the efficiency of solutions with a pH of 4.0 to 5.0.

Another source⁽⁴⁷⁾ states that modern practice in cobalt electrodeposition favours a high cobalt concentration 65 to 100 g/l, a temperature of 50 to 55°C and a pH in the range of 3.5 to 4.0 in order to deposit cobalt smoothly with a high efficiency at relatively high current densities of 3.5 to 5.5 A/dm^2 .

3.2.1 Properties of Electrodeposited Cobalt.

3.2.1.1 Hardness.

Hardness of electrodeposited cobalt ranged from 180 to

443 Hv, depending on the conditions of deposition and indentation load. The softer deposits (about 180 Hv) were relatively coarse-grained coatings from cobalt fluoborate baths at 45°C.⁽⁴⁹⁾ Harder deposits (250 to 330 Hv) were reported by Endicott⁽⁵⁰⁾ for cobalt from a sulphamate bath and a sulphate solution. Brenner⁽⁵¹⁾ reported that hardness in the range of 330 to 443 Hv was measured for cobalt deposited from a chloride bath. He has stated that electrodeposited cobalt of 99.7% purity, when heated regained a large part of its initial room temperature hardness and in some instances increased in hardness if the maximum temperature had not been too high.

The microhardness of cobalt has been shown to be dependent upon crystal orientation as reported by Morral et al⁽⁵²⁾. Lozinsky and Fedotov⁽⁵³⁾ showed that, when measuring hardness by the indentation methods, the hardness versus modulus of elasticity data at 20°C for most metals fell along a straight line. Hexagonal cobalt was one of the exceptions, its hardness having too high a value with respect to the magnitude of its modulus of elasticity. A sharp softening was observed slightly above room temperature. At temperatures above 480°C where cobalt has a face-centred-cubic lattice, its hardness was correctly related to the modulus of elasticity and the representative point for cobalt fell on the straight line.

3.2.1.2 Strength and Ductility.

Electrodeposited cobalt is stronger than soft nickel electroplate but not so ductile. The tensile strength and ductility properties for cobalt electrodeposited from chloride, sulphate-chloride and sulphamate-bromide solutions were investigated by Endicott⁽⁵⁰⁾, and the results shown in Table (V).

Table V

Tensile Strength and Ductility of
Cobalt Electrodeposits.

Type of solution	Tensile strength KN/mm ²	Elongation %
1) Chloride	0.54	2
2) Sulphate-chloride	1.18	0.019
3) Sulphamate-bromide	0.48	1-3

A decrease in the pH of a sulphate-chloride bath from 2 to 1.5 increased the tensile strength of the deposit from 0.66 to 1.186 KN/mm² and improved ductility slightly as reported by Lindsay et al⁽⁴⁹⁾. An increase in pH from 2.0 to 4.0 reduced ductility.

3.2.1.3 Internal Stress.

The tensile strength in cobalt deposits is usually about

twice that for nickel deposits from similar solutions at similar plating conditions. For example, cobalt deposited from a sulphate-chloride bath had a stress of 0.55 kN/mm^2 compared to 0.27 kN/mm^2 for nickel from the same type of solution⁽⁵¹⁾. A stress of 0.137 kN/mm^2 was reported by Barrett⁽⁵⁴⁾ for cobalt deposited from a sulphamate bath.

The harder deposits exhibited high stress values as a rule. Fisher⁽⁵⁵⁾ added 1.6 g/l of saccharin to a cobalt chloride bath at 25°C and it reduced the stress in the deposit from 0.186 to only 0.093 kN/mm^2 at a current density of 1.6 A/dm^2 .

3.2.2 Structure.

The microstructure of cobalt electrodeposits is usually columnar or fibrous. McFarlen⁽⁵⁶⁾ observed a fibrous structure in cobalt deposits plated in a sulphamate bath at 49°C . A mixture of hexagonal-close-packed and face-centred-cubic lattice structures has been observed in cobalt and cobalt rich alloy electrodeposits. At pH values below 2.5 the fcc form for cobalt was favoured, whereas either a high pH or a high temperature increased the proportion of hexagonal cobalt in deposits produced in a sulphate bath with organic addition agents as reported by Gaigalas et al⁽⁵⁷⁾. With no organic additive the hexagonal form was predominant. The hexagonal structure was also approached for cobalt deposited in sulphate baths contain-

ing no addition agents when the pH was more than 2.9 as reported by Okund⁽⁵⁸⁾. A high deposition temperature also induced the hexagonal structure for cobalt deposited in a chloride bath. High current densities favoured the cubic form for cobalt deposited in sulphamate solution as shown by Sard et al⁽⁵⁹⁾. Transformation from the hexagonal to the cubic form was observed upon heating to 425°C by Chabb⁽⁶⁰⁾. A high degree of preferred orientation has been observed for cobalt deposited in sulphate baths but cobalt deposited in chloride solutions was randomly oriented. Current densities affected the orientation, high current densities favoured a random distribution⁽⁵⁸⁾.

3.3 Iron Electrodeposition.

Iron is the cheapest metal available and the physical properties of electrodeposited iron are of potential interest in many applications. Furthermore it is easily electroplated from several types of electrolytes. Despite these advantages iron is not widely used as an electrodeposit. It has no decorative applications even though electrodeposited iron is somewhat more corrosion-resistant than ordinary iron, probably because of its higher purity. Uses of iron plating include some electroforming applications such as production of phonograph record stampers and iron moulds for rubber, glass, and plastics; iron foils with special magnetic properties and the restoration of worn parts. The properties of iron deposits are extremely sensitive to the purity of the electrolyte and the operating conditions, especially the pH and concentration of ferric ion.

Iron is plated from baths containing the ferrous iron (II) ion. Presence of ferric or iron (III) ion in more than trace concentrations may lower cathode efficiency and may also lead to brittle, stressed, and pitted deposits, as discussed by Connor⁽⁶¹⁾. Precipitation of Fe (III) hydrate in the cathode deposit is probably the cause of some of these difficulties.

The most commonly used iron-plating baths are the ferrous sulphate and the ferrous chloride baths, or mixtures of the two. Iron fluoborate and sulfamate

solutions also have been used. As the chloride is much more soluble and has a higher conductivity than the sulphate it is more commonly used. Most ferrous salt baths are fairly concentrated, e.g. as high as 140 g/l of dissolved iron. Addition of other salts can be made to increase the electrolyte conductivity. In sulphate baths ammonium sulphate is commonly added, or the double salt, ferrous ammonium sulphate, $\text{FeSO}_4 \cdot (\text{NH}_4)_2\text{SO}_4 \cdot 6\text{H}_2\text{O}$, is also used. In ferrous chloride baths calcium chloride is often added. Potassium chloride can be used when harder deposits are desirable. The compositions and operating conditions of the major plating solutions that have been used are given in Table (VI) by Lowenheim⁽⁴⁸⁾.

3.3.1 Types of Iron Plating Baths.

3.3.1.1 The Ferrous Sulphate Bath.

The ferrous sulphate bath can be operated at room temperature to produce deposits that are smooth, normally light grey in colour but brittle. The most common sulphate bath is the one containing the double salt, ferrous ammonium sulphate, see Table No. (VI). It has been used principally for building up undersized machined parts and also to apply a hard facing to stereotypes as shown by Lamb⁽⁶²⁾. Dilute solutions containing 50 to 100 g/l of ferrous ammonium sulphate gave excellent deposits but only at current densities up to 0.3 A/dm^2 . However, if the concentration was raised almost to saturation at

Table VI Composition and Operating Conditions for Iron Plating Baths. (48)

Type of solution	Component salts	Concentration g/l	Temperature °C	pH	Cathode current density A/dm ²
1. Sulphate	$\text{FeSO}_4(\text{NH}_4)_2\text{SO}_4 \cdot 6\text{H}_2\text{O}$	350	25	2.8-3.4	2
a) low pH	or $\text{FeSO}_4 \cdot 7\text{H}_2\text{O}$ $(\text{NH}_4)_2\text{SO}_4$	250 120	60	2.1-2.4	6-10
b) high pH	The same as (a)	The same as (a)	25	4.0-5.5	2
2. Hot chloride (Fisher-Langbein Solution)	$\text{FeCl}_2 \cdot 4\text{H}_2\text{O}$ CaCl_2	300 335	90	0.8-1.5	6.5
3. Fluoborate	$\text{Fe}(\text{BF}_4)_2$ NaCl	226 10	55-60	2.0-3.0	2-10
4. Sulphate- Chloride	$\text{FeSO}_4 \cdot 7\text{H}_2\text{O}$ $\text{FeCl}_2 \cdot 4\text{H}_2\text{O}$ NH_4Cl	250 42 20	40-43	3.5-5.5	5-10

about 410 g/l deposits equally as good as those obtained from the dilute solution could be obtained at current densities as high as 2 A/dm^2 ; i.e. about seven times the rate in the former case.

It is shown in Table VI that two ranges of pH are used for the sulphate bath at 25°C . These distinct ranges result from the fact that iron (III) hydroxide precipitates at a pH of about 3.5, whereas iron (II) hydroxide precipitates at a pH of about 6.0. In the low pH range, even in a well-reduced bath, some iron (III) ion is present because of air oxidation, therefore, operation at a pH too close to 3.5 results in dark-coloured excessively stressed deposits, probably caused by inclusion of basic iron (III) salts in the deposits. Operation at a pH below the recommended minimum for the low pH range results in lower cathode efficiency and increased deposit stress. The high pH sulphate bath has better covering power and yields deposits that are less stressed than those from the low pH bath. Deposits with minimum stress are obtained at pH values in the range 4.0-5.0.

At the high operating temperatures, sludging due to air oxidation is rapid at high pH. Therefore only the lower pH range is recommended for operation at elevated temperatures. Deposits from the sulphate bath do not become significantly ductile even if the bath is operated at the boiling point. However, the advantage of an elevated temperature is the higher permissible

current density.

3.3.1.2 The Ferrous Chloride Bath.

The important and distinctive characteristics of the chloride baths are that they yield ductile deposits when operated at temperatures higher than about 85°C. The most commonly used bath is the Fisher-Langbein solution, U.S. Patent 992,951⁽⁶³⁾, which consists of a slightly acid solution of ferrous and calcium chlorides. This bath yields dark-coloured, hard, highly stressed deposits at 25°C. At increasingly higher temperatures the deposits become gradually lighter coloured, softer and less stressed.

The composition of the Fisher-Langbein solution, as modified by Thomas and Blum, is shown in Table (VI), No.2. The lower concentrations introduced by Thomas and Blum⁽⁶⁴⁾ permitted the use of moderate current densities and did not lead to crystallisation of the salts when the bath was cooled. It was found that the concentrations of ferrous chloride and calcium chloride were not critical for this bath. The high concentration of ferrous chloride increased the permissible current density and calcium chloride increased the conductivity. Experiments by Thomas and Blum showed that the acidity of the bath was found to be more important than the concentrations of the salts, the free hydrochloric acid should be about 0.01N, corresponding to a pH of about 2.

Thomas, Klingenmaier and Hardesty⁽⁶⁵⁾ investigated iron plating from the ferrous chloride-calcium chloride bath at different salt concentrations. It was noted that the deposits became dark-coloured and brittle at temperatures below 70°C but the most troublesome aspect was the rapid oxidation of ferrous to ferric ion in the electrolyte. This oxidation was accelerated by high acid concentration and high temperature. When the Fe (III) was above 0.8 g/l pitting occurred.

The solution produced by McGeough and Lai⁽⁶⁶⁾ contained 80 g/l of calcium chloride and unlike the calcium chloride containing solution used by Thomas no pitting problems were encountered. Provided that the electrolyte temperature was above 86°C and the current density was in the range 10 to 30 A/dm² bright smooth deposits were obtained. With this bath the ratio of ferrous to ferric ion in the solution remained below 0.02 over a six months period while in use and after the electrolyte had been left idle for a further nine months the ratio of ferric to ferrous ion had only risen to 0.09.

Numerous modifications of the Fisher-Langbein chloride bath have been described in which calcium chloride has been eliminated. Solutions of ferrous chloride alone were used or replaced by other alkali or alkaline earth chlorides. The presence of a low concentration of manganese chloride has been claimed by Stoddard⁽⁶⁷⁾ to result in deposits of finer grain size and to permit a

wider range of operating conditions than did the ferrous-calcium chloride bath.

Elimination of calcium chloride from the bath enables the use of higher ferrous chloride concentrations which permits the use of higher current densities. For rapid deposition at current densities as high as 30 A/dm^2 Kasper⁽⁶⁸⁾ used a solution of ferrous chloride alone at concentrations from 400 to 500 g/l $\text{FeCl}_2 \cdot 4\text{H}_2\text{O}$. He found that in order to obtain a relatively soft ductile deposit from such a bath the following four requirements must be met:-

- (i) The solution should be clear green in colour, i.e. nearly free from ferric salts.
- (ii) The ferrous chloride concentration should be at least 4N since with lower concentrations more brittle deposits are obtained.
- (iii) The acidity should be controlled within fairly close limits. Insufficient free acids lead to brittle deposits while excess acidity lowers the cathode efficiency.
- (iv) The temperature should be controlled within close limits. It is the most important single factor, variations of 5°C can produce marked changes in the properties.

3.3.1.3 The Ferrous Sulphate-Ferrous Chloride Bath.

A bath for the application of iron plating to electrotyping must give a relatively stress free deposit at temperatures below the softening point of electroplaters' wax, e.g. about 35°C to 40°C. In making an electrottype shell removable non-adherent deposits are required. The metal, therefore, must be deposited in such a way that no strains are set up in the deposit otherwise peeling or separating would take place. The electrottype shell must be ductile enough to permit stripping from the mould without breaking. Schaffert and Gonser⁽⁶⁹⁾ developed a sulphate-chloride iron electrolyte of the composition and operating conditions given in Table (VI), No.(4), which meets the above requirements successfully. The iron deposits produced were less brittle than with either normal sulphate or chloride baths. A series of plating tests were made at different bath compositions and the results showed that the composition had a great effect on the deposit characteristics. A plain ferrous sulphate solution will normally produce dark crumbly deposits except at very low current densities. Addition of sufficient amounts of ammonium chloride permits a current density of about 10 A/dm² without darkening, but the deposit is quite brittle and trouble with peeling and cracking is encountered. Addition of relatively small amounts of both ammonium and ferrous chloride to the ferrous sulphate solution, allows good deposits to be obtained at high current densities without peeling or

cracking and with considerably less brittleness. Ferrous chloride added alone to the sulphate solution gives dark deposits at high current densities.

It appears that the ammonium ion is necessary for deposition at high current densities. A lower concentration of ammonium chloride will improve ductility of the iron deposits when relatively low current densities are used. It is also noted that the "Covering power" of the bath is better than that of the chloride bath. This is also thought to be due to the presence of ammonium ions.

3.3.2 Properties of Electrodeposited Iron.

It is very difficult to attribute the variation of any property of electrodeposited iron unambiguously to a single operating parameter independently of the others. Acting simultaneously these parameters determine the condition of the cathode layer and the processes occurring at the cathode solution interface and consequently the properties of the deposit.

Data from different sources refers to deposits produced from solutions of different compositions operating under different conditions, to give various deposit thicknesses. Consequently, it is very difficult to compare the results of different investigators and to establish the general trends of a property or condition of a deposit with the

conditions under which it was produced.

A representative selection of data on mechanical properties is given in Table (VII). This data is not sufficient to give a complete picture of the relationships between operating conditions and deposit properties but is nevertheless very useful. It is seen that deposits from the sulphate bath are harder than those from chloride baths. No work has been reported on the mechanical properties of deposits from the sulphate-chloride bath although it might be expected that the hardnesses of these deposits would be similar to those from the ferrous ammonium sulphate bath. It is seen that hardness, tensile strength and stress decreased with increase of bath temperature and that in general an increase in current density increased the hardness.

3.3.2.1 Hardness.

The hardness of iron deposited from a chloride bath depends mainly on the temperature of the solution. At 70°C a hard deposit of 450 HV could be produced. The hardness decreased markedly as the temperature was increased and at 88°C the deposit was very soft. Thomas et al⁽⁶⁵⁾ reported a value of 125 HV. At the lower temperatures deposits plated at low current densities were softer than those plated at higher current densities, whereas at the higher temperatures, 90-95°C, the hardnesses were nearly the same for all current densities. Additions of

ammonium, magnesium, potassium, or sodium sulphate increased the hardness of iron deposited in fluoborate baths but citric acid additions had even greater effect on hardness as reported by Mukai et al⁽⁷⁰⁾. Deposits from the sulphate baths at slightly above room temperature were harder than those from the hot chloride baths. Schaffert and Gonser⁽⁷¹⁾ reported Brinell hardness numbers ranging from 150 to 750, which were extremely high compared with a maximum hardness number of about 350 Brinell reported by MacNaughton⁽⁷²⁾ for deposits from a bath of similar type.

3.3.2.2 Tensile Strength and Ductility.

Iron with a coarse-grained structure electrodeposited in chloride solutions exhibited tensile strengths ranging from 0.26 to 0.6 kN/mm² but 0.88 kN/mm² was reported for fine-grained iron deposited in a chloride solution containing glycerol. The tensile strength of iron deposited in sulphamate and chloride-fluoborate solutions ranged from about 0.69 - 1.07 kN/mm². No systematic study of the influence of thickness on tensile properties has been reported. However, Stoddard and Diggin⁽⁶⁷⁾⁽⁷³⁾ claimed that increasing the thickness from 0.2 to 1 mm appeared to have little effect on the strength or ductility of iron deposited in a ferrous chloride-manganous chloride solution.

Kasper⁽⁶⁸⁾ investigated the mechanical properties of

Table (VII) Mechanical Properties of Electrolytic Iron
From Lowenheim (48)

Type of Solution	Operation Condition				Elongation %	Hardness Brinell	Stress N/mm ²
	pH or acidity	Temperature °C	Current density A/dm ²	Tensile Strength kN/mm ²			
$\text{Fe}(\text{NH}_4)_2(\text{SO}_4)_2 \cdot 6\text{H}_2\text{O}$	3.4	20	0.5	-	-	263	-
	3.4	20	2.0	-	-	354	-
	4.4	19	0.5	-	-	182	-
	4.4	41	5.0	-	-	240	-
$\frac{1}{4} 5\text{NFeCl}_2$	0.06N	97	10	0.515	5	167	-
	0.06N	100	10	0.430	18	135	-
	0.04N	100	20	0.765	0	228	-
$\text{FeCl}_2 + \text{CaCl}_2$	0.01N	90	6.0	0.390	20	-	-
	0.05N	88	6.0	0.545	-	-	795
	0.05N	93	12.0	0.475	-	-	60
	0.10N	65	6.0	-	-	-	365
Deposit from either Sulphate or chloride baths annealed at 90°C	-	-	-	316	40	70-90	-

iron deposited from a chloride solution under various conditions of pH, temperature and current density. The specimens were prepared by depositing onto nickel and the tests were carried out without removing the nickel. The ultimate tensile strengths ranged from 0.42 to 0.79 kN/mm², with elongations of 0 - 18%. This agrees well with the data by Thomas and Blum⁽⁶⁴⁾ who reported a tensile strength of 0.4 kN/mm² and an elongation of 20% for metal deposited from a chloride bath at a current density of 6.5 A/dm² and a temperature of 90°C. A deposit obtained at 18.6 A/dm² and 95°C had a tensile strength of 0.78 kN/mm² and an elongation of 4%.

Stoddard⁽⁶⁷⁾ carried out work on the mechanical properties of iron from a ferrous chloride solution to which manganese chloride had been added and obtained strengths ranging from 0.33 to 0.77 kN/mm² with elongations of 50% to 10% respectively.

3.3.3 Structure.

Grain size is one of the most important characteristics of an electrodeposit because it affects many other properties. Stoddard⁽⁶⁷⁾ ran tests with different addition agents in a ferrous chloride solution in an attempt to control grain size without causing embrittlement. He found that a small amount of manganese chloride was effective in producing pit-free, ductile, fine grained deposits.

Pitting is eliminated by the use of a compatible wetting agent. After trying several wetting agents such as 2,7-naphthalene disulphonic acid sodium salt, formaldehyde, ferrous oxalate and alkanols, he found that Gardinal WA* was perfectly stable in the solution and relieved pitting to a remarkable extent without interfering with the ductility of the deposit as did other wetting agents.

In general, under given conditions, grain size increased with increasing plate thickness but with manganese in the solution (about 5 g/l $\text{MnCl}_2 \cdot 4\text{H}_2\text{O}$) it was possible to build up heavy deposits as thick as 1.5 mm without having the grain size increase to any appreciable extent. Levy and Hutton⁽⁷⁴⁾ attempted to correlate the structure of the deposits from a mixed fluoborate-chloride bath with the operating parameters temperature, current density and pH. At a current density of 5 A/dm^2 and a temperature of 60°C , the deposits were fine grained and smooth. On increasing the temperature to 70°C the deposits were more uniformly light grey in appearance and the grain size was noticeably larger resulting in an increase in surface roughness. At a current density of 10 A/dm^2 and a temperature of 60°C , the deposits were shiny, smooth and light grey in colour but were very highly stressed as evidenced by the presence of many minute cracks over their entire surfaces. On increasing the temperature to 70°C the deposits were still light grey and contained few cracks.

* Proprietary product.

CHAPTER FOUR

4. ALLOY ELECTRODEPOSITION.

Surface coatings are extensively employed to satisfy industrial requirements ranging from decoration to wear resistance and from corrosion protection to electrical conductivity. The development of alloy electrodeposits began at the same time as the single metal electrodeposits.

The first alloys produced were of brass and bronze. The main reason for alloy plating is to obtain electrodeposits with better properties such as hardness, higher wear resistance and better magnetic properties since these properties are not always obtained by deposition of single metals. The alloys produced by electrodeposition are true metallurgical alloys in that they normally contain phases which are shown by the phase diagram as being stable for the temperature at which the electrodeposit was formed. However there are some notable exceptions such as Ni Sn, i.e. there is no Ni-Sn phase on the equilibrium diagram.

The deposition of alloys may be classified into five types⁽⁴¹⁾:-

- (I) Regular co-deposition
- (II) Irregular co-deposition
- (III) Equilibrium co-deposition

(IV) Anomalous co-deposition

(V) Induced co-deposition.

Types I - III are known as normal co-deposition and types IV - V as abnormal co-deposition since from elementary considerations it would seem that co-deposition of these elements should not be possible.

(I) Regular co-deposition of alloys is normally under diffusion control and therefore the effects of plating variables on the composition of the deposits are determined by changes in the concentrations of metal ions in the cathode diffusion layer and are predictable from simple diffusion theory.

The percentage of the more noble metal in the deposit is increased by those agencies that increase the metal ion content of the cathode diffusion layer. i.e. increase in total metal content of bath, decrease of current density, elevation of bath temperature and increased bath agitation. Regular co-deposition is most likely to occur in baths containing simple metal ions but may occur in baths containing complex ions.

(II) Irregular co-deposition is normally controlled by the characteristics of the potentials of the metals against the solution rather than by diffusion processes. The effects of some of the plating variables on the composition of the deposits are in accord with simple

diffusion theory and the effects of others are contrary to diffusion theory. Also, the effects of plating variables on the composition of the deposit are much smaller than with the regular alloy plating systems. Irregular co-deposition is not likely to occur with solutions of complex ions, particularly with systems in which the static potentials of the parent metals are markedly affected by the concentration of the complexing agent, for example, the potential of copper or zinc in a cyanide solution.

(III) Equilibrium co-deposition is not very common and only a few of these systems have been investigated such as the copper-bismuth and lead-tin acid baths. The solutions are in chemical equilibrium with both of the parent metals and the ratio of metals in the deposit is the same as their ratio in the bath.

(IV) Anomalous co-deposition type baths are fairly rare and usually contain one or more of the iron group metals, iron, cobalt or nickel. It is referred to as anomalous because the less noble metal deposits preferentially.

(V) Induced co-deposition baths are characterised by the deposition of alloys containing molybdenum, tungsten and germanium which cannot be deposited from aqueous solution alone. The alloys most likely to be formed are those iron group metals. The iron group ions present in the bath are termed inducing metal ions and molybdenum,

tungsten or germanium ions are called the reluctant metal ions.

In order that an alloy may be obtained from a plating solution it is required that the deposition potential of the two metals are fairly close together. The reason for this is that the more noble a metal the easier it will deposit and therefore if the difference in deposition potential of the two metals is great then the more noble metal will deposit preferentially, frequently to the complete exclusion of the less noble metal.

Electrode potentials: The static potential of each metal in the alloy bath may be given by the Nernst equation⁽⁷⁶⁾:-

$$E = E^0 + \frac{RT}{zF} \ln a^{z+} \dots\dots\dots(1)$$

where

E = static electro potential

E⁰ = standard electrode potential

R = gas constant

T = absolute temperature

F = Faraday

z = valency

a^{z+} = activity of metal ions charged in solution.

The static potential serves as a guide to the feasibility of metal deposition but is not necessarily applicable under the dynamic conditions of electrodeposition.

4.1 Electrochemical Aspects of Electrodeposition.

When any deposition or electrode process occurs at an electrode, its potential departs from its equilibrium or steady state value and the electrode is said to be polarised. Concentration polarisation⁽⁷⁷⁾ is due to a change in concentration of metal ions around the electrode during the plating operation, with the solution adjacent to the cathode becoming depleted of metal ions while at the same time the solution around the anode becoming more concentrated as the reaction proceeds. If when using conventional plating techniques the speed of deposition is increased, i.e. by raising the current density, the concentration polarisation becomes greater and finally the electrolyte next to the cathode becomes so denuded of metal ions that further deposition becomes difficult and finally impossible. If the concentration of metal ions around the cathode finally becomes zero, the current density which would be required to obtain this complete denuding is referred to as the limiting current density and it is the raising of this limiting current density that is the requirement to achieve high speed plating⁽⁷⁶⁾. If the concentration around the electrode changes, i.e. when depletion has occurred then the electrode potential changes.

$$E_1 = E^0 + \frac{RT}{zF} \ln a_1^{M^{z+}} \dots\dots\dots(2)$$

The concentration polarisation is the potential difference, G , between E (equation (1)) and E_1 (equation

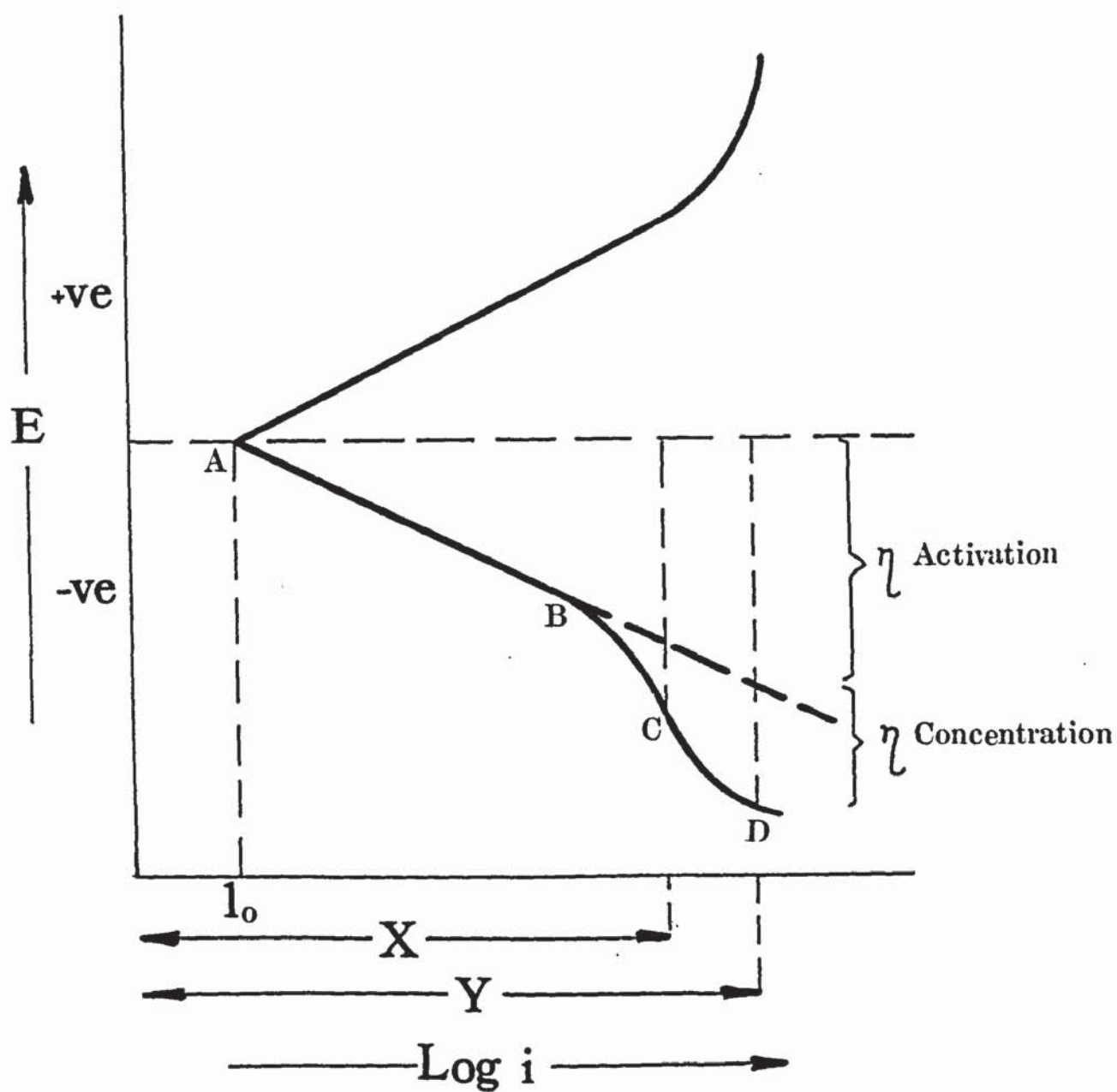
(2)). By reference to the Nernst equation the potential has become less noble as the deposition rate increases, i.e. E_1 is less noble than E .

If the current density of the plating operation is increased, then the faster the depletion of metal ions around the electrode and so the greater the concentration polarisation. Eventually an alternative cathode reaction will occur and this is usually one of gas liberation such as the evolution of hydrogen. High speed plating has the major problem of how to speed up the deposition rate without causing an alternative reaction.

In many cases this can be prevented by simply stirring the electrolyte and thus increasing the rate of replenishment of metal ions in the depleted regions; the current density can be increased without an immediate denuding of metal ions near the working electrode⁽⁷⁸⁾. Ultrasonic agitation is an alternative means of agitating a plating bath to achieve a higher limiting current density. This concentration effect causes deviation from the Tafel⁽⁷⁹⁾ relationship shown in Figure(2)⁽⁸⁰⁾.

$$\eta = a + b \log_e i \quad \text{.....Tafel Equation.}$$

In the region A-B, as long as a greater external potential is applied then so the current density will increase. Metal deposition occurs along this line with the number of metal ions being discharged in unit time,



X : Cathode limiting current density

Y : Anode limiting current density

Fig(2) Effect of concentration polarisation .

increasing with increasing current density.

In the region B-C, the limiting current density has been reached. As soon as metal ions reach the cathode surface from the bulk solution they are discharged or deposited. B-C is the limiting current density region, above which no increase in the rate of deposition can occur because the reaction is diffusion controlled.

In the region C-D, any further increase in applied potential produces an alternative cathode reaction. i.e. liberation of hydrogen.

In addition to diffusion, migration and convection effect the transfer of ions.

If a process is under diffusion control

$$i_{\text{limiting}} = \frac{D \cdot z \cdot F \cdot a}{(1-t)\delta}$$

D : Diffusion coefficient of metal ions in solution

a : Activity of metal ions in solution

t : Transport number of ion

δ : Thickness of cathode diffusion film

z : Valency of metal ions in solution

If the limiting current density is to be raised, that is if the rate of metal deposition is to be increased then (D) and (a) must be increased and/or (δ) decreased.

- (D) can be raised by increasing the temperature.
- (a) may be increased by making the solution more concentrated.
- (δ) can be decreased by agitation.

CHAPTER FIVE

5. NICKEL-COBALT ALLOY ELECTRODEPOSITION.

5.1 Bath Formulations for the Electrodeposition of Nickel-Cobalt Alloys.

Nickel-cobalt alloy electrodeposits have been in commercial use for about 35 years as this alloy was one of the first successful methods of depositing "bright-nickel" coatings when used in conjunction with either nickel formate⁽⁸¹⁾ or nickel formate and formaldehyde⁽⁸²⁾. Although the alloys have generally been superseded by commercial bright nickel systems containing organic brighteners interest is periodically revived in the alloys when nickel is either in short supply or prohibitive in price. Recent work on this alloy for decorative purposes carried out by Mathieson and Sedghi⁽⁸³⁾ was occasioned by such a shortage. The alloy has been successfully deposited from chloride⁽⁸⁴⁾, sulphate⁽⁸⁵⁾, mixed chloride/sulphate⁽⁸⁶⁾ and sulphamate baths⁽⁸⁷⁾. The recent work on this alloy system for electroforming purposes has been carried out by Belt et al⁽⁴¹⁾⁽⁸⁸⁾ and McFarlen⁽⁵⁶⁾ and Wearmouth⁽⁸⁹⁾. These investigators all used the sulphamate bath to produce alloys over a wide range of compositions for engineering applications.

These investigations illustrated that an alloy containing about 35% cobalt possessed the highest hardness and

greatest strength. The bath used by McFarlen⁽⁵⁶⁾ was the conventional sulphamate bath containing 75 g/l nickel and cobalt sulphamate whereas that employed by Belt et al⁽⁴¹⁾⁽⁸⁸⁾ and Wearmouth⁽⁸⁹⁾ was the concentrated bath based on the "Ni-Speed" (Trade name of the International Nickel Company Ltd.) electrolyte (600 g/l nickel sulphamate). The deposits obtained by McFarlen⁽⁵⁶⁾ gave slightly higher strengths than those obtained by Belt et al⁽⁸⁸⁾. This composition is very close to the composition found by Belt et al⁽⁴¹⁾ to give the highest hardness. The work of Wearmouth⁽⁸⁹⁾ is interesting as it is mainly a study of electroforming applications for the nickel-cobalt alloy solutions developed by Belt and co-workers⁽⁴¹⁾⁽⁸⁸⁾.

5.1.1 Nickel-Cobalt Sulphate Bath.

The sulphate bath for the deposition of nickel-cobalt is well known being based on the Watts bath. The alloy plating baths are prepared by adding the appropriate quantity of cobaltous sulphate to a Watts type nickel solution containing:

Nickel Sulphate	$\text{NiSO}_4 \cdot 7\text{H}_2\text{O}$	240 - 300 g/l
Nickel Chloride	$\text{NiCl}_2 \cdot 6\text{H}_2\text{O}$	20 - 50 g/l
Cobaltous sulphate	$\text{CoSO}_4 \cdot 7\text{H}_2\text{O}$	29 g/l
Boric acid	H_3BO_3	20 - 30 g/l.

As cobalt is preferentially deposited in the presence of nickel a calibration curve of concentration of cobalt

in solution against % cobalt in the alloy deposit was required. This was constructed initially by formulating solutions which would give required alloy deposits. The data for this was obtained from results published by Still⁽⁷⁸⁾ as shown in Figure (3).

5.1.2 Nickel-Cobalt Sulphamate Bath.

The sulphamate baths for alloy deposition of nickel-cobalt are prepared in a similar manner to the sulphate ones; that is by adding an appropriate quantity of cobaltous sulphamate to a nickel sulphamate bath containing:

Nickel sulphamate	$\text{Ni}(\text{SO}_3\text{NH}_2)_2 \cdot 4\text{H}_2\text{O}$	600 g/l
Nickel chloride	$\text{NiCl}_2 \cdot 6\text{H}_2\text{O}$	10 g/l
Boric acid	H_3BO_3	40 g/l.

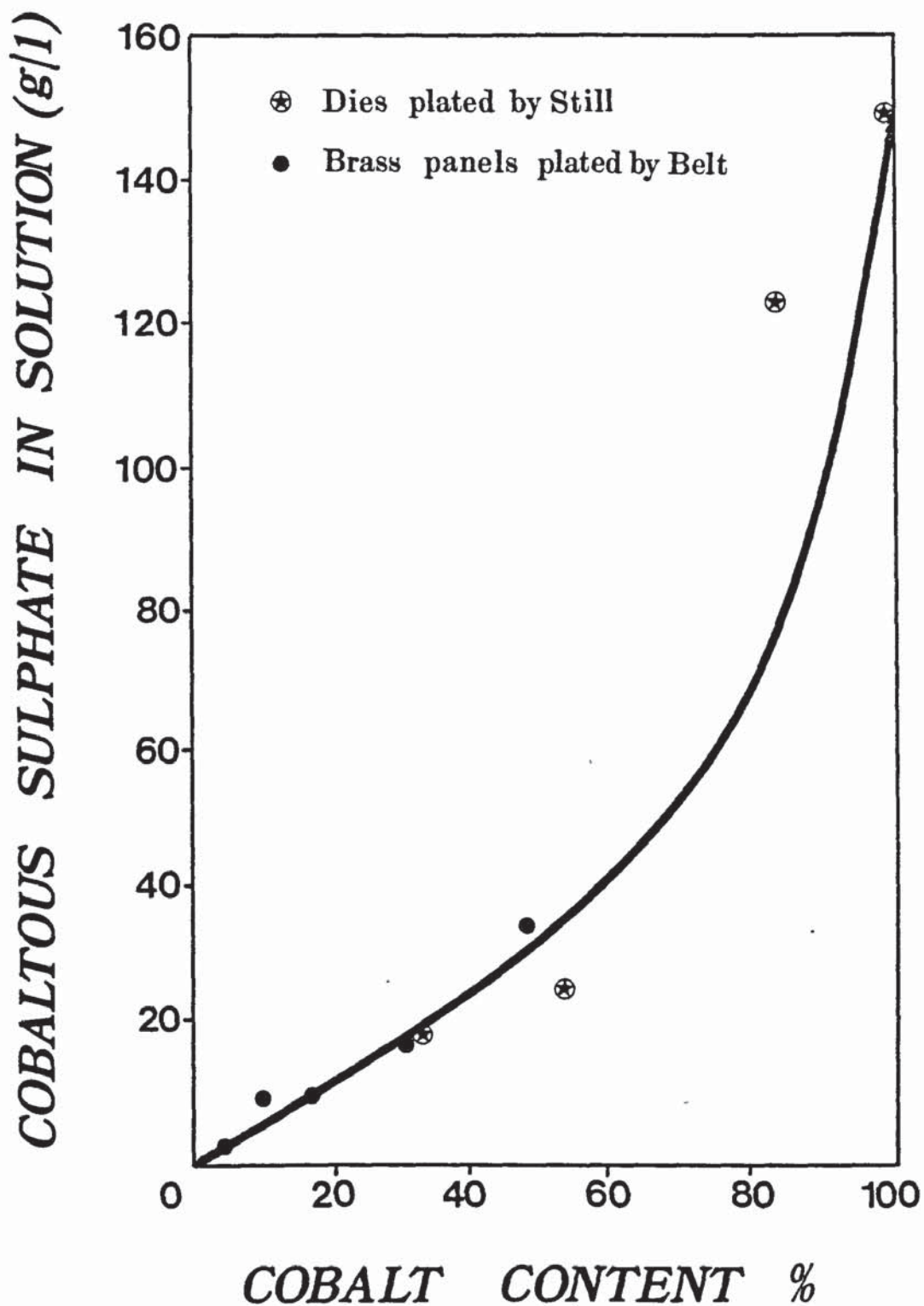


Fig (3) Relationship between the concentration of cobaltous sulphate in solution and the percentage cobalt obtained in the deposit by Belt (41) and Still (78).

5.2 The Effects of Plating Variables on Nickel-Cobalt Deposition.

5.2.1 Effect of Current Density on the Composition of the Deposit.

In general the cobalt content of a nickel-cobalt alloy deposited from simple salt baths is found to decrease with increasing current density. However due to the anomalous nature of this system the effects of current density on the deposit may be divided into various current density levels. At low current density levels Glasstone and Speakman⁽⁸⁵⁾ and Piontelli and Patuzzi⁽⁸⁷⁾ found that the alloy deposited normally (i.e. nickel deposited preferentially being more noble). Then at a higher range of current density (approximately 1 - 3 A/dm²) the cobalt content in the deposit reached a maximum. This maximum was reached at approximately 1 A/dm² in the case of the sulphate bath of Glasstone and Speakman⁽⁸⁵⁾. In an intermediate range of current density the cobalt in the alloy increased with current density. Deposition of the alloy at high current densities resulted in an impoverishment of the cathode diffusion layer mainly in cobalt ion, and caused the deposition to come under diffusion control.

At higher current densities (i.e. 2 - 6 A/dm²) a decrease in cobalt content takes place. This is due to depletion of cobalt ions in the cathode diffusion layer

causing the system to come under diffusion control.

5.2.2 Effect of Bath Temperature on the Composition of the Deposit.

Increasing the bath temperature of the cobalt-nickel alloy system, as with other alloy systems of the anomalous type, increases the diffusion rate of metal ions and replaces cobalt ions in the diffusion layer at a faster rate leading to an increase in cobalt content of the deposit. The relationship between current density and temperature is shown by Glasstone and Speakman⁽⁸⁵⁾. Their work using an acid sulphate bath containing 10% cobalt metal showed that if the current density was greater than 1.3 A/dm^2 the cobalt content of the deposit increased with increasing temperature, but at a current density of less than 0.3 A/dm^2 the opposite was the case. This behaviour is obviously very closely related to the change from normal to abnormal co-deposition associated with the current density.

5.2.3 Effect of the Metal Ratio of the Bath on Deposit Composition.

The effect of the metal ratio of the bath on the alloy content of the deposit from the anomalous co-deposition of cobalt-nickel has been investigated by numerous workers but the results obtained were all very similar. Piontelli et al^(87,90) using a sulphamate bath and Glasstone et al^(85,91) using a sulphate bath found that

a small percentage of cobalt present in the bath resulted in a high percentage of cobalt in the deposit. This effect is to be expected due to the anomalous nature of co-deposition (i.e. the less noble cobalt deposits preferentially).

The concentration of alloying element in induced co-deposition baths generally indicates that initially the baths behave in a similar manner to the anomalous type, in that low metal ion concentrations of the reluctant metal in the bath produce higher concentrations of reluctant metal in the deposit. They eventually reach a limiting value for the percentage alloying element present in the deposit.

5.2.4 Effect of the Total Metal Content of the Bath on Deposit Composition.

The total metal content of the bath has little effect on the composition of alloys of the anomalous co-deposition type. The work of Glasstone and Speakman⁽⁸⁵⁾ and Fink and Lah⁽⁹²⁾ show that in a simple sulphate bath for the deposition of cobalt-nickel alloys an increase in total metal content of approximately seven times produces only a slight increase in cobalt content of the deposit. The increase in concentration of the more readily deposited element in the deposit, with an increase in the total metal ion content of the bath is typical of diffusion controlled systems due to the



increased concentration gradient across the cathode film.

5.2.5 Effect of pH.

The effect of pH on the anomalous deposition of cobalt-nickel is that the cobalt content of the deposit increases slightly at low pH values. This has been reported by Glasstone and Speakman⁽⁸⁵⁾ when investigating the sulphate bath, and Piontelli and Patuzzi⁽⁸⁷⁾ when investigating the sulphamate bath. The largest increase in cobalt occurs below pH 2 - 3 and is accompanied by a decrease in cathode current efficiency. This effect was explained by Glasstone and Speakman⁽⁸⁵⁾ as being caused by disruption of the cathode film by hydrogen evolution due to the low cathode current efficiency experienced at these pH values.

5.2.6 Effect of Agitation on the Deposit.

Increase in agitation usually increases the proportion of the more noble metal in the deposit, thus offsetting the effect of an increase in current density. Fresh solution is transported to the cathode face by agitation and it decreases the thickness of the cathode film, consequently it offsets the normal tendency for more rapid depletion of the more noble metal in the cathode film. This effect is usually less pronounced when the metals are associated with complex ions than when they

are in the form of simple ions, and more pronounced when the two metals are associated with the same anion than when they are complexed by different anions.

5.2.7 Effect of Complexing Agents.

Although it is possible to produce nickel-cobalt alloys from complex baths there is little point in doing so as simple salt baths produce quite adequate results. Consequently work in this field is almost limited to the work of Sree and Rama Char⁽⁹³⁾ on the deposition of the alloys from a pyrophosphate bath containing ammonium citrate. The effect of the complexing agents on the bath was found to inhibit the deposition of cobalt with the result that the metal ratio of nickel-cobalt in the deposit was almost the same as in the bath over a wide range of current density. The effects of complexing agents on induced co-deposition have been studied with respect to neutral and alkaline baths.

5.3 Properties of Nickel-Cobalt Alloy Electrodeposits.

The properties of electrodeposited nickel are adequate for many engineering and electroforming applications where a tough, wear resistant surface with good corrosion resistance is required. The hardness may vary between 150 and 600 HV, or in exceptional cases a slightly higher figure. Some factors which influence hardness are current density, solution temperature and presence of addition agents. Higher hardnesses are obtained by the addition of organic compounds to the electrolyte⁽⁹⁴⁾.

Nickel-cobalt alloys have been studied extensively for magnetic applications. For engineering applications, alloying with cobalt hardens the nickel in a sulphur-free form that is not embrittled on heat-treatment. Using cobalt as a hardener instead of sulphur simplifies control. Moreover, the hard nickel-cobalt deposits are more ductile than those hardened by sulphur-containing additives.

Applications for nickel-cobalt alloy plating have been centred on electronic gear such as recording tapes, discs, and drums. Thus considerable data have been developed on magnetic properties. Such properties are critically dependent on solution formulation and operating conditions.

The operating conditions as mentioned before are the

current density, temperature of solution, pH, and agitation in the solution. In the case of the sulphate bath, modifications of these conditions greatly alter the composition of the alloy electroplate reported by Glasstone et al⁽⁸⁵⁾ and Fink et al⁽⁹²⁾; this also applies, though to a lesser extent, to the sulphamate bath claimed by Piontelli⁽⁹⁰⁾. However, in the case of the chloride bath, these result in only very slight changes in composition reported by Belt et al⁽⁴¹⁾. In a general way, it may be said that decreasing the current density, decreasing the pH, increasing the temperature, or increasing the agitation causes an increase in the cobalt content of the electrodeposited alloy. The easiest way to control the composition within relatively narrow limits is to use the chloride bath. For this type of bath the cathode efficiency is 88% or more. Deposits obtained from the chloride bath containing no brightening agents are often bright or semi-bright, and cross-sections show a banded structure, whereas only dull plates with a columnar structure are deposited from the sulphamate bath shown by Belt et al⁽⁴¹⁾. Alloy plate containing 45% Co and 55% Ni, deposited from a sulphate-chloride bath at pH4.0, showed a mixed fibrous and banded structure.

5.3.1 Hardness.

Previous investigators, Endicott⁽⁵⁰⁾ and Ericson,⁽⁹⁵⁾ have examined the influence of operating variables on nickel-cobalt alloy deposits produced from conventional

nickel sulphamate and concentrated (Ni-Speed) nickel sulphamate solutions containing cobalt. The results showed increases in hardness and tensile strength. Belt et al⁽⁸⁸⁾ reported an increase in hardness with increasing cobalt content to a maximum of 510 HV at a cobalt content of 35%. The actual hardness depends on the solution and conditions adopted for depositing the alloy.

A recent detailed study was made of the effect of cobalt additions to the Ni-speed solution by Wearmouth⁽⁹⁴⁾. The results showed the effect on deposit hardness of increasing the cobalt concentration in solution from 0 to 20 g/l or the cobalt content of the deposit from 0 to 80 percent. As the concentration of cobalt ions is progressively increased there is a steady increase in hardness up to a maximum of approximately 525 HV. The maximum hardness is obtained with a cobalt ion concentration in solution of 6 - 7 g/l, and a cobalt content in the deposit of 33 - 40%.

Kendrick⁽⁴¹⁾ reported that the addition of cobalt to nickel plating solutions increases the stress in the deposit, and therefore for electroforming applications cobalt can be used only with the Ni-speed solution, which under appropriate conditions can be operated to give compressively stressed deposits. At 33 - 40% cobalt the stress is too high to be able to exploit maximum hardness and therefore a somewhat lower hardness value, in the range 300 - 400 HV, has to be used.⁽⁹⁴⁾ The deposit stress

is also affected by solution temperature and current density⁽⁸⁸⁾.

Endicott et al⁽⁵⁰⁾ reported a maximum of 500 HV for an alloy containing 50% cobalt deposited from a sulphamate bromide bath.

Heat treating at 232 - 332°C had no effect on the hardness of nickel-cobalt alloys deposited in sulphamate-bromide baths⁽⁵⁰⁾, but a slight reduction in hardness was reported for a 300°C heat treatment of alloys deposited in sulphamate-chloride solutions⁽⁸⁸⁾. After heat treatment at 600 to 620°C, hardness of alloys from both baths decreased appreciably to values of 300 HV, or less⁽⁵⁰⁾⁽⁸⁸⁾. The nickel-cobalt alloy containing 25% cobalt, deposited from sulphate-chloride bath was found to have a hardness of 360 - 412 HV.⁽⁹²⁾

5.3.2 Tensile Strength and Ductility.

Tensile strength and ductility of electrodeposits may be of great importance to the performance of the plated article. They are important factors in determining the degree to which the plated article will resist stress corrosion cracking, this term includes any combined action of static tensile stress and corrosion which leads to failure by cracking, and it takes many forms. These properties also are important in preplated strip and wire. If the coating is lacking in strength and

ductility, it will fail during fabrication. The tensile properties of electrodeposited nickel-cobalt alloys obtained from sulphamate solution were investigated by Endicott, tensile strengths from 1.37 to 1.88 kN/mm² were reported⁽⁵⁰⁾ for alloys containing 40 to 50% cobalt. Ductility increased with decreasing cobalt content to values ranging from 2 to 4 percent elongation at 45% cobalt before heat treatment and 4 to 10% after heating at 630°C. The most ductile alloys, having elongations from 3 to 9% before heating and 8 to 22% after heating at 630°C, contained 20 to 30% cobalt, using sulphamate-bromide solution.

McFarlen⁽⁵⁶⁾ reported the tensile strength and yield strength of electrodeposited nickel-cobalt alloys containing 50% cobalt from a concentrated sulphamate bath as 1.76 - 1.88 kN/mm² and 1.24 kN/mm² respectively. In general, however, McFarlen⁽⁵⁶⁾ reported higher values of strength than those measured with deposits from concentrated sulphamate baths and reported by Wearmouth.⁽⁹⁴⁾ The values of UTS and elongation obtained at the annealing temperature of electrodeposited nickel-cobalt alloys from a concentrated sulphamate electrolyte reported by Belt et al⁽⁸⁸⁾ were lower than corresponding values measured at room temperature after annealing. UTS decreased rapidly with increase in heat treatment temperature and declined to a value of 0.1 kN/mm² after 17 hours at 600°C. Ductility values were also lower, but this time elongation reached a maximum at 400°C (1 hour and 17 hours) before

falling sharply at 500°C and 600°C, reaching 3% and 2% after one hour and 17 hours respectively at 600°C.

McFarlen⁽⁵⁶⁾ found that as the cobalt content of the alloy electrodeposited from sulphamate solution was raised, ultimate tensile strength reached a maximum of 1.9 kN/mm² at 38.5% cobalt. This value is similar to that at which maximum hardness was observed by Belt et al⁽⁴¹⁾ using concentrated nickel sulphamate electrolytes. He also found that strength, measured at room temperature, decreased with increase in the temperature of his four hour heat treatments.

The results of these investigations show that the hardness of deposits after a period of heating, measured either at room temperature or the heat treatment temperature, is always higher for nickel-cobalt alloys than for nickel. This finding applies over the temperature range 200 - 600°C, and for heat treatment times of 1 and 17 hours. The difference is often considerable: thus, the room temperature hardness of nickel 35% cobalt after 17 hours at 400°C is 382 HV, compared with the value 203 HV for unalloyed nickel similarly heat treated⁽⁸⁸⁾.

These observations suggest that nickel-cobalt deposits might be suitable as a hard coating in applications where service temperature, or even fabrication temperature, would lead to embrittlement of nickel hardened by means of sulphur-bearing addition agents. A second range of applications might lie in electroforming in those

instances where some internal stress can be accepted in exchange for sulphur-free hardening. A recent review by Bailey⁽¹²⁸⁾ of applications of electroforming in Europe drew attention to the possible application of nickel-cobalt for electroforming moulds for zinc-based alloy diecasting where the die must operate, in part at least, at elevated temperatures. Possible extensions of this application are moulds for aluminium and for glass. In order that the moulds may be electroformed with the necessary precision, however, it is necessary that deposit stress should be far lower than those previously reported by Belt et al⁽⁸⁸⁾. One way of lowering stress would be to add a stress reducer, but the addition agent used would have to be sulphur-free in order to preserve the desirable high temperature properties of the alloys.

For certain applications a sulphur-free stress reducing addition agent might be advantageous, since it would offer the possibility of achieving zero stress while depositing the hardest alloys of the nickel-cobalt system. However a process allowing production of relatively hard, low stress, nickel-cobalt alloy electroforms without addition agents is a desirable alternative, having the added attraction of freedom from addition agent breakdown products and associated problems of control.

Belt et al⁽⁸⁸⁾ reported the possibility of producing low stress nickel-cobalt alloy deposits with a surface

hardness in excess of 400 HV from concentrated sulphamate solution (600 g/l Nickel sulphamate; 10 g/l Nickel chloride) by careful selection and control of operating variables, in particular cobalt concentration in solution and cathode current density. A relatively high current density may be necessary in order to reduce total production time but it should be noted that increased current density caused increased tensile stress under practically all conditions in spite of the fact that the cobalt content usually fell.

5.3.3 Macrothrowing Power.

Alloy plating baths have been developed which have fairly good throwing power over a wide current density range. Since current density change can alter the composition of an alloy plate, there is a question of uniform plate composition associated with throwing power. Whenever the plate composition is critically dependent on current density, "the throwing power of composition" will be critical. Fortunately, alloy deposition baths can often be developed for which the current density range is wide enough to permit a good throwing power of composition over fairly irregular shapes. A knowledge of the current density effect on composition and current efficiency will give a good indication of expected throwing power, covering power, and plate composition uniformity over a surface for the particular type of bath being used.

The throwing power of the nickel-cobalt (Watts Bath) is somewhat improved by increase in pH, temperature and chloride content. At high current densities, the low pH of the bath is only slightly inferior to other formulations; and by increasing the chloride content sufficiently, the throwing power can be made superior to them⁽⁹⁶⁾. Belt et al⁽⁸⁸⁾ reported that the throwing power of the nickel-cobalt alloy obtained from concentrated "Ni-speed" (600 g/l nickel sulphamate solutions) containing cobalt was higher than that of conventional nickel sulphamate plating solutions.

As reported by Weisberg⁽⁹⁷⁾ in a study of nickel-cobalt alloy plating, the levelling power of the sulphate baths can be greatly enhanced by adding formic acid. The presence of cobalt corresponding to about 1% in the deposit produces better levelling than is obtained with nickel alone. The presence of chloride ions has two main effects, it assists anode corrosion and increases the diffusion coefficient of the metal ions thus permitting a higher limiting current density. An excessive amount of chloride should be avoided because this increases the magnitude of tensile stress in the deposit.

5.4 Structure.

The structure of an electrodeposit depends on the relative rates of formation of nuclei and the growth of existing ones. If the conditions favour the formation of fresh nuclei then fine-grained deposits are formed, while preferential growth of existing nuclei leads to the production of large-grained deposits. Usually fine-grained deposits are smoother, brighter, harder and less ductile than coarse-grained ones, although exceptions to this generalisation do occur.

In general, any change in the plating conditions that results in an increase in cathode polarisation leads to a reduction in grain size. An increase in current density causes a reduction of the metal ion concentration in the cathode film with a consequent increase in concentration overpotential and decrease in grain size. If other factors remain constant, an increase in the degree of agitation lowers the concentration overpotential and hence results in a larger grain size. An increase in temperature similarly leads to a reduction in cathode polarisation. The type of solution and its composition also influences the characteristics of the deposits. Cobalt alloy electrodeposits usually have a banded or fibrous structure.

A fibrous structure was obtained by Safranek⁽⁹⁸⁾ for cobalt alloy deposited from sulphamate solution containing

17 to 22% nickel. A banded structure was obtained for cobalt alloys containing 53 to 75% nickel by Endicott et al⁽⁵⁰⁾ and by McFarlen⁽⁵⁶⁾ using sulphamate solution

Heat treated nickel-cobalt alloy specimens obtained from a sulphamate bath revealed a fine-grained banded structure. A mixed fibrous and banded structure was detected in a nickel-cobalt alloy deposited from sulphate-chloride solution⁽²⁷⁾. A mixture of hexagonal-close packed and face-centred-cubic lattice structures has been observed by several investigators in the case of cobalt rich alloy electrodeposits, whereas the face-centred-cubic structure is characteristic of cobalt alloys containing more than 30% nickel as reported by Weil et al⁽⁹⁹⁾. Sree et al⁽⁹³⁾ have reported that alloys containing 14 to 72% cobalt, deposited from a pyrophosphate solution, had an fcc structure but that if the nickel content was below 14% then a c.p.h. structure occurred.

5.5 The Magnetic Properties of Alloys.

Over the past decade the growing importance of magnetic alloys for computer and telecommunication applications has focused attention on the electrodeposition of thin films of nickel, cobalt, iron and their alloys. The relative ease with which these metals can be codeposited in alloy form from aqueous solutions of their salts and the controllability of the alloy composition and hence magnetic properties by change of concentration, makes electrodeposition a most attractive technique.

The magnetic properties of the electrodeposited film depend, as expected, on its composition, pH, solution additives, temperature and all the usual known and unknown foibles of normal plating techniques. For the sake of clarity it is proposed to deal with the coating normally applied to peripheral storage systems followed by the thinner coatings applied for high-speed computer magnetic film memories.

The achievement of controlled magnetic properties was a great challenge to the electrodepositor whose main preoccupation had probably been bounded by porosity, thickness, speed of application, brightness, hardness or corrosion resistance⁽¹⁰⁰⁾.

5.5.1 Properties of the Magnetic Materials.

Magnetic coatings for computer systems are important for both static and dynamic switching. Hard magnetic coatings with a high coercive force above 200 oersteds are needed for high-density permanent storage (typically on drums or discs), whereas soft magnetic coatings with a coercivity of only about 2 oersteds are desired for fast switching memory devices. Thus coercivity is an important property of cobalt and cobalt alloy coatings intended for computer systems.

Coercivity of a coating is dependent on the crystalline structure, thickness and composition of the material. For cobalt, increasing thickness usually reduces coercivity. A hexagonal-close-packed structure appears to favour high coercivity in comparison with a mixture of hexagonal and face-centred-cubic structures. Buffering agents and stress reducers have profound effects on the crystalline structure and magnetic properties of electro-deposited cobalt. Temperature, pH, and current density also affect the magnetic properties.

Low coercive forces of 9 to 12 oersteds have been reported by Fisher⁽⁵⁵⁾ for 7 μm thick deposits obtained at a current density of 1.6 A/dm² in a 25°C, dilute cobalt chloride solution containing 0.5 to 1.6 g/l saccharin added to reduce stress.

Cobalt alloy electrodeposits containing 10% chromium from a sulphate bath showed coercivities < 50 as reported by Safranek⁽⁹⁸⁾. Wolf⁽¹⁰¹⁾ reported lower coercivities < 7 for cobalt alloy electrodeposits 64% nickel - 14% iron obtained from a sulphate-chloride solution.

Cobalt alloy containing only 5% phosphorus obtained from a chloride bath exhibited relatively higher coercivities 600 - 850 oersteds as reported by Bondar⁽¹⁰²⁾. Bate et al⁽¹⁰³⁾ reported that higher coercivities of 1400 to 1750 oersteds were obtained for cobalt alloys containing 19% nickel plus 2% or 3% phosphorus obtained from a sulphate bath.

Magnetic properties have been mentioned briefly for completion but will not be investigated in the present project.

CHAPTER SIX

6. NICKEL-IRON ALLOY ELECTRODEPOSITION.

Magnetic recording and switching applications have been the principal stimuli for research on electrodeposition of nickel-iron alloys. Particular interest leans toward optimizing the magnetic properties of thin films. Many researchers have investigated the reduction of internal stress by adding organic compounds to the plating bath, although one report indicates the beneficial effect of ultrasonic agitation⁽¹⁰⁴⁾. Saccharin is the most widely used additive for reducing stress in nickel-iron alloys.

Nickel-iron alloys have been deposited from a variety of plating baths. Brenner⁽⁴⁷⁾ has discussed the deposition of these alloys from simple salts as well as from complexes variously based on cyanide, alkali, pyrophosphate, amino acids, hydroxy acids and ammoniacal solutions.

Much of the attraction of bright nickel-iron alloy deposition is directly related to the significant metal cost savings which can be achieved. The economic aspects are not the only inducements, there are distinct process advantages as compared to conventional bright nickel processes. This is true when plating on steel since, any iron which is accidentally introduced into the solution from the parts themselves is readily dissolved and co-deposited. The acceptance of the decorative alloy

electrodeposit is broadly illustrated by the great diversity of products now being plated with bright nickel-iron coatings and overplated with a chromium deposit. Current applications include kitchen and bathroom ware, tubular furniture and jewellery⁽¹⁰⁵⁾. However, concern for the usefulness of these alloy deposits is justified because the corrosion potentials of the nickel-iron alloys lie between those of nickel and of iron, the former being more cathodic to steel. Comparative corrosion results from salt-spray, humidity, and static industrial exposure test programmes for various coatings which included nickel, nickel-cobalt and nickel-iron has been discussed in the literature^(106,107). As most tests were performed on alloy deposits without a final chromium layer, this data is of limited use for decorative and protective applications. Subsequent corrosion tests^(105,108) on nickel-iron alloys have been directly related to decorative coating systems. These coating are generally described as suitable for moderate or dry exposure conditions as outlined in Service Condition 2 and 1 in ASTM Standard B.456.

Despite numerous advertisements, in a variety of trade journals^(109,110) extolling the benefits of nickel-iron alloys for decorative applications, published corrosion data remains scarce on nickel-iron coating systems suitable for outdoor applications, that is, meeting the requirements of Service Conditions 3 and 4 in ASTM B.456. Two papers outlining corrosion potential

studies of nickel and of nickel-iron alloy deposits containing up to 41% iron have been published^(105,108). Although potentials were measured in different solutions and the values showed experimental scatter, the overall results are not unexpected. As the iron content of the alloy increases, the potential of the alloy becomes more negative; i.e. the alloy becomes more base.

6.1 The Decorative Bright Nickel-Iron Process.

Bright nickel-iron alloy deposits can be produced which are comparable to 100% nickel deposits in brightness, levelling and ductility⁽¹¹¹⁾. Decorative nickel-iron alloy electrodeposits have been established as a practical, viable finish in the USA for almost eight years since a paper by Clause and Tremmel⁽¹¹²⁾ first described such a process in 1973. During the past four years, solutions for electroplating the bright, levelling alloy have reached a volume of nearly 3,800,000 litres in the USA alone⁽¹¹³⁾. A large number of solution systems capable of depositing such coatings have been developed and they all utilise one or more salts of nickel, one or more salts of iron and a complexing agent.

There are two different types of process; one uses an electrolyte of conventional strength and a chemical reducing stabiliser to maintain a high concentration of iron in the ferrous state, whereas the other employs a solution of about half the strength of a standard nickel plating bath and a special complexant which ties up any ferric iron, which, under normal operating conditions, should not exceed 20% of the total iron in solution. As the latter type is more widely established in the U.K., where virtually all plating baths operate on the lower strength, ferric-complexed system, the following discussion will therefore be confined to this type of operation.

6.2 Development of Nickel-Iron Plating Solutions.

The main problem in the deposition of a nickel-iron alloy is that iron exists in such an environment as two species; ferrous Fe^{2+} and ferric Fe^{3+} . As ferric ion forms insoluble hydroxides in solutions above a pH of 2.5 , it is necessary to develop a bath which can operate either without the formation of ferric ion or, if formed, prevent the precipitation of the insoluble hydroxide. In addition the solution formulation must also permit the effective use of addition agents in order to achieve bright, levelled and ductile alloy deposits.

Numerous well documented compounds may be used to stabilise both ferrous and ferric ions so that the hydroxide does not form. However, many of these are either unstable in the type of plating solutions needed to produce bright, ductile, levelled deposits or react unfavourably to the passage of current due to the chemical reaction with hydrogen and oxygen which are produced at the electrodes.

6.3 Corrosion Behaviour of Nickel-Iron Electrodeposition.

Nickel-iron electrodeposition has been extensively evaluated as a decorative protective coating. The alloy can be used as a replacement for bright nickel in many mild and moderate exposure conditions as outlined in Service Conditions 2 and 1 in the ASTM Standard B.456. Within the last four years, considerable corrosion testing has been undertaken on nickel-iron deposits in severe corrosive conditions to evaluate their suitability for various applications.

These include products such as bicycle parts, marine work and automotive components, that is, meeting the requirements of Service Conditions 3 and 4 in the ASTM B.456. The significant difference between nickel and nickel-iron observed in these severe conditions was the tendency for the alloy deposit to develop a brown corrosion stain. It has been reported that there is no apparent stain in nickel-iron deposits containing less than 13% iron. As a result of this observation a multilayer deposit has been developed. It consists of a top layer having a lower iron content than the thicker lower layer. This can be achieved using either, two solutions that produce alloys of differing iron content, or a single solution with different degrees of agitation. The results from corrosion tests exploiting such coatings are reported in the paper by Tremmel⁽¹¹¹⁾.

The static tests showed that an undercoat of copper is important in increasing the protective value of the plating system. The mobile tests showed that the components plated with the alloy deposit were equal or superior to the equivalent components plated with nickel.

6.4 Plating Baths.

6.4.1 Solution Composition.

The preferred solution composition for the electro-deposition of nickel-iron is dilute (37 g/l) total nickel metal, compared with conventional nickel which contains 81 g/l of nickel metal.

Commercial Nickel-Iron Solution Compositions

	g/l		
	UDYLITE	CANNINGS	PERMALITE
$\text{NiSO}_4 \cdot 7\text{H}_2\text{O}$	49-105	150	60-110
$\text{NiCl}_2 \cdot 6\text{H}_2\text{O}$	47-100	60-70	60-110
$\text{FeSO}_4 \cdot 7\text{H}_2\text{O}$	10-18	12.5	8-16
H_3BO_3	45	45	30-45
Stabilizer	15-35	25	10-30

Typical examples of base solutions as supplied by three companies.

The lower concentration of nickel salts allows the deposition of high iron alloy deposits without the need for maintaining an excessively high iron concentration in the solution, as well as minimising the stabilizer requirements. Essentially the salts function in the same manner as they do in bright nickel plating baths, the nickel sulphate acts as a source of metal ions, the chloride promotes anode dissolution and increases

plating speed, and the boric acid serves as a buffer.

6.4.2 Oxidation States of Iron in Plating Baths.

Although the iron is always introduced into the bath as the ferrous ion, a portion of it will normally be oxidised to the ferric ion. The relative concentrations of ferrous and ferric ions influence some characteristics of the deposit. Generally, to avoid adverse effects on levelling, ductility and cathode efficiency, it is desirable that the ferric ion concentration should not exceed 60% of the total iron. A high percentage of ferrous iron is maintained in solution, by controlling the pH and by ensuring that there is always an adequate area of nickel anodes to prevent polarisation. Ferric iron is, in any case, constantly being reduced to the ferrous state during electrolysis, by virtue of the strongly reducing environment at the cathode. Thus under normal operating conditions, the ferric ion concentration will not exceed 20% of the total iron in solution.

Plating solutions with a ferric content of less than 5% retain the clear green colour characteristic of conventional nickel baths, whereas solutions containing much ferric iron tend to a slate-grey green, and the depth of this colour forms a useful instant indication of the general state of the bath.

6.4.3 Addition Agents.

The addition agents which function most effectively in an iron-nickel alloy solution have some similarity to those which function in bright nickel solutions, as well as having some important differences. For example, primary brighteners are not effective once the iron content of the deposit exceeds about 10%. Furthermore, even the brightener compounds, such as saccharin and certain aromatic sulphonamides are only useful up to a maximum of 45% of iron in the alloy deposit. Alloys higher in iron become brittle and highly stressed, and have little value. Many secondary brighteners, such as quarternary amines, nitriles, and some unsaturated compounds have limited value in a nickel-iron solution. However, primary and secondary acetylenic alcohols are quite effective although, in the presence of a stabilizer, they may function at different concentrations or in different combinations as compared to regular bright nickel.

An addition of 1 g/l saccharin to the solution, a current density 80 A/dm^2 at a 50°C , and ultrasonic agitation at 22 kHz with sufficient intensity to cause cavitation are reported capable of giving deposition of a stress-free nickel-iron alloy⁽¹¹⁴⁾.

6.4.4 Operating Parameters.

The operating pH for various commercial nickel-iron baths lies in the range of 2.8 - 4.2. Higher pH values tend to favour the formation of undesirable ferric ions accompanied by a gradual loss of brightness and ductility, whereas a lower pH reduces cathode efficiency and prevents the organic brightening compounds from functioning properly. Although the solution is much more dilute in metal salts than is usual, it nonetheless may be operated within the current density range 1.0 to 8.5 A/dm², the same as commonly used for bright nickel plating. Voltage requirements to maintain the recommended current density are the same or slightly higher than for normal bright nickel solutions.

The iron content of the alloy deposits is changed by the type, and to a lesser extent the degree of agitation. The use of agitation is encouraged for several reasons:

- (I) It permits the utilisation of higher average current densities.
- (II) It allows low concentrations of iron in solution while resulting in high iron content in the deposit.

A cathode rod agitated solution needs about twice as much iron in solution as an air agitated bath in order to produce the same alloy composition. With air, the degree of vigour has allowed the deposition of a variable composition deposit usually having an iron content of

about 30% by weight as a first layer onto which is plated a second nickel-iron layer containing from 5 to 14% iron⁽¹¹⁵⁾.

Agitation should be fairly mild, as unnecessarily vigorous air agitation increases the tendency for the oxidation of iron. The air should be directed towards the cathode to give maximum impingement on the work surfaces whilst leaving the solution largely undisturbed in the vicinity of the anodes.

6.4.5 Properties of the Bath.

When the correct stabilizer is used the nickel-iron process is claimed to be no more susceptible to contamination than a modern bright nickel. Common impurities such as copper and zinc can be readily removed by plating out, zinc being removed most readily at higher pH values.

The cathode efficiency of nickel-iron plating baths usually exceeds 90% and is primarily dependent upon three factors, temperature, ferric ion concentration, and organic impurities. Since the nickel-iron solutions are more dilute than conventional nickel baths their efficiencies are very temperature dependent. Normally, no major loss of efficiency occurs until the temperature falls below about 55°C.

An increase in ferric ion concentration lowers the cathode efficiency. However, high ferric ion levels are rarely ever attained whereby a noticeable loss of cathode efficiency can be observed.

6.4.6 Structure.

Fedorova⁽¹¹⁷⁾ has shown that iron alloys containing 8 to 18% nickel exhibit a body-centred-cubic lattice structure, whereas alloys containing 31% nickel consist of mixed face-centred-cubic and body-centred-cubic structures. With 52 to 80% nickel, only the face-centred-cubic structure was detected. She has examined, by X-ray diffraction, the structures of nickel-iron alloys containing 9 to 86% nickel electrodeposited from sulphate-citrate solutions. Alloys containing 82 and 91% iron crystallised with a bcc lattice while those containing 14, 36 and 48% iron had an fcc lattice. The alloy containing 69% iron was a mixture of bcc and fcc⁽¹¹⁷⁾. Lamellar microtextures were reported by Levy⁽¹¹⁶⁾ for high-strength alloys containing 25 to 50% iron deposited from a chloride-sulphate solution with or without sodium 1,3,6-naphthalene sulphonate as a stress reducer.

6.4.7 Properties of Electrodeposited Nickel-Iron.

The properties of the decorative alloy deposits are similar to those of bright nickel in some respects and quite different in others. Although the levelling of

nickel-iron alloy deposits is comparable to bright nickel plate, the factors which effect its ability to smooth out surface irregularities are numerous. Obviously the addition agent system must be compatible with a particular compound used to stabilize or complex the ferrous and ferric ions. Furthermore, other factors such as temperature, pH, ferric ion concentration, and alloy composition can have a notable effect on levelling.

The amount of iron co-deposited effects levelling in that as the iron in the alloy increases, levelling decreases⁽¹⁰⁵⁾. The throwing power of the process is at any iron content similar to that of a Watts nickel.

Generally, such factors as hardness, ductility and internal stress of alloy deposits are functions of alloy composition, brightener concentration, pH and temperature. These alloy deposits are significantly more stressed than bright nickel deposits.

Nickel alloy deposits containing 25 to 40% iron are about equal in strength to nickel alloys containing 40 to 50% cobalt, but harder than nickel alloys of cobalt or tungsten reported by Endicott⁽⁵⁰⁾ and McFarlen⁽⁵⁶⁾.

Levy⁽¹¹⁶⁾ reported that an ultimate tensile strength of 1.37 kN/mm^2 and elongation of 2 - 3% were obtained for nickel alloys containing 15 to 60% iron deposited in a chloride-sulphate bath containing 7.5 g/l sodium 1,3,5-

naphthalene trisulphonate as a stress reducer. The nickel-iron deposit possesses quite strong magnetic characteristics.

Particular emphasis has been placed on the deposition of alloys of the permalloy type, 80%Ni-20% Fe, due to their low coercivity and high permeability, hence their name of Permalloy. These have very rapid response, allowing very short switching times for data storage as shown by Levy⁽¹¹⁶⁾.

A citrate-complexed bath which can produce nickel-iron films of varying thickness with properties comparable to films made by vacuum deposition has been reported by Venkatasetty⁽¹¹⁸⁾. The bath has a higher plating efficiency and longer useful life, and the process has a higher degree of reproducibility than the sulphate bath.

CHAPTER SEVEN

7. EXPERIMENTAL PROCEDURE.

7.1 Equipment.

The apparatus which was used for electroplating was as follows:-

1. The plating cell consisted of a plastic tank of volume 10 litres. This was a suitable size to enable it to fit into the ultrasonic tank unit. The cathode panel 10 cm x 5 cm was clamped mid-way between the two anodes placed at either end of the bath. The cathode together with the anodes were submerged completely into the solution and the cell was covered with a plastic lid. A three-phase rectified D.C. supply was used. Two series of experiments were carried out, one using ultrasonic agitation and the other using air agitation.

2. The ultrasonic equipment consisted of two main parts:

A) The frequency generator which gave a maximum output of 350 watts per transducer at a frequency of 13 kHz. The transducers could be tuned and the output power varied.

B) The tank unit shown in Fig.(4) which consisted of a free standing container housing two magneto-strictive transducers fixed in the bottom of a stainless steel

tank. Ledges were provided inside the tank to enable the use of a sheet of stainless steel as a platform on which to stand the plating cell. It was assumed that a 15% power loss occurred as described in section (9.1).

The plating cell was immersed to approximately $\frac{3}{4}$ of its height in the ultrasonic tank containing water.



Fig.(4) The power unit and ultrasonic tank.

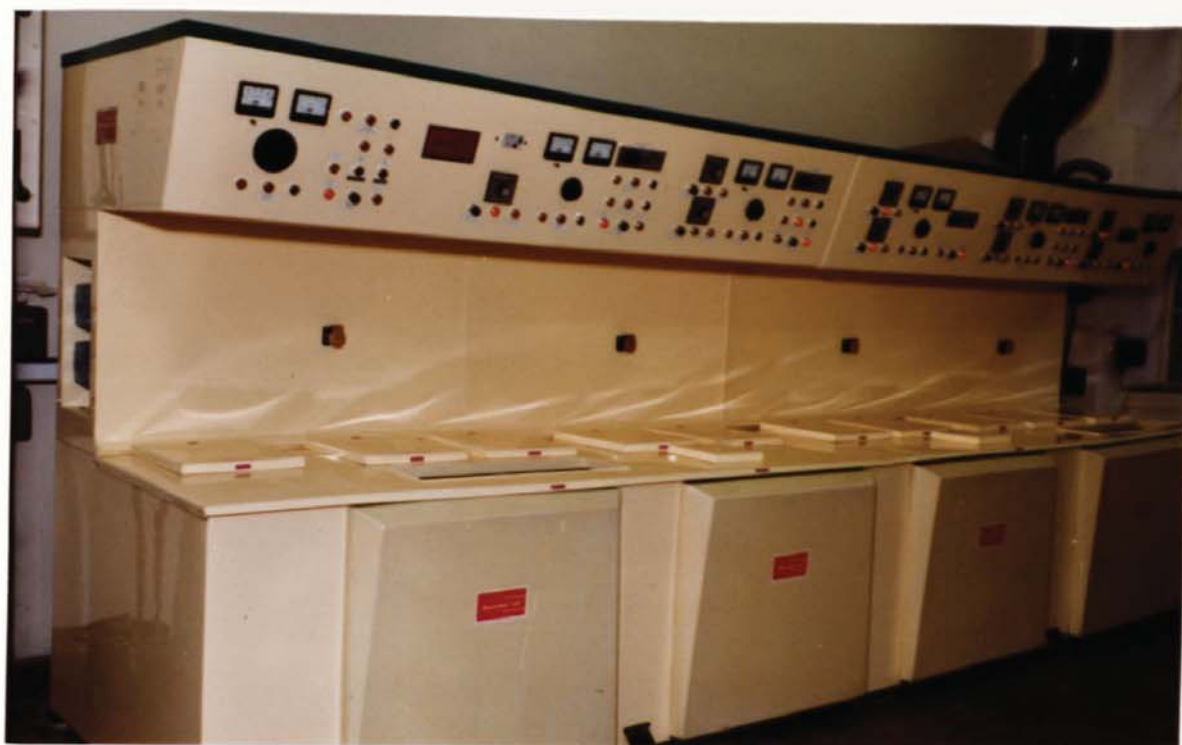


Fig.(5) The Electroplating Plant.

7.2 Electroplating Procedure.

The 10 cm x 5 cm flat mild steel panels were plated in nickel, cobalt, nickel-cobalt and nickel-iron solutions in the plastic cell using ultrasonic agitation. The air agitated nickel, cobalt and nickel-cobalt panels were also plated in the same cell but the air agitated nickel-iron samples were plated in a 55ℓ tank as described in section (7.2.5)

The pre-electroplating cleaning sequence employed was as shown below and all these operations were undertaken in the plating plant illustrated in Fig.(5).

Cleaning sequence.

1. Clean in acetone for three minutes.
2. Anodic treatment in hot commercial alkaline solution, 4 A/dm^2 , 70°C for three minutes.
3. Swill in running water.
4. Dip in 50% HCl for 30 seconds.
5. Swill in running water.
6. Anodic treatment in cyanide solution, 4 A/dm^2 at room temperature for 2 minutes.
7. Swill in running water.
8. Dip in sulphuric acid solution, 20% v/o concentrated acid for 30 seconds.
9. Rinse in water.
10. Electroplate at appropriate conditions.

Most panels were plated at 4 A/dm^2 for 40 minutes and the rest at 8 A/dm^2 for 20 minutes. These panels were used for hardness determination, the study of surface topography and analysis.

7.2.1 Plating of Hounsfield Test Pieces.

Flat brass strip-type Hounsfield test pieces were plated in both alloy plating solutions in the 10ℓ tank. Both modes of agitation were used and all samples were plated for 40 minutes at 4 A/dm^2 . The cleaning sequence employed is shown below.

Cleaning sequence.

- 1) Soak in acetone for three minutes.
- 2) Polish surface with 100 grit wet emery paper.
- 3) Swill in running water, dry.
- 4) Polish surface with 600 grit wet emery paper.
- 5) Swill in running water, dry.
- 6) Polish surface with 1200 grit wet emery paper.
- 7) Swill in running water.
- 8) Polish using Brasso.
- 9) Water swill.
- 10) Soak in acetone for 2 minutes.
- 11) Soak in commercial alkaline cleaner for 2 minutes at temperature 70°C .
- 12) Water swill.
- 13) Cathodic clean in a commercial cyanide solution for two minutes, 4 A/dm^2 at room temperature.

- 14) Swill in running water.
- 15) Dip in sulphuric acid solution, 20% v/o for 30 sec.
- 16) Rinse in water.
- 17) Electroplate.

7.2.2 Nickel Solution.

The solution used for the electrodeposition of nickel was based on the Watts bath (sulphate/chloride solution).

The plating solution consisted of:-

Constituents		g/l
Nickel Sulphate	$\text{NiSO}_4 \cdot 7\text{H}_2\text{O}$	290
Nickel Chloride	$\text{NiCl}_2 \cdot 6\text{H}_2\text{O}$	40
Boric acid	H_3BO_3	40

Plating conditions were:-

pH	4
temperature	55-60°C

The solution was purified before use by treating with 20 g/l activated carbon to remove organic impurities and by plating at low current density ($0.5 - 1.0 \text{ A/dm}^2$) for several hours to remove metallic contamination.

The electrodeposits obtained from this bath proved to be ductile and low stressed, using either air or ultrasonic agitation.

7.2.3 Cobalt Solution.

The bath used for the electrodeposition of cobalt was based on the Watts nickel type bath, that is the nickel content was replaced by cobalt salts. The solution composition was as follows:-

Constituents		g/l
Cobaltous sulphate	$\text{CoSO}_4 \cdot 7\text{H}_2\text{O}$	300
Cobaltous chloride	$\text{CoCl}_2 \cdot 6\text{H}_2\text{O}$	45
Boric acid	H_3BO_3	30

The plating conditions were:

pH	4
temperature	55°C

The electrodeposits obtained from this concentrated cobalt bath proved to be very brittle and stressed using either air or ultrasonic agitation. In an attempt to improve the quality of the cobalt deposit a solution of half the above strength was prepared with a pH of 3.5. The deposits obtained from this solution were relatively ductile, had a lower stress and a bright appearance using both air and ultrasonic agitation. Consequently this dilute bath was used for all the experimental work reported.

7.2.4 Nickel-Cobalt Sulphate/Chloride Bath.

The mixed sulphate/chloride bath for the deposition of nickel-cobalt is well known, being based on the Watts nickel bath. The alloy plating bath was prepared by adding the appropriate quantity of cobaltous sulphate solution to a Watts type nickel solution containing $\text{NiSO}_4 \cdot 7\text{H}_2\text{O}$, NaCl and H_3BO_3 . The solution was purified before use by treating with 20 g/l activated carbon to remove organic impurity and then by plating at low current density ($0.5 - 1.0 \text{ A/dm}^2$) for several hours to remove metallic contamination. The solution chosen for the initial work was a nickel-cobalt alloy plating solution consisting of:-

Nickel sulphate	$\text{NiSO}_4 \cdot 7\text{H}_2\text{O}$	290 g/l
Nickel chloride	$\text{NiCl}_2 \cdot 6\text{H}_2\text{O}$	40 g/l
Cobalt sulphate	$\text{CoSO}_4 \cdot 7\text{H}_2\text{O}$	10 g/l
Boric acid	H_3BO_3	40 g/l.

The operating conditions chosen when plating flat mild steels were:-

pH	4
temperature	$50-60^\circ\text{C}$.

Solution density 1.18 g/cm^3 at room temperature.

Rolled nickel anodes were used and the concentration of cobalt in the solution was maintained by addition of cobalt sulphate.

In order to vary the cobalt content of deposits, further plating solutions were prepared having 35; 60; 85 and 110 g/l cobaltous sulphate.

7.2.5 Nickel-Iron Solution.

A proprietary bright-levelling nickel-iron solution was prepared as recommended by the manufacturers. The solution produced a bright reflective deposit with excellent levelling, low stress and good ductility for a fully bright deposit.

The solution chosen for the work was a nickel-iron alloy plating solution consisting of:-

Constituents		g/l
Nickel Sulphate	$\text{NiSO}_4 \cdot 7\text{H}_2\text{O}$	130
Nickel Chloride	$\text{NiCl}_2 \cdot 6\text{H}_2\text{O}$	100
Boric acid	H_3BO_3	40
Ferrous sulphate	$\text{FeSO}_4 \cdot 7\text{H}_2\text{O}$	12.5
Complexing agent		20
Saccharin		2
Initial brightener*	(Wetting agent, saccharin leveller and brightener)	10 ml/l

* Proprietary solution.

In addition to the standard steel panels plated in the 10 l cell, as described in section (9.2), nickel-iron solution in a 55 l tank of the main plating plant was used to electrodeposit nickel-iron alloys onto flat mild steel panels 10 cm x 7.5 cm using vigorous air agitation.

Plating conditions were as follows:-

pH	4
temperature	68°C
current density	4 and 8 A/dm ²

The reason for plating in this tank rather than the 10 l one was to keep the solution in optimum working condition. Not only was it possible to keep the metal ion concentration constant but by regular plating it was possible to prevent excessive formation of ferric iron. These electroplated panels were used for hardness tests, analysis, surface topography and x-ray structural analysis.

7.2.5.1 Plating Conditions.

7.2.5.1.1 pH Value.

The pH value of this solution was maintained within the range 3.8 - 4.2, this range was dictated by the need to keep the trivalent iron at a low level, since a high rate of formation of Fe^{+3} was favoured by high operating pH. If the pH fell below 3.8 levelling was reduced.

Nickel carbonate was used to raise the pH to its recommended value. If the pH rose above 4.2 there was a loss of brightness in the low current density areas and the ductility was reduced. The pH was lowered to the recommended value when necessary using dilute 20 v/o sulphuric acid. A Phillips digital pH meter was used for the pH measurement.

7.2.5.1.2 Temperature.

The solution temperature was maintained between 63°C and 70°C. At temperatures below 63°C there was a reduction in brightness, levelling and cathode current efficiency. Temperatures above 70°C caused harmful degradation products to form as a result of stabilizer breakdown.

7.2.5.1.3 Cathode Current Density.

Although the solution was much more dilute in metal salts than is usual it nonetheless was operated within the current density range 1 to 8.5 A/dm². For normal operations the usual current density range was 4 to 8 A/dm², but higher current densities were possible when using ultrasonic agitation.

7.2.5.1.4 Density.

The density of the solution was 1.14 - 1.155 g/cm³ at 65°C.

7.2.5.2 Maintenance of the Bath.

The iron was present in the bath as ferrous (Fe^{+2}) and ferric (Fe^{+3}) ions. It was important that the ferric iron concentration did not exceed 40% of the total iron concentration in the bath otherwise, loss of ductility and cathode current efficiency resulted. If the bath was operated at pH values higher than recommended, the ferric iron concentration had a tendency to rise. Under normal operating conditions, the ferric ion concentration did not exceed 20% of the total iron in solution because ferric iron is constantly being reduced to ferrous at the cathode as discussed in section (6.4.2).

7.2.5.2.1 Brightener Additions.

The brightening and levelling properties of the solution were maintained by regular additions of a single maintenance brightener at the rate of 500 ml. per 1000 Ah of operation.

7.2.5.2.2 Anti-pit Agents (Wetting Agents).

Maintenance additions of wetting agent were added as necessary to prevent pitting.

7.2.5.3 Anodes.

Nickel-iron alloy (75% Ni - 25% Fe) in granular form was contained in a titanium anode basket. This was enclosed in a well washed cotton anode bag. An alternative system using the individual metals as anode can be employed. In this case the iron should be of a suitably pure grade containing less than 0.15% total impurities (usually C, Si and Mn) and nickel of the sulphur activated type is generally preferred.

7.2.6 Evaluation of Plating Deposits.

As the aim of the project was to investigate the effect of the ultrasonic agitation on the deposition of the nickel-cobalt and nickel-iron alloys, the individual experiments were designed to compare the results of ultrasonic agitation with vigorous air agitation. Specimens were plated using air agitation and then similar ones were produced using ultrasonic agitation. Hardness, tensile strength, ductility, structure, early stages of growth, analysis, cathode current efficiency, limiting current density and macrothrowing power were studied.

7.2.6.1 Hardness.

The hardness of electrodeposits was measured using the micro-hardness (Vickers photoplan) tester. Samples for hardness tests were cut from the centre of the plated mild steel panels. They were mounted in conducting bakelite. The specimens were polished using a Vibromet polisher. They were left for three days in the polisher in order to ensure a suitable flat surface for the tests and etched in a 50/50 v/o mixture of concentrated nitric and acetic acids, in order to distinguish between the coating and substrate.

Hardness tests were then carried out on mounted cross sections of the deposits using a load of 20 g. Ten readings were taken from each sample and the average calculated.

7.2.6.2 Tensile Tests.

The widths and thicknesses of specimens were measured before and after plating. A nominal 5 cm gauge length was scribed on them and the edges chamfered to remove the thick coating from these high current density regions so that premature edge cracking did not occur. The exact distance between the scribed crosses was measured accurately by a Vernier travelling microscope. The specimens were fixed into the grips of a Hounsfield tensometer and the strain applied manually. Elongation

and load were recorded. An initial measurement was taken shortly after the appearance of small cracks or other tiny defects in the deposit. The test piece was unloaded and the permanent elongation of the gauge length measured together with the applied load. The specimen was reloaded and extended until final failure occurred. The final elongation was calculated and the maximum load recorded on the moving drum chart was noted. Triplicate results were obtained in all cases.

7.2.6.3 Structure and Surface Topography.

The structures of the deposits were examined by high resolution Transmission Electron Microscopy (model - Jem 100B) Fig.(6); Philips X-ray diffractometer and X-ray texture goniometer. Surface topography was studied using a scanning electron microscope (model - Cambridge-150), illustrated in Fig.(7).

7.2.6.3.1 Transmission Electron Microscopy (T.E.M.)

Thin foils were prepared by electroplating from cobalt, nickel-cobalt and nickel-iron solutions on to stainless steel panels using both air and ultrasonic agitation. The stainless steel panels were used in order to facilitate the removal of the electrodeposit. Samples were taken from the foils and thinned using a Struers Polipower jet-polisher, illustrated in Fig.(8). A solution of 5% Perchloric acid and 2-Butoxyethanol. The object was to

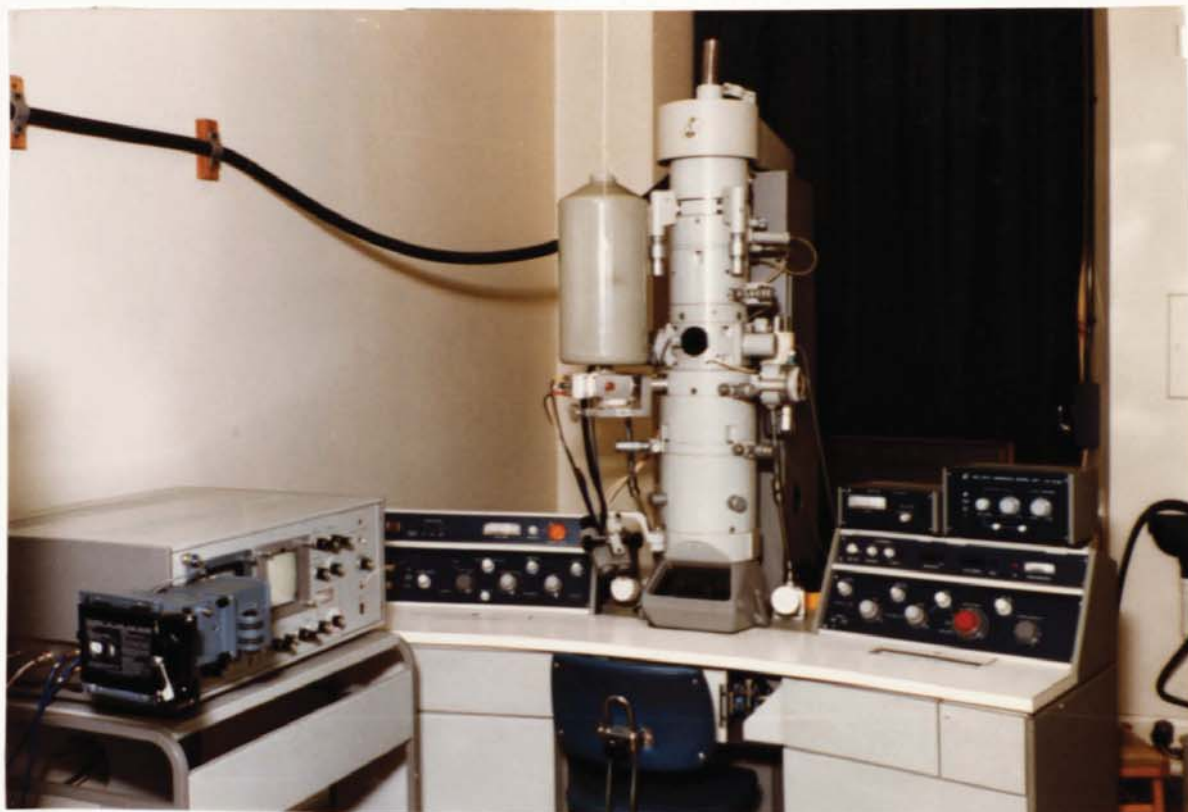


Fig.(6) High resolution Transmission
Electron Microscope Model Jem 100B.





Fig.(7) Scanning Electron Microscope
Model Cambridge - 150.

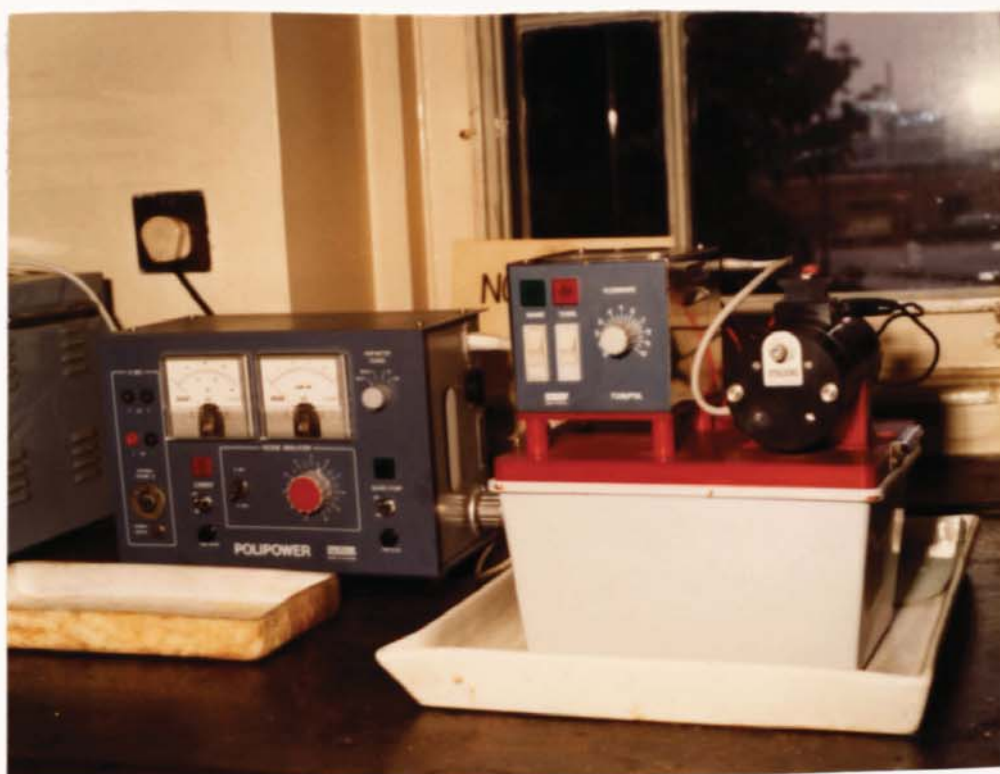


Fig.(8) Struers Polipower jet-polisher.

produce a large area of specimen transparent to the electron beam.

7.2.6.3.2 Scanning Electron Microscopy (S.E.M.)

The surface topography of a selection of the electroplated deposits of nickel-cobalt and nickel-iron was examined using the scanning electron microscope.

Specimens 1 cm x 1 cm were cut from the plated panels, mounted on stubs in the usual manner and viewed directly.

7.2.6.3.3 X-Ray Diffractometer.

Attempts were made to study the structure of nickel-cobalt and nickel-iron electrodeposits by using an x-ray diffractometer, illustrated in Fig.(9). Samples were selected from electrodeposits produced by using air and ultrasonic agitation. Samples, 2 cm x 2 cm, were cut from the plated steel panels so that they would fit into the diffractometer. Traces were carried out using a cobalt K α source. Where the most intense peaks occurred, the 2θ angles were noted and using Bragg's law, $n\lambda = 2d \sin\theta$, the (d) spacings were calculated. These lattice spacings were subsequently used to index the traces using the x-ray diffraction powder file.

7.2.6.3.4 X-Ray Texture Goniometer.

The specimens used in this investigation were 5 mm x 5 mm



Fig.(9) Philips X-Ray diffractometer.

and were again cut from the plated steel panels. It was essential to ensure that the deposit thickness was greater than 0.12 mm so that it would not be penetrated by the x-ray beam. Schulz reflection method was used. The x-ray texture goniometer employed is shown in Fig.(10a, b).

7.2.6.3.5 Progressive Growth of Nickel-Cobalt Alloys.

The early fundamental investigation on the nucleation and growth of electrodeposits was confined to the deposition of nickel-cobalt alloys obtained from sulphate/chloride solution (10 g/l $\text{CoSO}_4 \cdot 7\text{H}_2\text{O}$ and 110 g/l). Deposition was carried out on "gold seal^{*}" steel panels. The surface topography of nickel-cobalt electrodeposits obtained from the above solutions at various time intervals of 1, 5, 10 and 15 minutes were studied using the replica technique. The plating conditions employed were pH4, current density 4 A/dm^2 , and temperature $50 - 55^\circ\text{C}$, using either air or ultrasonic agitation.

Preparation of replicas.

Thin, electron transparent, replicas of electrodeposit surfaces were produced using a two stage plastic/carbon replica technique. This involved coating the prepared metal surface with a layer of nitrocellulose dissolved

* Proprietary product of Pyrene Ltd.



Fig.(10)(a) The Texture Goniometer.

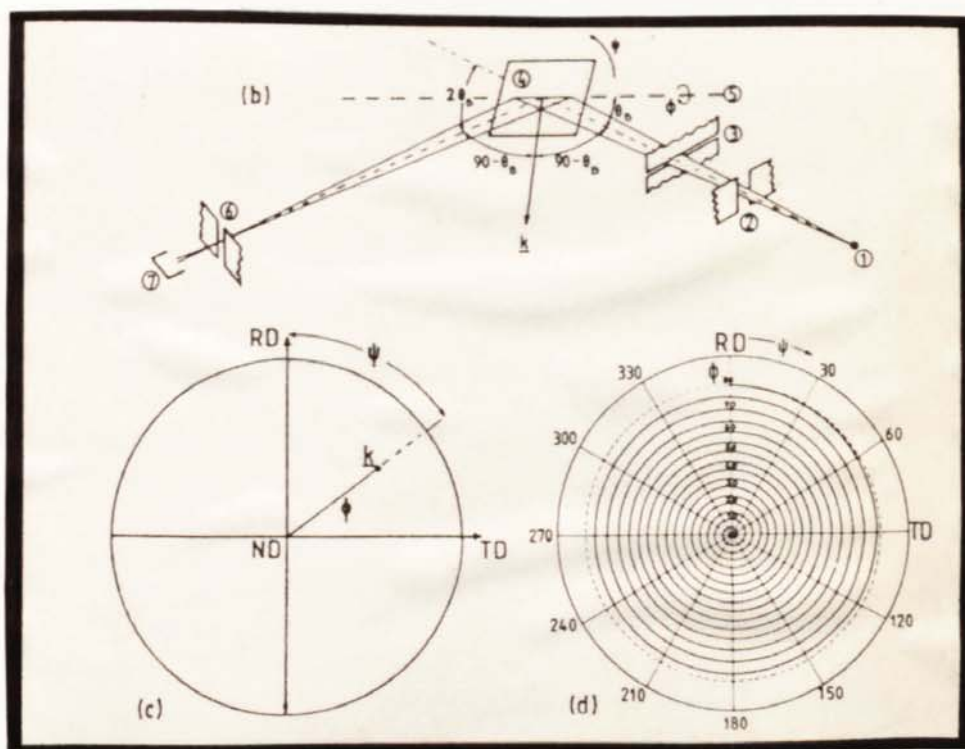


Fig.(10)(b) A schematic diagram which explains the geometrical arrangement of the goniometer,
 (c) The corresponding stereographic projection showing the diffracting vector \underline{k} ,
 (d) Spiral path of the diffracting vector.

in amyl acetate and allowing it to dry. The dried film was stripped from the surface with cellulose adhesive tape. An electron dense metal (Au/Pd) alloy was vacuum evaporated onto the plastic copy of the surface. While still under vacuum, carbon was also evaporated from an arc struck between two carbon electrodes onto the Au/Pd shadowed plastic. The carbon arc was directly above the specimen but shadowing, using the alloy, was carried out at a 10° angle. Small squares approximately 1.5×1.5 mm were cut from the sample and placed face up in a petri dish containing petroleum ether. Solution of the cellulose tape glue by the petroleum ether enabled removal of the plastic film, together with the carbon and Au/Pd coating from the cellulose tape. The small sections of the replica were floated onto copper electron microscope grids. Heat from the electron beam in the microscope would decompose the nitrocellulose so this was removed by dissolving in amyl acetate. Replicas were placed on filter papers, soaked in amyl acetate and left over night to completely remove the nitrocellulose. The replica consisting of the Au/Pd shadowing on the carbon film supported by the copper grid, was then ready for examination in the electron microscope.

7.2.6.4 Analysis.

The differences in composition of the deposits produced by the two agitation methods were determined by electron probe microanalysis, atomic absorption spectrophotometry

and wet chemical analysis.

7.2.6.4.1 Electron Probe Microanalysis.

The Cambridge MK5 electron probe microanalyser, illustrated in Fig.(11), was used to check the composition of electrodeposited alloys. Samples were cut from the centre of the plated steel panels; they were then mounted in conductive bakelite and polished by conventional methods. Analysis was performed at 20 kV and data corrected by computer for absorption effects.

7.2.6.4.2 Atomic Absorption Spectrophotometry.

The Perkin-Elmer atomic absorption spectrophotometer model 303, shown in Fig.(12), was used to determine the composition of plating solutions and electrodeposited alloys. Calibration was carried out using solution of known metal content.

7.2.6.4.2.1 Nickel-Cobalt Plating Solution.

10 ml of the nickel-cobalt solution were diluted with deionized water in a 1000 ml graduated flask. Further dilution was carried out by transferring 10 ml of diluted solution to a 100 ml graduated flask and making up to the volume with deionized water. This dilution resulted in a concentration of approximately 5 ppm cobalt. A water blank was run between each sample or standard to



Fig.(11) Electron Probe Microanalyser
Model Cambridge Microscan V.



Fig.(12) Perkin-Elmer Atomic Absorption
Spectrophotometer Model 560.

verify baseline stability. Ten readings were obtained for cobalt and the average calculated.

Nickel-Cobalt Alloy Deposits.

In order to analyse electrodeposits thin foils of nickel-cobalt alloys were weighed, dissolved in warm 50/50 v/o HCl and then made up to 50 ml in a graduated flask. The same procedure was used as above for analysis.

7.2.6.4.2.2 Nickel-Iron Plating Solution.

Nickel-iron solutions were not analysed by atomic absorption spectrophotometry since it was not possible to distinguish between ferric and ferrous iron.

Nickel-Iron Alloy Deposits.

Foils were dissolved in hydrochloric acid in the same way as for nickel-cobalt alloys. In this case the standard iron solution was made up to contain approximately the same amount of nickel as the "unknown" solution in order to take into account interference effects.

7.2.6.4.3 Wet Chemical Analysis.

7.2.6.4.3.1 Nickel-Cobalt Plating Solution.

Cobalt Analysis.

10 ml of solution was transferred to a 600 ml beaker, diluted to 400 ml and 10 ml of concentrated hydrochloric acid added. The solution was brought to the boil and 50 ml of freshly prepared 1-nitroso-2-naphthol in acetic acid were added. It was allowed to stand for one hour, filtered through ashless filter paper and the precipitate washed with 1% hydrochloric acid. The precipitate and filter paper were ignited to constant weight at 600°C in a crucible.

Calculation.

$$\text{Wt of Co}_3\text{O}_4 \times 0.7342 \times 100 = \text{g/1 Co}$$

Analysis of Nickel

10 ml of solution was made up to exactly 100 ml. 5 ml. of this dilute solution was transferred to a 400 ml. beaker, diluted to 200 ml, 4 gm tartaric acid were added and the solution was heated to nearly boiling. The solution was then made just ammoniacal and 50 ml. of a 1% solution of dimethylglyoxime in alcohol were added. It was left in a warm place for 30 minutes then filtered

through a weighed sintered glass crucible. The precipitate was washed with hot water then dried in an oven at 120°C to constant weight.

Calculation.

Wt of nickel dimethylglyoxime \times 0.203 \times 2000 = g/1 Ni.

Nickel-Cobalt Alloy Electrodeposits.

Weighed electrodeposited foils of nickel-cobalt alloy were dissolved in 50/50 nitric acid and then made up to 50 ml in a graduated flask. Suitable aliquots were taken for analysis by the same methods described in the previous section.

7.2.6.4.3.2 Nickel-Iron Plating Solution.

Nickel-iron solution was analysed to determine both the ferrous (Fe^{2+}) and ferric (Fe^{3+}) iron content.

Ferrous Iron.

25 ml of 10 v/o sulphuric acid together with two drops of 1,10 phenanthroline ferrous sulphate complex as indicator were added to 10 ml of nickel-iron plating solution contained in a titration flask. The solution was titrated with 0.1N ceric sulphate solution until the colour changed from orange to bright green indicating

the oxidation of all ferrous ions to ferric.

Calculation.

Titration value x 0.56 = g/l Ferrous iron

(Factor calculated on the basis that 1 ml 0.1N solution is equivalent to 0.0056 gms iron).

Ferric Iron

50 ml of nickel-iron solution, 10 ml concentrated hydrochloric acid, 10 ml 10% potassium iodide, and 3 ml cuprous iodide slurry were added to a 500 ml flask and shaken for 15 seconds then allowed to stand for 5 minutes. The ferric iron liberated an equivalent amount of iodine which was titrated with 0.1N sodium thiosulphate solution to a pale straw colour. Starch was added as an indicator and titration continued until the purple colour was discharged.

Calculation.

Titration value x 0.112 = g/l Ferric iron.

7.2.6.5 Cathode Current Efficiency.

The cathode current efficiencies of solutions were determined when using both air and ultrasonic agitation. This was carried out by plating the test panel in series

with a brass panel of size 10 cm x 5 cm in a two litre plastic tank containing 150 g/l copper sulphate ($\text{CuSO}_4 \cdot 5\text{H}_2\text{O}$) and 50 g/l H_2SO_4 . The test panels were cleaned in the appropriate manner then dried and weighed. They were then cleaned once more and plated for one hour. Air agitation was used in the copper coulometer in both cases. After plating the panels were washed in water, dried in acetone and re-weighed. The weight differences gave the quantities of copper and alloy deposited by the same number of coulombs. The cross section from the alloy deposit was mounted in conducting bakelite and polished for analysis by electron probe microanalysis. Later, samples were also analysed by atomic absorption spectrophotometry.

7.2.6.6 Limiting Current Density.

From a practical point of view, this is the highest current density at which sound deposits can be obtained. Beyond this value deposits are generally dark and powdery, having a burned appearance. Such deposits are due to hydrogen discharge, with consequent increase of pH at the cathode surface to the point where metal hydroxide or a basic salt is precipitated and becomes included in the deposit. The effect of ultrasonic and air agitation on the limiting current density was investigated using mild steel test pieces 1.25 cm x 5 cm so that high current densities could be achieved. The initial work was carried out by setting the current

density to 4 A/dm^2 for 40 minutes. When the current density was increased the plating time was decreased by the appropriate amount in order to maintain a constant deposit thickness, i.e. the number of coulombs passed was kept constant. All test pieces were examined visually for differences in appearance.

7.2.6.7 Macrothrowing Power.

For evaluation of macrothrowing a 267 ml Hull Cell was employed using mild steel cathodes $7.5 \text{ cm} \times 10 \text{ cm}$. The anode was fitted at the rectangular end of the box and a cathode plate 100mm long and 7.5 mm high was placed along the sloping side.

The cell was immersed in the water bath of the ultrasonic tank to maintain the temperature of the plating solution at $50 - 55^\circ\text{C}$ for nickel-cobalt and $63 - 68^\circ\text{C}$ for nickel-iron. Ultrasonic agitation was used and 1A was passed through the cell for 40 mins. The cleaning sequence for mild steel was used. For comparison, plating tests were carried out using an air agitated Hull cell for nickel, cobalt and both alloy solutions.

CHAPTER EIGHT

8. RESULTS

8.1 HARDNESS AND DEPOSIT COMPOSITION.

8.1.1 Nickel-Cobalt Deposits.

The hardness values obtained using the nickel-cobalt solution containing 10 g/l cobaltous sulphate are shown in Table VIII. Each hardness value shown is the average of ten hardness readings.

The effects of ultrasonic agitation on hardness and cobalt content are shown in Figs. 13 and 14. After each three hours of plating the Ni-Co solution was analysed by atomic absorption spectrophotometry and then replenished by adding cobaltous sulphate to bring it back to its original concentration.

The air agitation results shown in Table VIII indicate that the hardness and cobalt content of the deposits were approximately the same at 4 and 8 A/dm². The hardness at 4 A/dm² varied between 254 and 280HV, and at 8 A/dm² between 258 and 282HV. The cobalt content at 4 A/dm² was between 19.6% and 26.5% while at 8 A/dm² it was between 19.4% and 24.8%.

Table No.VIII

Hardness and Cobalt Content of Ni-Co Alloys Deposited
Using Air or Ultrasonic Agitation. Cobalt Sulphate
Content of Solution 10 g/l; Temperature 55°C; pH 4.

Agitation	Current Density A/dm ²	Cobalt Content %	Hardness HV
Air	4	20.2	261
Air	4	24.7	254
Air	4	25.8	277
Air	4	26.5	263
Air	4	19.6	259
Air	4	22.9	280
Air	8	19.4	264
Air	8	23.1	268
Air	8	23.8	261
Air	8	22.4	282
Air	8	24.8	275
Air	8	20.6	258
Ultrasonic 20 watt	4	23.3	268
Ultrasonic 20 watt	4	22.0	264
Ultrasonic 20 watt	4	22.6	263
Ultrasonic 40 watt	4	21.3	266
Ultrasonic 40 watt	4	20.9	257
Ultrasonic 40 watt	4	21.4	259
Ultrasonic 100 watt	4	20.2	267
Ultrasonic 100 watt	4	19.8	266
Ultrasonic 100 watt	4	19.7	269
Ultrasonic 200 watt	4	19.2	277
Ultrasonic 200 watt	4	19.3	280
Ultrasonic 200 watt	4	19.1	283
Ultrasonic 350 watt	4	18.0	345
Ultrasonic 350 watt	4	18.4	337
Ultrasonic 350 watt	4	18.8	354
Ultrasonic 20 watt	8	22.8	274

Agitation	Current Density A/dm ²	Cobalt Content %	Hardness HV
Ultrasonic 20 watt	8	21.6	265
Ultrasonic 20 watt	8	21.7	268
Ultrasonic 40 watt	8	20.5	269
Ultrasonic 40 watt	8	20.8	266
Ultrasonic 40 watt	8	20.3	270
Ultrasonic 100 watt	8	19.2	272
Ultrasonic 100 watt	8	19.0	269
Ultrasonic 100 watt	8	18.9	270
Ultrasonic 200 watt	8	18.3	286
Ultrasonic 200 watt	8	18.1	281
Ultrasonic 200 watt	8	18.2	288
Ultrasonic 350 watt	8	18.0	357
Ultrasonic 350 watt	8	18.0	356
Ultrasonic 350 watt	8	17.9	361

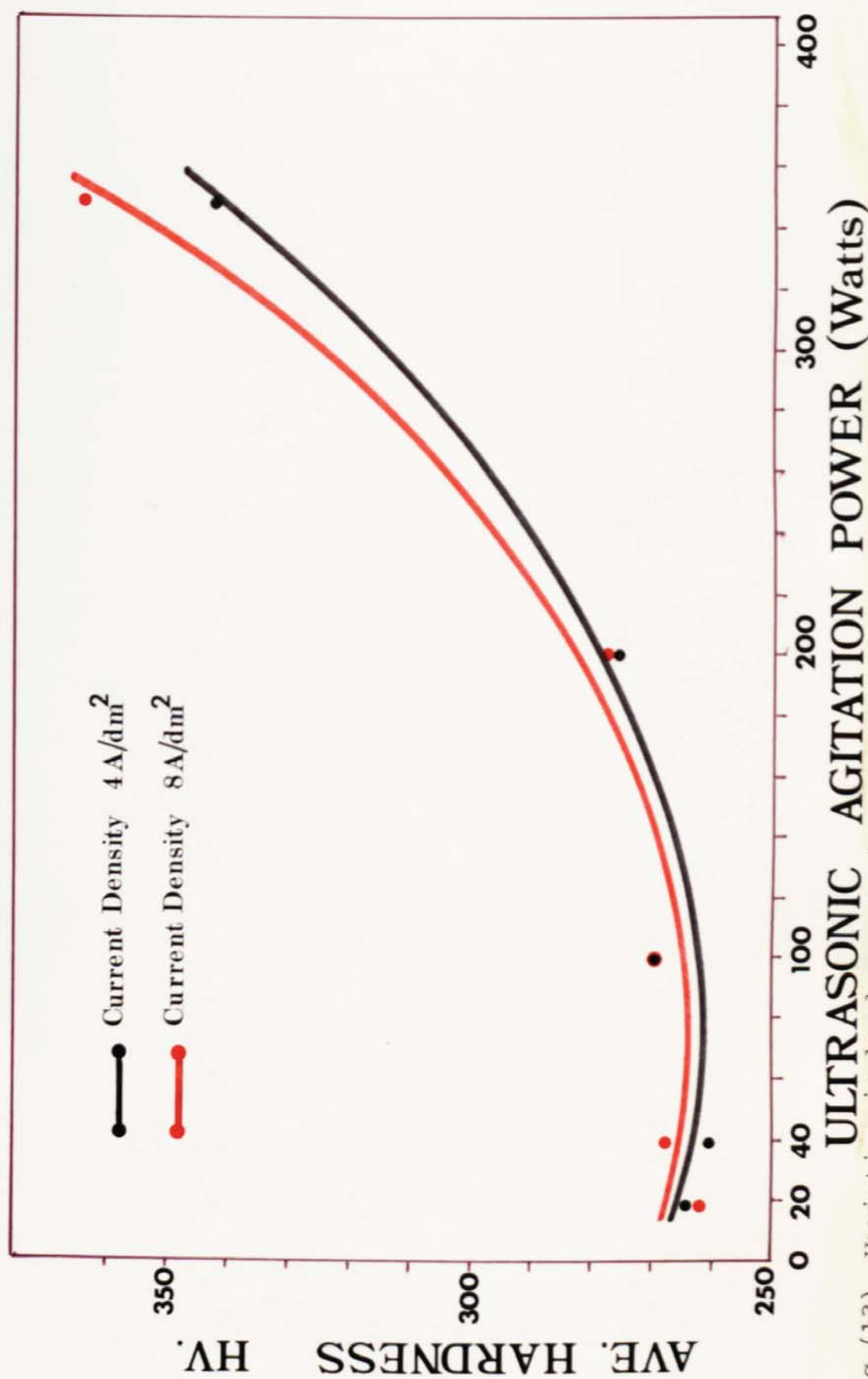


Fig. (13) Variation in hardness of nickel-cobalt alloys with degree of ultrasonic agitation.
(Plating solution containing 10 g/l cobalt sulphate.)

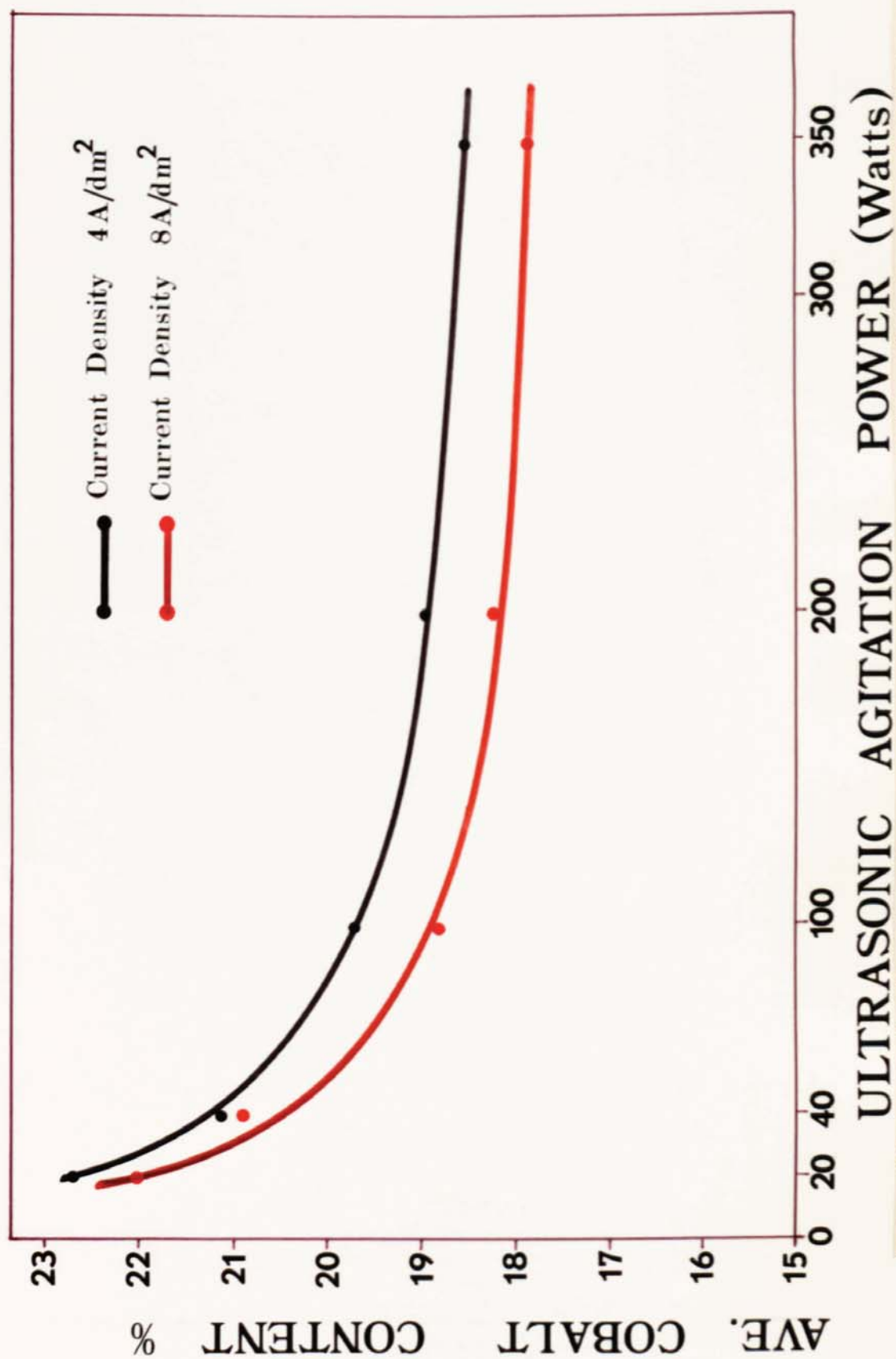


Fig. (14) Variation in nickel-cobalt alloy composition with degree of ultrasonic agitation. (Plating solution containing 10g/l cobalt sulphate.)

Deposits obtained from nickel-cobalt solution using ultrasonic agitation showed that the hardness and cobalt content in the deposit depend on the degree of ultrasonic agitation power and current density. Results from Table VIII show that at 4 A/dm^2 the cobalt content in the deposit varied from 18.0% to 23.3% whilst the hardness varied from 257 to 354 HV by transmitting different power intensities to the 10 litre electroplating bath ranging from 20 to 350 watts, but at 8 A/dm^2 the cobalt content in the deposit varied from 17.9 to 22.8% while the hardness varied from 265 to 361 HV. From these results it is evident that ultrasonic agitation had a far greater effect on hardness than on cobalt content in the deposit, although there was greater scatter in the hardness results using ultrasonic agitation.

The average hardness for air agitation at 4 A/dm^2 was 265.6 HV and for the highest ultrasonic power of 350 watts at 4 A/dm^2 was 345 HV.

Since air agitation gave an average cobalt content in the deposit of 23.3% and an average hardness of 265.6 HV whilst ultrasonic agitation power of 350 watts gave an average cobalt content of 18.4% and an average hardness of 345.3 HV. It seems reasonable that the increase in hardness is due to the ultrasonic agitation effect.

8.1.1.1 Effect of Change in Solution Composition.

Further work was carried out using plating solutions having the compositions shown below in Table IX. The plating conditions for all solutions were pH 4, temperature 55°C and current density 4 A/dm² unless otherwise stated, using either air or ultrasonic agitation, averages of ten readings were taken for cobalt content and hardness.

It was apparent that the small percentages of cobalt in the bath resulted in high percentages of cobalt in the electrodeposit. This effect is to be expected due to the anomalous nature of codeposition (i.e. the less noble cobalt deposits preferentially). The cobalt contents of the alloy deposits are given in Table IX and displayed graphically together with cobaltous sulphate contents in Fig.(15).

Table IX

The effect of the concentration of cobalt sulphate in solution
 on hardness and on the percentage cobalt obtained in the deposit,
 using either air or ultrasonic agitation, pH4; 55°C.

Cobalt Sulphate Content g/l	Agitation	Current Density A/dm^2	Cobalt Content %	Hardness HV
35	Air	4	51	280
35	Air	8	48	278
35	Ultrasonic 200 watts	4	43.5	335
35	Ultrasonic 350 watts	4	42	372
60	Air	4	66.4	289
60	Air	8	64.1	294
60	Ultrasonic 200 watts	4	61.2	351
60	Ultrasonic 350 watts	4	58.4	386
85	Air	4	71.7	300
85	Air	8	70.3	306
85	Ultrasonic 200 watts	4	66.4	359
85	Ultrasonic 350 watts	4	63.8	390

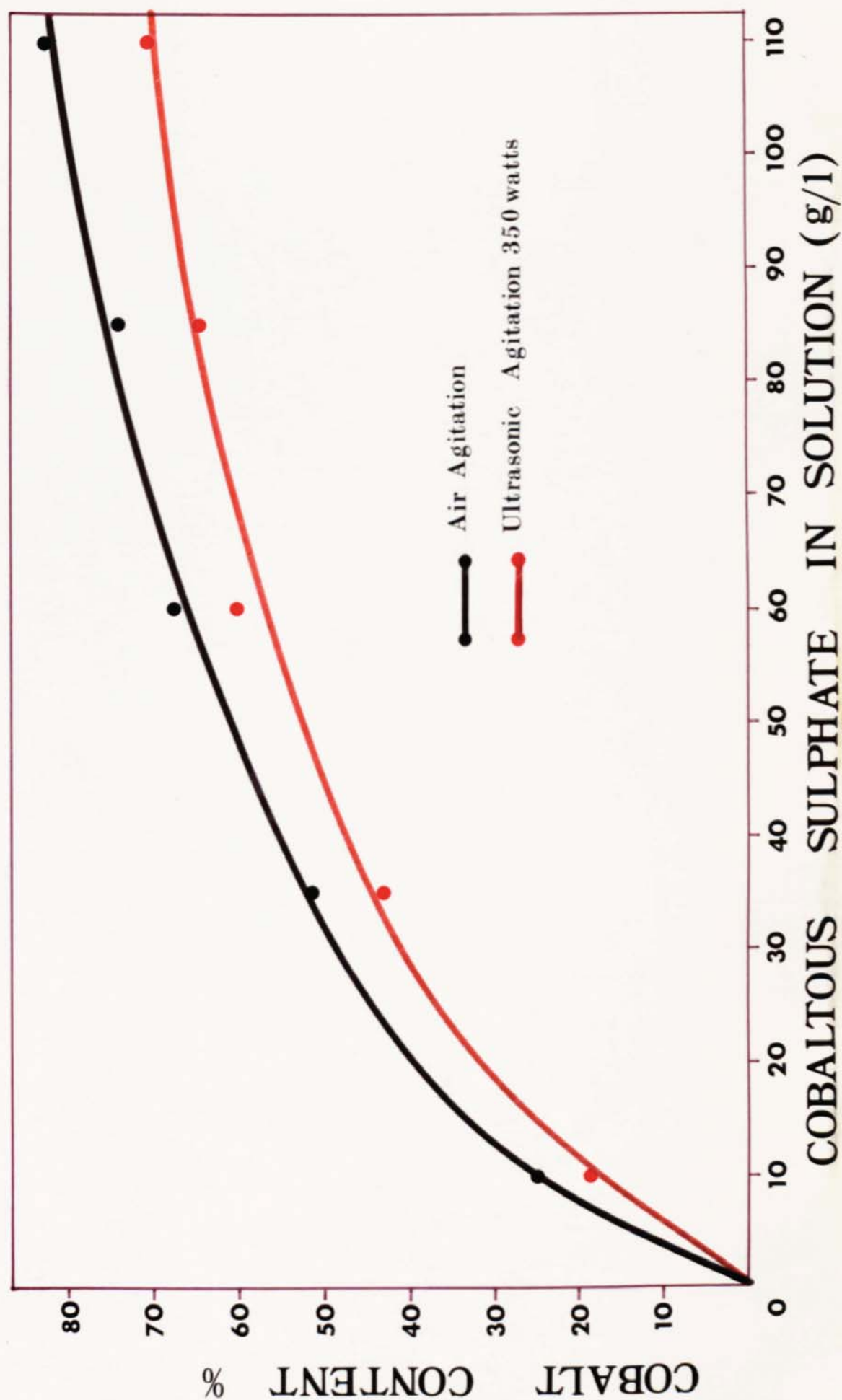


Fig.(15) Relation between cobalt sulphate concentration in solution and cobalt content in deposit

8.1.2 Nickel-Cobalt Solution Containing 110 g/l of Cobalt-Sulphate.

Hardness results and cobalt contents are given in Table X.

Table X

Hardness and composition of nickel-cobalt alloy deposits obtained using air or ultrasonic agitation, pH4, temperature 55°C. Plating solution containing 110 g/l cobalt sulphate.

Agitation	C.D ₂ A/dm ²	Cobalt Content %	Hardness HV
Air	4	81.8	308
Air	8	81.2	312
Ultrasonic 20 watts	4	64.8	297
Ultrasonic 40 watts	4	72.4	296
Ultrasonic 100 watts	4	71.5	308
Ultrasonic 200 watts	4	69.5	328
Ultrasonic 350 watts	4	68.3	383

The compositions of the deposits produced by the two agitation methods were determined by electron probe microanalysis, as shown in Table X. The cobalt content of the deposit using air agitation was initially 81.8% and dropped to 68.3% at 350 watts ultrasonic agitation.

The hardness obtained using different ultrasonic agitation intensities ranged from 296 - 383 HV as shown

in Table X. Deposits with hardnesses of 308 and 312 HV were obtained by applying vigorous air agitation at 4 and 8 A/dm² respectively. The more intense the ultrasonic agitation the harder were the electrodeposits as shown in Fig.(16), and the greater the intensity of the ultrasonic agitation the lower the cobalt content, after an initial rise at 40 watts, as shown in Fig.(17).

A comparison between hardness results obtained from this solution and that of 10 g/l cobaltous sulphate using ultrasonic agitation is illustrated in Fig.(16).

8.1.3 Nickel Deposits.

Electrodeposits obtained from dull nickel solution were analysed by electron probe microanalyser for nickel and cobalt content, the same samples were used for hardness tests. The following results were obtained as shown in Table XI. It is apparent that some cobalt was present as impurity. Electrodeposited nickel ranged in hardness from 247 - 253 HV when deposited using vigorous air agitation and current densities of 4 and 8 A/dm². Harder deposits about 258.6 - 312 HV were obtained using ultrasonic agitation of different power intensities. Average hardness versus ultrasonic agitation power (watts) is illustrated in Fig.(18).

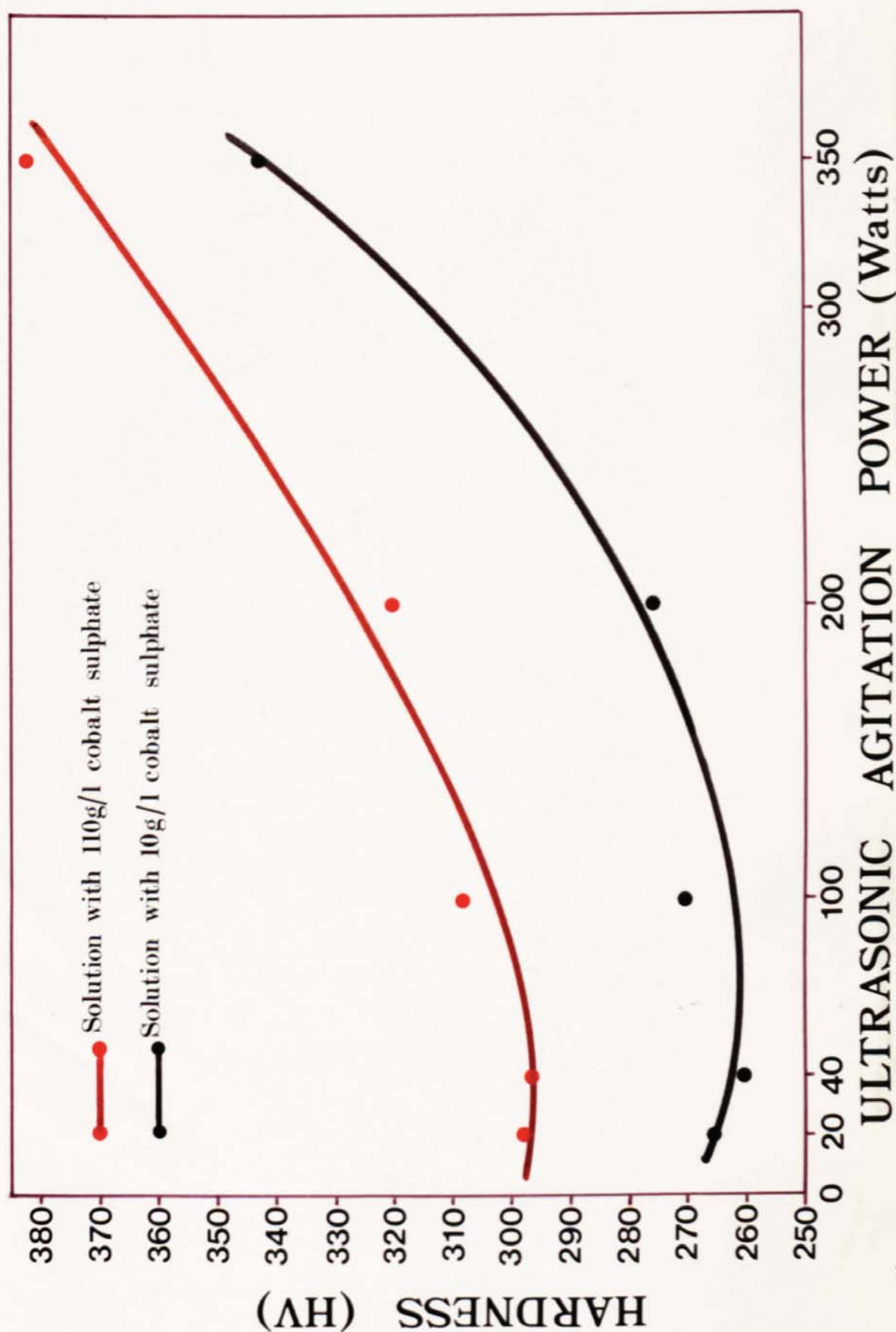


Fig.(16) Variation in hardness of nickel-cobalt alloys with degree of ultrasonic agitation (Plating solutions containing 10 g/l and 110 g/l cobalt sulphate.)

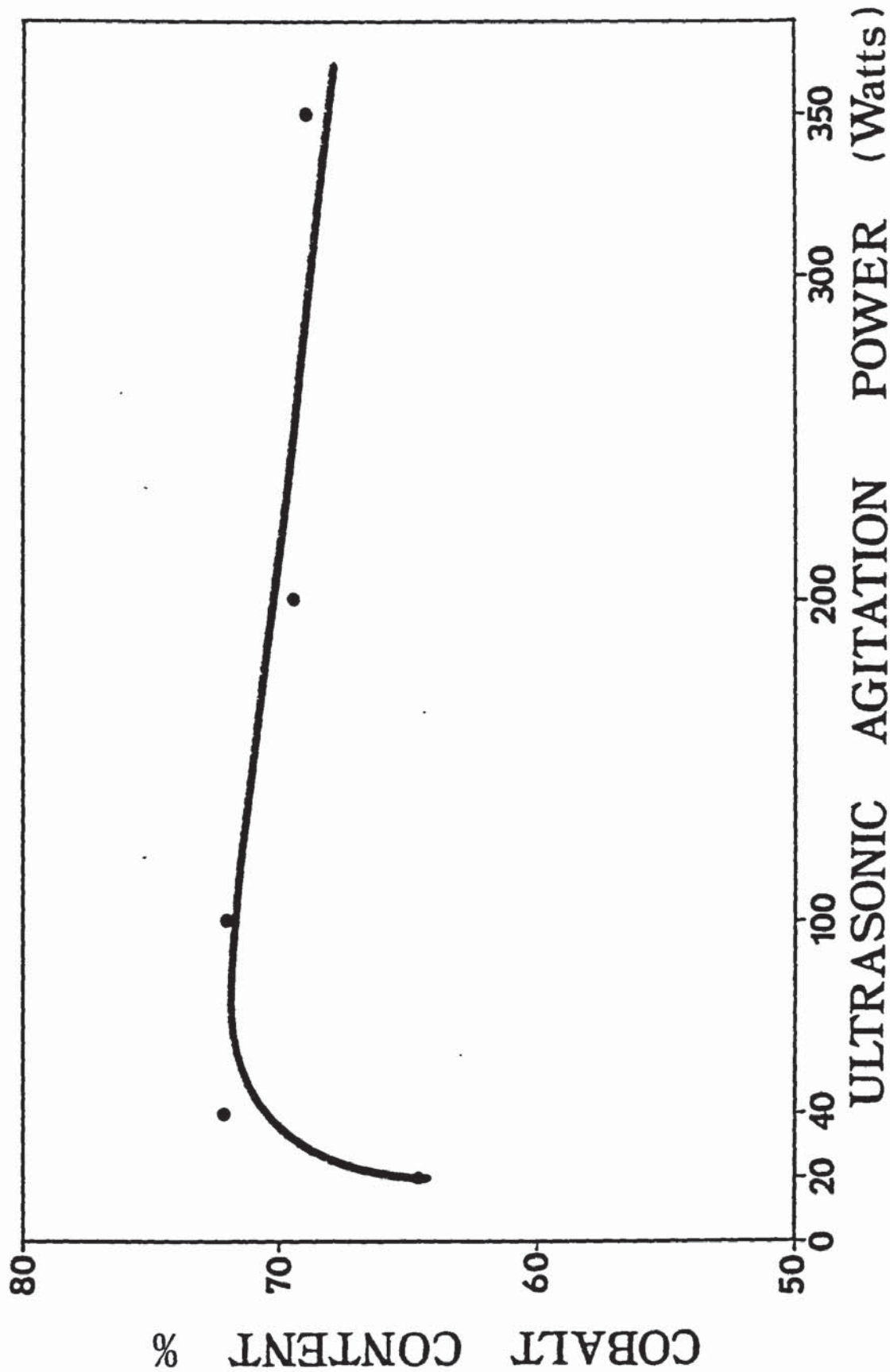


Fig.(17) Variation in nickel-cobalt alloy composition with degree of ultrasonic agitation. (Plating solution containing 110g/l cobaltous sulphate.)

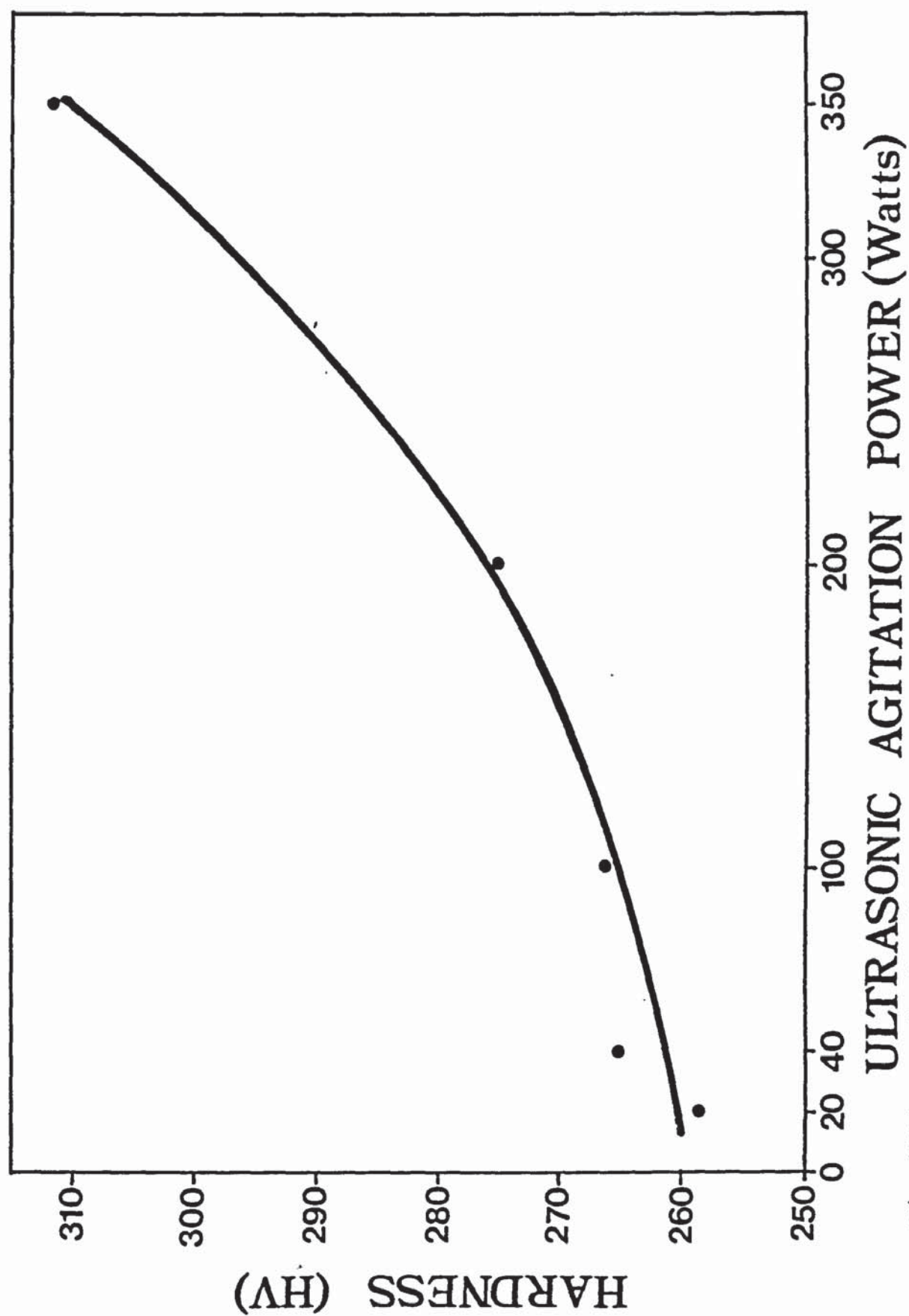


Fig. (18) Variation in hardness of dull nickel alloys with degree of ultrasonic agitation.

Table XI

Hardness and composition of nickel electrodeposits obtained using air or ultrasonic agitation. pH4; temperature 55°C and current density 4 A/dm² unless otherwise stated.

Agitation	Nickel Content %	Cobalt Content %	Hardness HV
Air	94.47	5.88	247
Air 8A/dm ²	92.16	8.32	253
Ultrasonic 20 watt	94.61	5.62	258.6
Ultrasonic 40 watt	94.02	6.1	264.8
Ultrasonic 100 watt	94.09	6.3	265.4
Ultrasonic 200 watt	94.19	5.86	275
Ultrasonic 350 watt	94.31	5.70	312

It is apparent from Table XI that by increasing the power intensity of ultrasonic agitation the percentage of cobalt in the alloy decreased slightly and the hardness of the deposit increased.

8.1.4 Cobalt Deposits.

Deposits obtained from cobalt solution were analysed by electron probe microanalyser for cobalt and nickel content and the same samples were used for hardness tests.

Hardnesses of electrodeposits obtained by using air agitation were 284 and 287 HV, using current densities of 4 and 8 A/dm² respectively. Deposits of hardnesses 292.6 to 361.9HV were obtained using ultrasonic agitation of different power intensities as shown in Table XII.

Table XII

Hardness of cobalt electrodeposits obtained using air or ultrasonic agitation. pH 4; temperature 55°C.

Agitation	C.D. A/dm ²	Cobalt Content %	Nickel Content %	Hardness HV
Air	4	99.87	0.21	284
Air	8	99.7	0.33	287
Ultrasonic 20 watt	4	99.58	0.44	294.6
Ultrasonic 40 watt	4	99.68	0.43	292.6
Ultrasonic 100 watt	4	99.7	0.35	304
Ultrasonic 200 watt	4	99.68	0.41	322
Ultrasonic 350 watt	4	99.65	0.45	361.9

The more intense the ultrasonic agitation the harder was the cobalt electrodeposit, as shown graphically in Fig.(19).

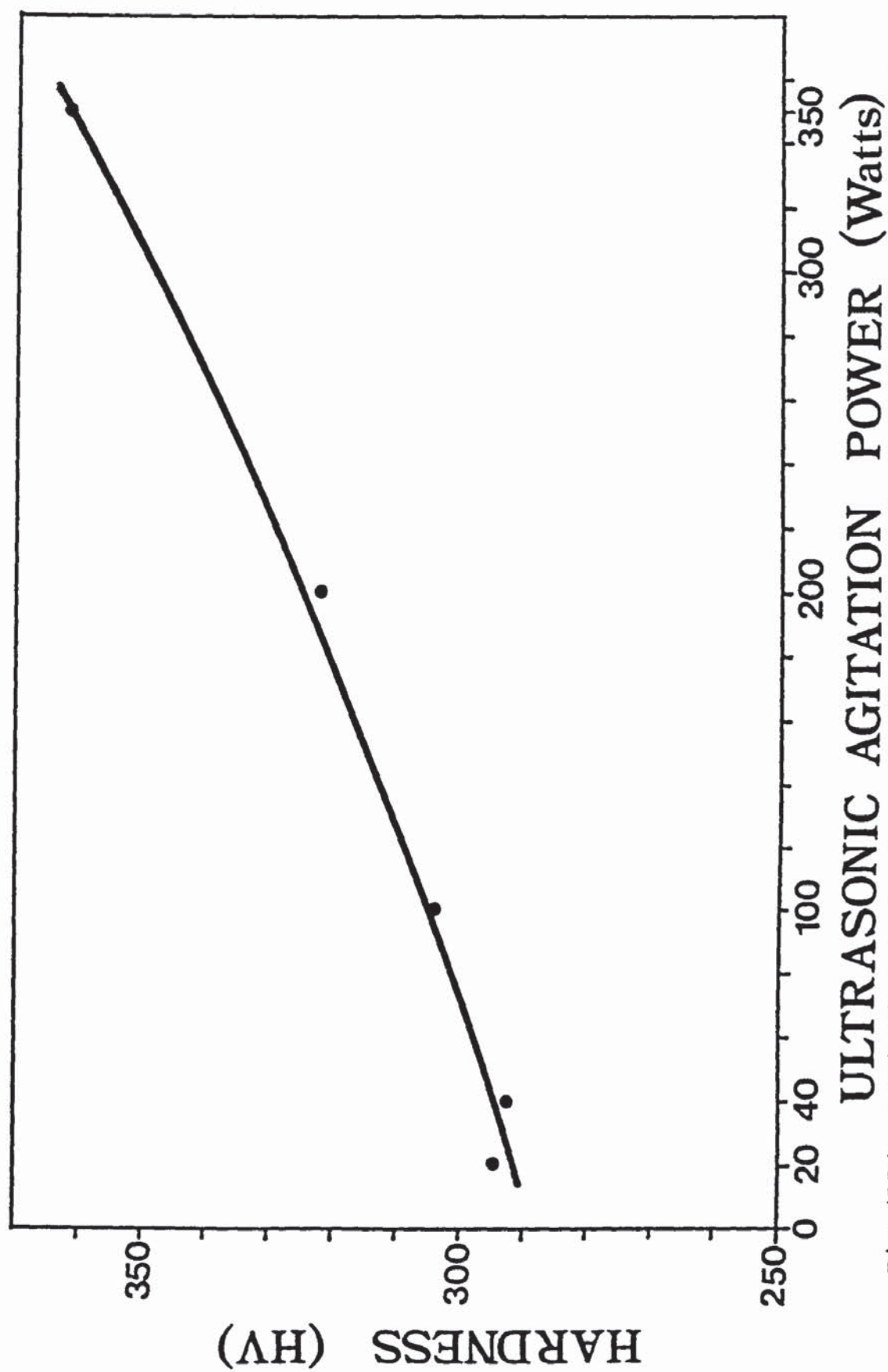


Fig.(19) Variation in hardness of cobalt with degree of ultrasonic agitation.

8.1.5 Nickel-Iron Deposits.

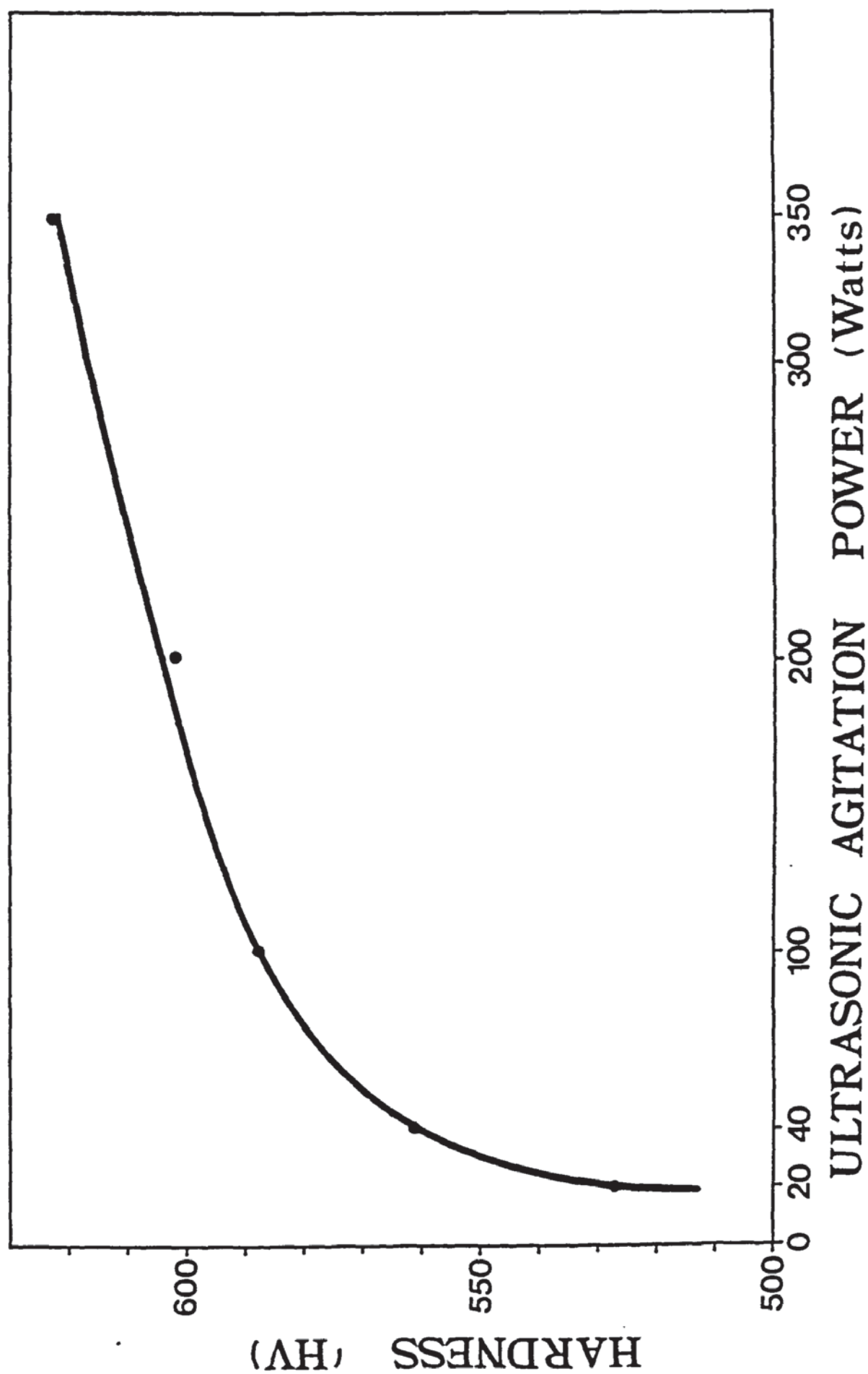
Hardnesses of nickel-iron alloy electrodeposits ranged from 523 - 538.8 HV using vigorous air agitation and current densities of 4 and 8 A/dm². Harder deposits were obtained, 527.3 - 623.4 HV, using ultrasonic agitation with different power intensities as shown in Table XIII.

The more intense the ultrasonic agitation the harder was the electrodeposit.

The samples were analysed to determine the composition of the deposits by electron probe microanalyser. The iron content of the deposit using air agitation was 24.78%. When ultrasonic agitation was applied the iron content varied between 19.42% at 20 watts to 26% at 350 watts. The microhardness results are given in Table XIII and displayed graphically in Fig.(20).

The same samples were analysed by atomic absorption spectrophotometry for nickel and iron content.

Results obtained by electron probe microanalysis and atomic absorption spectrophotometry are displayed graphically in Fig.(21) and show good agreement.



ULTRASONIC AGITATION POWER (Watts)

Fig. (20) Variation in hardness of nickel-iron alloys with degree of ultrasonic agitation.

8.1.5.1 Effect of Different Types of Agitation on Composition.

The different methods of agitation used to study their effects on composition were as follows:-

- i) Air agitated.
- ii) Ultrasonically agitated using different powers 20, 40, 100, 200 and 350 watts.
- iii) Both air and ultrasonic agitation together with different power intensities 40, 100, 200 and 350 watts.
- iv) No agitation.

The deposits were analysed by electron probe microanalyser and atomic absorption spectrophotometry. Results are shown in Table XIII. The use of air and ultrasonic agitation together did not show significant differences from using ultrasonic agitation alone. When no agitation was used the iron content of deposits was lower than when using any form of agitation but the hardness was similar to that achieved using air agitation.

Table XIII

Variation in nickel-iron contents with agitation using air, ultrasonic, both air and ultrasonic together, and with no agitation. Both electron probe microanalysis and atomic absorption spectrophotometry were used. Plating condition pH 4, Temperature 65°C and Current Density 4 A/dm² unless otherwise stated.

Agitation	Average Iron Content (%) A.A.	Probe	Average Nickel Content (%) A.A.	Probe	Hardness HV
Air	25.79	24.78	75.11	75.9	523.2
Air 8 A/dm ²	21.83	20.3	79.9	81.2	538.8
Ultrasonic 20 watts	20.03	19.42	81.1	81.7	527.3
Ultrasonic 40 watts	19.2	20.1	82.7	80.3	561.9
Ultrasonic 100 watts	21.74	22.54	79.8	77.8	588.5
Ultrasonic 200 watts	22.7	23.5	78	76.7	602.1
Ultrasonic 350 watts	26.27	26.00	74.1	74.5	623.4
Air and ultrasonic 40W	20.1	19.96	79.5	80.85	559.4
Air and ultrasonic 100W	21.2	21.7	79.9	80.8	555.1
Air and ultrasonic 200W	20.8	19.64	79.4	79.24	610
Air and ultrasonic 350W	22.45	22.8	78.5	79.3	635
No agitation 4 A/dm ²		18.2			518
No agitation 8 A/dm ²		16.8			502

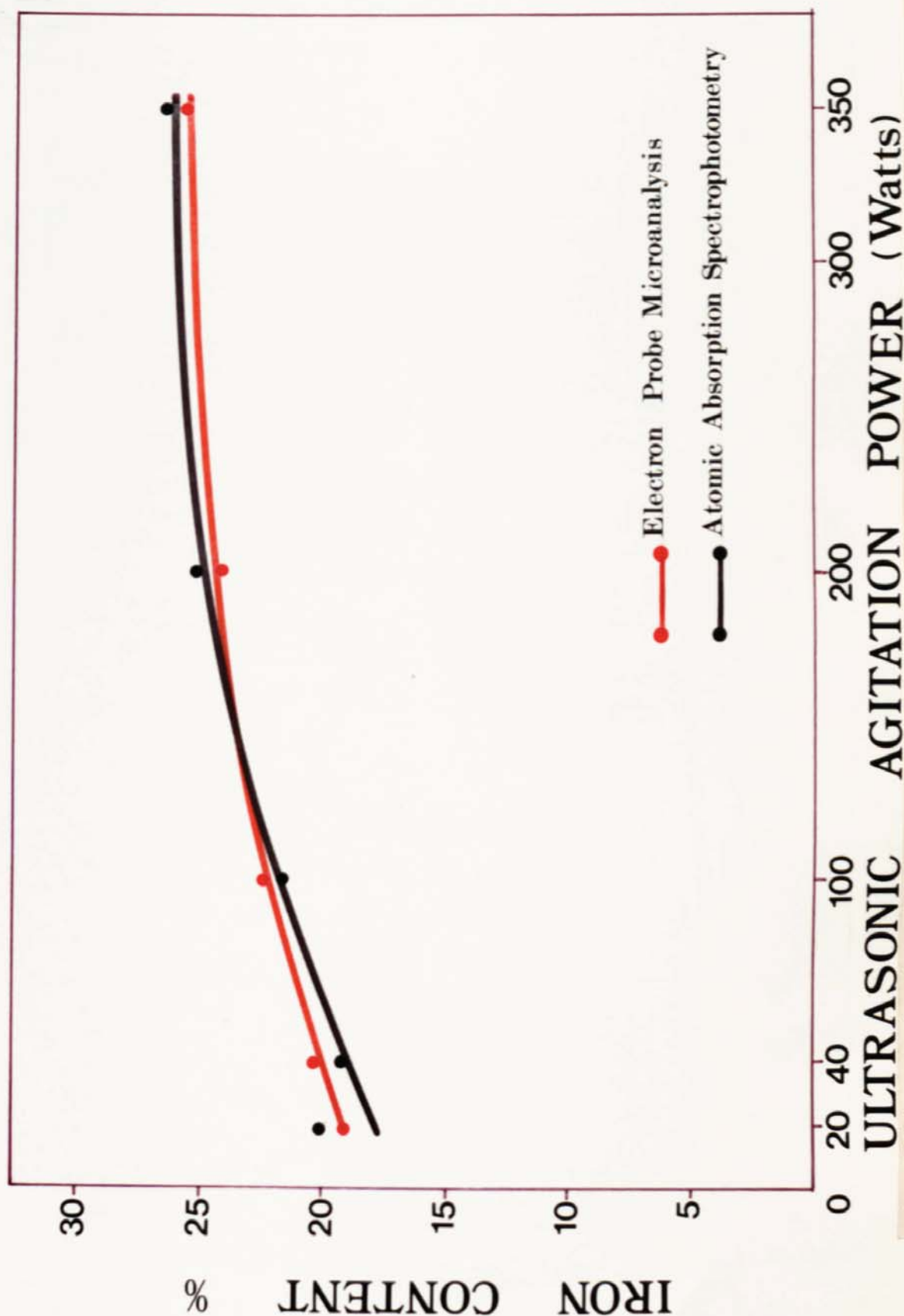


Fig. (21) Variation in nickel-iron alloy composition with degree of ultrasonic agitation. Results determined by Electron Probe Microanalysis and Atomic Absorption spectrophotometry.

8.2 Tensile Strength and Ductility.

8.2.1. Nickel-Cobalt.

The tensile test pieces were electroplated in nickel-cobalt solution (10 g/l cobaltous sulphate), using either air or ultrasonic agitation. Triplicate results were obtained in all cases for both the tensile strength of the coating and the compound plated test bar. The tensile strength of nickel-cobalt alloy deposits on brass substrates was determined using the method described by Brook.⁽¹¹⁹⁾

The individual results are given in Tables XIV to XVII and displayed graphically in Fig.(22), which shows typical load-extension curves for a brass specimen, OAB, and for an electroplated brass specimen, OC. During the testing of the nickel-cobalt electrodeposited specimens, fracture was always preceded by cracking of the deposit and fracture usually started from one of the edge defects. Thus it appears probable that fracture initiates in the nickel-cobalt electrodeposit and if this is completely ruptured before failure starts in the brass the load carried by the brass will be no longer equivalent to AD but to CD, which is greater than the ultimate tensile strength of the brass. The brass will then fail without further noticeable elongation at an extension OD. If on the other hand, failure starts in the brass before fracture in the deposit is complete,

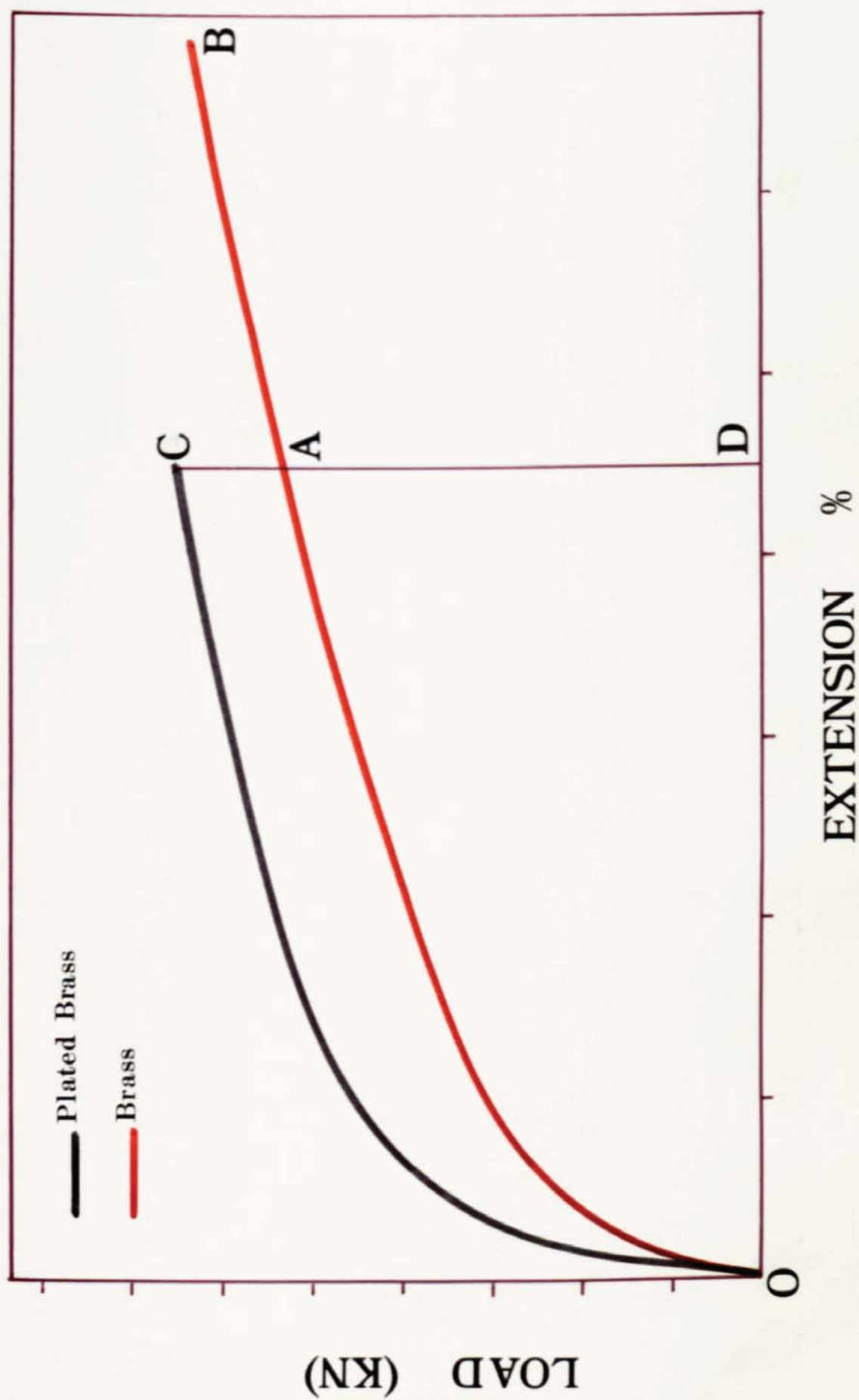


Fig. (22) Load-Extension curves for brass, and for a nickel-cobalt plated brass specimen.

the specimen will behave as if it were homogeneous. No test result was accepted unless the nickel-cobalt alloy and brass remained bonded throughout the test. The ultimate tensile strength of the plated test piece was calculated using the equation $(U.T.S.) = \frac{P_{\max}}{A_o}$ where P_{\max} is the maximum load and A_o is the original cross-sectional area of the specimen. The true ultimate tensile strength was calculated by dividing the breaking load by the cross-sectional area at failure. The U.T.S. of the deposit was calculated by dividing the load CA by the cross-sectional area of the coating. The U.T.S. of the brass test piece was determined by dividing the load DA by the original cross-sectional area of the brass before coating.

During the tests, the first cracks in the coating were recorded and elongation at that stage measured as shown in Table XIV and average elongation at first crack shown in Table XVI. The percentage elongation is the ratio of the increase in the length of the gauge section of the specimen to its original length, expressed as a percentage.

$$\% \text{ Elongation} = \frac{L_f - L_o}{L_o} \times 100$$

Where L_f is equal to gauge length after extension and L_o is original gauge length.

The results in Table XVI show that at specimen failure the average ultimate tensile strengths of nickel-cobalt

alloy electrodeposits, obtained using ultrasonic agitation, were slightly higher than those for the electrodeposits obtained by air agitation.

The ductility of plated specimens was significantly higher when the nickel-cobalt coating was applied using ultrasonic agitation instead of air as shown in Table XV. The U.T.S. of plated specimens was hardly affected by the use of ultrasonic agitation instead of air as shown in Table XV, and their averages are shown in Table XVII.

The tensile tests were repeated using samples plated in solution containing 110 g/l cobaltous sulphate. The results are shown in Table XVIII. It is apparent that the tensile strength results are approximately the same as those for deposits obtained from the more dilute nickel-cobalt solution containing 10 g/l cobaltous sulphate. However the ductility results were lower than those from the dilute bath.

The tensile strength results of air agitated test pieces were marginally lower than those obtained by ultrasonic agitation but the ductilities of the test pieces were improved by applying ultrasonic agitation from an average of 21.2% using air agitation to an average of 32.06% by ultrasonic 350 watts as shown in Table XIX.

Table XIV

Tensile strength and ductility of plated Nickel-Cobalt coatings obtained from solution containing 10 g/l $\text{CoSO}_4 \cdot 7\text{H}_2\text{O}$ determined in situ on brass substrates.

Method of Agitation	First Cracks		Stress in Brass		U.T.S. of Coating	
	Load KN	Elongation %	At first cracks kN/mm ²	At failure of test piece kN/mm ²	At first cracks kN/mm ²	At failure of test piece kN/mm ²
Air (1)	4.656	8.7	0.156	0.29	1.26	0.72
Air (2)	6.125	11.9	0.2251	0.29	1.26	0.96
Air (3)	5.5	12.67	0.2	0.289	1.142	0.83
Ultrasonic 100 watt (1)	5.25	21.6	0.188	0.29	1.172	1.09
Ultrasonic 100 watt (2)	6.468	21.2	0.244	0.29	1.2	1.06
Ultrasonic 100 watt (3)	5.563	18.9	0.21	0.3	1.02	0.75
Ultrasonic 200 watt (1)	6.28	27	0.244	0.295	1.02	0.9
Ultrasonic 200 watt (2)	5.125	22.3	0.186	0.299	1.1	0.91
Ultrasonic 200 watt (3)	6.25	26	0.244	0.2996	0.99	0.88
Ultrasonic 350 watt (1)	6.125	30	0.238	0.3	0.99	0.77
Ultrasonic 350 watt (2)	5.84	28.5	0.218	0.3	1.142	0.925
Ultrasonic 350 watt (3)	5.844	27.7	0.22	0.3	1.02	0.83

Table XV

Tensile strength and ductility of test pieces plated with Nickel-Cobalt coating obtained from solution containing 10 g/l $\text{Co.SO}_4.7\text{H}_2\text{O}$. and uncoated brass

Method of Agitation	Load at failure of plated test piece kN	U.T.S. of plated test piece kN/mm ²	True U.T.S. of plated test piece kN/mm ²	Elongation %
Air (1)	7	0.312	0.465	35.66
Air (2)	7.25	0.323	0.464	37.2
Air (3)	7.05	0.315	0.464	38.6
Ultrasonic 100 watt (1)	7.35	0.33	0.47	40.36
Ultrasonic 100 watt (2)	7.35	0.33	0.475	41.4
Ultrasonic 100 watt (3)	7.25	0.323	0.478	41.9
Ultrasonic 200 watt (1)	7.25	0.323	0.478	41.78
Ultrasonic 200 watt (2)	7.35	0.33	0.487	42.7
Ultrasonic 200 watt (3)	7.33	0.33	0.485	43.2
Ultrasonic 350 watt (1)	7.3	0.33	0.494	46.95
Ultrasonic 350 watt (2)	7.4	0.33	0.49	46.25
Ultrasonic 350 watt (3)	7.3	0.33	0.49	43.39
Unplated Brass (1)	6.75	0.315	0.459	69.95
Unplated Brass (2)	6.8	0.17	0.466	69.73
Unplated Brass (3)	6.85	0.319	0.464	70.01

Table (XVI)

Average tensile strength and ductility of plated nickel-cobalt coatings obtained from solution containing 10 g/l $\text{CoSO}_4 \cdot 7\text{H}_2\text{O}$, determined in situ on brass substrates.

Method of Agitation	First Cracks			Average Stress in Brass		Average U.T.S. of Coating	
	Average load kN	Average elongation %	At first cracks kN/mm ²	At failure of test piece kN/mm ²	At first cracks kN/mm ²	At failure of test piece kN/mm ²	
Air	5.43	11.1	0.194	0.29	1.22	0.836	
Ultrasonic 100 watt	5.76	20.6	0.214	0.29	1.13	0.97	
Ultrasonic 200 watt	5.885	25	0.225	0.298	1.04	0.896	
Ultrasonic 350 watt	5.94	28.7	0.225	0.3	1.05	0.841	

Table XVII

Average tensile strength and ductility of test pieces plated with nickel-

cobalt coating obtained from solution containing 10 g/l $\text{CoSO}_4 \cdot 7\text{H}_2\text{O}$. and uncoated brass

Method of Agitation	Average load at failure of plated test piece. kN	Average U.T.S. of plated test piece kN/mm^2	Average true U.T.S. of plated test piece kN/mm^2	Average elongation %
Air	7.1	0.32	0.464	37.15
Ultrasonic 100 watt	7.32	0.328	0.474	41.22
Ultrasonic 200 watt	7.31	0.328	0.483	42.56
Ultrasonic 350 watt	7.33	0.33	0.49	45.53
Unplated Brass	6.8	0.317	0.463	69.9

Table XVIII

Tensile strength and ductility of test pieces plated with Nickel-Cobalt coating obtained from solution containing 110 g/l $\text{CoSO}_4 \cdot 7\text{H}_2\text{O}$.

Method of Agitation	Load at failure of plated test piece kN	U.T.S. of plated test piece kN/mm ²	True U.T.S. of plated test piece kN/mm ²	Elongation %
Air (1)	7.02	0.311	0.454	20.2
Air (2)	7.1	0.308	0.466	22.0
Air (3)	6.8	0.314	0.455	21.3
Ultrasonic 100 watt (1)	7.2	0.326	0.474	24.6
Ultrasonic 100 watt (2)	7.0	0.328	0.461	22.4
Ultrasonic 100 watt (3)	7.23	0.3285	0.47	25.6
Ultrasonic 200 watt (1)	7.2	0.33	0.468	27.8
Ultrasonic 200 watt (2)	7.13	0.33	0.474	28.6
Ultrasonic 200 watt (3)	7.23	0.33	0.478	28.2
Ultrasonic 350 watt (1)	7.28	0.332	0.488	31.4
Ultrasonic 350 watt (2)	7.12	0.334	0.482	31.8
Ultrasonic 350 watt (3)	7.31	0.335	0.485	33.0

Table XIX

Average tensile strength and ductility of test pieces plated with nickel-cobalt coating obtained from solution containing 110 g/l $\text{CoSO}_4 \cdot 7\text{H}_2\text{O}$

Method of Agitation	Average load at failure of plated test piece kN	Average U.T.S. of plated test piece kN/mm ²	Average true U.T.S. of plated test piece kN/mm ²	Average elongation %
Air	6.97	0.311	0.458	21.2
Ultrasonic 100 watt	7.14	0.328	0.468	24.2
Ultrasonic 200 watt	7.19	0.33	0.473	28.2
Ultrasonic 350 watt	7.24	0.334	0.485	32.06

8.2.2 Nickel-Iron

Triplicate results were obtained in all cases, as for nickel-cobalt deposits and the results are shown in Tables XX to XXIII. The results in Table XX show that erratic values were obtained for the ultimate tensile strength of nickel-iron coatings obtained using ultrasonic agitation. The ductilities of deposits produced by ultrasonics were much higher than those obtained by air agitation as shown in Table XX and XXII. The U.T.S. of plated specimens was hardly changed by variation in the type and degree of agitation, as shown in Tables XXI and XXIII. The average ductility value of the plated specimens was 22% when using air agitation but increased to 34.8% when using ultrasonic agitation, 350 watts, as shown in Table XXIII.

Table XX

Tensile strength and ductility of plated nickel-iron coatings determined in situ
on brass substrates.

Method of Agitation	First cracks		Stress in Brass		U.T.S. of Coating	
	Load kN	Elongation %	At first cracks kN/mm ²	At failure of test piece kN/mm ²	At first cracks kN/mm ²	At failure of test piece kN/mm ²
Air (1)	4.125	1.19	0.126	0.25	1.38	1.02
Air (2)	4.53	1.23	0.139	0.24	1.5	1.26
Air (3)	4.563	2.6	0.154	0.26	1.23	0.72
Ultrasonic 100 watt (1)	4.78	6.9	0.145	0.254	1.62	1.23
Ultrasonic 100 watt (2)	4.4	3.4	0.140	0.276	1.3	0.78
Ultrasonic 100 watt (3)	4.84	6.7	0.158	0.275	1.41	1.129
Ultrasonic 200 watt (1)	4.0	6.7	0.116	0.269	1.47	1.02
Ultrasonic 200 watt (2)	5.75	5.9	0.21	0.291	1.142	0.56
Ultrasonic 200 watt (3)	4.94	6.1	0.18	0.29	1.08	0.53
Ultrasonic 350 watt (1)	4.3	9.2	0.14	0.285	1.23	0.97
Ultrasonic 350 watt (2)	5.06	10.1	0.146	0.288	1.86	0.956
Ultrasonic 350 watt (3)	5.4	10.5	0.19	0.292	1.26	0.91

Table XXI

Tensile strength and ductility of test pieces plated with Nickel-Iron coatings.

Method of Agitation	Load at failure kN	U.T.S. kN/mm ²	True U.T.S. kN/mm ²	Elongation %
Air (1)	6.375	0.284	0.452	22.5
Air (2)	6.5	0.29	0.456	20.5
Air (3)	6.25	0.278	0.459	23
Ultrasonic 100 watt (1)	6.72	0.30	0.463	25.27
Ultrasonic 100 watt (2)	6.72	0.30	0.465	30.4
Ultrasonic 100 watt (3)	7.06	0.315	0.469	30
Ultrasonic 200 watt (1)	6.81	0.304	0.468	30.3
Ultrasonic 200 watt (2)	6.8	0.303	0.471	30.78
Ultrasonic 200 watt (3)	6.8	0.303	0.47	32.1
Ultrasonic 350 watt (1)	7.1	0.3167	0.472	33.4
Ultrasonic 350 watt (2)	7.15	0.319	0.473	34.7
Ultrasonic 350 watt (3)	7.2	0.3212	0.481	36.15

Table XXII

Average tensile strength and ductility of plated nickel-iron coatings determined in situ on brass substrate.

Method of Agitation	First Cracks		Average Stress in Brass		Average U.T.S. of Coating	
	Average load kN	Average elongation %	At first cracks kN/mm ²	At failure of test piece kN/mm ²	At first cracks kN/mm ²	At failure of test piece kN/mm ²
Air	4.41	1.67	0.139	0.25	1.37	1
Ultrasonic 100 watt	4.7	5.7	0.148	0.27	1.44	1.05
Ultrasonic 200 watt	4.9	6.2	0.168	0.28	1.23	0.7
Ultrasonic 350 watt	4.92	9.9	0.159	0.29	1.45	0.95

Table XXIII

Average tensile strength and ductility of test pieces plated with nickel-iron coating.

Method of Agitation	Average load at failure kN	Average U.T.S. kN/mm ²	Average true U.T.S. kN/mm ²	Average elongation %
Air	6.38	0.284	0.456	22
Ultrasonic 100 watt	6.83	0.305	0.466	28.56
Ultrasonic 200 watt	6.8	0.303	0.47	31.1
Ultrasonic 350 watt	7.15	0.319	0.475	34.75

8.3 Structure.

8.3.1 Nickel-Cobalt.

The structures of the nickel-cobalt alloy electrodeposits plated from solution containing 10 g/l cobaltous sulphate were examined by transmission electron microscopy.

The following samples were deposited from nickel-cobalt solution containing 10 g/l cobaltous sulphate and examined.

- i) Air agitated
- ii) Ultrasonically agitated 20 watts.
- iii) Ultrasonically agitated 100 watts.
- iv) Ultrasonically agitated 200 watts.
- v) Ultrasonically agitated 350 watts.

Figures 23 to 27 illustrate a selection of the structures and diffraction patterns, deposited at 4 A/dm^2 , pH 4 and 55°C .

Fig.23 shows small uniform grains in the deposit but they were somewhat larger than for cobalt alone. Twin bands were usually very clearly defined and twinning was also indicated by the diffraction pattern in Fig.23D.

Deposits obtained at different ultrasonic agitation intensities of 20, 100, 200 and 350 showed a few large

grains with small ones fitted in between. The wide variation in grain size is emphasised by Figs.24 to 27.

8.3.1.1 Nickel-Cobalt Alloy Plating Solution Containing 110 g/l Cobaltous Sulphate.

Thin foils were also prepared from nickel-cobalt deposits plated in solutions containing 110 g/l cobaltous sulphate, using either vigorous air or ultrasonic agitation.

Figures 28 to 33 illustrate a selection of the structures and diffraction patterns, observed by electron microscopy.

The structure of deposits plated by means of air agitation at 4 A/dm^2 , as shown in Figs.28C and D had a very small grain size. The deposits seemed to be stressed as indicated by the diffraction pattern, Fig.28B. The electron diffraction spots were numerous and lay on concentric rings due to the small grain size.

The structure of deposits plated by means of air agitation at 8 A/dm^2 are shown in Fig.29. The grain size was much larger than at 4 A/dm^2 and the stress level was much lower.

Deposits obtained at different ultrasonic intensities of 20, 40, 200 and 350 are illustrated in Figs.30, 31, 32, 33 and emphasise the wide variation in grain size. Twinning appeared to be somewhat more extensive than in deposits plated by means of air agitation and the twin

bands were usually very clearly defined. The diffraction patterns indicate that the deposits were quite highly stressed.

8.3.2 Structure of Cobalt Electrodeposit.

The following samples were prepared from a cobaltous sulphate - cobaltous chloride solution.

- i) Air agitation 4 A/dm^2 .
- ii) Air agitation 8 A/dm^2 .
- iii) Ultrasonic agitation 20 watts.
- iv) Ultrasonic agitation 100 watts.
- v) Ultrasonic agitation 200 watts.

Figs.34 to 38 illustrate a selection of the structures and diffraction patterns, deposited at 4 A/dm^2 and 8 A/dm^2 , pH 4 and 55°C . The deposits plated using air agitation at 4 A/dm^2 had fairly uniform grain size as shown in Fig.34 but a few large grains occurred. The deposits seemed to be stressed as indicated by the streaky diffraction pattern shown in Fig.34D.

As the current density increased to 8 A/dm^2 the grains became much smaller as shown in Fig.35 and the electron diffraction spots became more numerous as the grain size decreased and lay on concentric rings as shown in Fig.35D. The deposits seemed to be stressed.

Ultrasonic agitation resulted in a mixed grain size,

some very large grain occurred in the deposits produced using 20 watts ultrasonic agitation. The structures are illustrated in Figs.36 to 38. The deposits produced using ultrasonic agitation were less stressed than those produced using air.

8.3.3 Structure of Nickel-Iron Deposits.

The following samples were prepared from a commercial bright nickel-iron solution:

- i) Air agitation 4 A/dm².
- ii) Air agitation 8 A/dm².
- iii) Ultrasonic agitation 20 watts.
- iv) Ultrasonic agitation 40 watts.
- v) Ultrasonic agitation 100 watts.
- vi) Ultrasonic agitation 200 watts.
- vii) Ultrasonic agitation 350 watts.

Figures 39-45 illustrate a selection of the structures and diffraction patterns, deposition having been carried out at 4 A/dm² and 8 A/dm², pH 4 and 68°C. The grain size of deposits obtained from the nickel-iron solution were so small that resolution of the structure was hardly possible even at a magnification of 500000 times.

The structures in Figs. 39 to 45 appeared to be almost identical regardless of the plating conditions. From results already obtained, it is apparent that organic additions which significantly affect physical and

mechanical properties also lead to a reduction in grain size.

The diffraction patterns obtained from all these deposits confirm that the grain size is extremely small resulting in complete rings of spots, as shown in Figs. 39D, 40D, 41D, 42D, 43D, 44D and 45D.

8.3.4 Determination of the Structure of Nickel-Iron Alloy Plated Deposits using X-Ray Techniques.

The results obtained from x-ray diffraction of nickel-iron alloy deposits are recorded in Table XXIV. For each diffraction trace obtained, the 2θ angles were recorded for diffraction peaks and the "d" spacings calculated.

Attempts were then made to index the diffraction data by reference to the ASTM powder diffraction file. The samples selected for investigation were as follows:

Air agitated 4 A/dm².

Ultrasonically agitated 350 watts.

In the case of air agitated samples, the "d" spacings were indexed as FCC structure iron, and the ultrasonically deposited alloy as a mixture of FCC and BCC iron at room temperature.

The following formulae were used to calculate the "d"

spacing of peaks and lattice parameters "a".

$$n\lambda = 2d\sin\theta$$

Bragg's law

and

$$a = d\sqrt{h^2 + k^2 + l^2}$$

where " λ " the wave length of cobalt is 1.791\AA , " 2θ " is the diffraction angle and "n" the other order of reflection which is equal to 1.

It has been shown that nickel-iron electrodeposits appear to be a mixture of FCC and BCC iron structures at room temperature when deposited using ultrasonic agitation but a BCC iron structure only was obtained at room temperature when using air agitation.

8.3.4.1 Plane Orientation of the Nickel-Iron Structure.

The crystal orientations of the air and ultrasonic agitated alloy deposits were found by determining their (200) pole figures, using the Schulz back reflection x-ray diffraction method.

By providing simultaneously a fast rotation through the angle ψ with a slow rotation through the angle ϕ , the diffracted intensity was determined along a spiral trace as indicated in Fig.(46). Typically, the radial angle ϕ is changed by 5° during a complete revolution around the ψ axis.

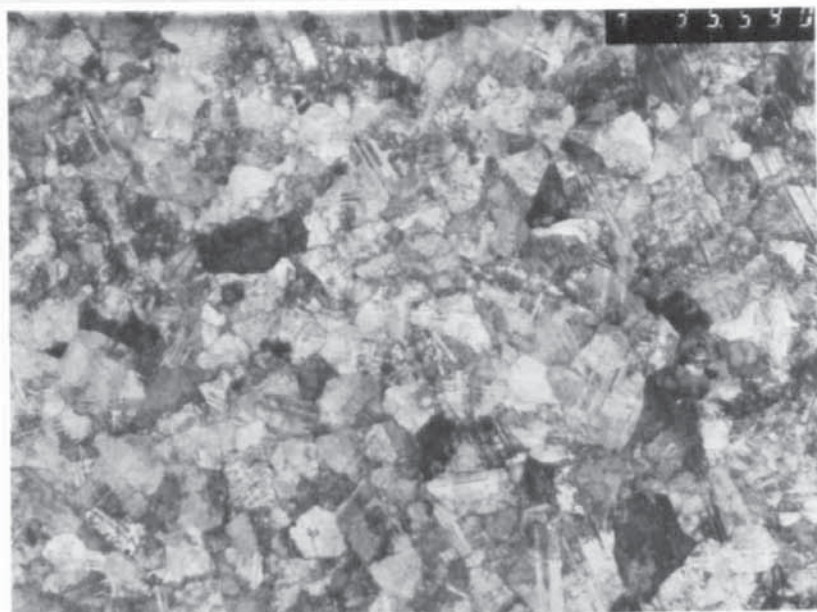
Positions of high measured intensity on sequential laps of the spiral track are then used to locate regions of high pole density on the pole figure, with points of equal intensity being joined together along contour lines.

Due to the similarity between the Bragg angles M_0K_α (Fe = 23.1° ; Ni = 23.2°) of the (200) peaks for Fe (FCC) and for Ni, separate pole figures could not be obtained. Consequently only one pole figure was determined showing the distribution of (200) planes for both nickel and iron (FCC). The results obtained from x-ray diffraction showed that the nickel-iron alloy deposit had a mixed [100] and [111] fibre texture for both air and ultrasonically agitated solutions.

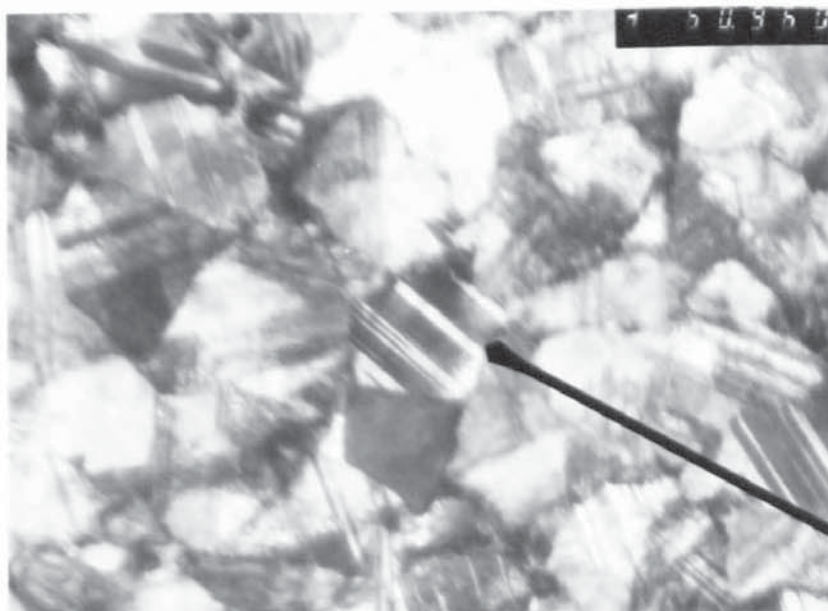
Table XXIV

Results obtained from x-ray diffraction of nickel-iron deposits, using either air or ultrasonic agitation.

Metal	{hkl}	ASTM Powder Index Information		Experimental Results		
		d, A°	2 θ Cobalt	d, A°	2 θ Cobalt	a, A°
Nickel FCC	111	2.034	52.21	2.050	51.8	3.55
	200	1.762	61.06	1.775	60.6	3.55
	220	1.246	91.84	1.248	91.7	3.53
	311	1.062	114.88	1.066	114.3	3.54
	222	1.017	123.32	1.02	122.8	3.53
Iron FCC Austenite (γ)	111	2.052	51.7	2.08	51.0	3.6
	200	1.777	60.49	1.805	59.5	3.61
	220	1.257	90.8	1.265	90.1	3.58
	311	1.072	113.23	1.078	112.3	3.58
	222	1.026	121.5	1.038	119.2	3.6
Iron BCC Ferrite (α)	110	2.027	52.41	2.039	52.1	2.884
	200	1.433	77.31	1.434	77.3	2.868
	211	1.170	99.82	1.171	99.8	2.868

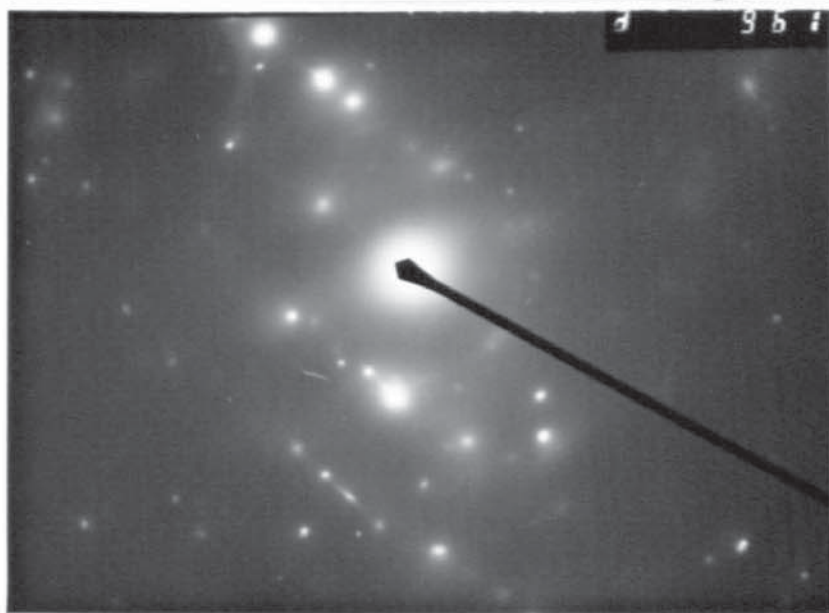


A Magnification X 35000

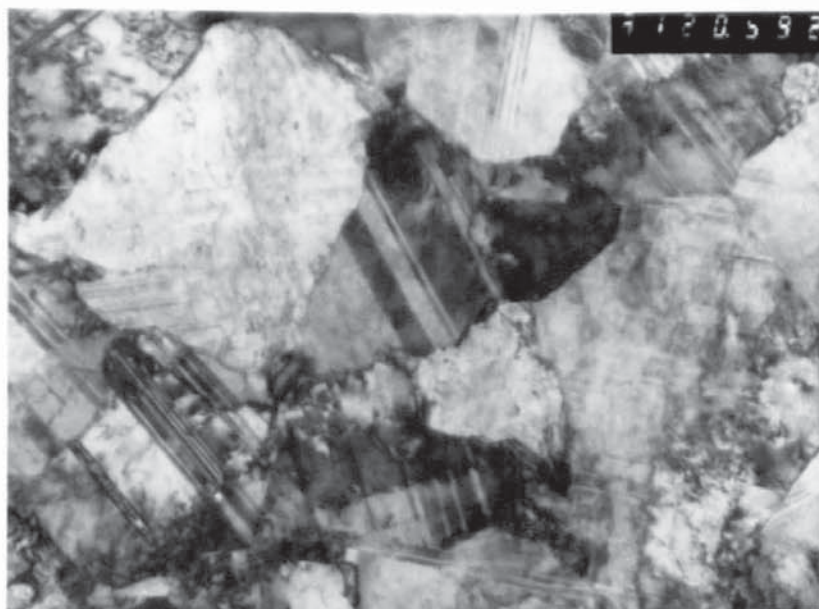


B Magnification X 60000

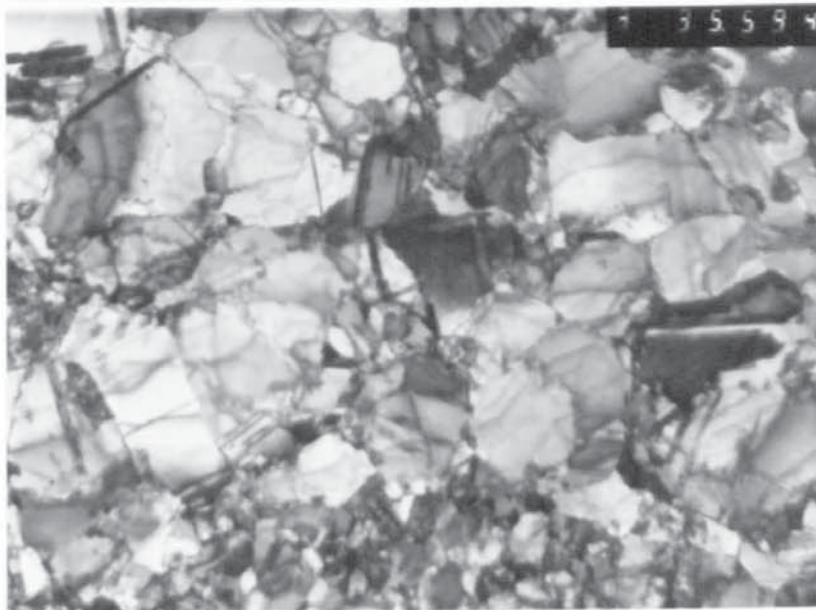
Fig.(23) T.E.M. micrographs of nickel-cobalt alloy deposit plated from solution containing 10 g/l $\text{CoSO}_4 \cdot 7\text{H}_2\text{O}$ at 4 A/dm^2 , 55°C and pH 4. Air agitated.



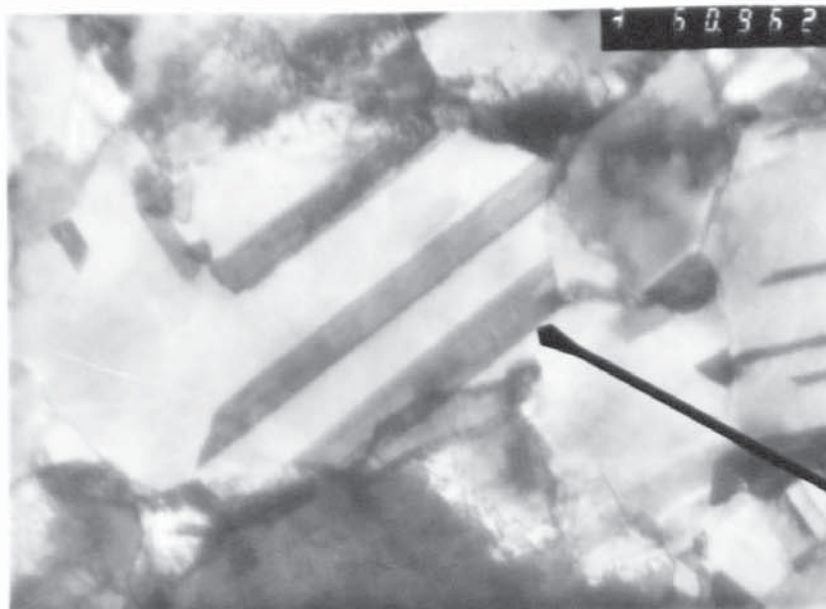
C Diffraction pattern of a grain shown in Fig.(23)B



D Magnification X 120000



A Magnification X 35000

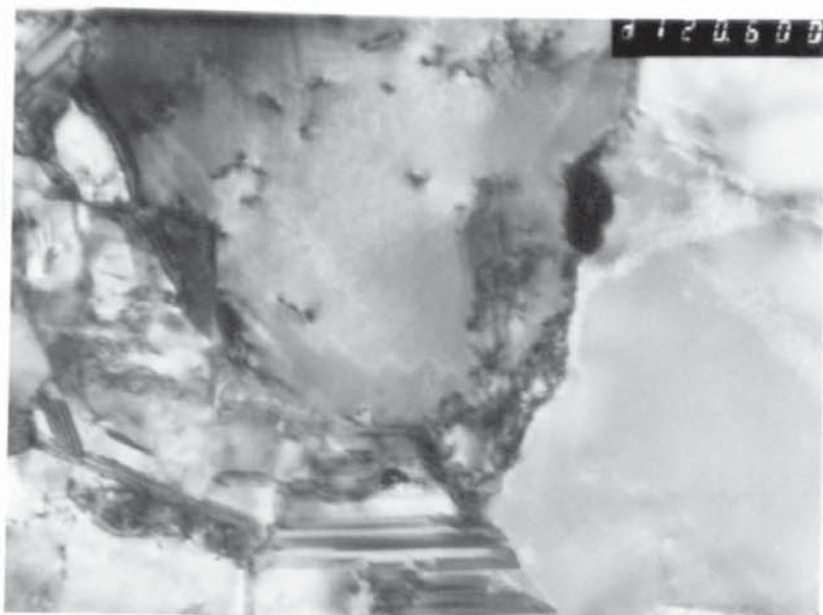


B Magnification X 60000

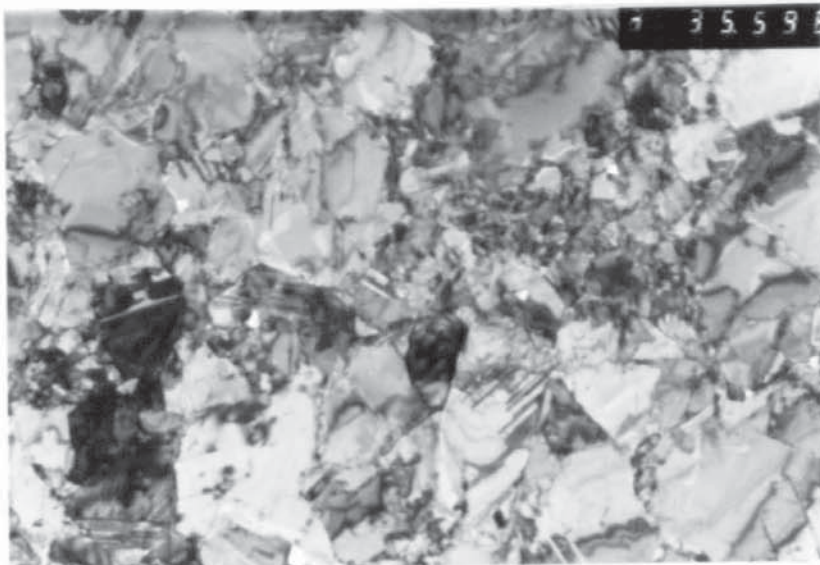
Fig.(24) Conditions as in Fig.(23) but
ultrasonically agitated 20 watts.



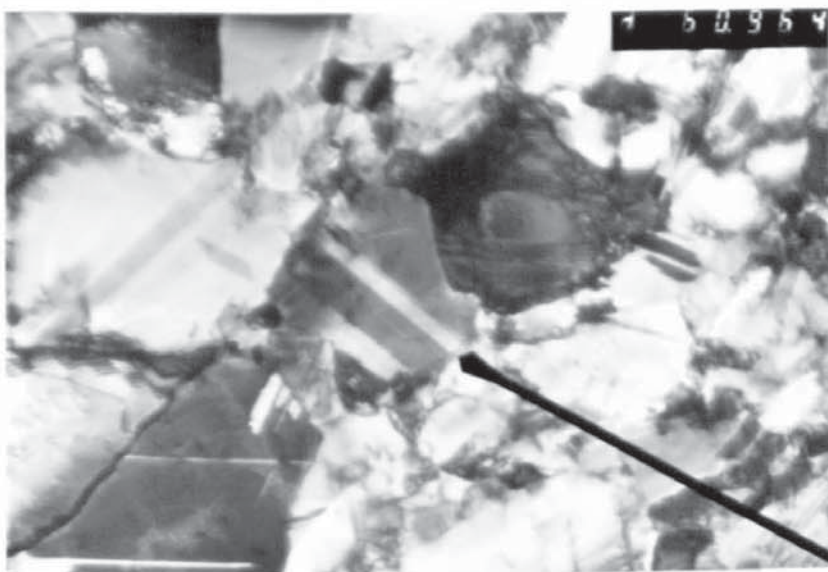
C Diffraction pattern of a grain shown in Fig. (24)B



D Magnification X 120000



A Magnification X 35000



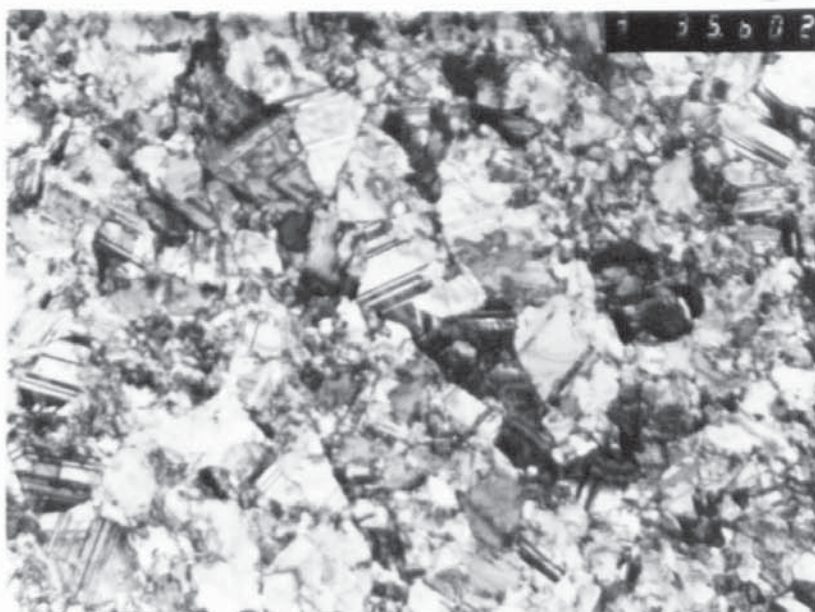
B Magnification X 60000



C

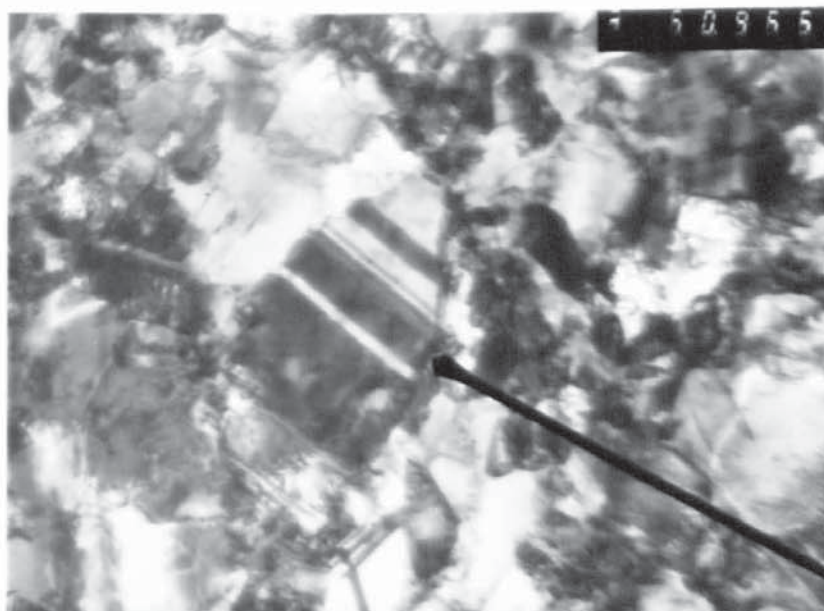
Diffraction pattern of a grain shown in Fig.(25)B

Fig.(25) Conditions as in Fig.(23) but
ultrasonically agitated 100 watts.



A

Magnification X 35000

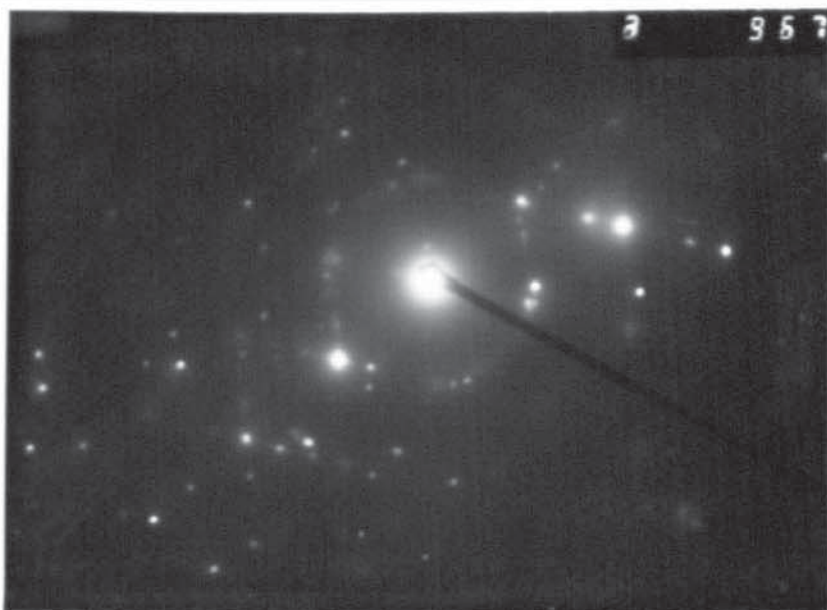


B

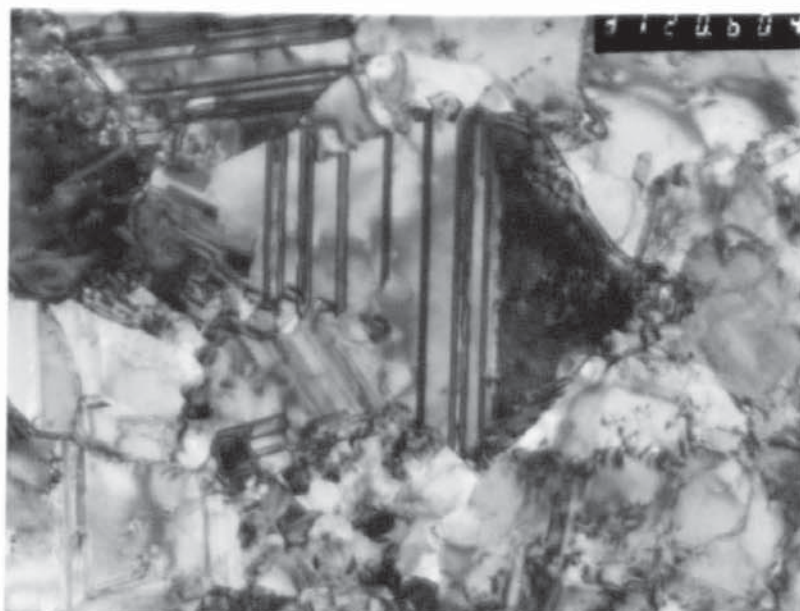
Magnification X 60000

Fig.(26) Conditions as in Fig.(23) but ultrasonically agitated 200 watts.

C

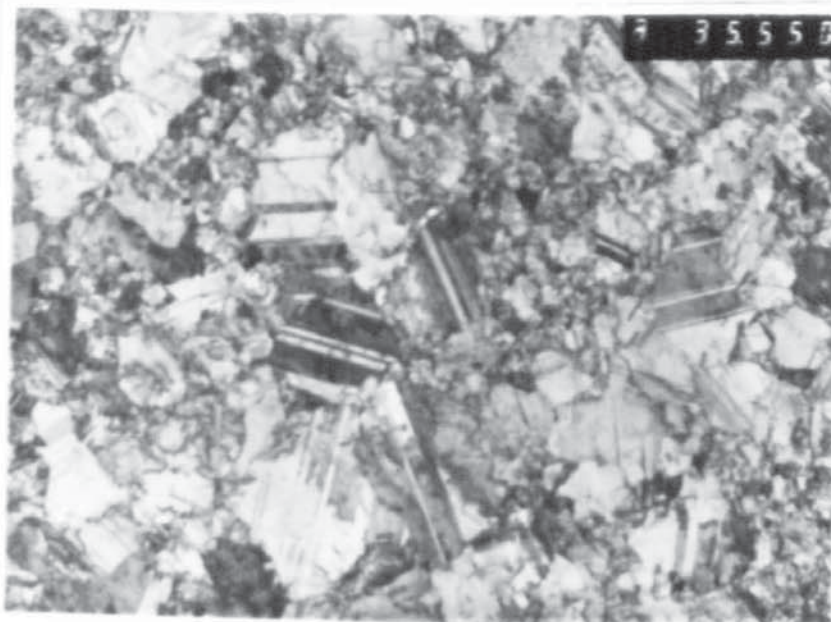


Diffraction pattern of a grain shown in Fig.(26)B



D

Magnification X 120000

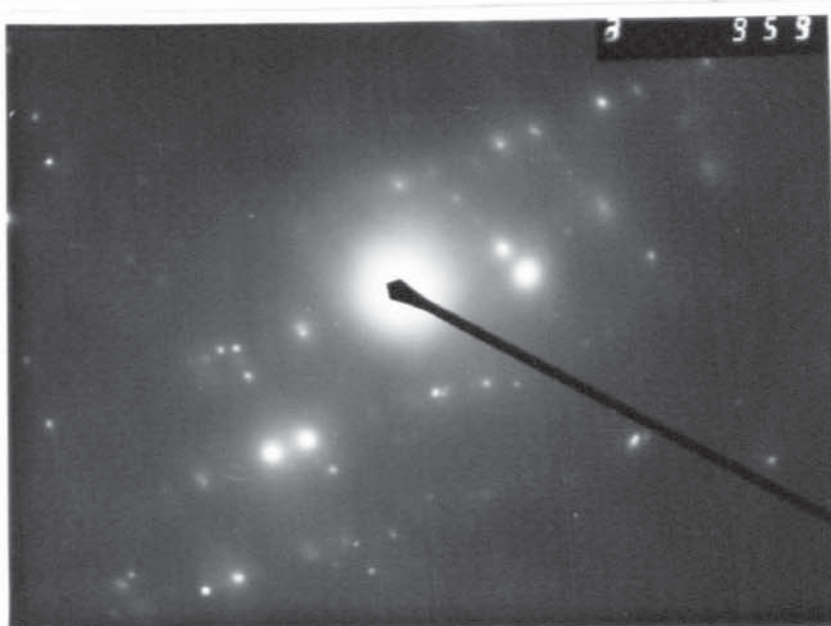


A Magnification X 35000



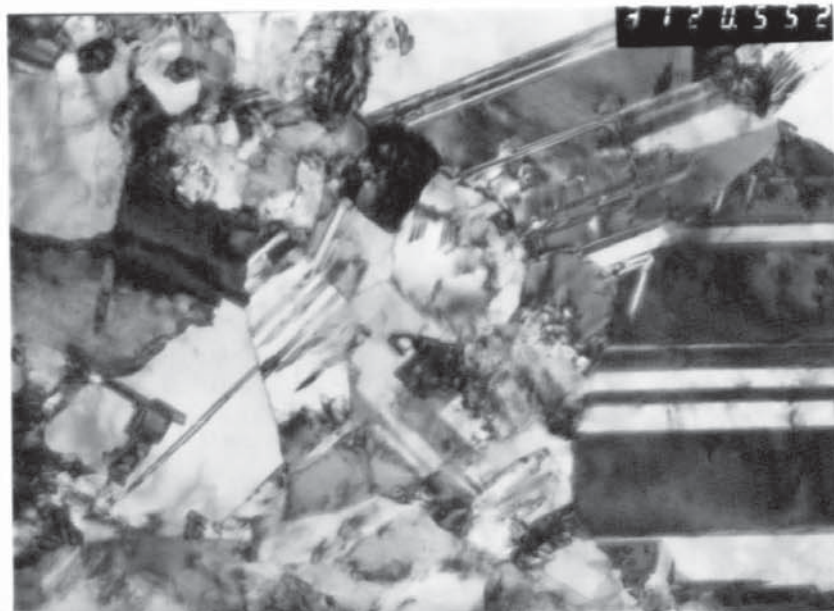
B Magnification X 60000

Fig.(27) Condition as in Fig.(23) but
ultrasonically agitated 350 watts.



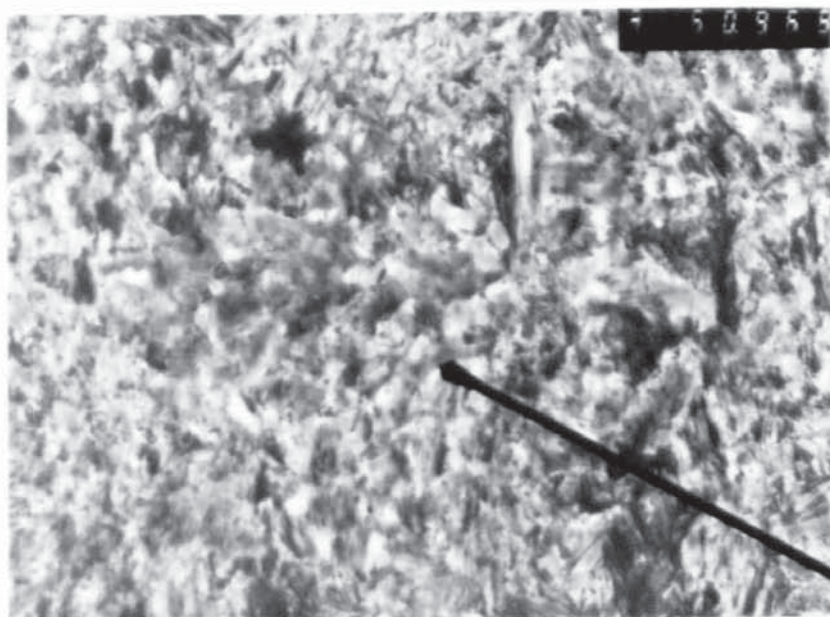
C

Diffraction pattern of a grain shown in Fig.(27)B

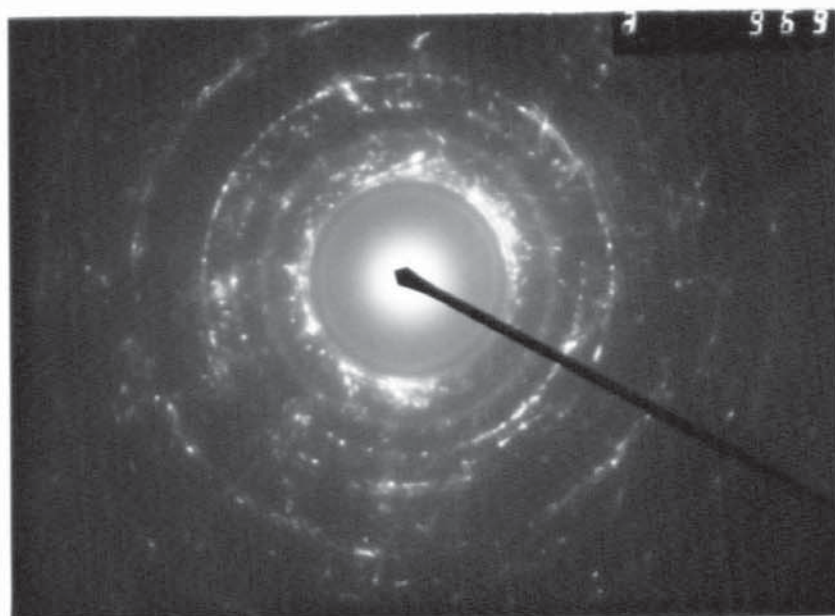


D

Magnification X 120000

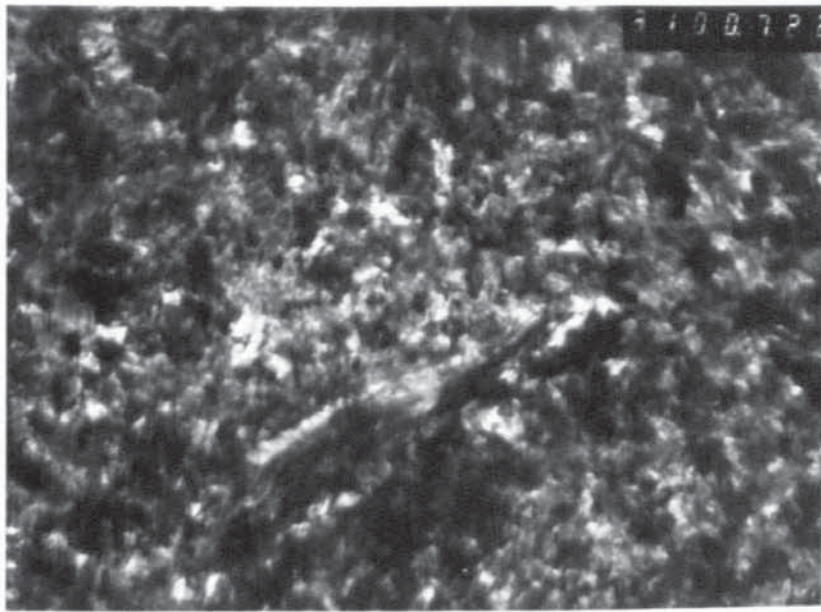


A Magnification X 60000

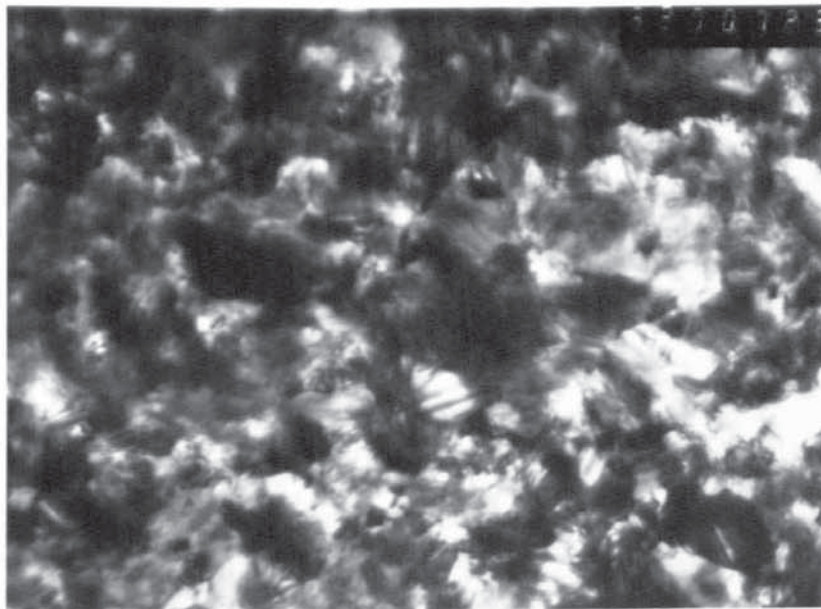


B Diffraction pattern of a grain shown in Fig.(28)A

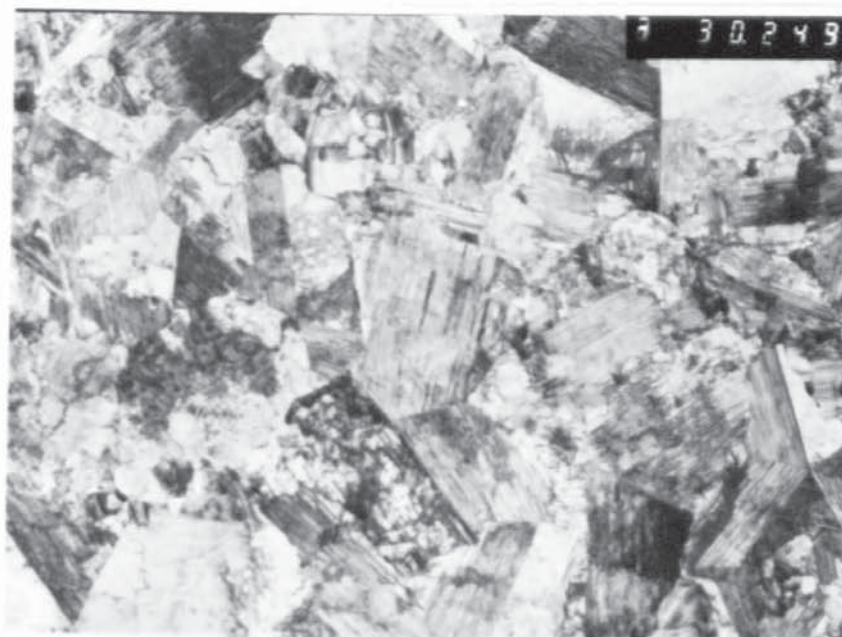
Fig.(28) Transmission electron micrograph of Ni-Co alloy deposit plated from solution containing 110 g/l $\text{CoSO}_4 \cdot 7\text{H}_2\text{O}$ at 4 A/dm², 55°C and pH 4. Air agitated.



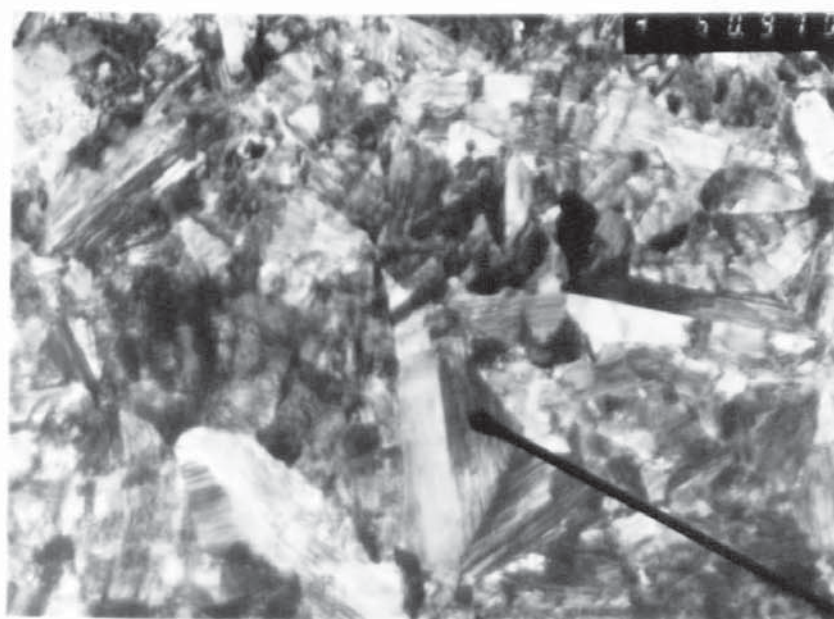
C Magnification X 100000



D Magnification X 200000

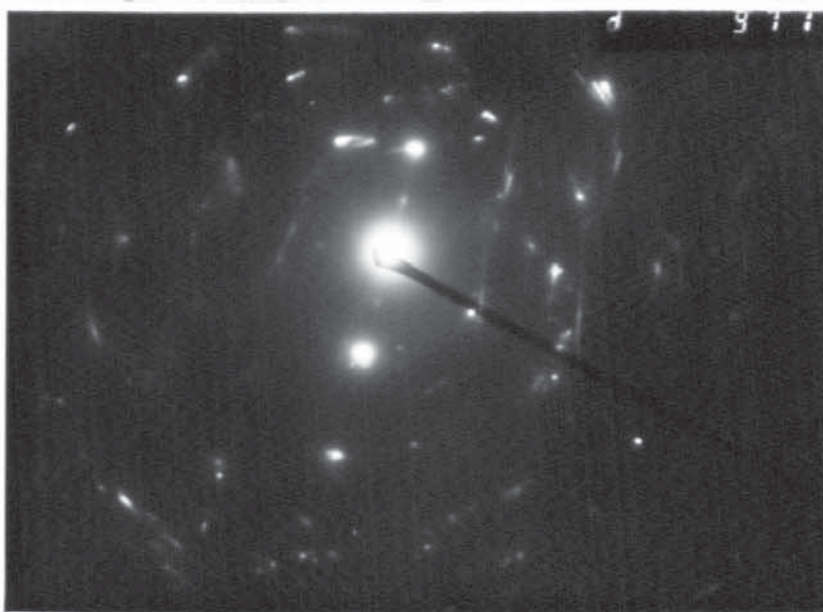


A Magnification X 30000

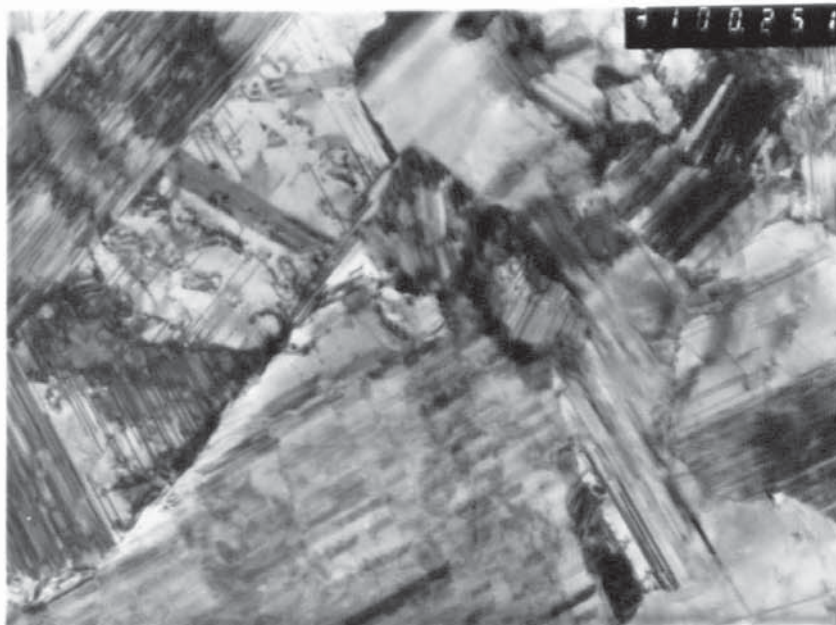


B Magnification X 60000

Fig.(29) Conditions as in Fig.(28) but
C.D. used 8 A/dm^2 , air agitated.



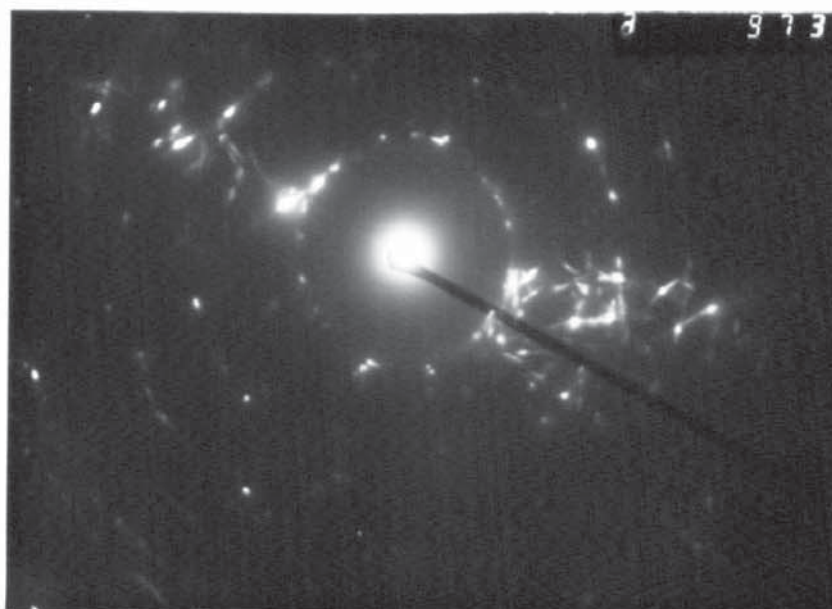
C Diffraction pattern of a grain shown in Fig.(29)B



D Magnification X 100000



A Magnification X 60000

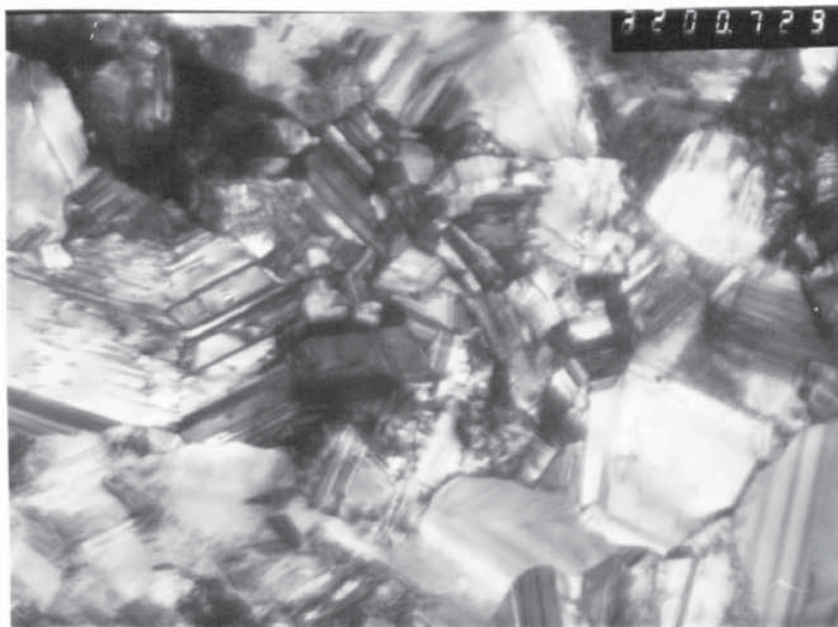


B Diffraction pattern of a grain shown in Fig.(30)A

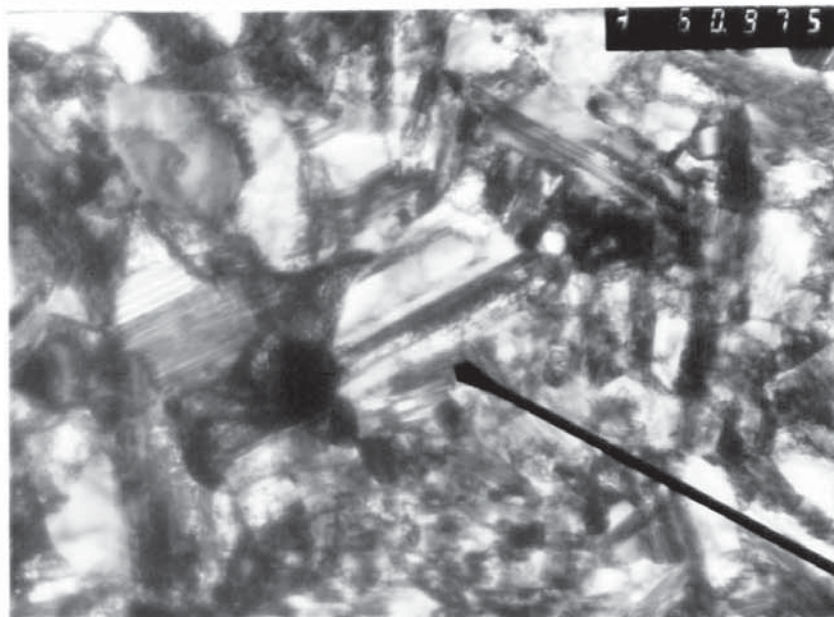
Fig.(30) Conditions as in Fig.(28) but
ultrasonically agitated 20 watts.



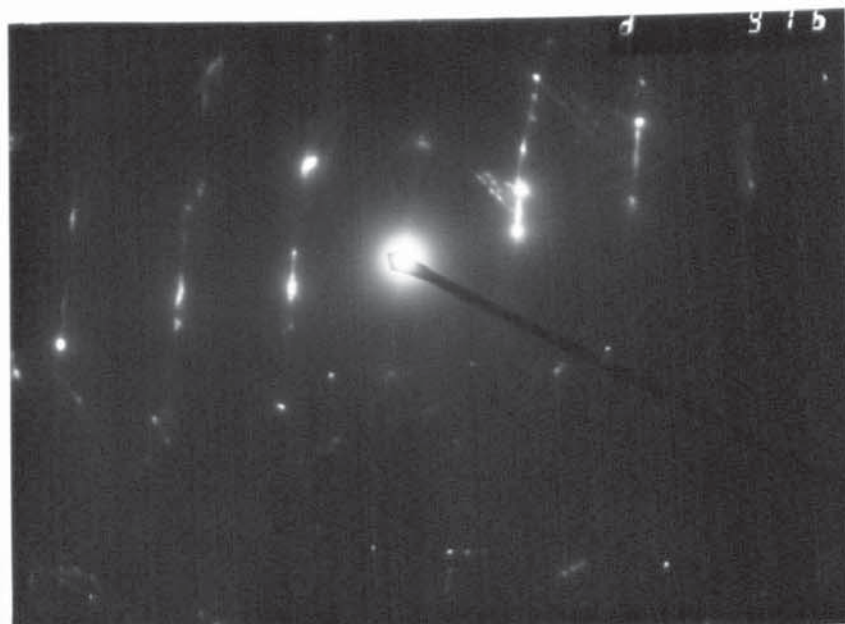
C Magnification X 100000



D Magnification X 200000

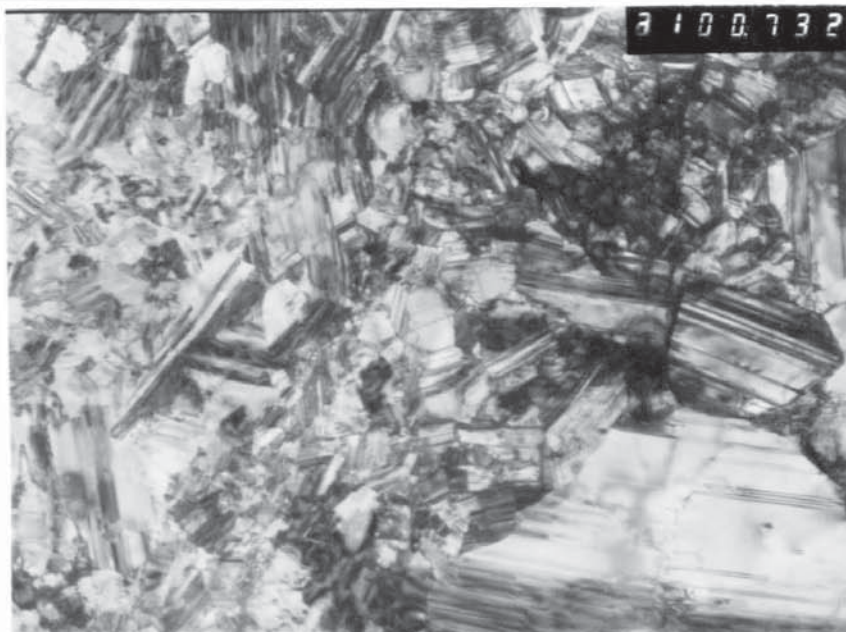


A Magnification X 60000

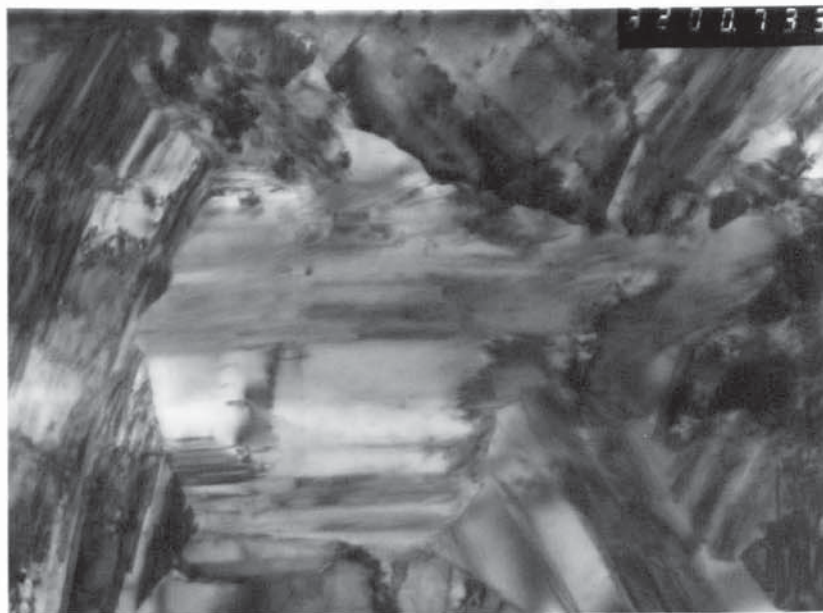


B Diffraction pattern of a large grain shown in Fig.(31)A

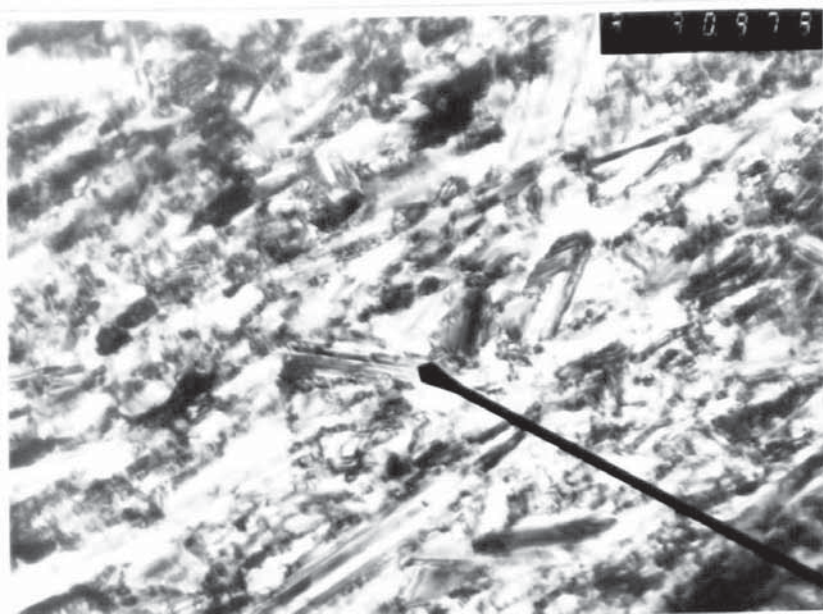
Fig.(31) Conditions as in Fig.(28) but ultrasonically agitated 40 watts.



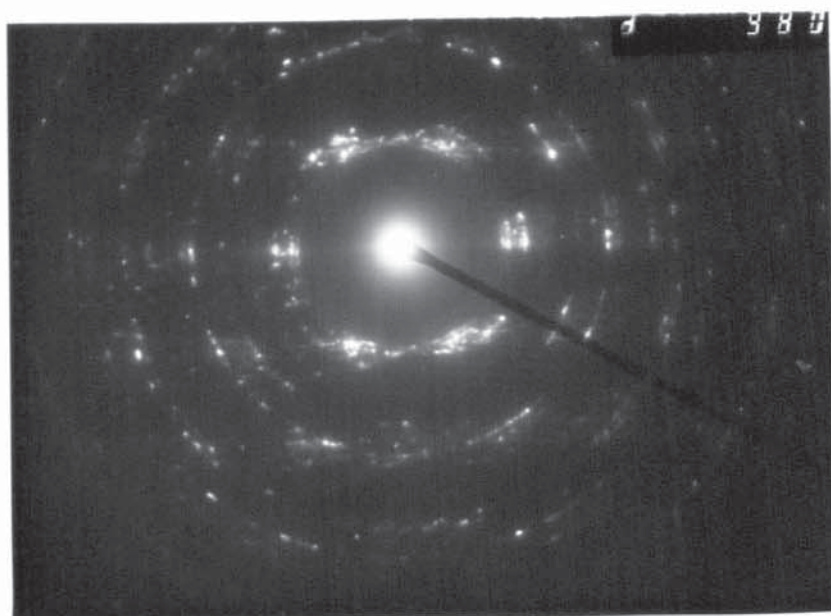
C Magnification X 100000



D Magnification X 200000



A Magnification X 90000

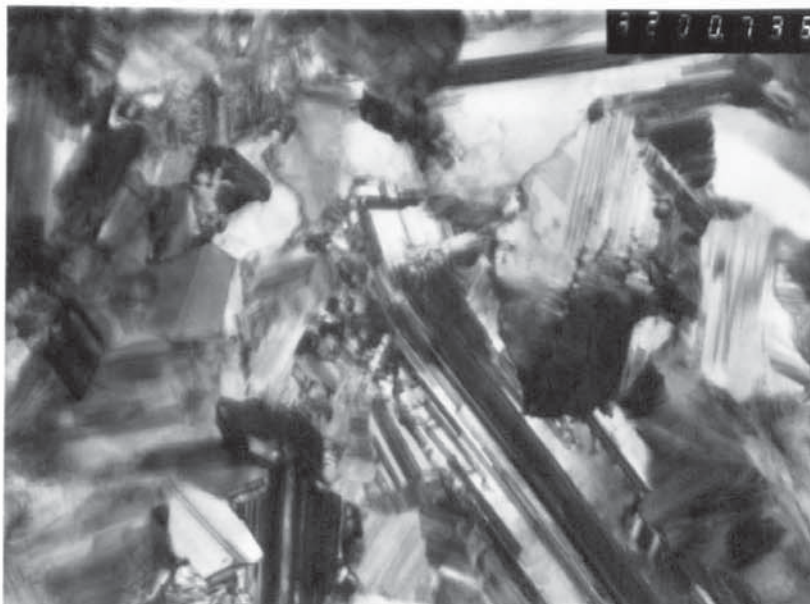


B Diffraction pattern of a large grain shown in Fig.(32)A

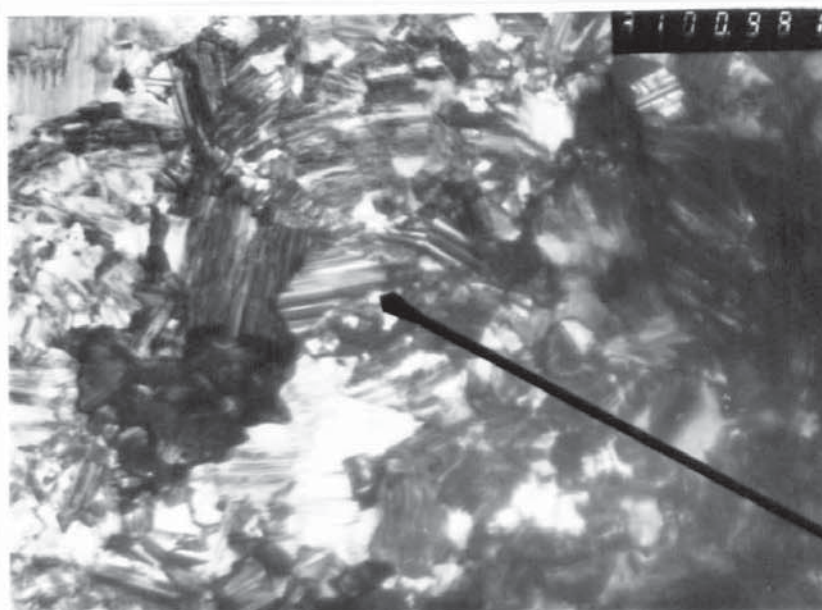
Fig.(32) Conditions as in Fig.(28) but ultrasonically agitated 200 watts.



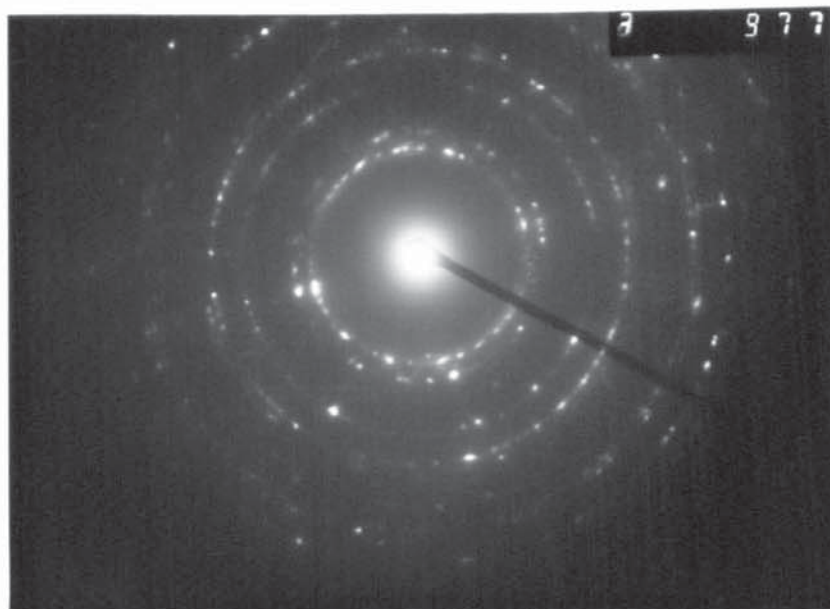
C Magnification X 100000



D Magnification X 200000

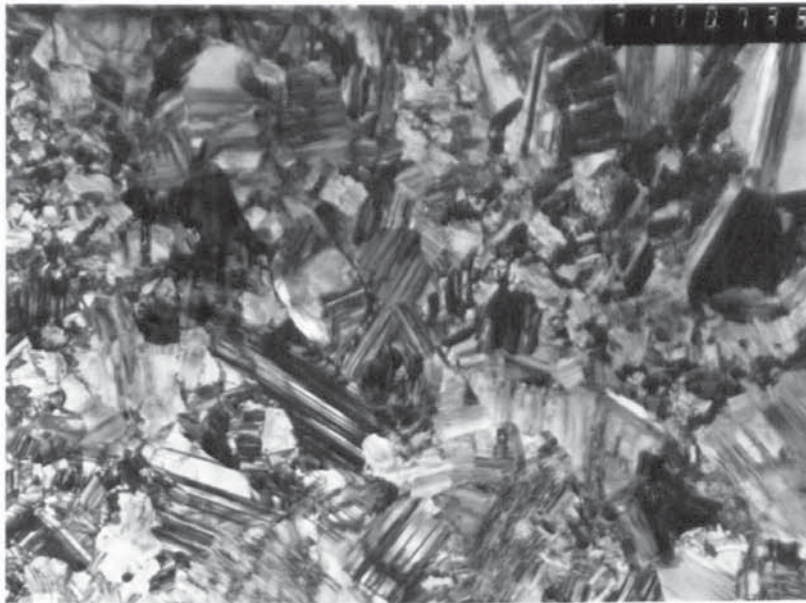


A Magnification X 100000



B Diffraction pattern of a large grain shown in Fig.(33)A

Fig.(33) Condition as in Fig.(28) but ultrasonically agitated 350 watts.



C Magnification X 100000



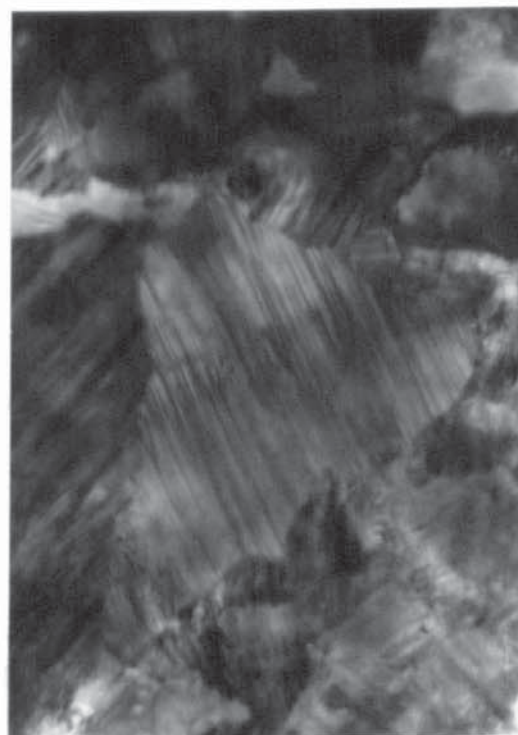
D Magnification X 200000



A Magnification X 60000



B Magnification X 100000

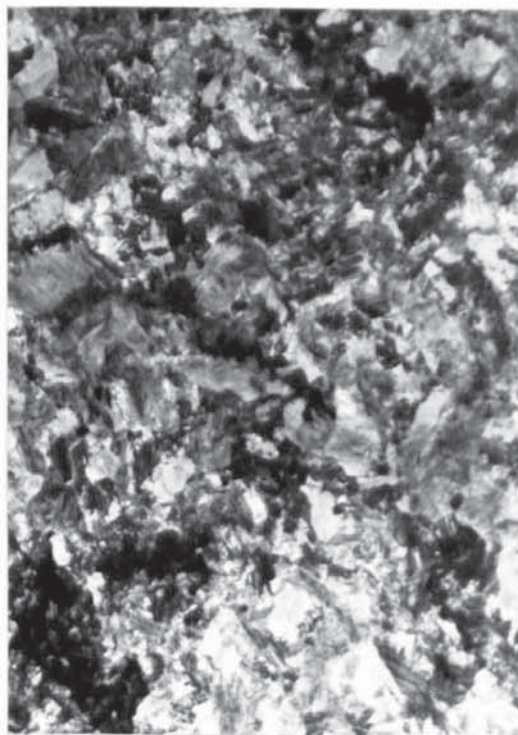


C Magnification X 200000

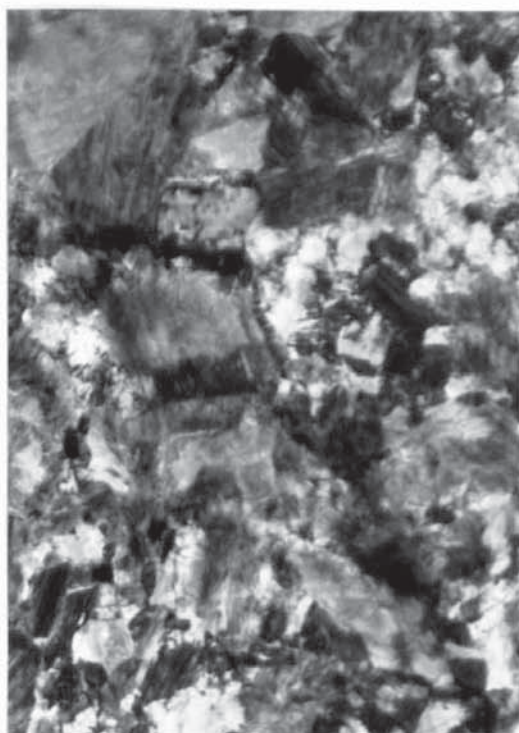


D Diffraction pattern of a large grain shown in Fig.(34)**C**

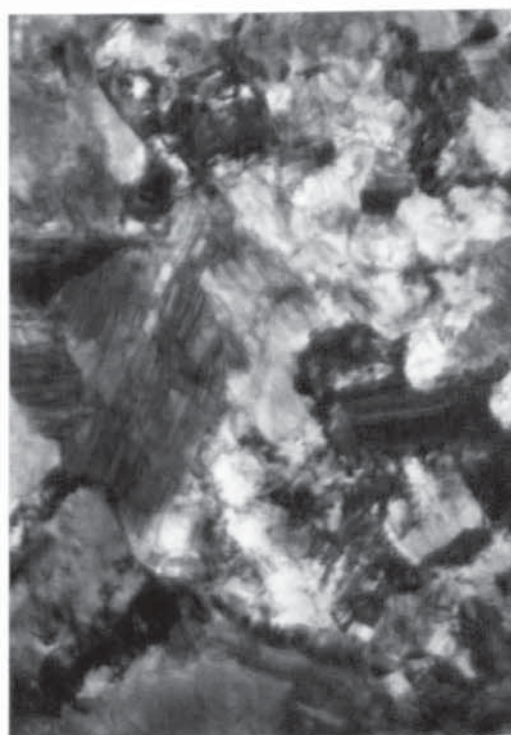
Fig.(34) T.E.M. micrograph of cobalt deposit plated at 4 A/dm², 55°C and pH 4, air agitated.



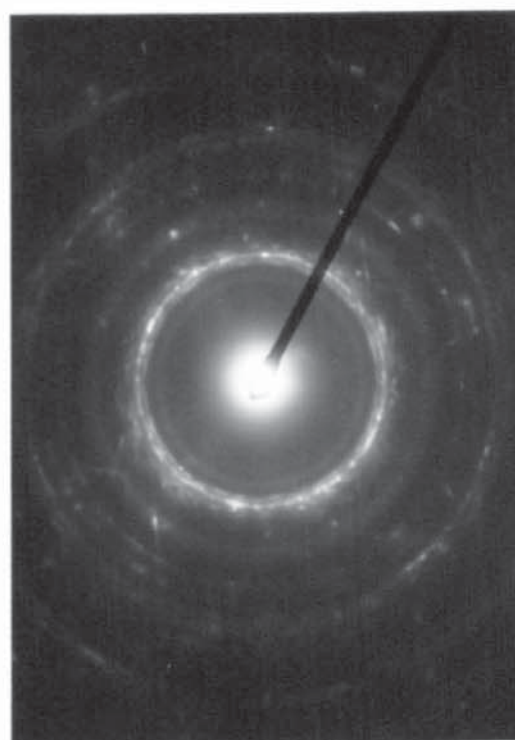
A Magnification X 60000



B Magnification X 100000



C Magnification X 200000

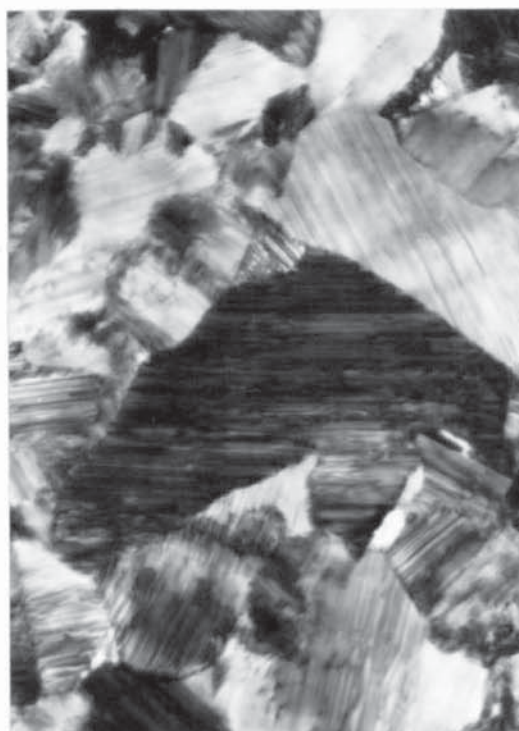


D Diffraction pattern of a large grain shown in Fig.(35)C

Fig.(35) Conditions as in Fig.(34) but deposit plated at $8A/dm^2$



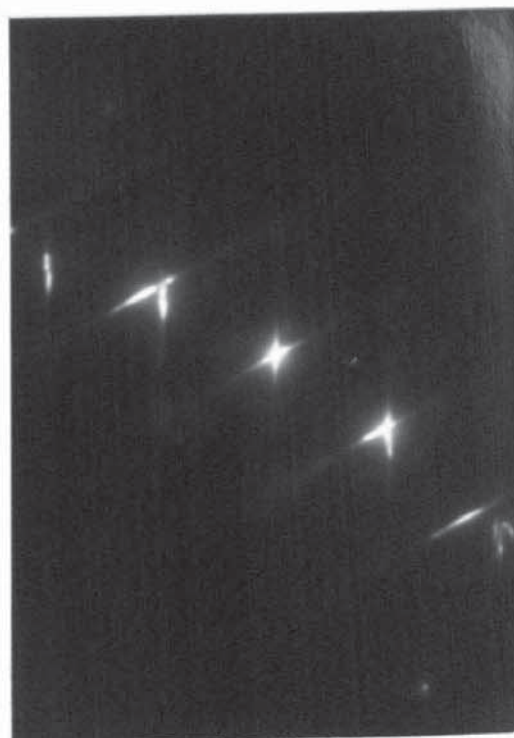
A Magnification X 60000



B Magnification X 100000



C Magnification X 200000

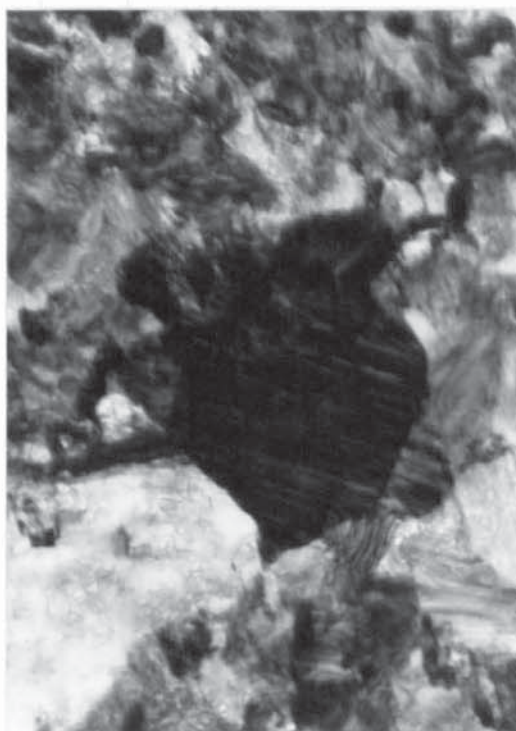


D Diffraction pattern of a large grain shown in Fig. (36)C

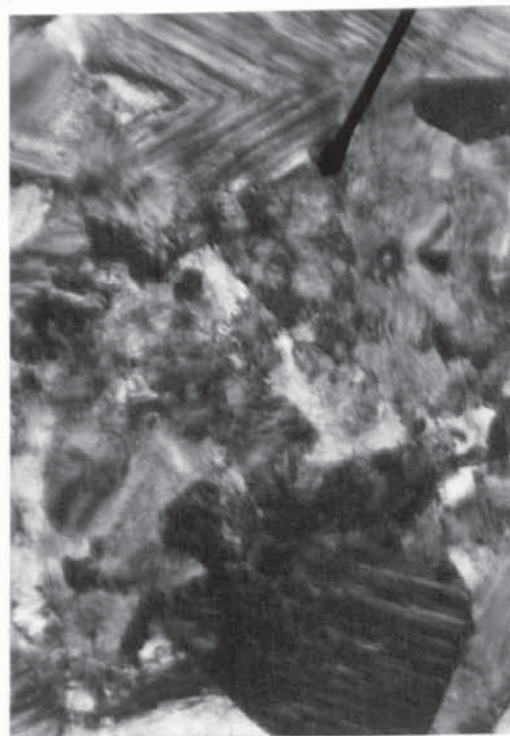
Fig. (36) Conditions as in Fig. (34) but ultrasonically agitated 20 watts.



A Magnification X 60000



B Magnification X 100000

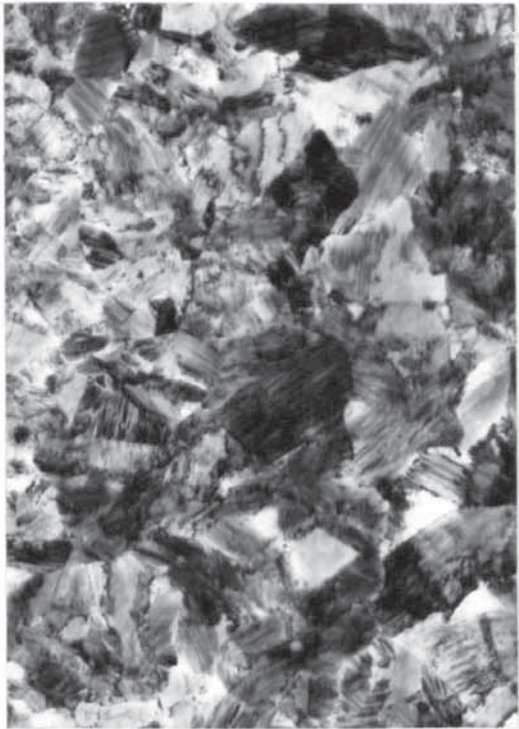


C Magnification X 200000

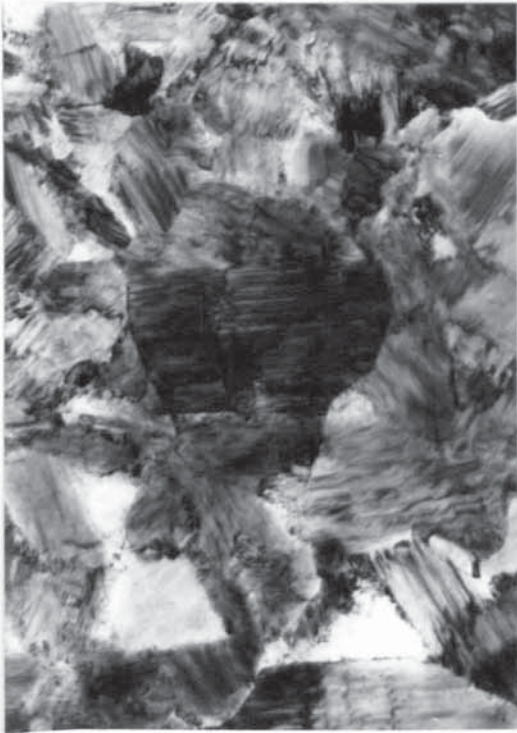


D Diffraction pattern obtained from a grain shown in Fig.(37)
C

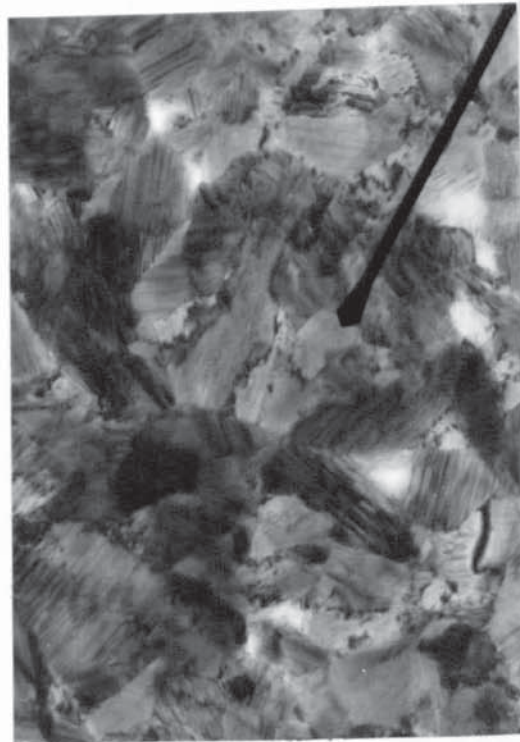
Fig.(37) Conditions as in Fig.(34) but ultrasonically agitated 100 watts



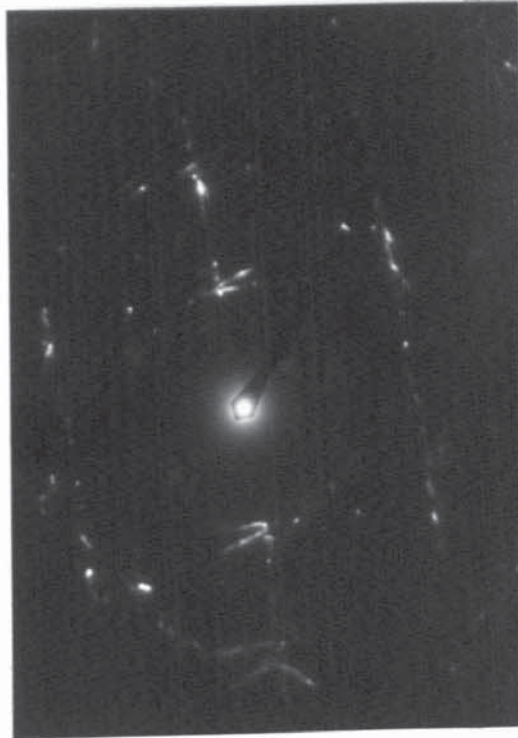
A Magnification X 60000



B Magnification X 100000

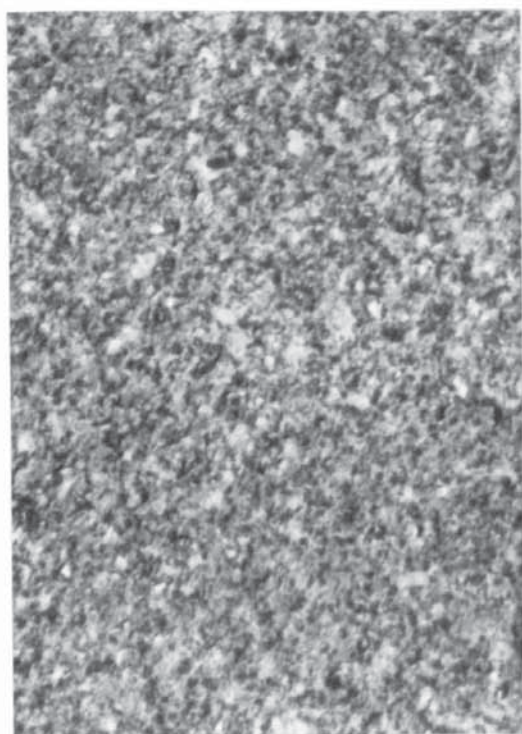


C Magnification X 200000

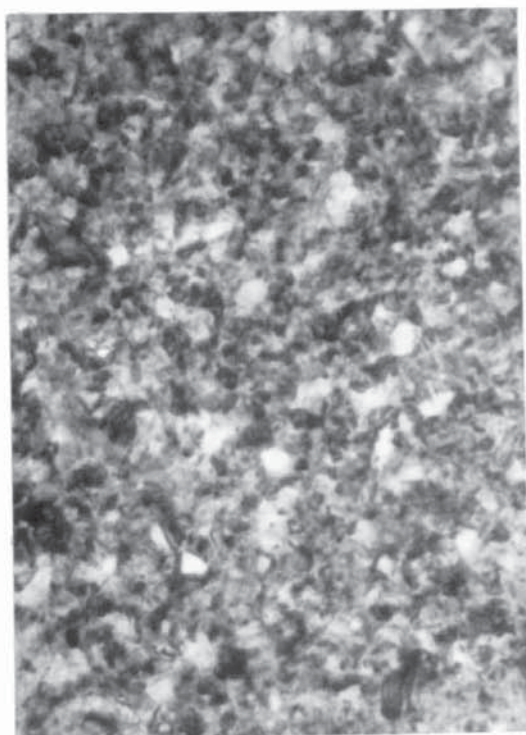


D Diffraction pattern of a large grain shown in Fig.(38)**C**

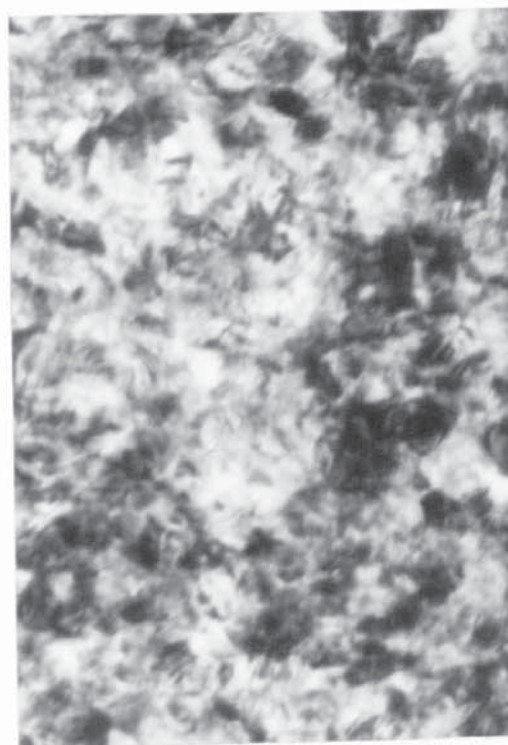
Fig.(38) Conditions as in Fig.(34) but ultrasonically agitated 200 watts



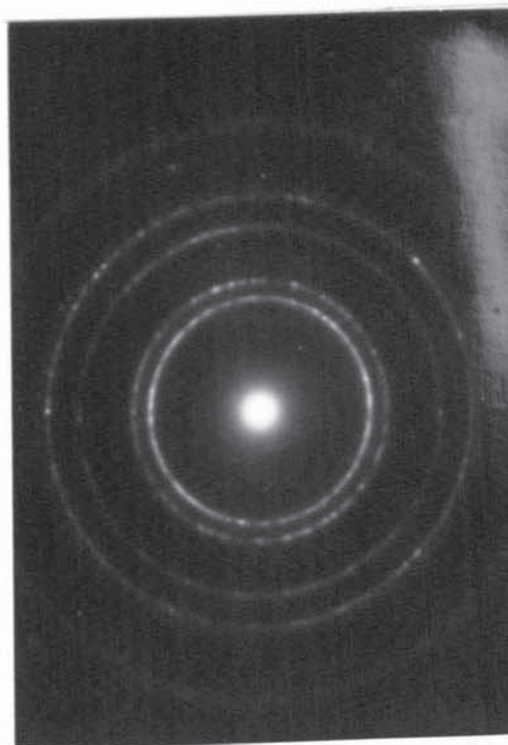
A Magnification X 100000



B Magnification X 250000

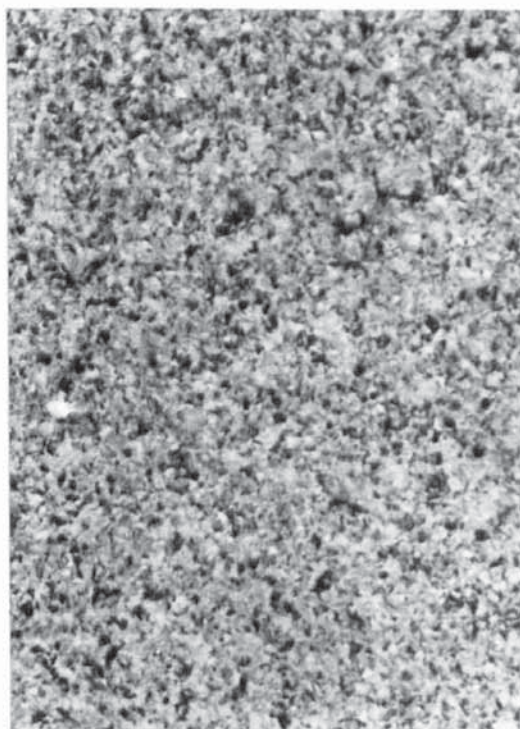


C Magnification X 500000

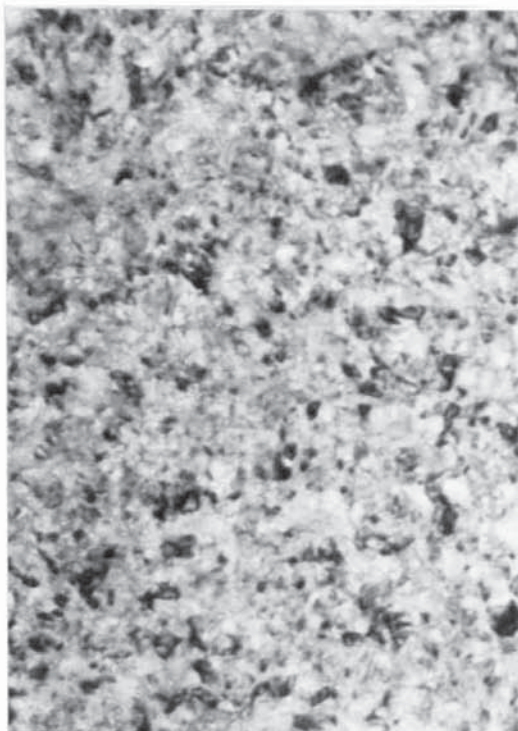


D Diffraction pattern
of grains in deposit

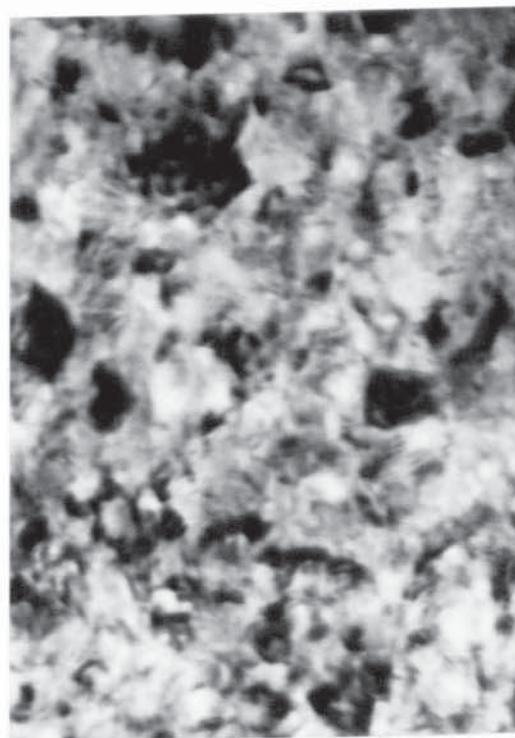
Fig. (39) S.E.M. micrograph of nickel-iron alloy deposit plated at 4A/dm^2 , 68°C and pH4, air agitated.



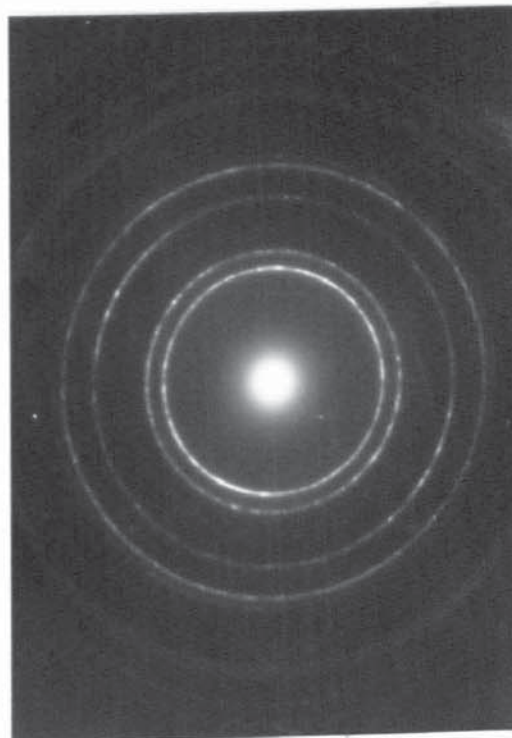
A Magnification X 100000



B Magnification X 250000

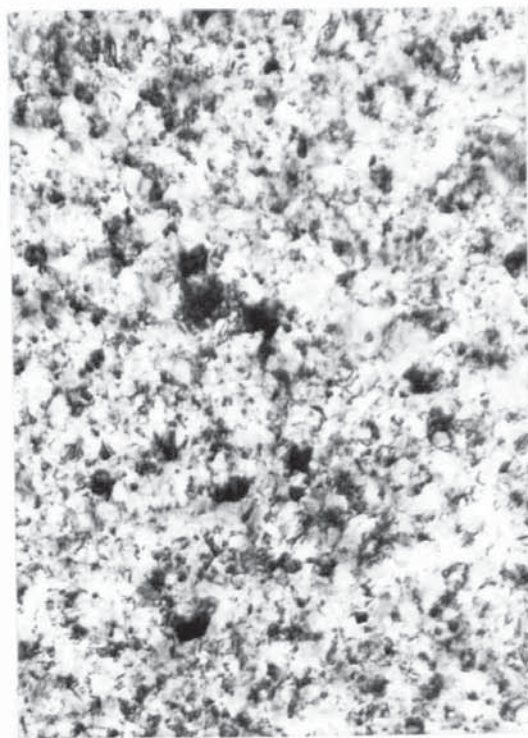


C Magnification X 500000

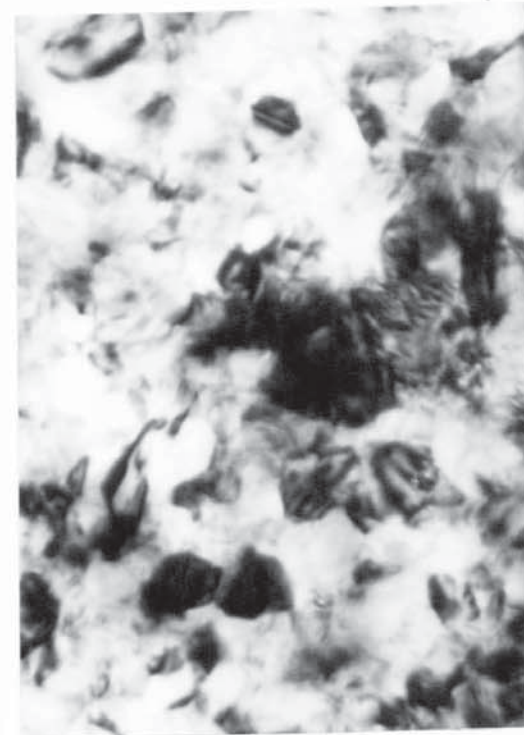


D Diffraction pattern
of grains in deposit

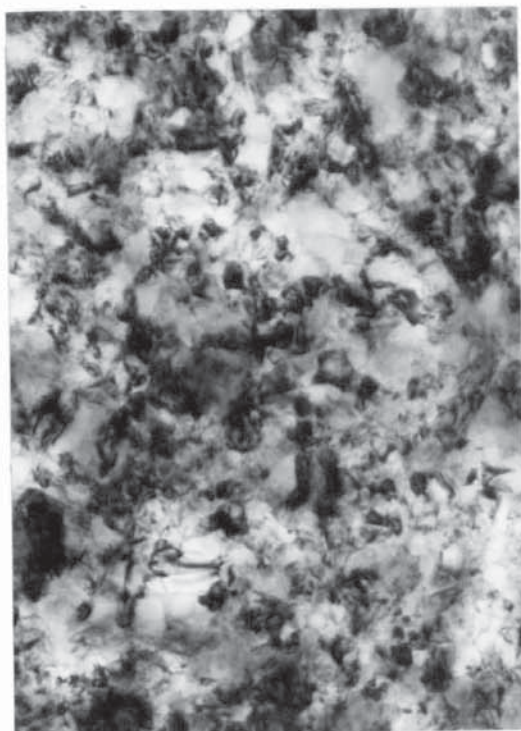
Fig. (40) Conditions as in Fig. (39) but deposit plated at 8 A/dm^2



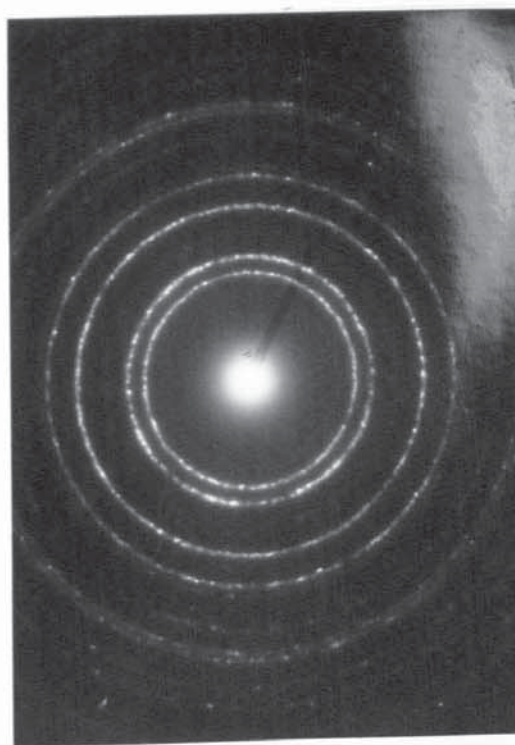
A Magnification X 100000



C Magnification X 500000

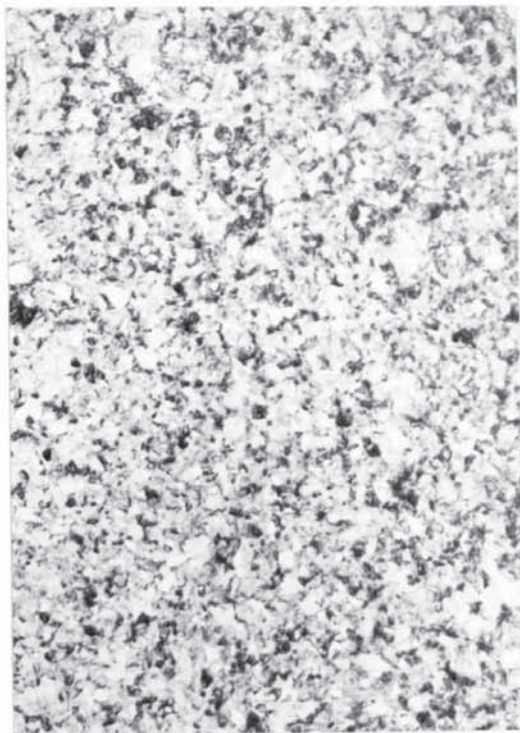


B Magnification X 250000

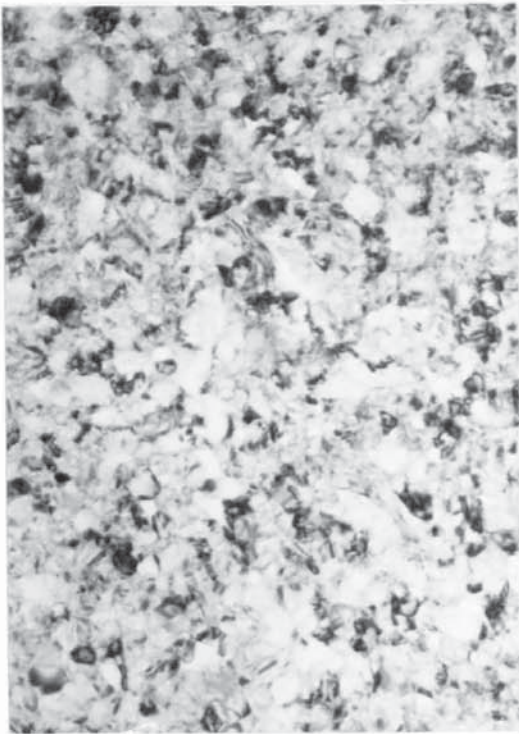


D Diffraction pattern
of grains in deposit

Fig. (41) Conditions as in Fig. (39) but ultrasonically agitated 20 watts



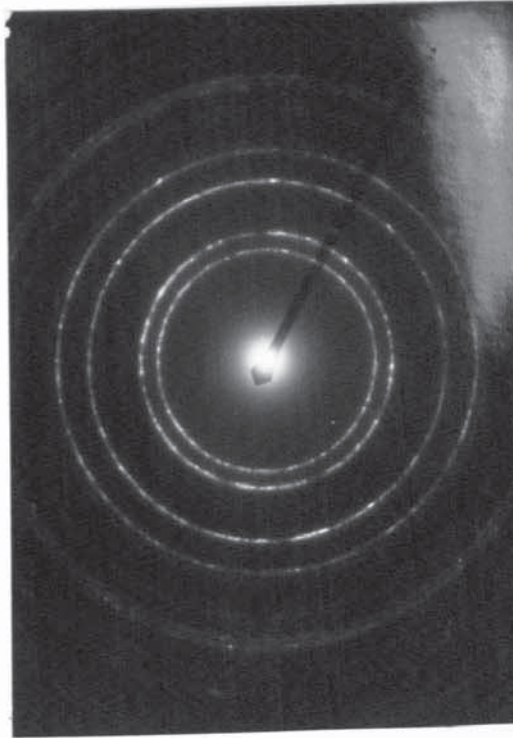
A Magnification X 100000



B Magnification X 250000

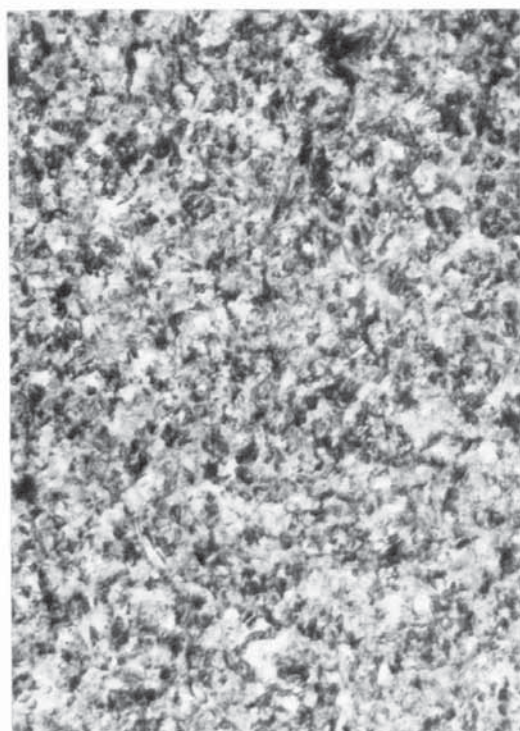


C Magnification X 500000

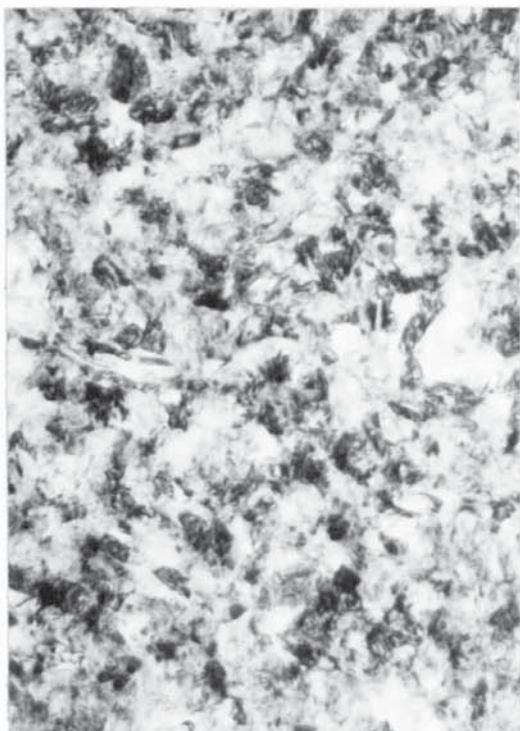


D Diffraction pattern
of grains in deposit

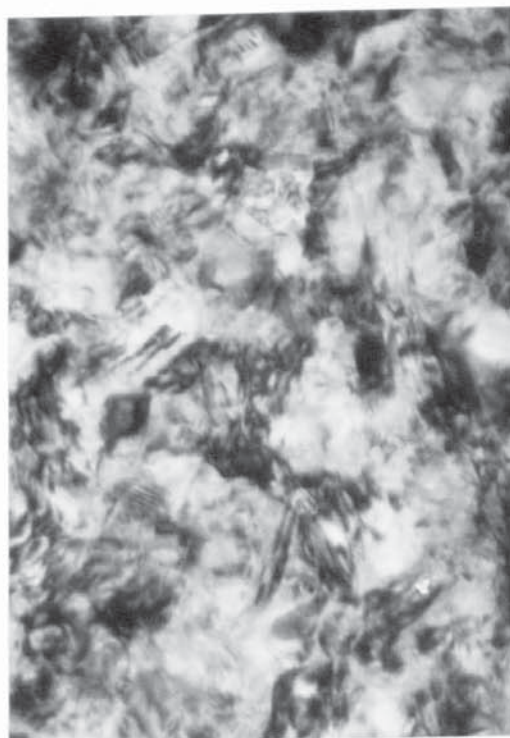
Fig. (42) Conditions as in Fig. (39) but ultrasonically agitated 40 watts



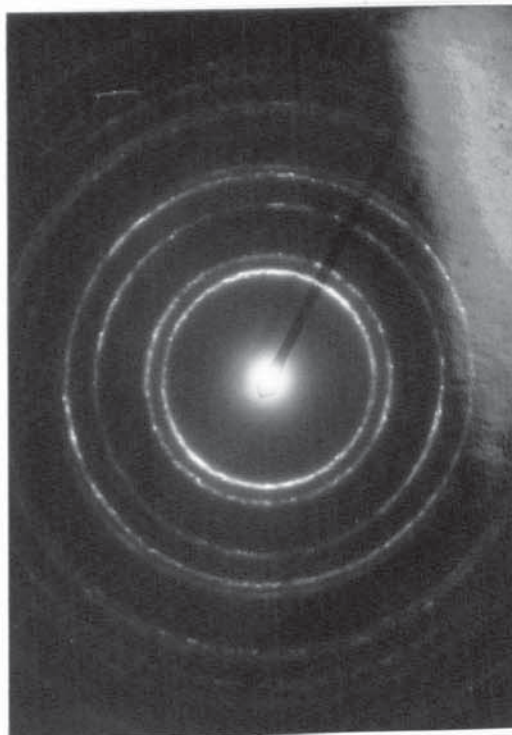
A Magnification X 100000



B Magnification X 250000

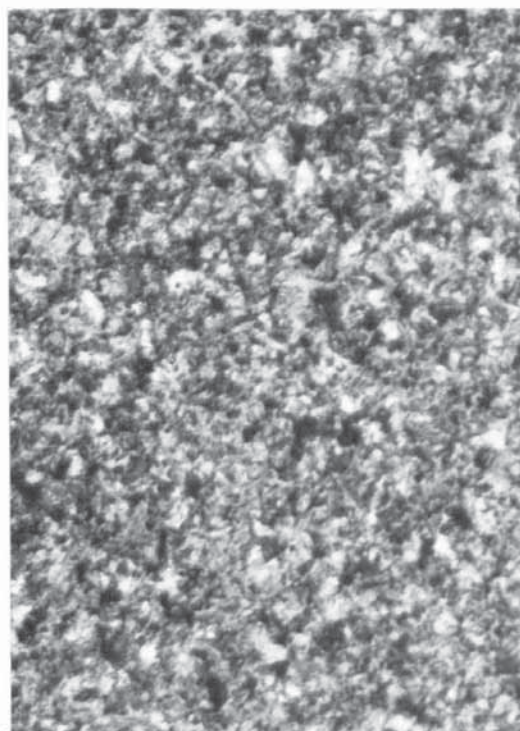


C Magnification X 500000

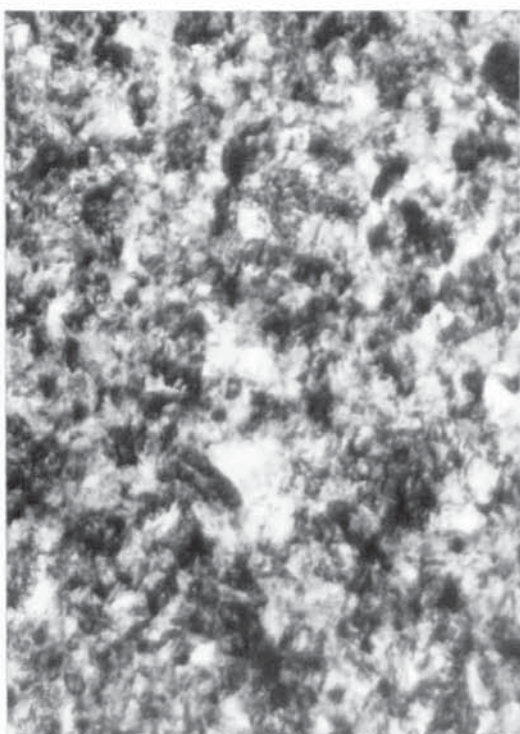


D Diffraction pattern
of grains in deposit

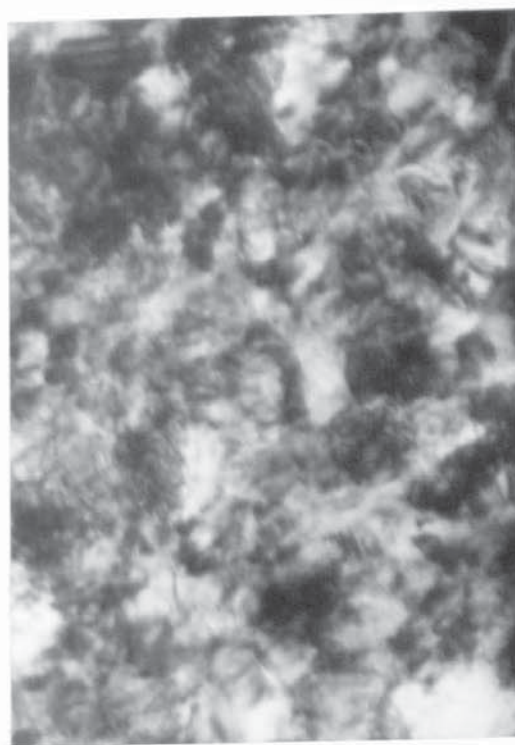
Fig.(43) Conditions as in Fig.(39) but ultrasonically agitated 100 watts



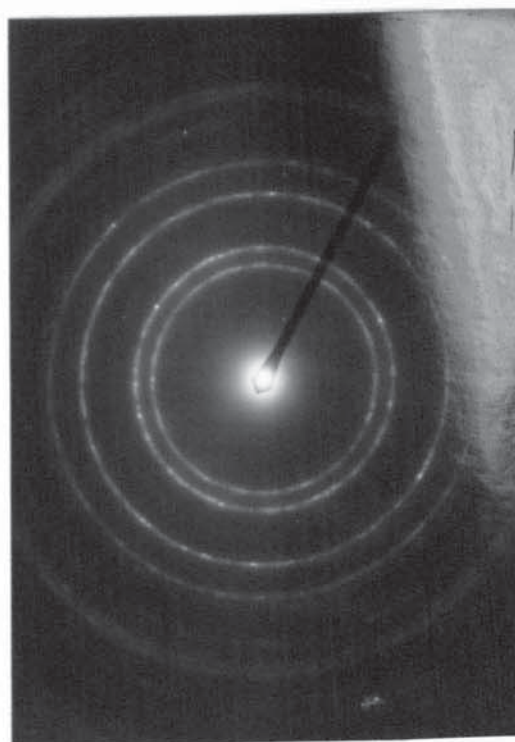
A Magnification X 100000



B Magnification X 250000

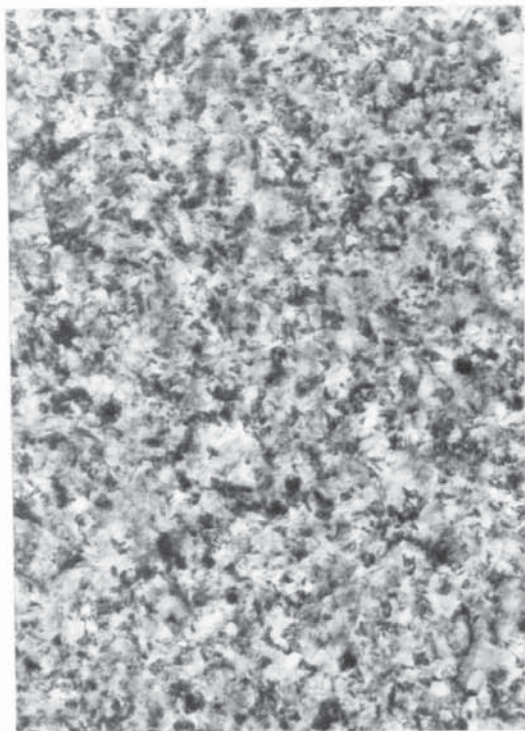


C Magnification X 500000

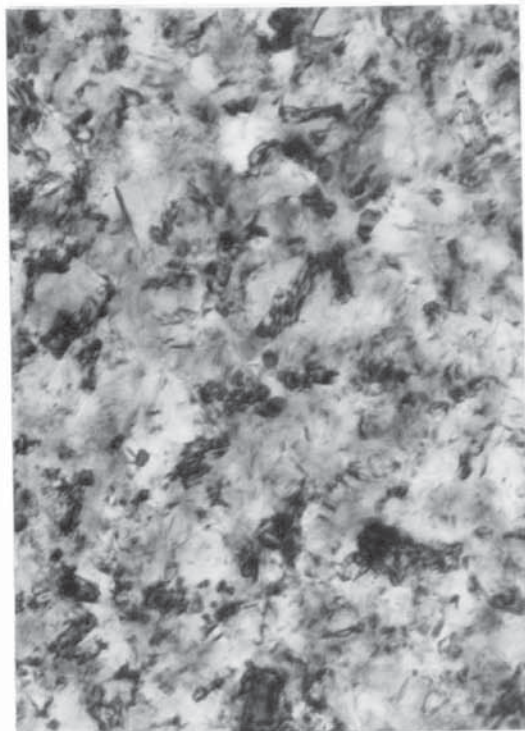


D Diffraction pattern
of grains in deposit

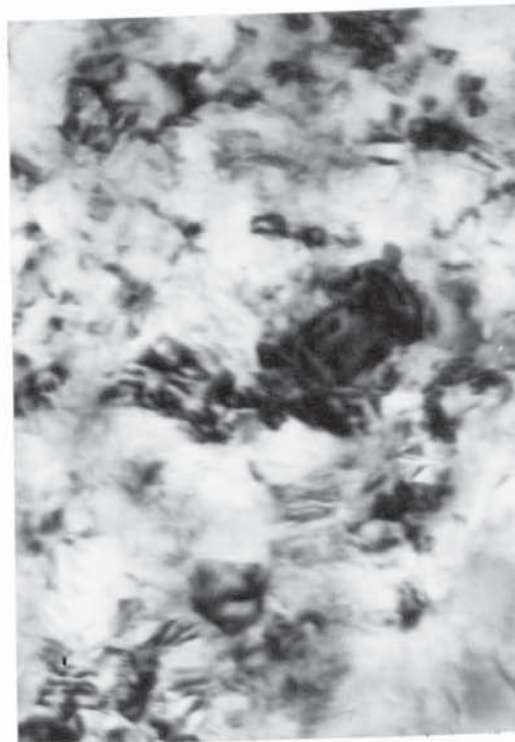
Fig. (44) Conditions as in Fig. (39) but ultrasonically agitated 200 watts



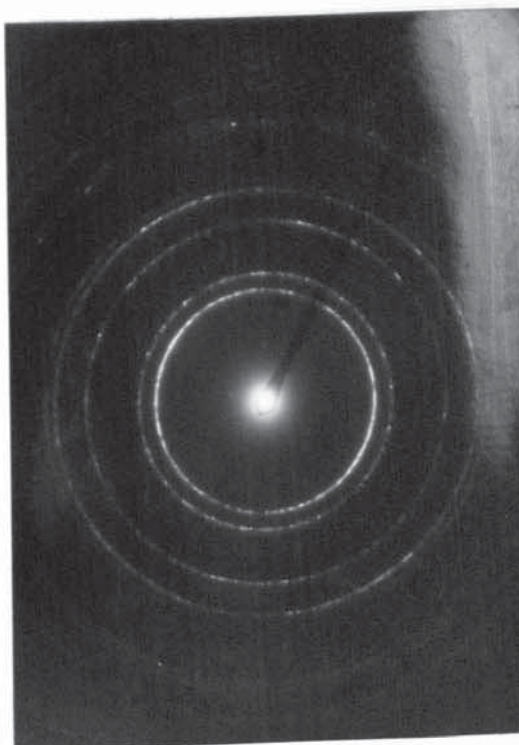
A Magnification X 100000



B Magnification X 250000



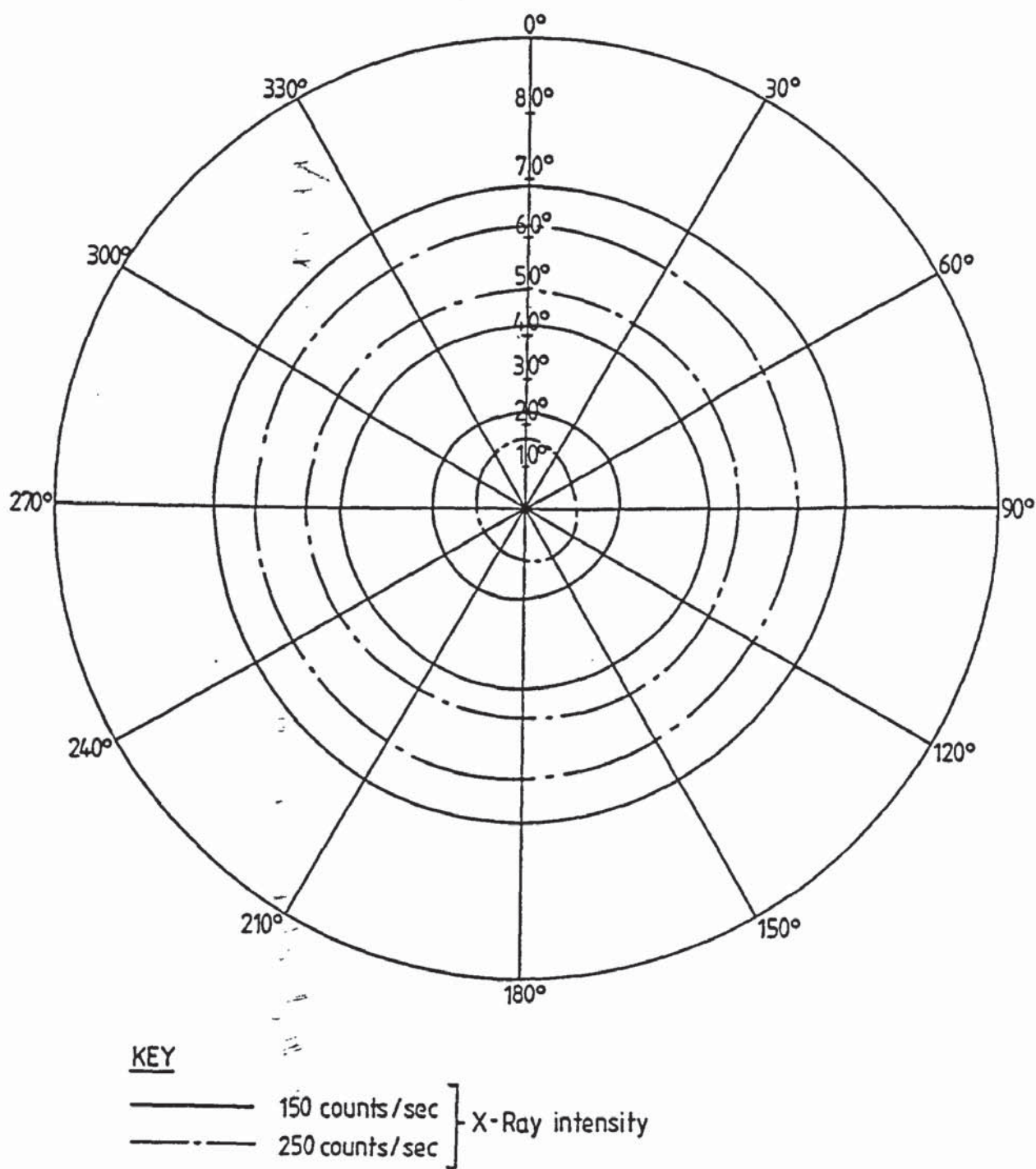
C Magnification X 500000



D Diffraction pattern
of grains in deposit

Fig. (45) Conditions as in Fig. (39) but ultrasonically agitated 350 watts

Fig(46) Pole figure of nickel-iron deposit obtained using either air or ultrasonic agitation



8.4 Surface Topography.

8.4.1 Nickel-Cobalt Deposits.

Surface topography of a selection of electroplated deposits of nickel-cobalt alloys deposited from solutions containing cobaltous sulphate contents of 10 g/l; 35 g/l; 60 g/l; 85 g/l and 110 g/l was examined using the scanning electron microscope.

It was apparent from the deposits obtained from nickel-cobalt solution containing 10 g/l cobaltous sulphate and using air agitation as shown in Fig.47 that the topographical features of the deposits were fine and of an irregular shape.

On the other hand the surface topographical features of deposits obtained from the same solution using ultrasonic agitation, 350 watts, were larger than those obtained by air agitation and were of regular pyramid shape as shown in Fig.48. By increasing the cobalt content to 4.2 g/l (35 g/l $\text{CoSO}_4 \cdot 7\text{H}_2\text{O}$) the structure changed from pyramid to granular shape for deposits obtained using ultrasonic agitation as shown in Fig.50. Increased cobalt content had little effect on the air agitated sample as shown in Fig.49.

On further increase in cobalt content to 7.2 g/l (60 g/l $\text{CoSO}_4 \cdot 7\text{H}_2\text{O}$), the structure of the deposits changed to a spaghetti structure using air agitation as shown in Fig.51 but still had a fine granular structure

when using ultrasonic agitation, 350 watts, Fig.52. By increasing the cobalt content to 10.2 g/l (85 g/l $\text{CoSO}_4 \cdot 7\text{H}_2\text{O}$) the surface topography changed to a spaghetti structure for deposits obtained using either air or ultrasonic agitation as shown in Figs.53 and 54. At 110 g/l cobaltous sulphate the spaghetti structure still occurred when using air agitation as shown in Fig.55 but in the case of ultrasonic agitation, at both 100 watts and 350 watts, the structure became feathery in appearance, Figs.56 and 57.

8.4.2 Nickel-Iron Deposits.

The following samples were prepared from a commercial bright nickel-iron solution, pH 4, current density 4 A/dm² and temperature 68°C.

- i) Air agitation.
- ii) Ultrasonic agitation 100 watts.
- iii) Ultrasonic agitation 200 watts.
- iv) Ultrasonic agitation 350 watts.

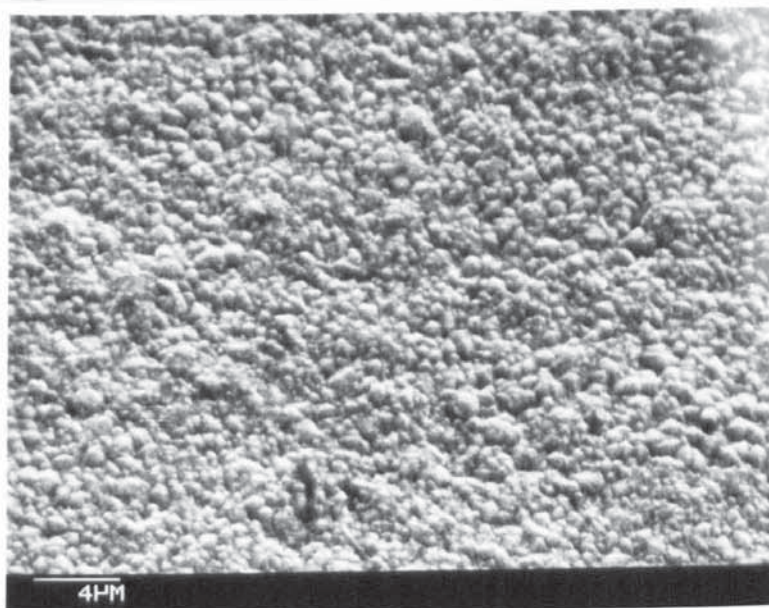
Scanning electron microscope photographs of a selection of the nickel-iron alloy electrodeposits are shown in Figs. 58 to 61. Fig.58 shows a tiny defect in the bright smooth surface of a nickel-iron deposit obtained by air agitation. The surface was almost completely free of surface features; the area shown is not typical of the general surface. This indicates the smooth level nature of the surface. Figs. 59 to 61 illustrate the less bright

surface of the nickel-iron alloy deposits obtained by ultrasonic agitation. The smooth, rounded, directionally orientated nodules were characteristic of nickel-iron alloys produced using ultrasonic agitation.

8.4.2.1 The Effect of Ultrasonic Agitation on the Brightness of the Nickel-Iron Deposits.

Ultrasonic waves significantly reduced the brightness of the commercial bright nickel-iron alloy deposits. The loss of brightness increased as the intensity of the ultrasonic agitation was increased. Longitudinal parallel bright and dull bands were formed on the surface of the electrodeposited panel.

A



B

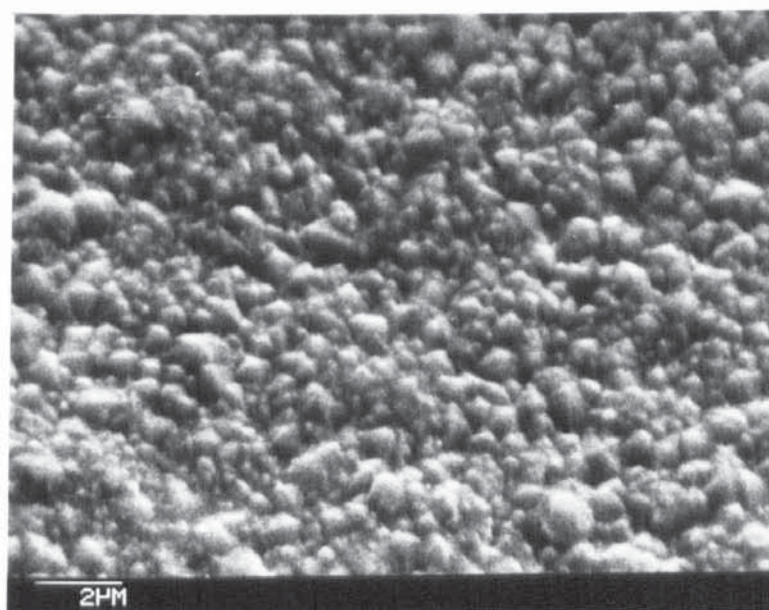
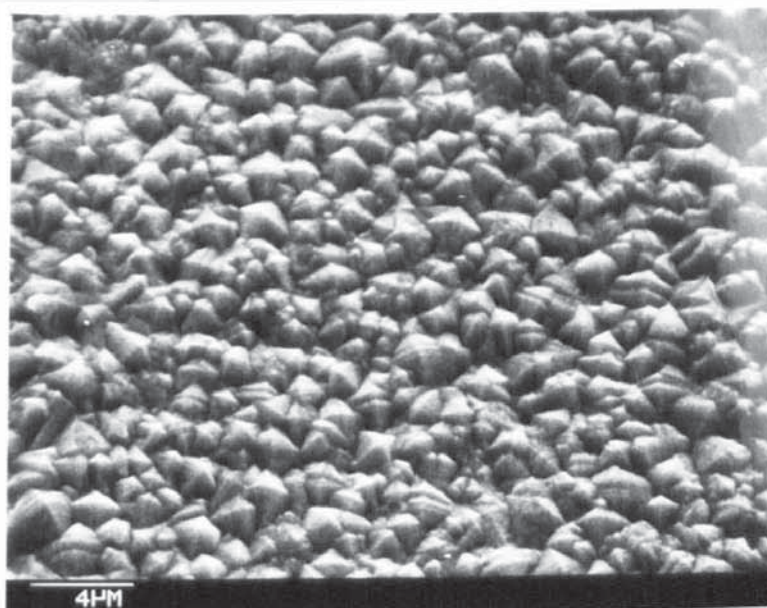


Fig. (47) Surface topography of nickel-cobalt deposit plated at $4A/dm^2$ from a solution containing 10g/l cobaltous sulphate. Air agitation.

A



B

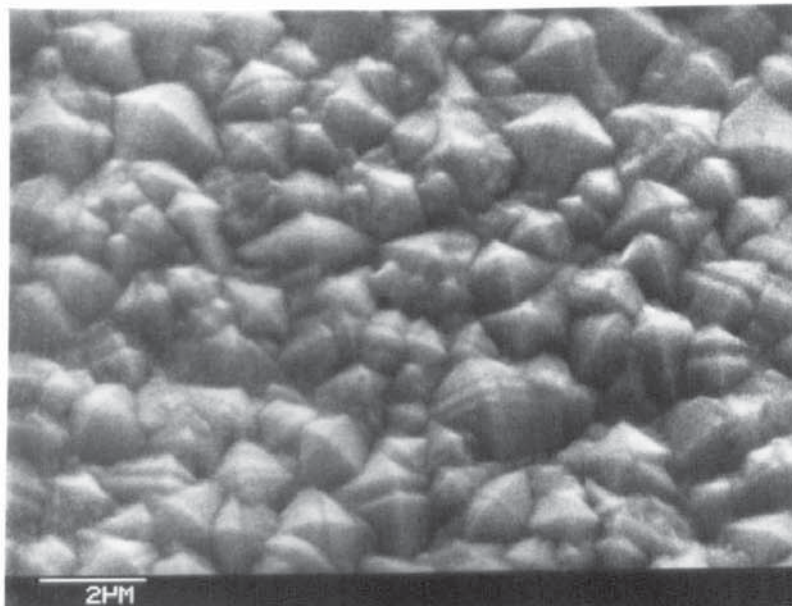
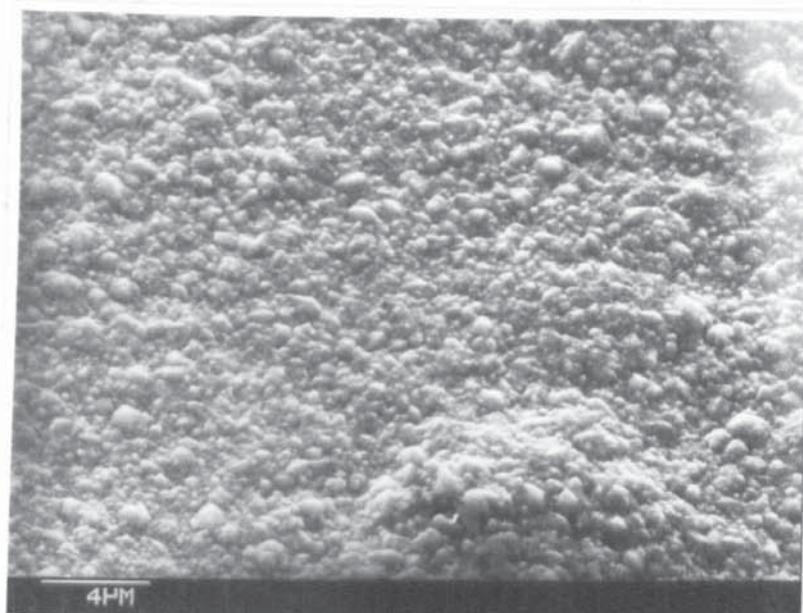


Fig. (48) Conditions as in Fig. (47) but ultrasonically agitated 350 watts.

A



B

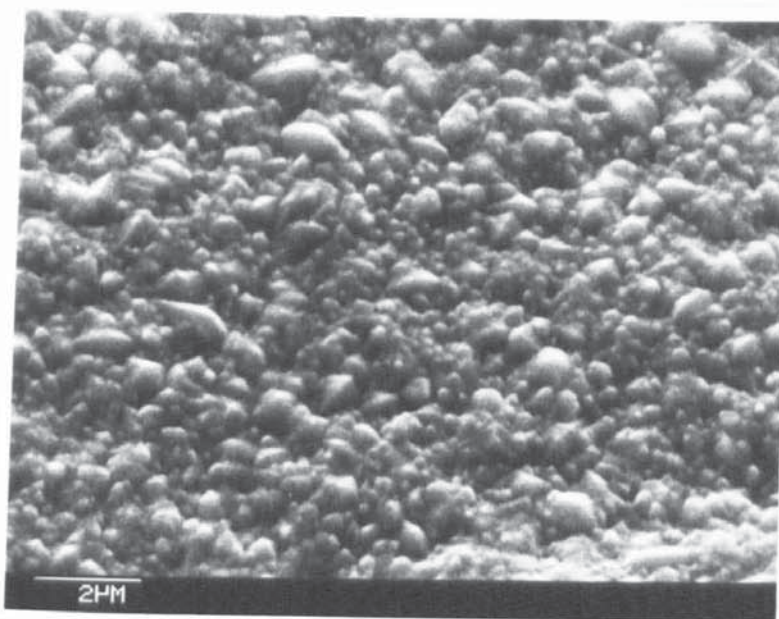
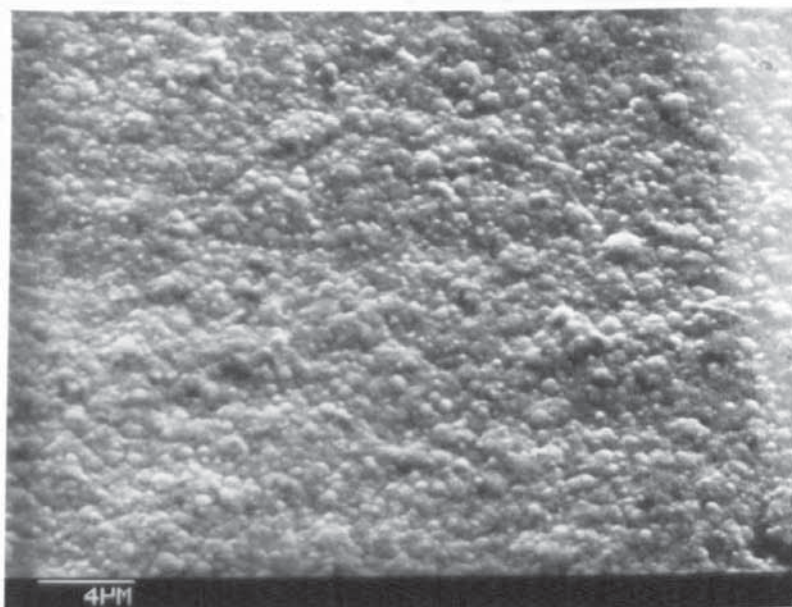


Fig.(49) Surface topography of nickel-cobalt deposit plated at $4A/dm^2$ from a solution containing 35g/l cobaltous sulphate. Air agitation.

A



B

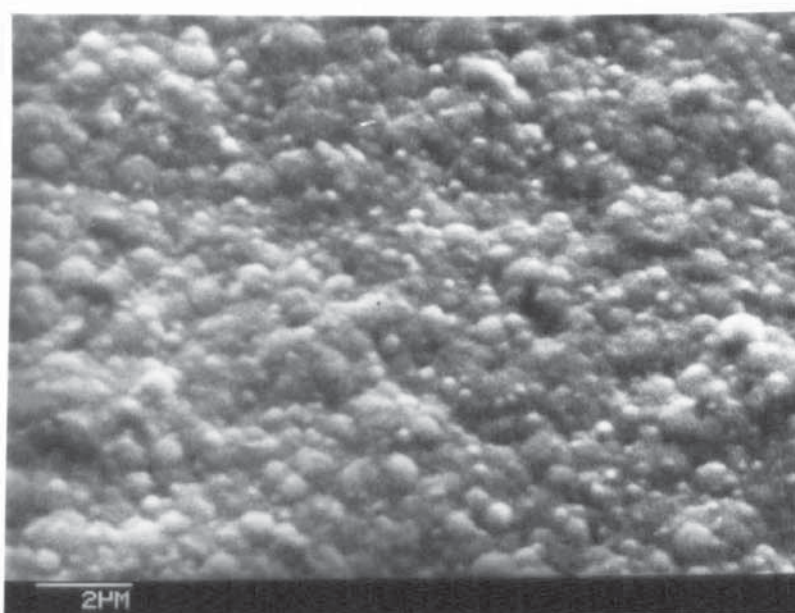
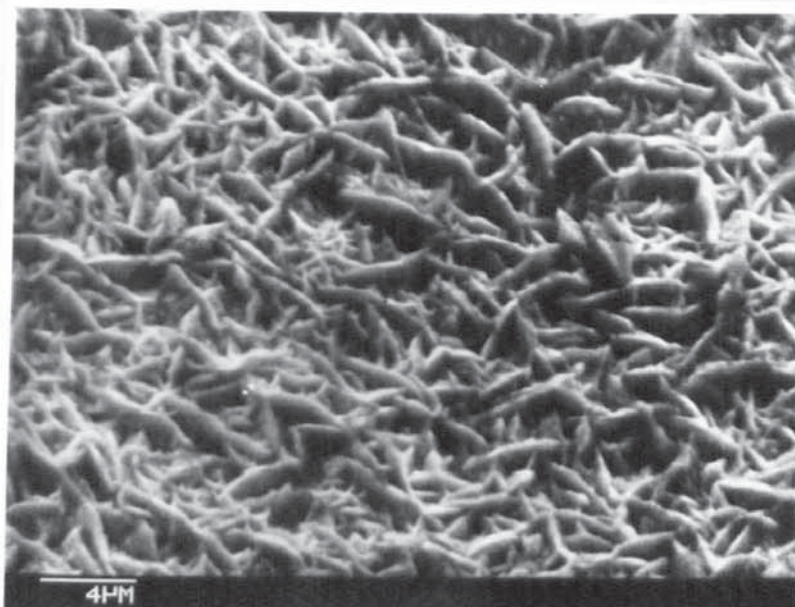


Fig.(50) Conditions as in Fig.(49) but ultrasonically agitated 350 watts.

A



B

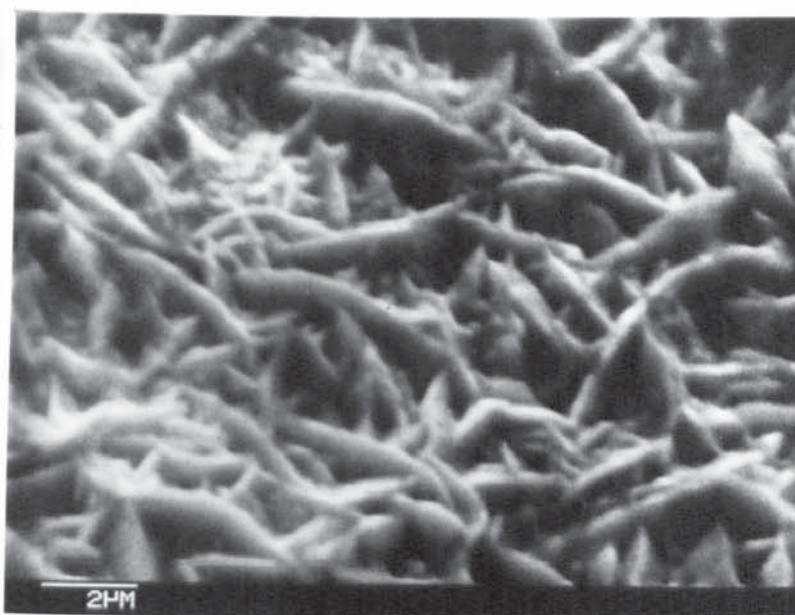
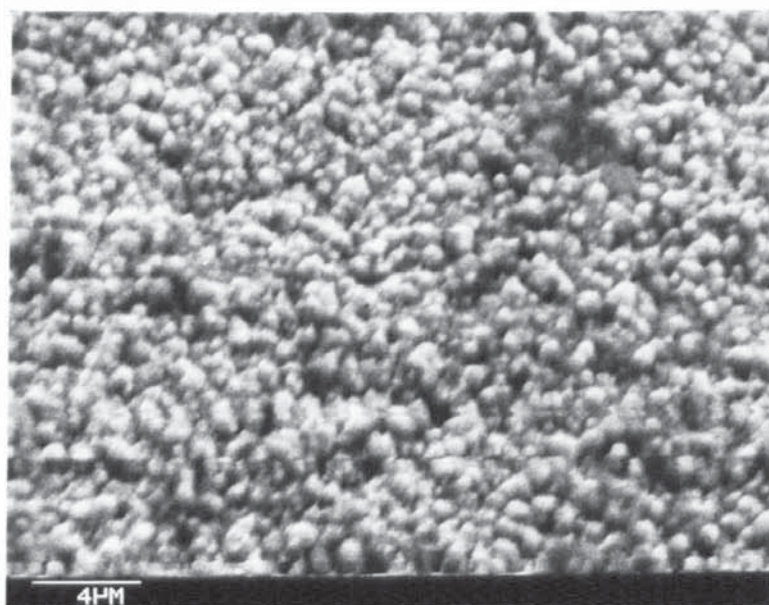


Fig.(51) Surface topography of nickel-cobalt deposit plated at 4A/dm^2 from a solution containing 60g/l cobaltous sulphate. Air agitation.

A



B

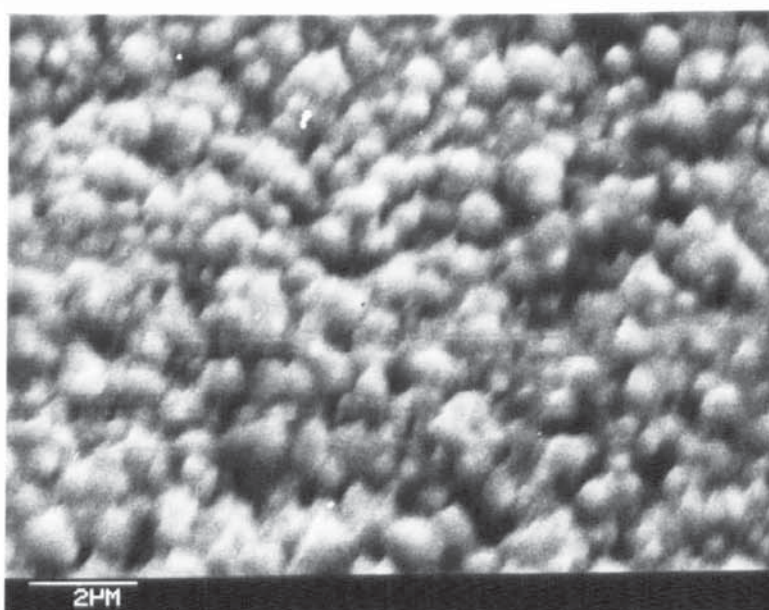
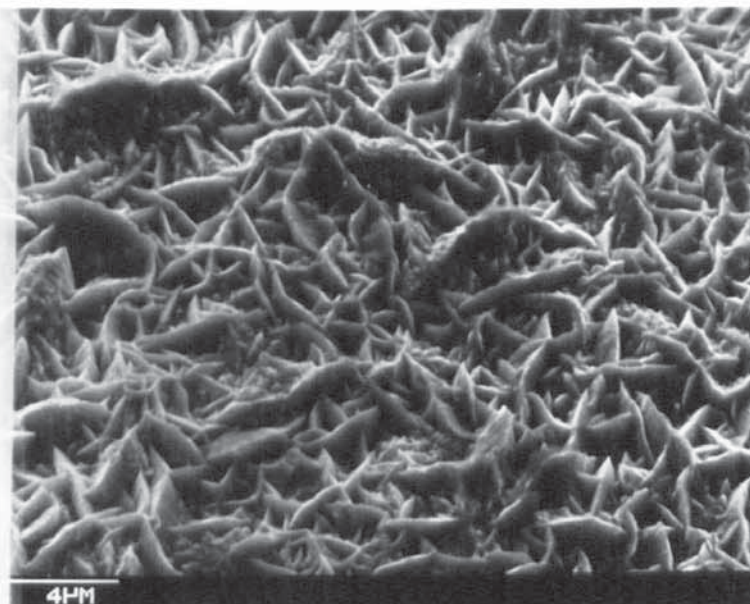


Fig.(52) Conditions as in Fig.(51) but ultrasonically agitated 350 watts.

A



B

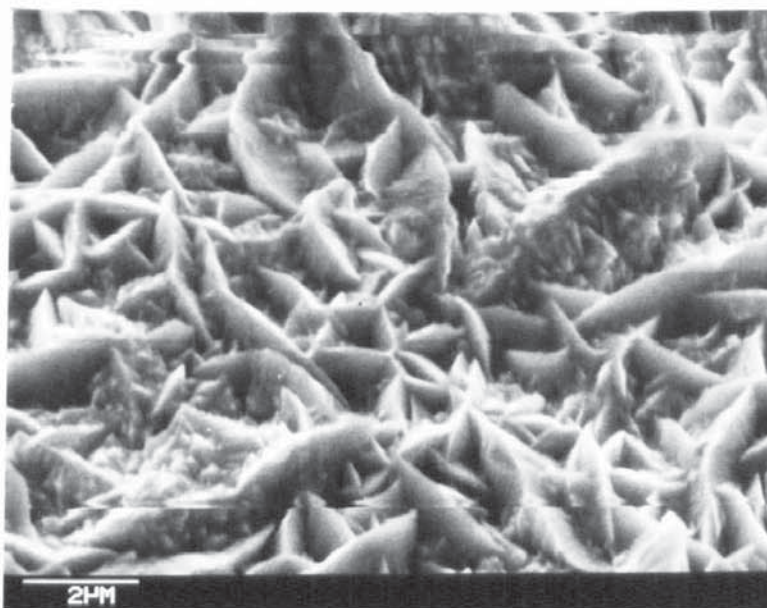
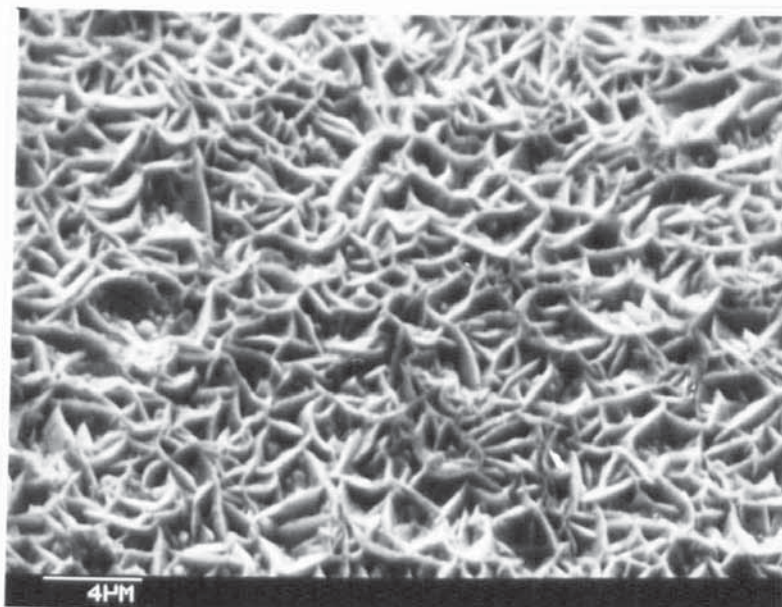


Fig.(53) Surface topography of nickel-cobalt deposit plated at $4A/dm^2$ from a solution containing 85g/l cobaltous sulphate. Air agitation.

A



B

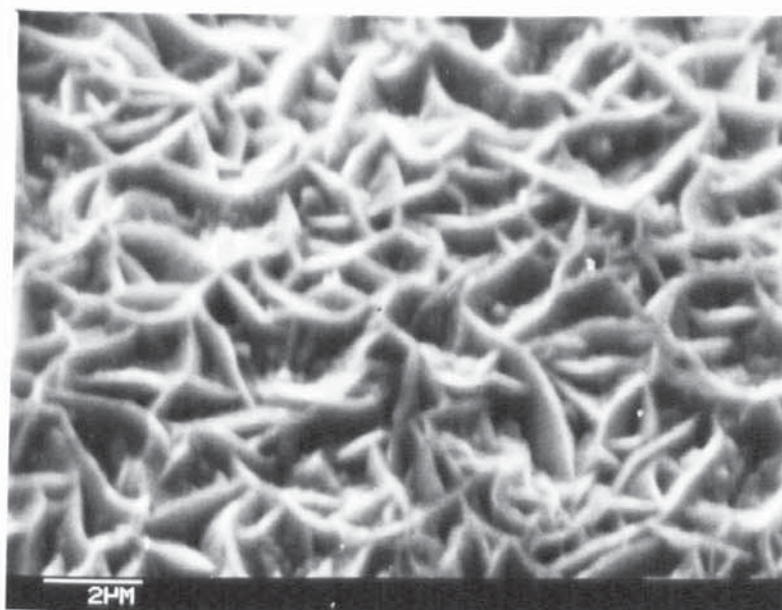
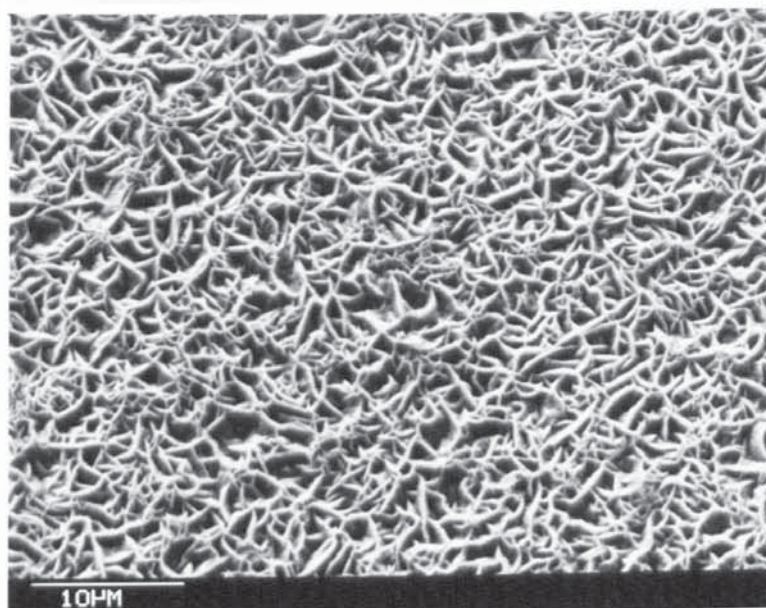


Fig.(54) Conditions as in Fig.(53) but ultrasonically agitated 350 watts.

A



B

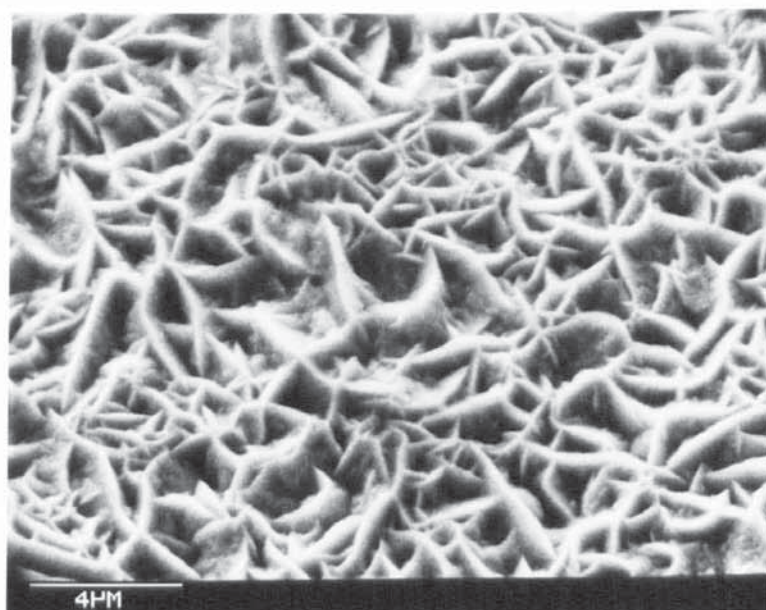
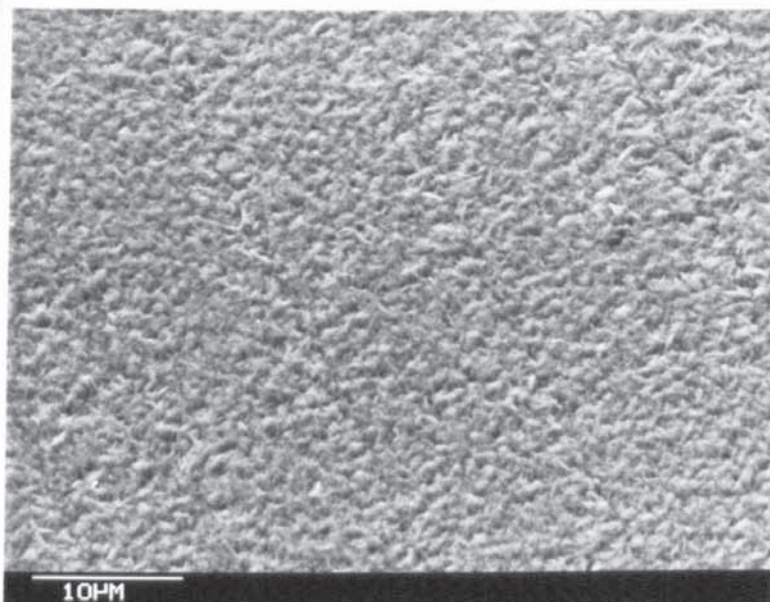


Fig.(55) Surface topography of nickel-cobalt deposit plated at 4A/dm^2 from a solution containing 110g/l cobaltous sulphate. Air agitation.

A



B

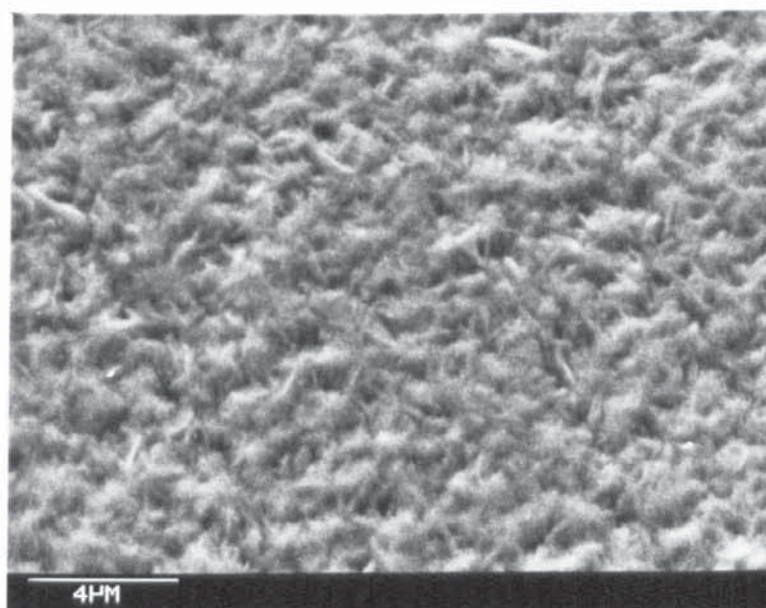
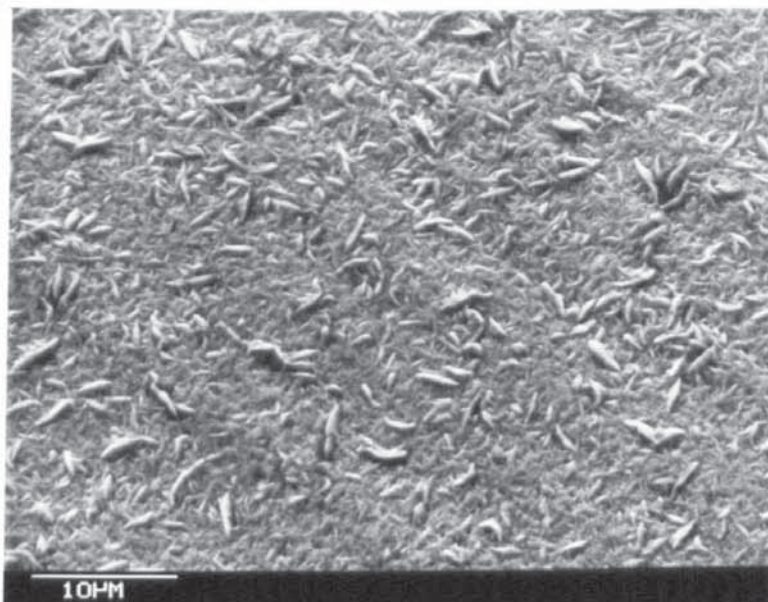


Fig.(56) Conditions as in Fig.(55) but ultrasonically agitated 100 watts.

A



B

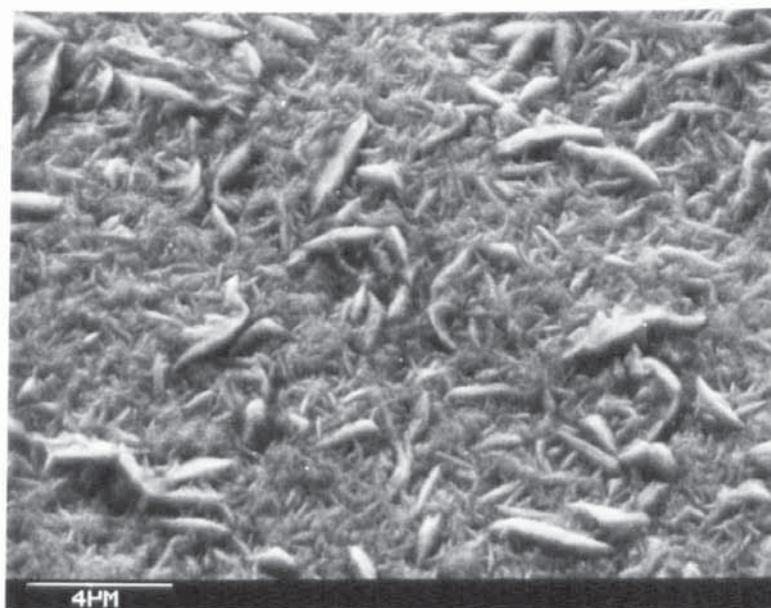


Fig.(57) Conditions as in Fig.(55) but ultrasonically agitated 350 watts.

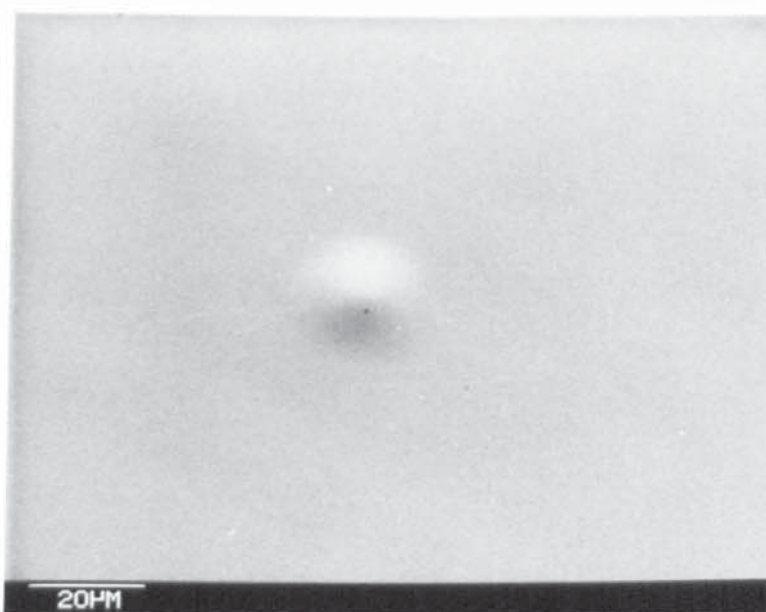
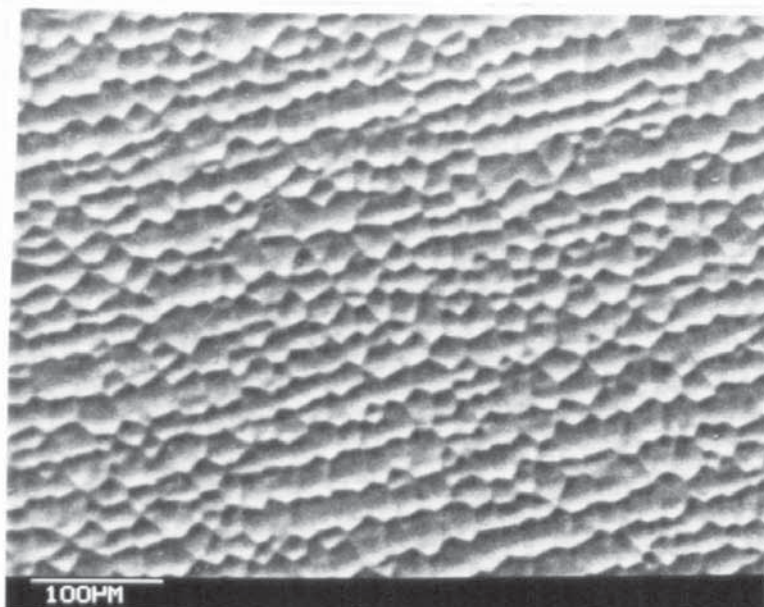


Fig.(58) Scanning Electron photomicrograph of nickel-iron alloy deposit plated at 4 A/dm^2 , 68°C and pH4, air agitated.

A



B

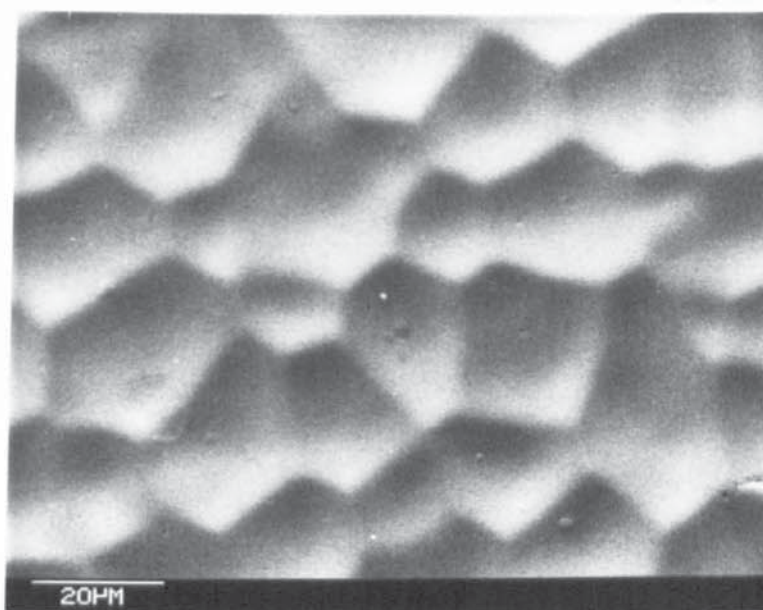


Fig.(59) Conditions as in Fig.(58) but
ultrasonically agitated 100 watts.

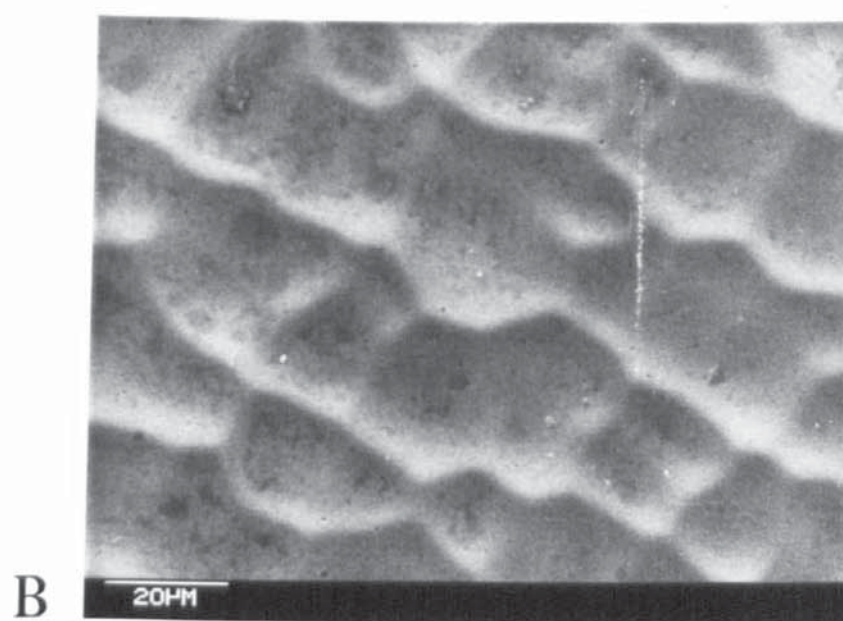
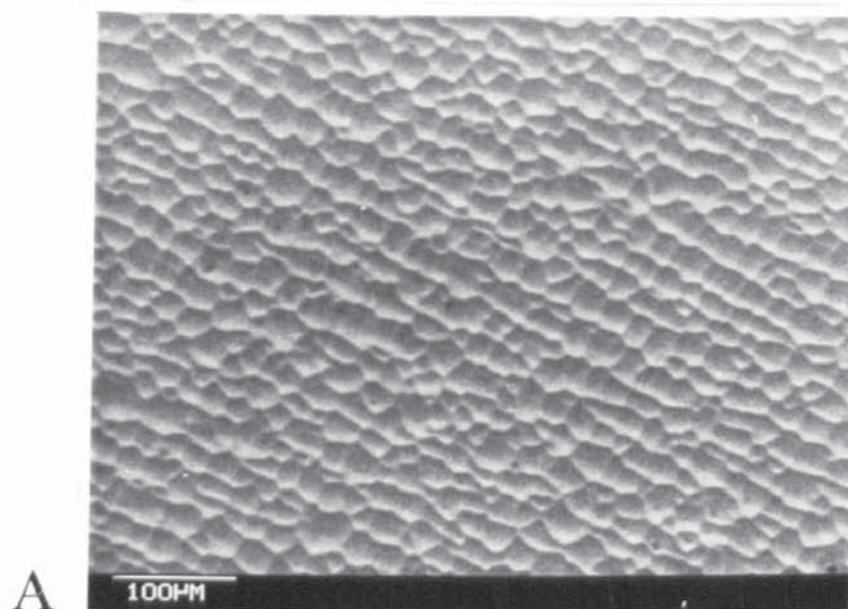


Fig.(60) Conditions as in Fig.(58) but
ultrasonically agitated 200 watts.

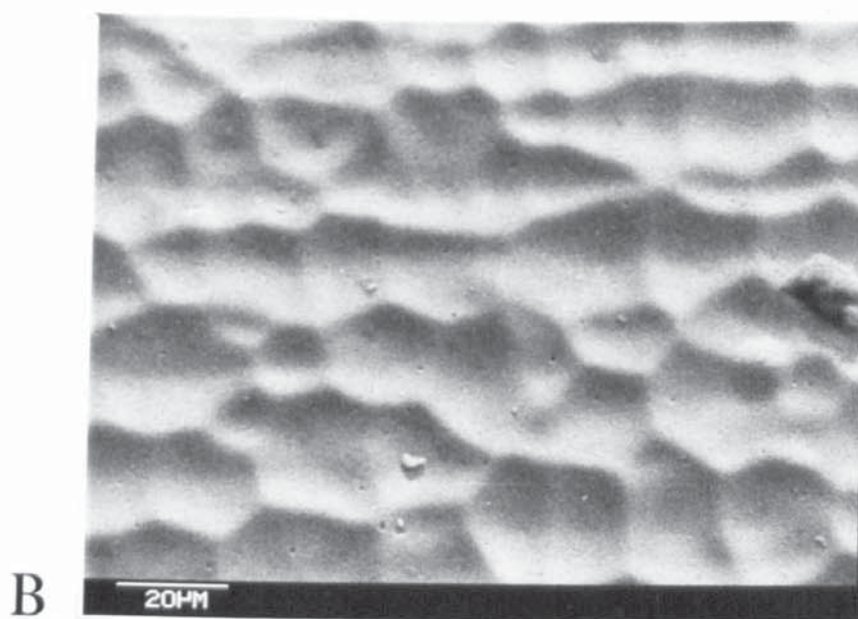
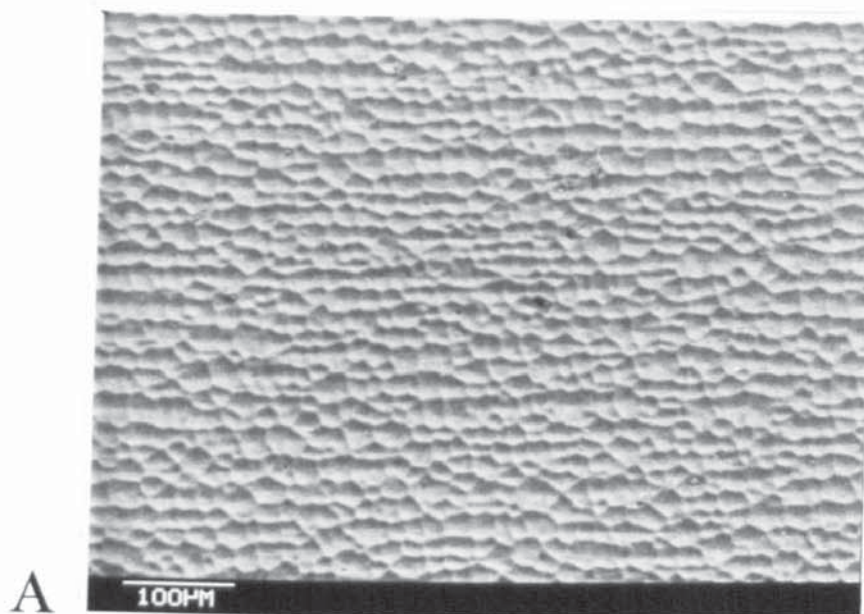


Fig.(61) Conditions as in Fig.(58) but
ultrasonically agitated 350 watts.

8.5 Progressive Growth of Deposits.

8.5.1 Nickel-Cobalt Deposits.

The development of the surface topography of nickel-cobalt electrodeposits with increasing plating time, using air agitation, on finely abraded "gold seal" steel panels, is illustrated by the electronmicrographs shown in Figs. 62, 63, 64 and 65. At the lowest thickness (after one minute plating) the fine abrasion marks in the substrate were still visible; on further plating the pyramid structure developed. The pyramids are uniform in size and smaller than those produced using ultrasonic agitation as shown in Figs. 62, 63, 64 and 65. Mixtures of pyramid and irregular rounded humps were obtained by using ultrasonic agitation, 350 watts as shown in Figs. 66, 67, 68 and 69. Otherwise no clear differences could be detected in the surface topography of deposits plated from nickel-cobalt solution containing 10 g/l $\text{CoSO}_4 \cdot 7\text{H}_2\text{O}$ using either air or ultrasonic agitation 350 watts at equal time intervals. The surface topography of nickel-cobalt deposits became very similar after 20 minutes plating regardless of the type of agitation. The plating tests were repeated using a solution containing 110 g/l $\text{CoSO}_4 \cdot 7\text{H}_2\text{O}$, the plating times remaining the same at 1, 5, 10 and 15 minutes.

The dendritic, acicular structure is very clear as shown in Figs. 71, 72 and 73 using air agitation. The surface

topography obtained using ultrasonic agitation, 350 watts was irregular and had unusual flat-topped peaks as shown in Figs. 75, 76 and 77. Layered structures were visible in some regions.

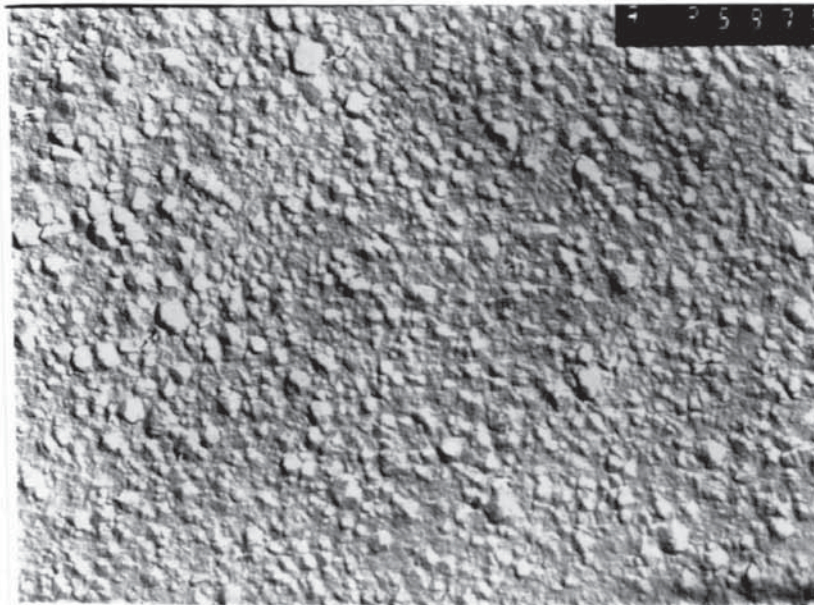


Fig.(62) Surface topography X 8.4k for 1
minute deposit using air agitation.

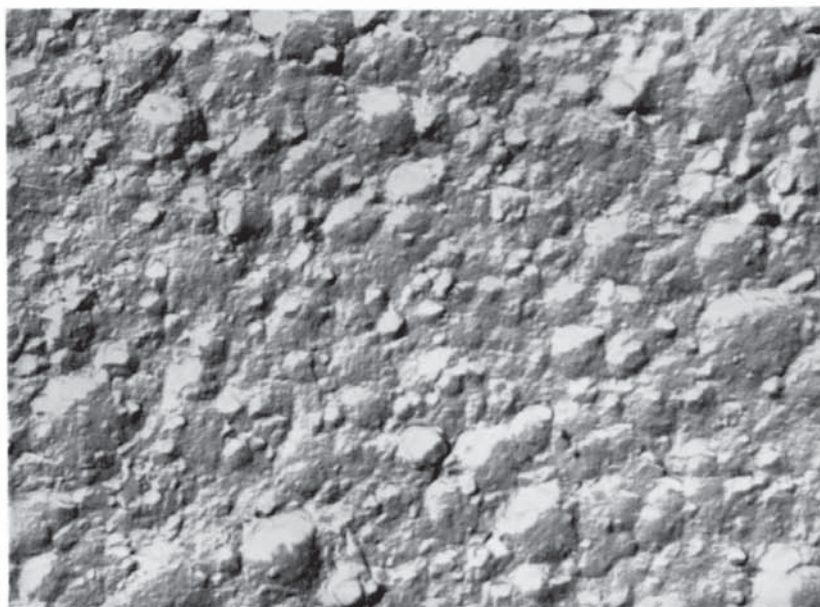


Fig.(63) Surface topography X 8.4k for 5
minutes deposit using air agitation.

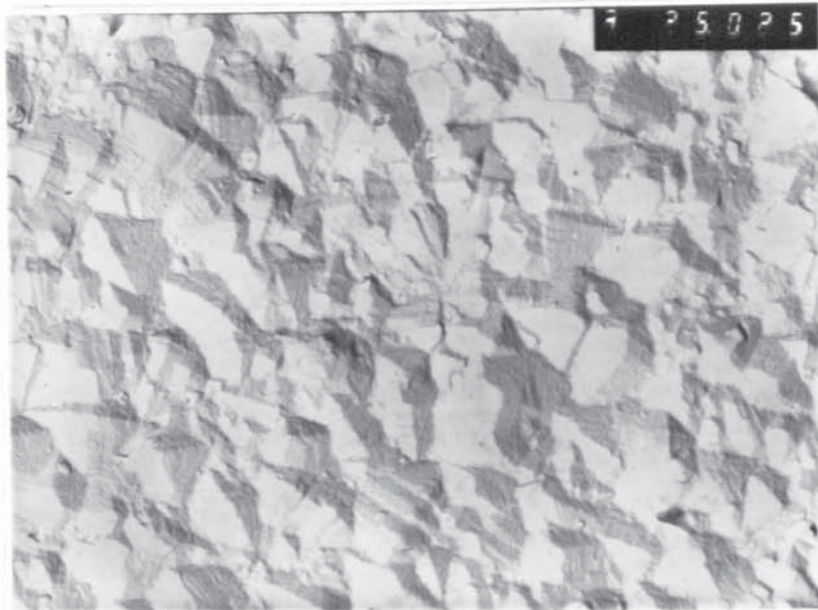


Fig.(64) Surface topography X 8.4k for 10 minutes deposit using air agitation.



Fig.(65) Surface topography x 8.4k for 15 minutes deposit using air agitation.

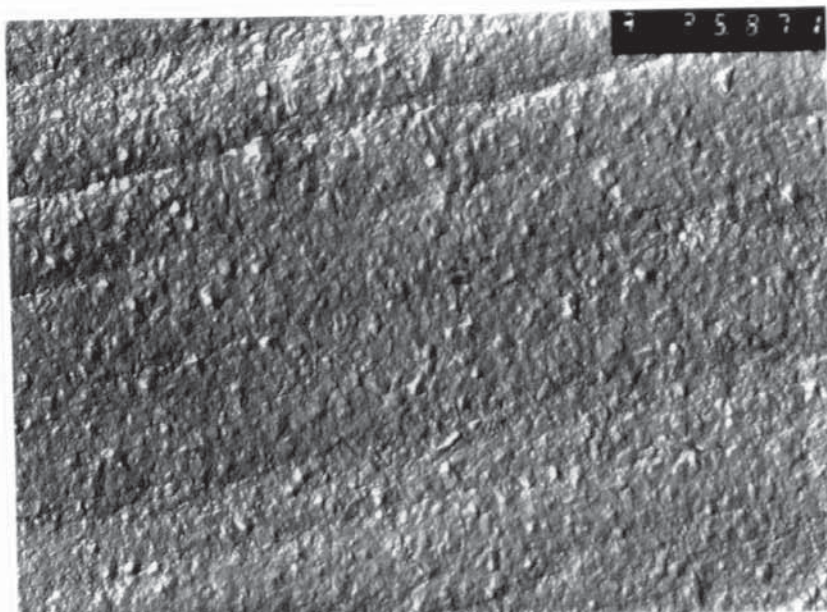


Fig.(66) Surface topography X 8.4k
for 1 minute deposit using
ultrasonic agitation 350 watts.

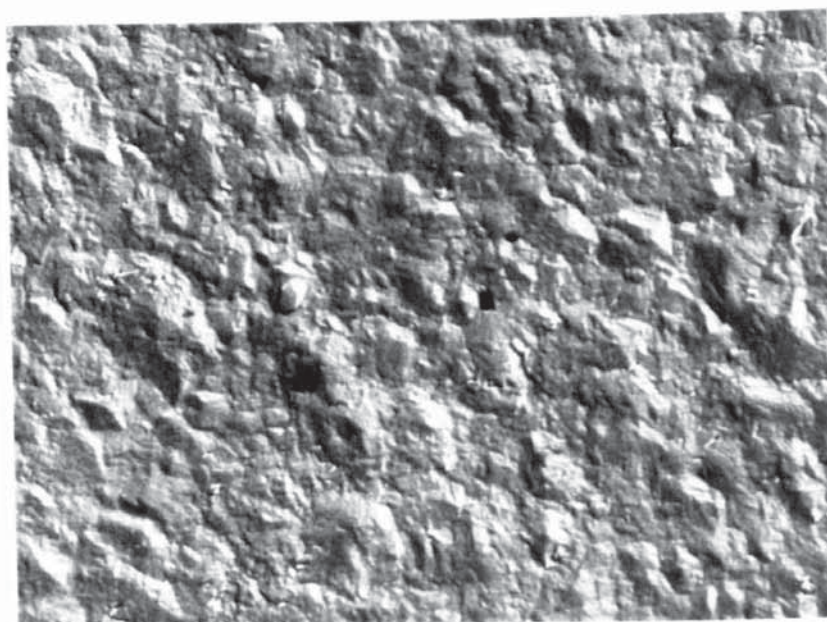


Fig.(67) Surface topography X 8.4k
for 5 minutes deposit using
ultrasonic agitation 350 watts.

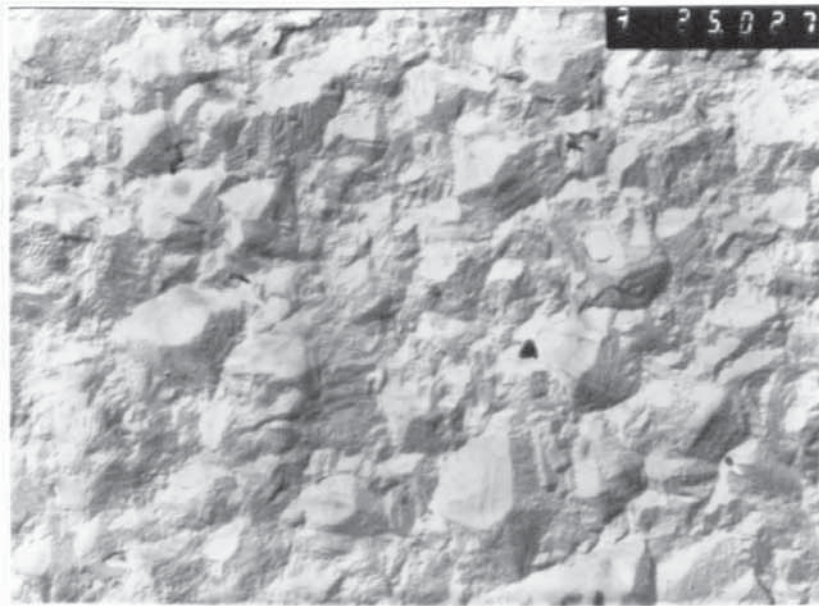


Fig.(68) Surface topography X 8.4k
for 10 minutes deposit using
ultrasonic agitation 350 watts.



Fig.(69) Surface topography X 8.4k
for 15 minutes deposit using
ultrasonic agitation 350 watts.

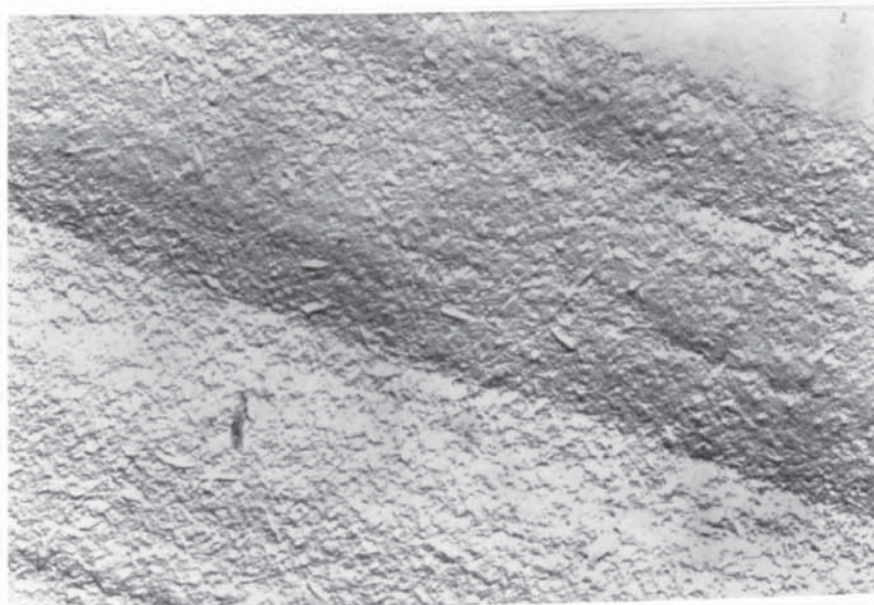


Fig.(70) Surface topography X 8.4k for 1 minute deposit using air agitation, solution containing 110 g/l $\text{CoSO}_4 \cdot 7\text{H}_2\text{O}$.



Fig.(71) Surface topography X 8.4k for 5 minutes deposit using air agitation, solution containing 110 g/l $\text{CoSO}_4 \cdot 7\text{H}_2\text{O}$.



Fig.(72) Surface topography X 8.4k for 10 minutes deposit using air agitation, solution containing 110 g/l $\text{CoSO}_4 \cdot 7\text{H}_2\text{O}$.



Fig.(73) Surface topography X 8.4k for 15 minutes deposit using air agitation, solution containing 110 g/l $\text{CoSO}_4 \cdot 7\text{H}_2\text{O}$.



Fig.(74) Surface topography X 8.4k for 1 minute deposit using ultrasonic agitation 350 watts, solution containing 110 g/l $\text{CoSO}_4 \cdot 7\text{H}_2\text{O}$.

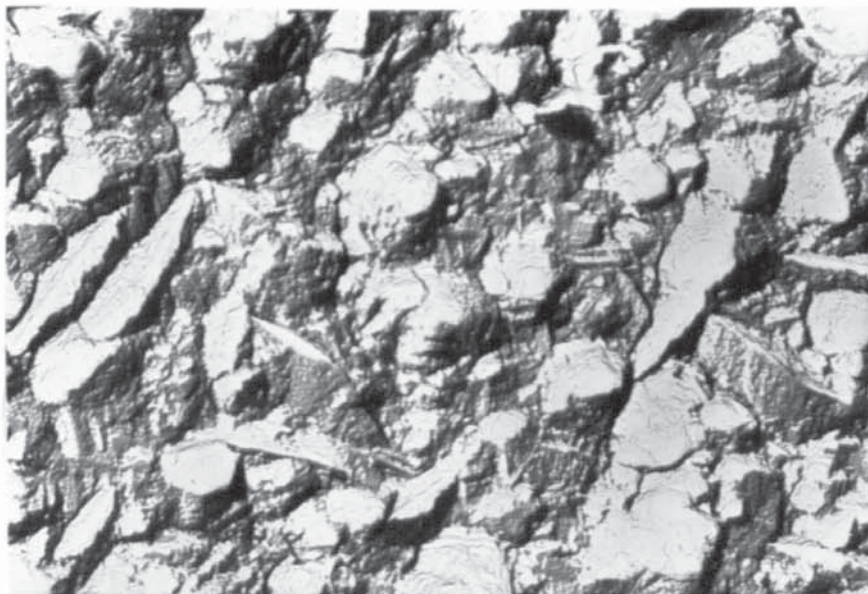


Fig.(75) Surface topography X 8.4k for 5 minutes deposit using ultrasonic agitation 350 watts, solution containing 110 g/l $\text{CoSO}_4 \cdot 7\text{H}_2\text{O}$.

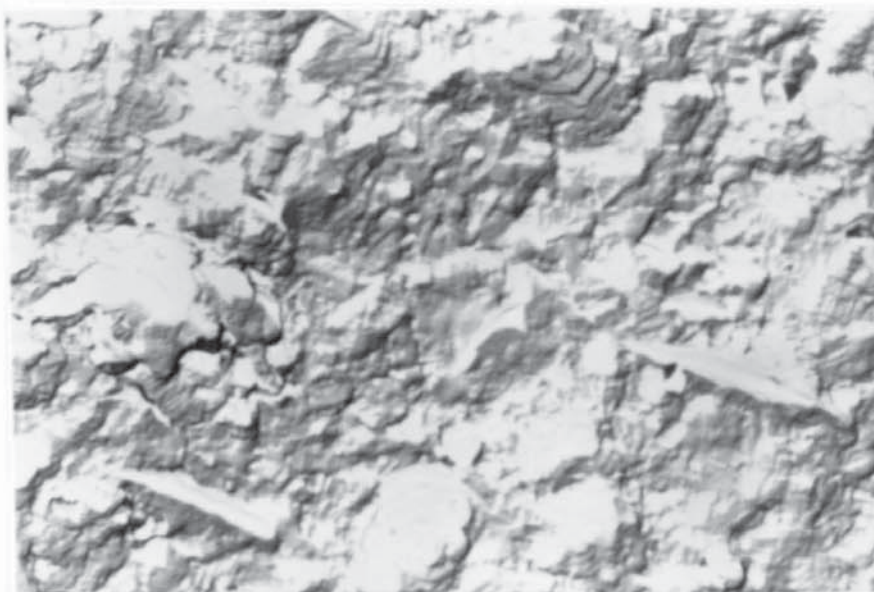


Fig.(76) Surface topography X 8.4k for 10 minutes deposit using ultrasonic agitation 350 watts, solution containing 110 g/l $\text{CoSO}_4 \cdot 7\text{H}_2\text{O}$.

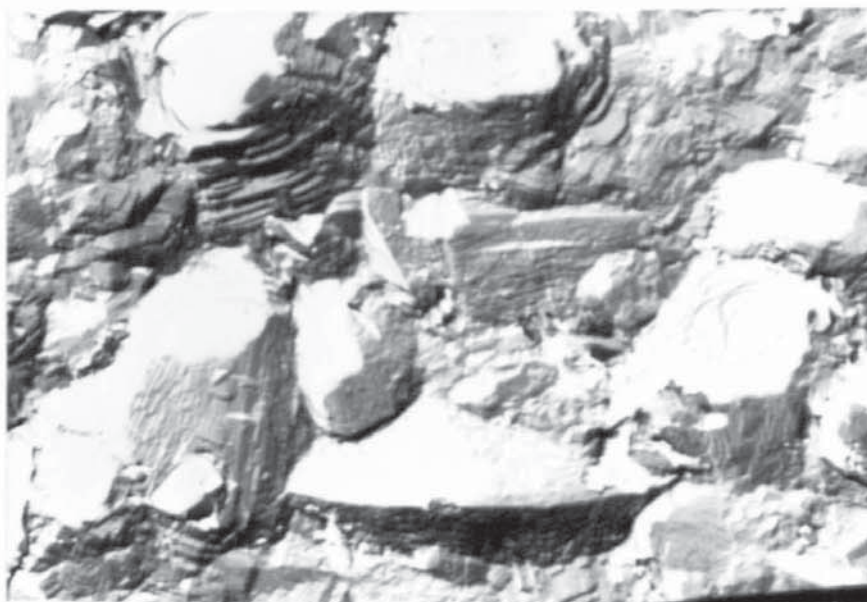


Fig.(77) Surface topography X 8.4k for 15 minutes deposit using ultrasonic agitation 350 watts, solution containing 110 g/l $\text{CoSO}_4 \cdot 7\text{H}_2\text{O}$.

8.6 Limiting Current Density.

8.6.1 Nickel-Cobalt.

Experimental work was carried out to investigate the effect of air and ultrasonic agitation on limiting current density, the results are shown in Tables XXV, XXVI and XXVII.

The current density up to which a satisfactory deposit could be obtained, (limiting current density) was dependent upon the degree of agitation as shown below:

Type of agitation	Limiting current density A/dm ²
Air	18
Ultrasonic 100 watt	20
Ultrasonic 350 watt	28

8.6.1.1 Hardness and Composition of Deposits Obtained Using Air Agitation.

Samples of electrodeposits obtained from limiting current density experiments using vigorous air agitation between 10 and 80 A/dm² obtained from Ni-Co solution containing 10 g/l CoSO₄.7H₂O; were analysed by electron probe microanalyser and the hardnesses of the electrodeposits were measured as shown in Table XXVIII and displayed graphically in Fig.(78). The variation of the cobalt content with the change of current density is displayed graphically in Fig.(79).

Table XXV

Limiting current density results using air agitation
pH 4; 55°C.

Plated Area dm ²	Current Density A/dm ²	Plating Time min.sec.	General Appearance of Panel
0.5	10	40.00	Dull sound deposit
0.5	14	28.35	"
0.5	16	25.00	"
0.5	18	22.12	"
0.25	20	20.00	Dull slight burn on the edges
0.25	22	18.12	"
0.25	24	16.38	"
0.25	26	15.24	Dull slight burn on the edges,
0.25	28	14.18	slight stress,,
0.25	30	13.22	"
0.25	32	12.30	"
0.25	34	11.46	"
0.25	36	11.07	Dull slight burn on the edges
0.125	40	10.00	gradually increasing, stressed
0.125	44	9.06	"
0.125	48	8.20	"
0.125	52	7.41	"
0.125	56	7.08	Dull burn increasing stressed
0.125	60	6.40	"
0.125	64	6.15	"
0.125	68	5.53	Severe stress burn increases
0.125	72	5.33	"
0.125	76	5.15	Burnt with powdery deposit
0.125	80	5.00	"

Table XXVI

Limiting current density results using ultrasonic agitation 100 watts, pH 4, 55°C.

Plated Area dm ²	Current Density A/dm ²	Plating Time min.sec.	General Appearance of Panel
0.5	10	40.00	Dull sound deposit
0.5	14	28.35	"
0.5	16	25.00	"
0.25	18	22.12	"
0.25	20	20.00	"
0.25	22	18.12	Dull slight burn on the edges
0.25	24	16.38	"
0.25	26	15.24	"
0.25	28	14.18	Slight burn on the edges slightly stressed
0.25	30	13.22	"
0.25	32	12.30	"
0.25	34	11.46	"
0.25	36	11.07	"
0.125	40	10.00	Burns on the edges gradually increasing and stressed
0.125	44	9.06	"
0.125	48	8.20	"
0.125	52	7.41	"
0.125	56	7.08	"
0.125	60	6.40	Burns increasing, stressed.
0.125	64	6.15	"
0.125	68	5.53	"
0.125	72	5.33	Burns increasing, severe stress
0.125	76	5.15	"
0.125	80	5.00	"

Table XXVII

Limiting current density results using ultrasonic agitation 350 watts; pH 4, 55°C.

Plating Area dm ²	Current Density A/dm ²	Plating Time min.sec.	General Appearance of Panel.
0.5	10	40.00	Dull sound deposit
0.5	14	28.35	"
0.5	16	25.00	"
0.5	18	22.12	"
0.25	20	20.00	"
0.25	22	18.12	"
0.25	24	16.38	"
0.25	26	15.24	"
0.25	28	14.18	"
0.25	30	13.22	Dull slight burn on the edges
0.25	32	12.30	"
0.25	34	11.46	"
0.25	36	11.07	"
0.125	40	10.00	"
0.125	44	9.06	Dull slight stress, burns on the edges gradually increasing
0.125	48	8.20	"
0.125	52	7.41	"
0.125	56	7.08	"
0.125	60	6.40	"
0.125	64	6.15	"
0.125	68	5.53	"
0.125	72	5.33	Dull burn increasing, stressed
0.125	76	5.15	"
0.125	80	5.00	Burnt with powdery deposit.

Table XXVIII

Variation in hardness and composition of nickel-cobalt alloy deposits with changes in current density using air agitation pH4; 55°C.

Current density A/dm ²	Cobalt content %	Nickel content %	Hardness HV
10	15.1	85.2	259
20	12.0	88.7	263
30	10.6	91.1	271
40	8.5	93.0	274
52	6.1	94.6	269
60	4.8	96.1	280
72	3.9	97.2	287
80	3.0	97.4	293

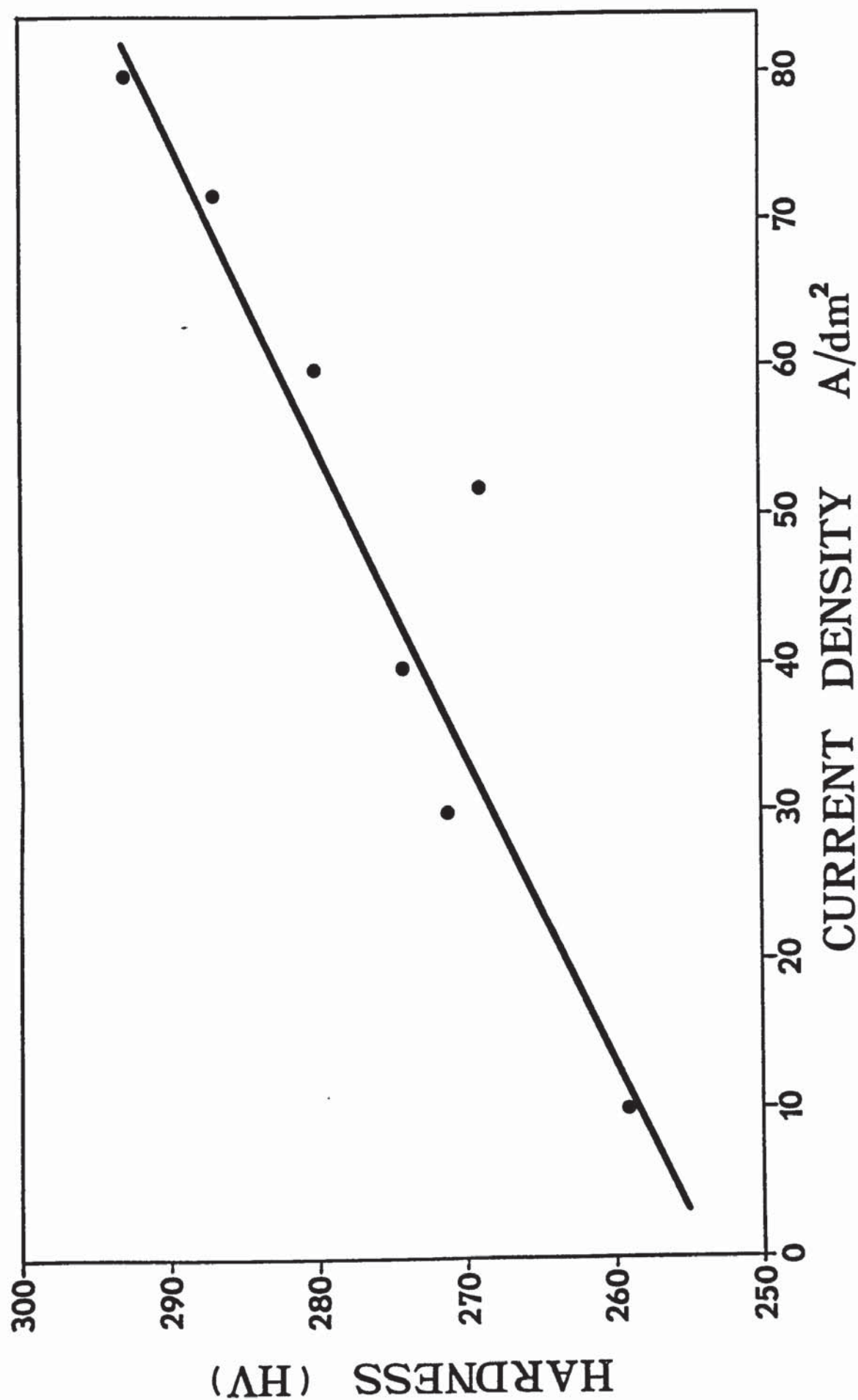


Fig.(78) Effect of variation of current density on the hardness of nickel-cobalt alloy deposit plated using air agitation.

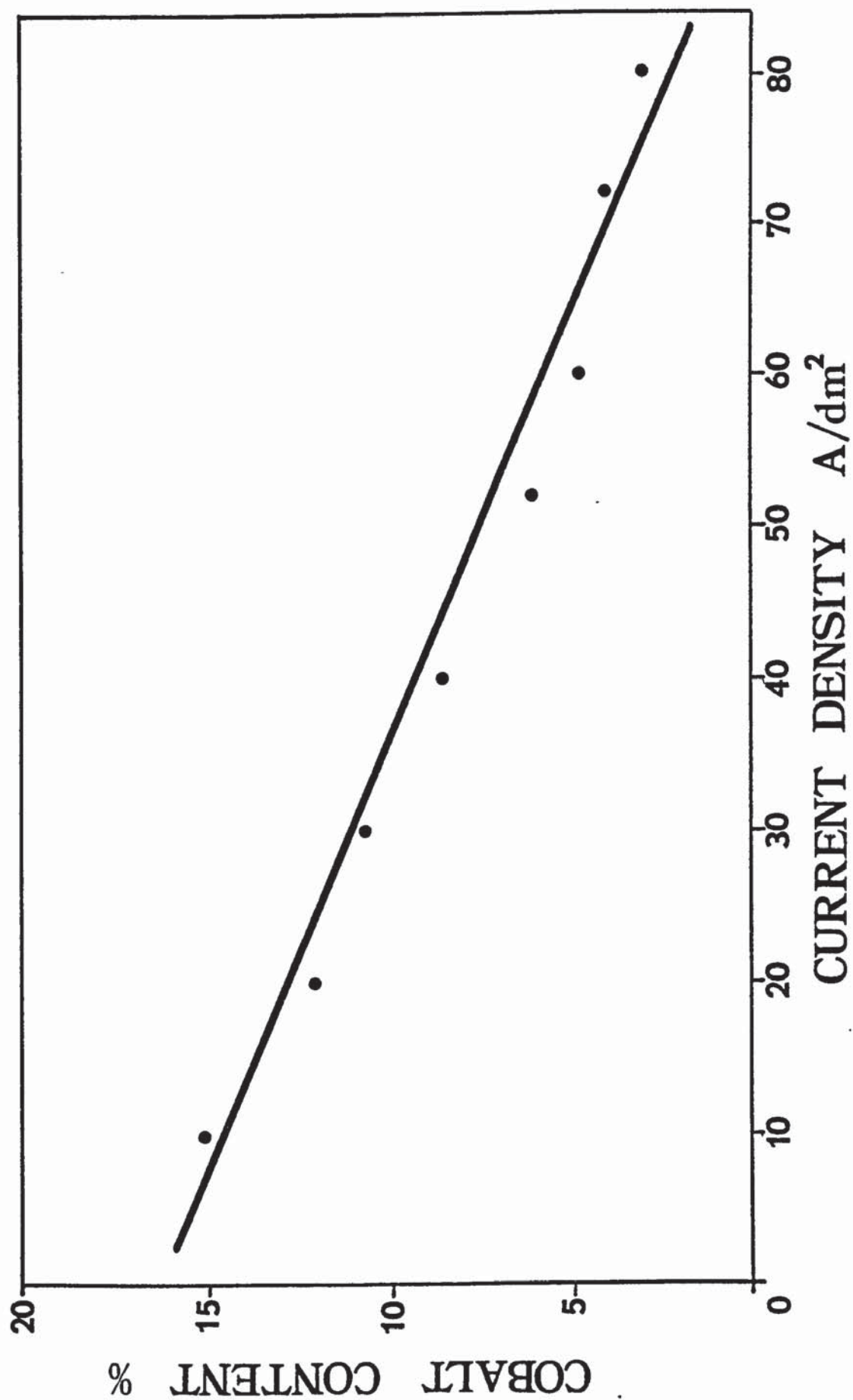


Fig.(79) Effect of variation of current density on the cobalt content of nickel-cobalt alloy deposit plated using air agitation.

8.6.1.2 Hardness and Composition Obtained Using
Ultrasonic Agitation 350 Watts.

Samples of electrodeposits obtained from limiting current density experiments using ultrasonic agitation, 350 watts and current densities between 10 and 80 A/dm² were examined in the same way as the air agitated samples. The results are listed in Table XXIX.

Table XXIX

Variation in hardness and composition of Ni-Co alloy deposits with changes in current density using ultrasonic agitation 350 watts, pH 4, 55°C.

Current density A/dm ²	Cobalt content %	Nickel content %	Hardness HV
10	16.9	83.8	311
20	15.3	84.9	318
30	12.9	89.1	329
40	11.5	89.7	345
52	10.3	90.8	339
60	9.1	91.6	356
72	7.9	93.3	364
80	5.3	94.8	370

The variation of hardness with the change of current density is graphically displayed in Fig.(80) and the variation of the cobalt content with the change of current density is displayed graphically in Fig.(81).

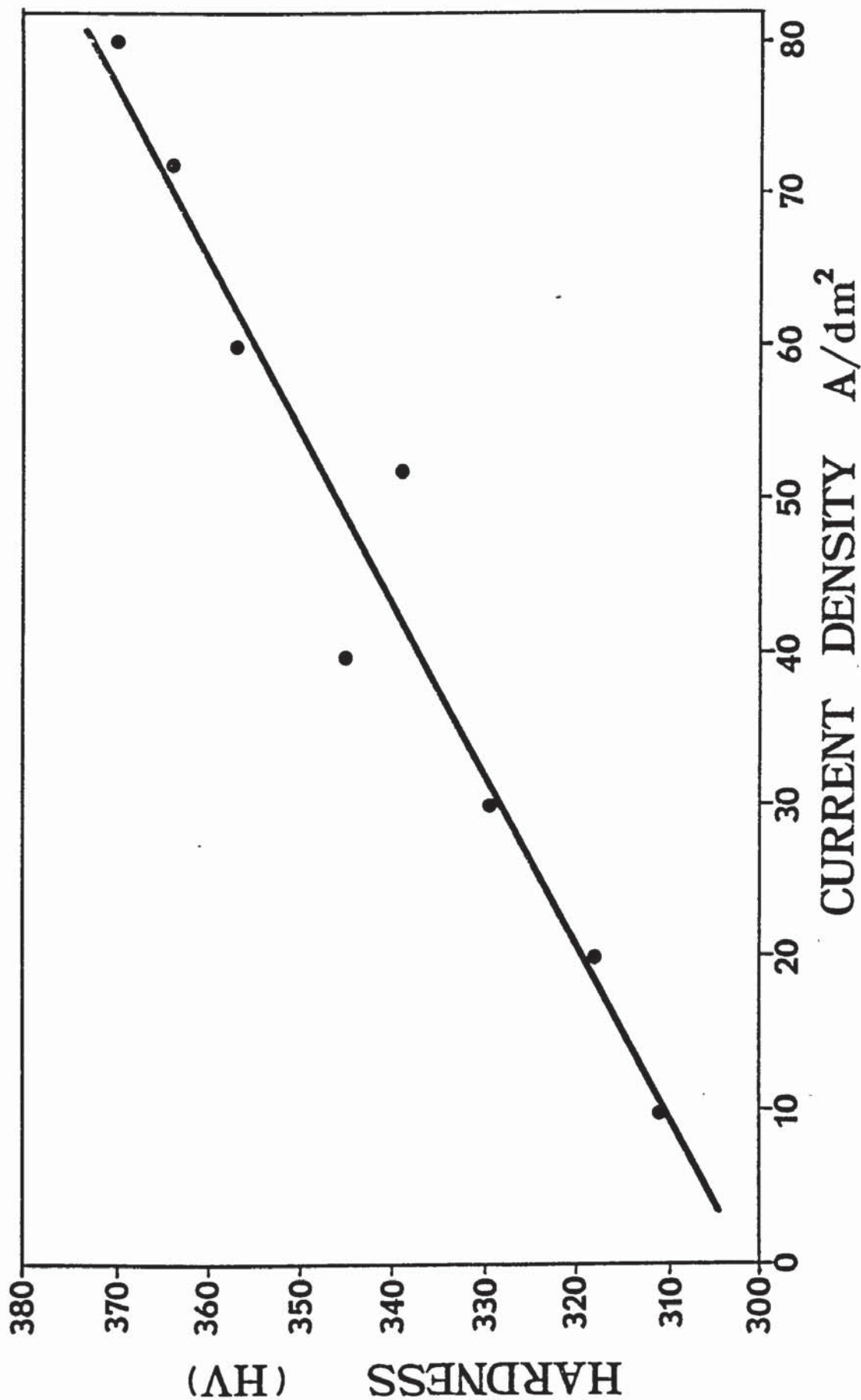


Fig.(80) Effect of variation of current density on the hardness of nickel-cobalt alloy deposit plated using ultrasonic agitation 350 watts.

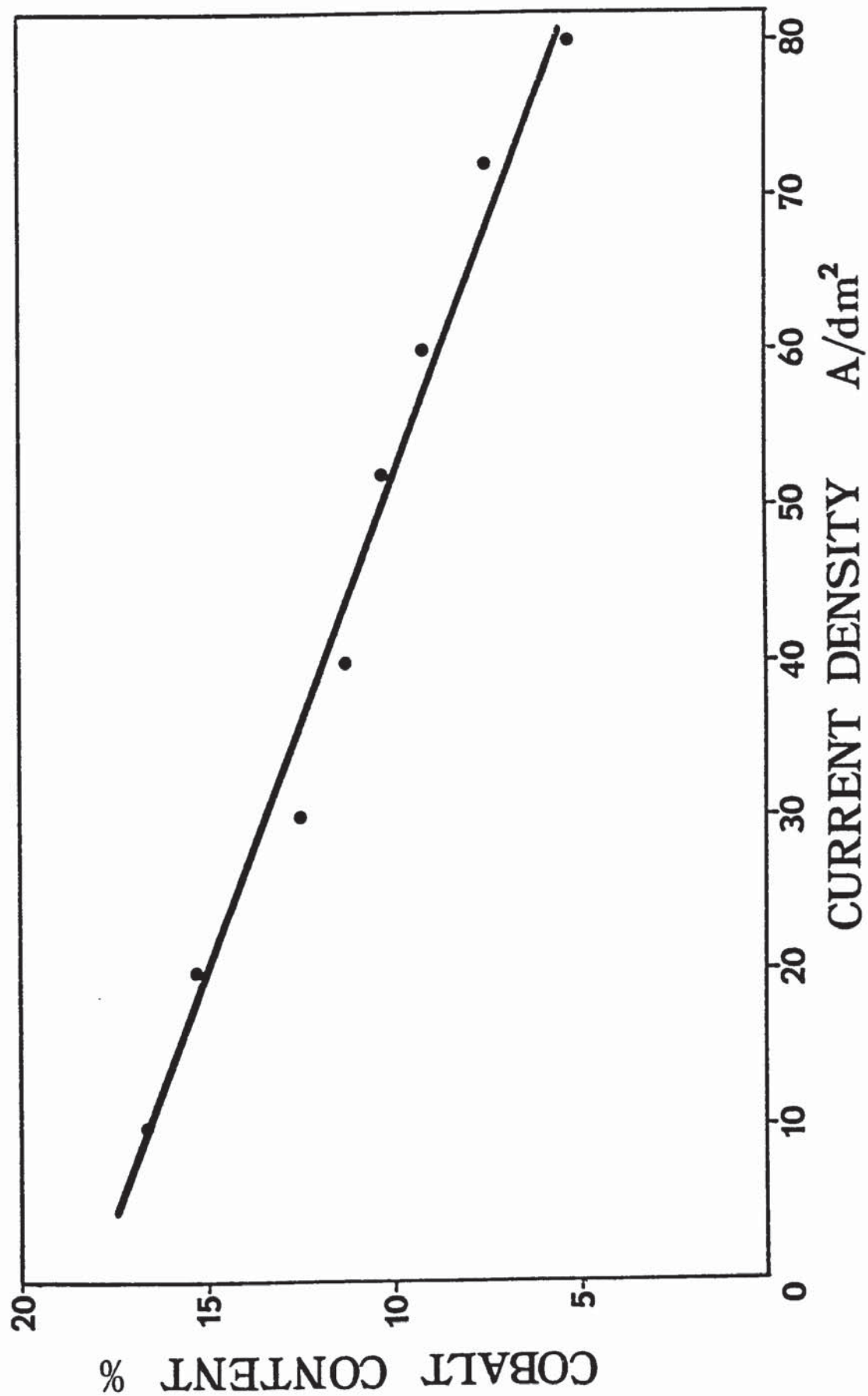


Fig.(81) Effect of variation of current density on the cobalt content of nickel-cobalt alloy deposit plated using ultrasonic agitation 350 watts

8.6.2 Nickel-Iron.

The results of experimental work carried out to investigate the effect of vigorous air agitation on limiting current density are shown in Table XXX.

Satisfactory, bright and sound electrodeposits were obtained between 10 to 16 A/dm² with no trace of edge burns. At 18 A/dm² an unsatisfactory powdery deposit appeared at the edges of the test pieces and these burns gradually increased as higher current densities were applied to the cathode. Test pieces are illustrated in Fig.(82).

The result of experimental work carried out to investigate the effects of ultrasonic agitation of various intensities on limiting current density as shown in Tables XXXI and XXXII.

Bright and sound deposits were obtained by using ultrasonic agitation 200 watts between 10 and 30 A/dm² with no trace of edge burns and commercially acceptable. At 32 A/dm² an unsatisfactory powdery deposit built up on the edges of the test piece and these burns gradually increased as higher current densities were applied to the plating solution.

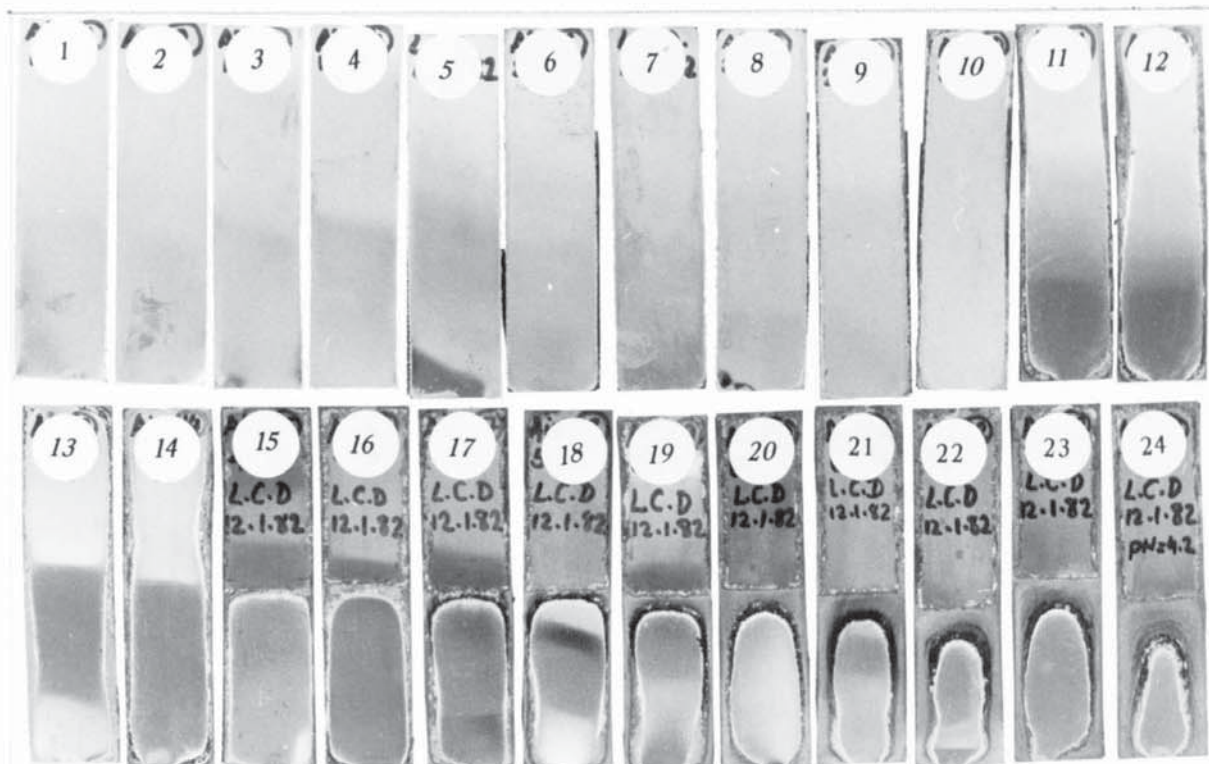


Fig.(82) Appearance of nickel-iron deposits plated at current densities ranging from 10 to 80 A/dm² using air agitation, pH 4, temperature 68°C.

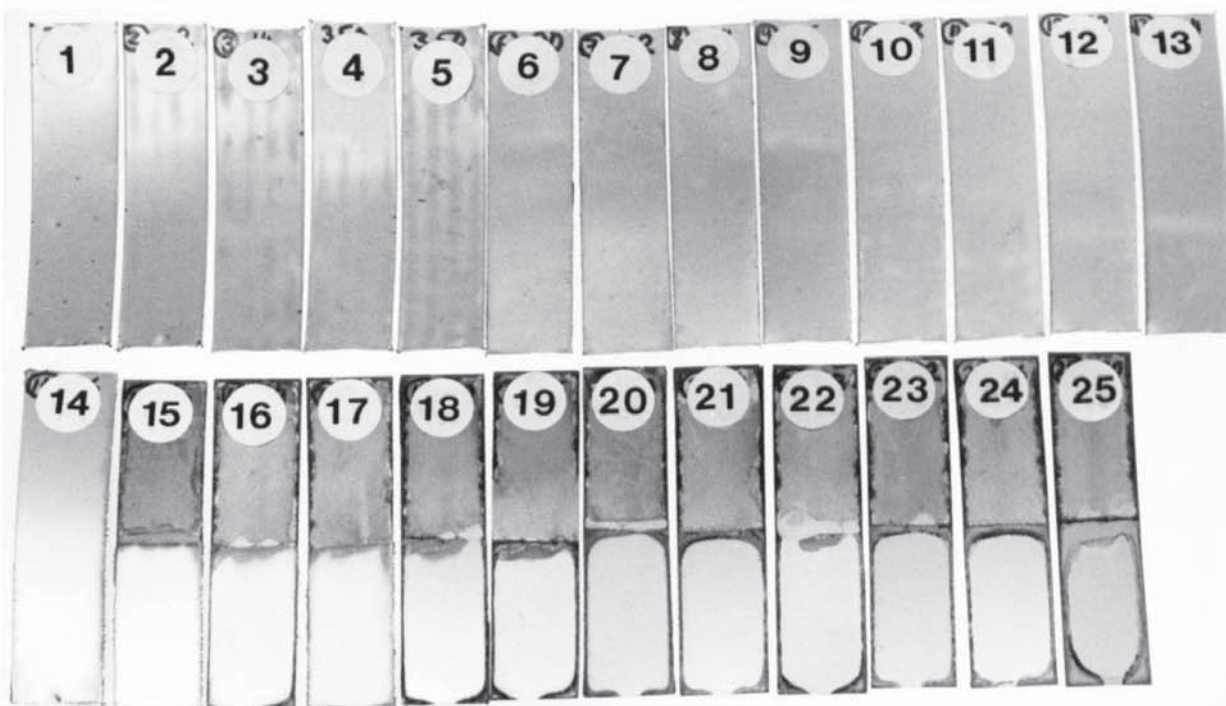


Fig.(83) Appearance of nickel-iron deposits plated at current densities ranging from 10 to 80 A/dm² using ultrasonic agitation 350 watts, pH 4, temperature 68°C.

Table XXX

Limiting current density results using air
agitation, pH 4, 68°C.

Plated Area dm ²	Current Density A/dm ²	Plating Time min.sec.	General Appearance of Deposit
0.5	10	40.00	Bright, sound deposit
0.5	12	33.20	"
0.5	14	28.35	"
0.5	16	25.00	"
0.25	18	22.12	Slight burns on the corners
0.25	20	20.00	"
0.25	22	18.12	"
0.25	24	16.38	Slight burns increasing gradually towards the centre, slightly stressed
0.25	26	15.24	"
0.25	28	14.18	"
0.25	30	13.22	"
0.25	32	12.30	"
0.25	34	11.46	"
0.25	36	11.07	"
0.125	40	10.00	Burns increasing on the edges
0.125	44	9.06	"
0.125	48	8.20	Burns increasing, stressed
0.125	52	7.41	"
0.125	56	7.08	"
0.125	60	6.40	Severe stress, burns all around
0.125	64	6.15	"
0.125	68	5.53	"
0.125	72	5.33	Severe stress, burn increased
0.125	76	5.15	"
0.125	80	5.00	"

Table XXXI

Limiting current density results using ultrasonic
agitation 200 watts, pH 4, 68°C.

Plating Area dm ²	Current Density A/dm ²	Plating Time min.sec.	General Appearance of Deposit
0.5	10	40.00	Bright, sound deposit
0.5	12	33.20	"
0.5	14	28.35	"
0.5	16	25.00	"
0.5	18	22.12	"
0.5	20	20.00	"
0.25	22	18.12	"
0.25	24	16.38	"
0.25	26	15.24	"
0.25	28	14.18	"
0.25	30	13.22	"
0.25	32	12.30	Slight burns on the edges
0.25	34	11.46	"
0.25	36	11.07	"
0.125	40	10.00	"
0.125	44	9.06	Slight burns increasing gradually
0.125	48	8.20	Slight burn increase, slight stress
0.125	52	7.41	"
0.125	56	7.08	"
0.125	60	6.40	Burns all around getting more stressed
0.125	64	6.15	"
0.125	68	5.53	Severe stress and burns increased
0.125	72	5.33	"
0.125	76	5.15	"
0.125	80	5.00	"

Table XXXII

Limiting current density results using ultrasonic agitation 350 watts, pH 4, 68°C.

Plating Area dm ²	Current Density A/dm ²	Plating Time min.sec.	General Appearance of Deposit
0.5	10	40.00	Bright, sound deposit
0.5	12	33.20	"
0.5	14	28.35	"
0.5	16	25.00	"
0.5	18	22.12	"
0.25	20	20.00	"
0.25	22	18.12	"
0.25	24	16.38	"
0.25	26	15.24	"
0.25	28	14.18	"
0.25	30	13.22	"
0.25	32	12.30	"
0.25	34	11.46	"
0.25	36	11.07	Slight burns on the edges
0.125	40	10.00	"
0.125	44	9.06	"
0.125	48	8.20	"
0.125	52	7.40	Slight burns increasing gradually towards centre and slightly stressed
0.125	56	7.08	"
0.125	60	6.39	"
0.125	64	6.15	"
0.125	68	5.52	"
0.125	72	5.33	Burns all around the test piece and highly stressed
0.125	76	5.13	"
0.125	80	5.00	"

Bright and sound deposits were obtained by using ultrasonic agitation 350 watts between 10 and 34 A/dm² with no traces of edge burns. At 36 A/dm² slightly burned deposits appeared at the edges.

Test pieces are illustrated in Fig.(83). The current density up to which a satisfactory deposit could be obtained from bright nickel-iron solution was dependent upon the degree of either air or ultrasonic agitation as shown below:

Type of Agitation	Limiting current density A/dm ²
Air	16
ultrasonic 200 watts	30
ultrasonic 350 watts	34

It is apparent from the results of the limiting current density experiments, that by applying ultrasonic agitation higher current densities could be satisfactorily used giving bright, sound deposit as shown in Table XXXII, and illustrated in Fig.(83).

8.6.2.1 Hardness and Composition of Deposits
Obtained Using Air Agitation.

The hardness and composition of deposits plated between 10 and 80 A/dm² from nickel-iron solution are shown in Table XXXIII for air agitation.

Table XXXIII

Variation in hardness and composition of nickel-iron alloy deposits with changes in current density using air agitation, pH 4, 68°C.

Current density A/dm ²	Iron content %	Nickel content %	Hardness HV
10	20.1	80.6	562.8
20	18.5	82.7	574.4
30	17.1	84.1	579.4
40	15.9	84.6	591.8
52	14.2	86.9	605.5
60	13.7	87.4	615.5
72	13.1	87.8	606.37
80	12.2	88.6	614.5

By increasing the current density in nickel-iron solution when using air agitation the hardnesses of the electrodeposits increased linearly as shown in Fig.(84) and the iron contents of the deposits decreased as shown in Fig.(85).

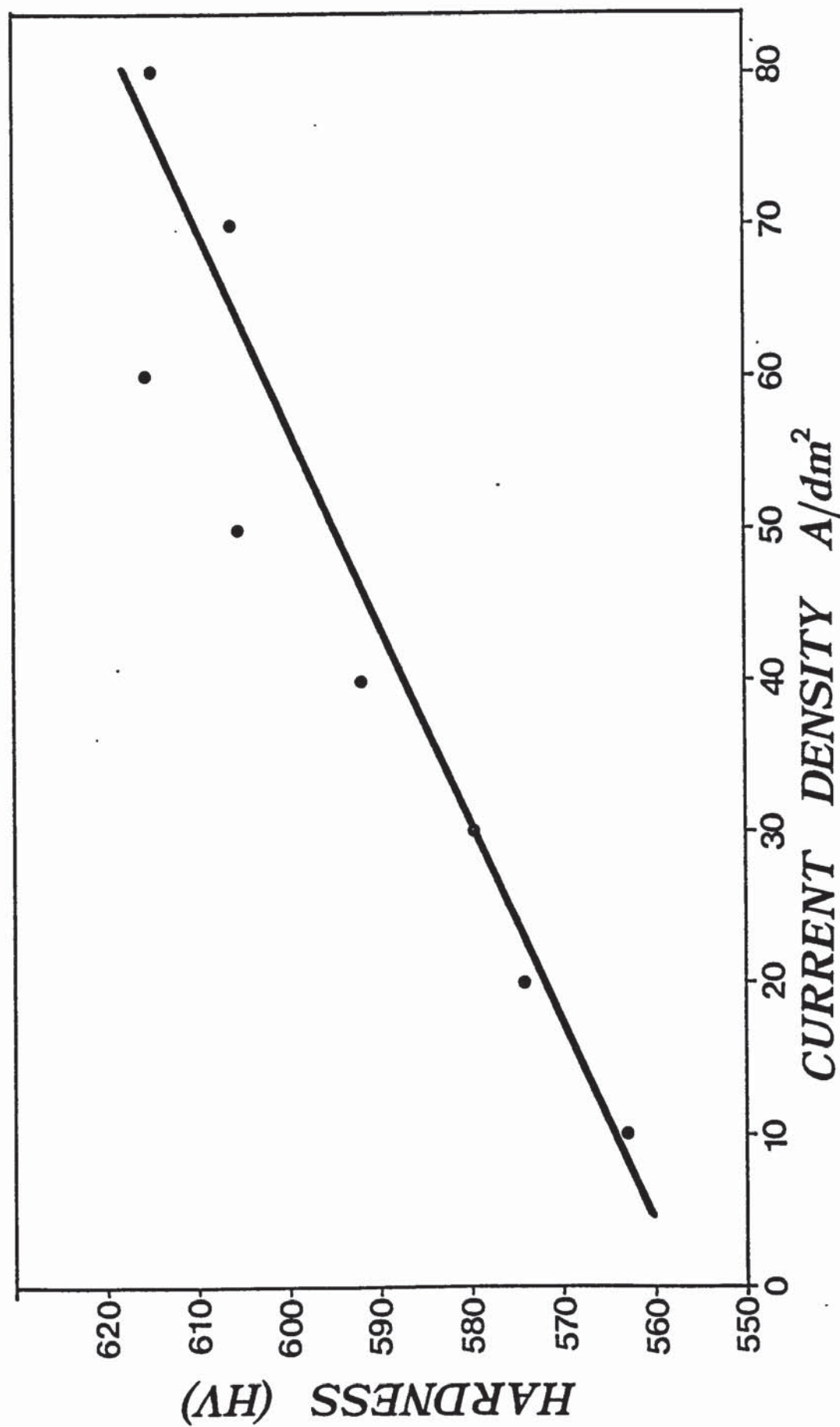


Fig. (84) Effect of variation of current density on the hardness of nickel-iron alloy deposit plated using air agitation.

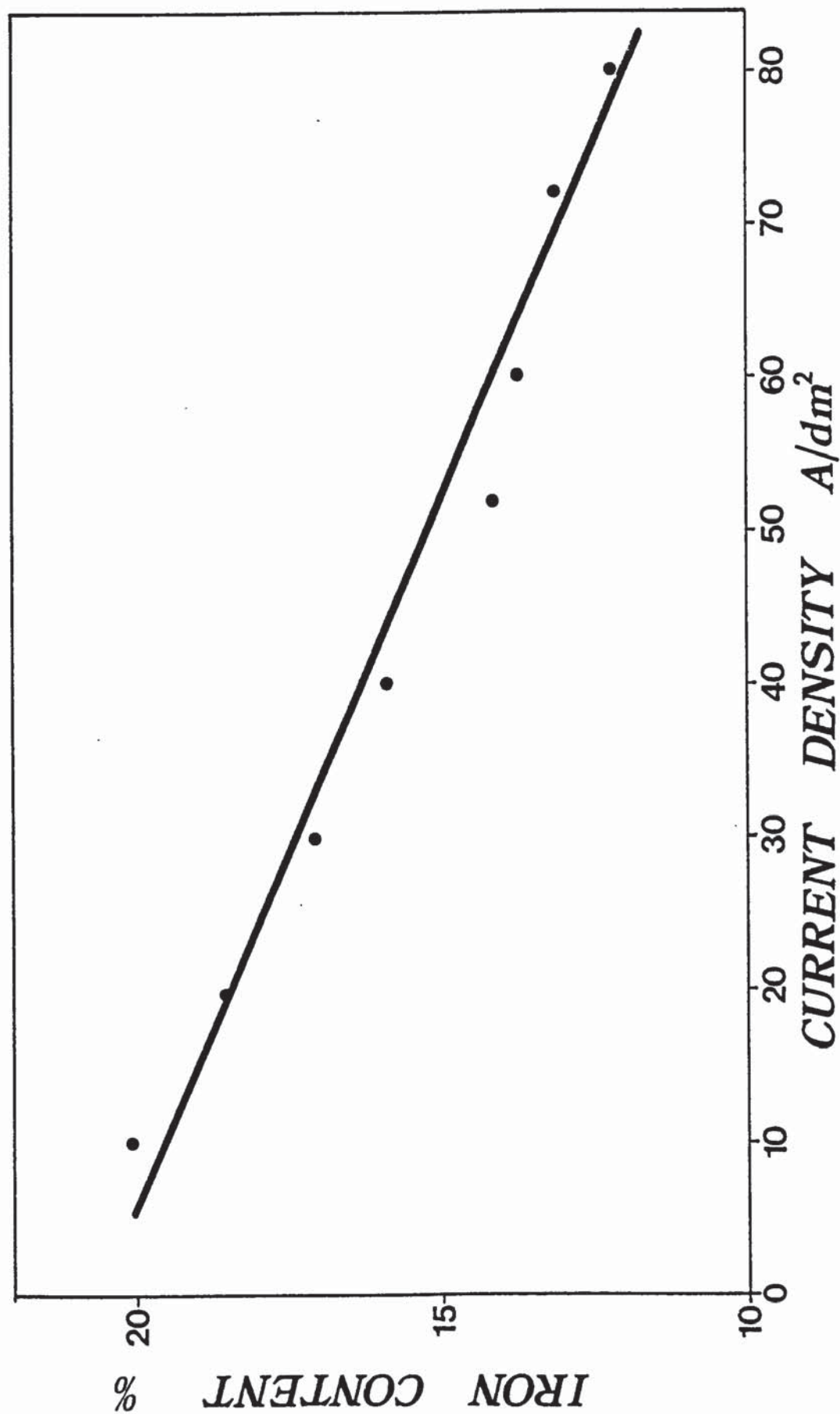


Fig.(85) Effect of variation of current density on the iron content of nickel-iron alloy deposit plated using air agitation.

8.6.2.2 Hardness and Composition of Deposits
Obtained Using Ultrasonic Agitation.

The composition and hardness results for ultrasonically agitated solutions are shown in Tables XXXIV and XXXV.

Table XXXIV.

Variation in hardness and composition of nickel-iron alloy deposits with changes in current density using ultrasonic agitation 200 watts, pH 4, 68°C.

Current density A/dm ²	Iron content %	Nickel content %	Hardness HV
10	19.6	81.4	609
20	18.3	82.7	612
30	16.8	85.1	615.3
40	15.6	84.9	621.4
52	14.5	86.3	629.1
60	13.5	87.4	632.7
72	12.3	88.4	630
80	11.6	89.3	645.3

Table XXXV

Variation in hardness and composition of nickel-iron alloy deposits with changes in current density using ultrasonic agitation 350 watts, pH 4, 68°C.

Current density A/dm ²	Iron content %	Nickel content %	Hardness HV
10	20.3	80.2	631
20	18.2	81.9	634
30	16.9	83.5	642
40	15.3	85.2	651
52	14.6	85.9	647
60	13.8	86.8	649.7
72	12.4	87.9	654.3
80	10.8	90.1	663.9

It is apparent from Figs. 86 and 88 that by increasing the current density for nickel-iron solution when using ultrasonic agitation of 200 and 350 watts the hardness of the electrodeposits increased and the iron content decreased, as shown in Figs. 87 and 89.

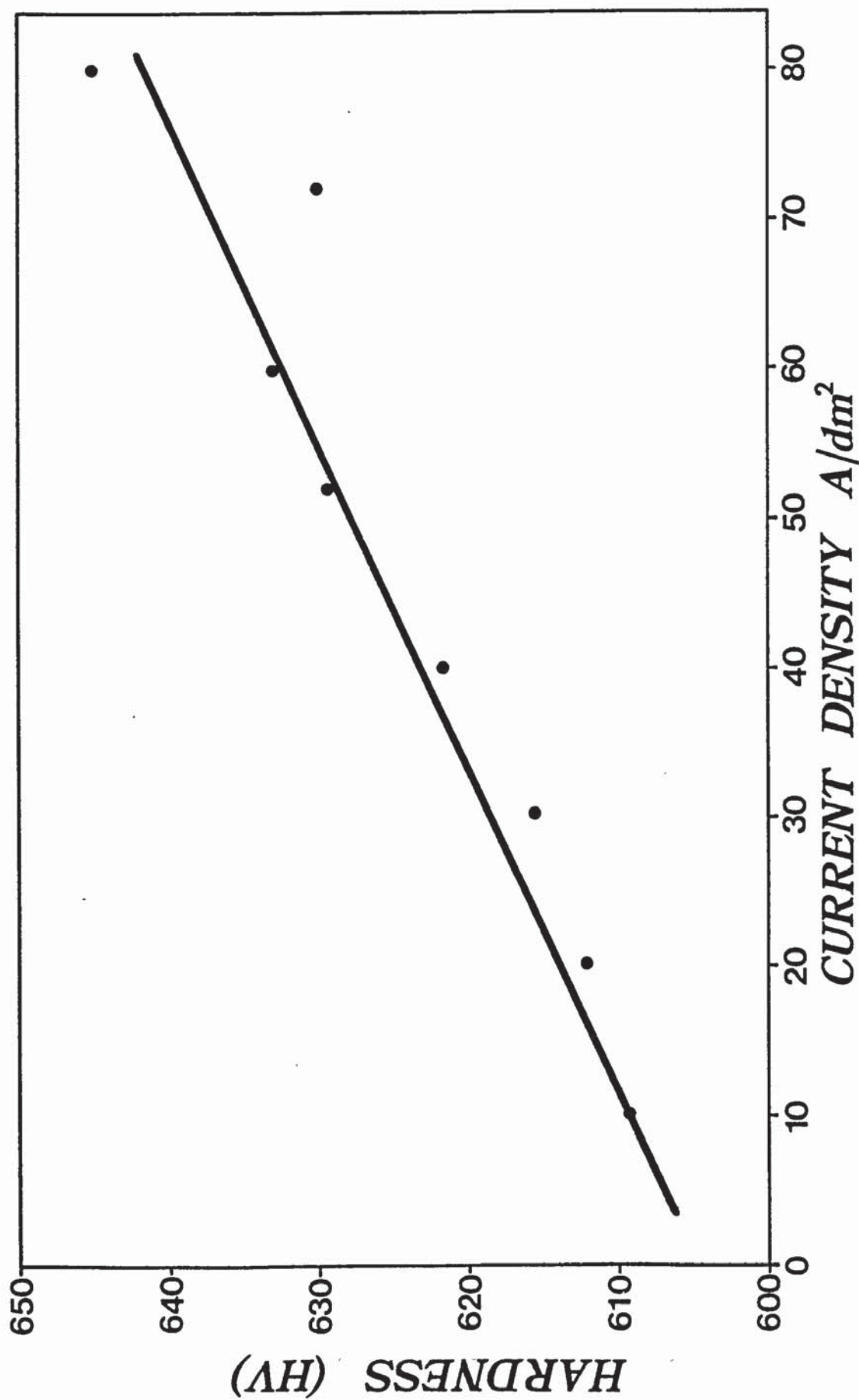


Fig.(86) Effect of variation of current density on the hardness of nickel-iron alloy deposit plated using ultrasonic agitation 200 watts.

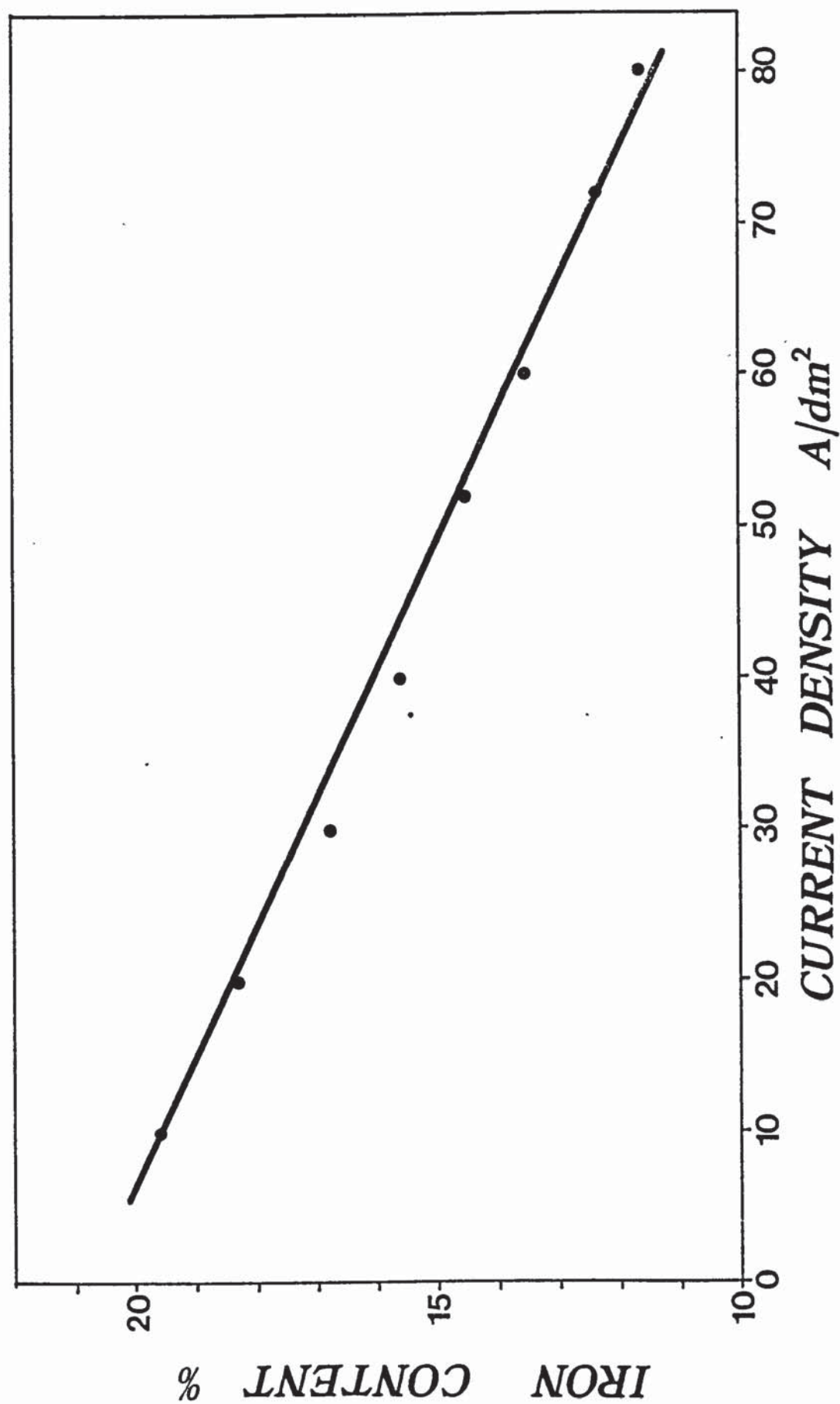


Fig.(87) Effect of variation of current density on the iron content of nickel iron alloy deposit plated using ultrasonic agitation 200 watts.

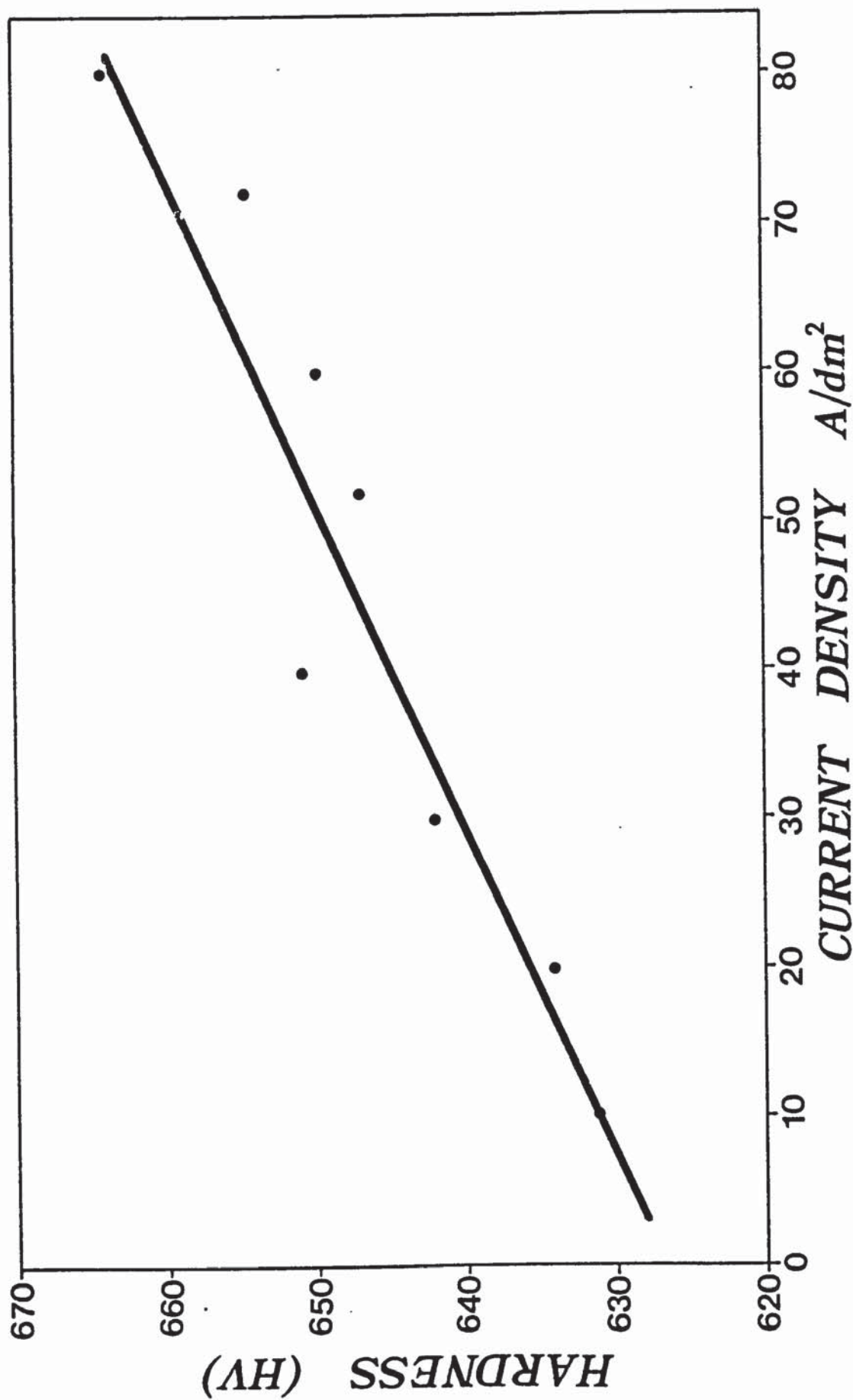


Fig.(88) Effect of variation of current density on the hardness of nickel-iron alloy deposit plated using ultrasonic agitation 350 watts.

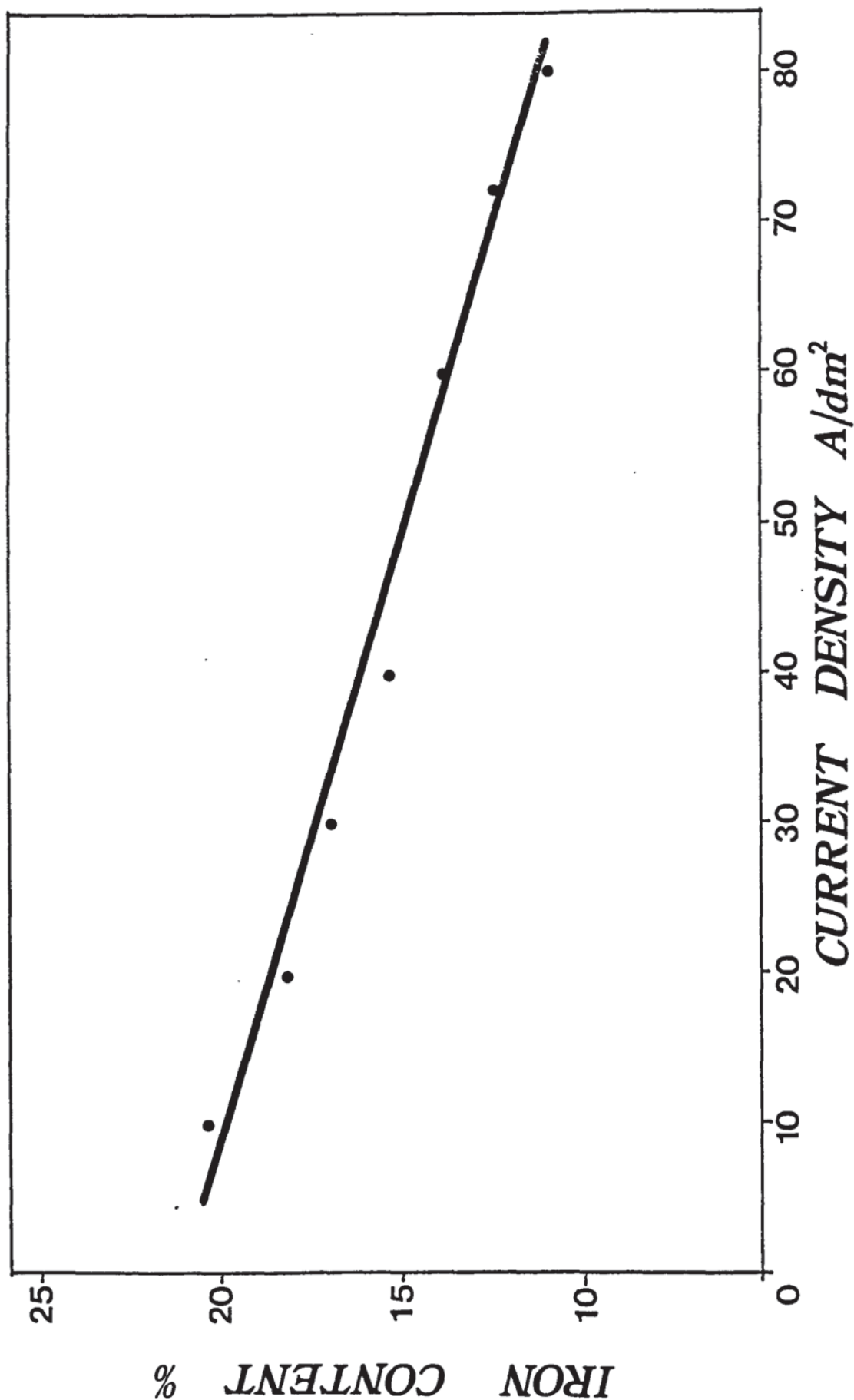


Fig.(89) Effect of variation of current density on the iron content of nickel-iron alloy deposit plated using ultrasonic agitation 350 watts.

8.7 Cathode Current Efficiency.

8.7.1 Nickel-Cobalt.

Calculations were made for cathode current efficiencies of the baths using either air or ultrasonic agitation respectively. The individual weights of nickel and cobalt were determined from the analytical results.

Example of calculation

8.7.1.1 Air Agitation.

Weight of nickel-cobalt alloy deposited = 3.899 g

Weight of copper deposited = 4.426 g

Weight of nickel deposited = 79.8% of alloy = 3.111 g

Weight of cobalt deposited = 20.2% of alloy = 0.7876 g

Number of gramme equivalents of Ni = $\frac{3.111}{29.345}$ = 0.106

Number of gramme equivalents of Co = $\frac{0.7876}{29.47}$ = 0.0267

Number of gramme equivalents of Cu = $\frac{4.426}{31.77}$ = 0.139

Number of gramme equivalents of Ni+Co = 0.106 + 0.0267
= 0.1327

Cathode current efficiency = $\frac{0.1327}{0.139} \times 100$ = 95.5%

The following cathode current efficiency results were found using air agitation, pH 4; current density 4 A/dm² and temperature 55°C.

95.5%; 95%; 96%; 95.4%; 95.2%; 95.8%; 94.6%; 95.3%; 96%; 95%.

Average 95.4%.

8.7.1.2 Ultrasonic Agitation.

The results obtained using ultrasonic agitation pH 4; current density 4 A/dm² and temperature 55°C are shown in Table XXXVI.

Table XXXVI

Relation between power of ultrasonic agitation and cathode current efficiency for nickel-cobalt solution containing 10 g/l CoSO₄·7H₂O.

Power Watts	Efficiency %	Average %
20	94.3	
20	94.5	94.53
20	94.8	
40	94.9	
40	95.2	94.9
40	94.8	
100	95.2	
100	94.9	94.83
100	94.4	
200	95.7	
200	96.6	96.23
200	96.4	
350	97.4	
350	97.9	98.03
350	98.8	

These results indicate that a small increase in cathode current efficiency was achieved by using the higher levels of ultrasonic agitation instead of air.

8.7.2 Nickel-Iron.

The cathode efficiency of nickel-iron plating baths which normally exceeds 90% is primarily dependent upon, three factors; temperature, ferric ion concentration, and organic impurities. Since the nickel-iron solution is more dilute than conventional nickel baths its efficiency is very temperature dependent. Normally, no major loss of efficiency occurs until the temperature falls below 55°C. An increase in ferric ion concentration lowers the cathode efficiency. However, high ferric ion levels are rarely ever attained whereby a noticeable loss of cathode efficiency can be observed. The formation of organic breakdown products, a problem common to bright nickel baths as well, influences cathode efficiency, but was successfully controlled through continuous filtration. The cathode current efficiency of the solution was determined using either air or ultrasonic agitation.

8.7.2.1 Air Agitation.

The following cathode current efficiency results were found for air agitated solution, pH 4; current density 4 A/dm² and temperature 68°C.

95.11%; 95.1%; 94.5%; 93%; 94.2%; 94.8%; 94.4%; 94.8%;
94.7%; 94.3%.

Average = 94.5%.

8.7.2.2 Ultrasonic Agitation.

The results obtained using ultrasonic agitation pH 4; current density 4 A/dm² and temperature 68°C are shown in Table XXXVII.

Table XXXVII

Relation between power of ultrasonic agitation and cathode current efficiency for nickel-iron solution.

Power, Watts	Efficiency %	Average %
20	94.7	
20	95.7	95.2
20	95.2	
40	95.44	
40	95.1	95.45
40	95.8	
100	96.6	
100	96.9	96.6
100	96.4	
200	96.66	
200	97.8	97.3
200	97.4	
350	98.4	
350	97.4	98.03
350	98.3	

It is apparent that the same general trend occurred for nickel-iron as for nickel-cobalt baths. The efficiency increased slightly as the degree of ultrasonic agitation.

was increased and it was even slightly higher at 20 watts than when using air agitation.

8.8 Macrothrowing Power.

8.8.1 Nickel-Cobalt Deposits.

The cathodes from the Hull cell plating tests were sectioned and the coating thicknesses measured using the optical system of the micro-hardness (Vickers photo-plan)tester. The metal distribution curves shown in Fig.(90) were plotted. In order to identify the current densities at specific positions of the cathode panel the following formula was used:-

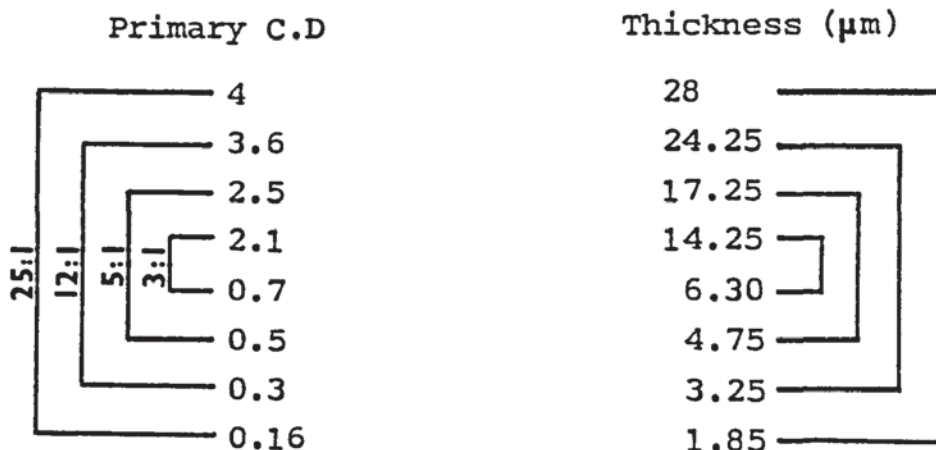
$$i = I(4.08 - 3.96 \log x)$$

Where (i) is the primary current density in A/dm^2 , (I) is the total cell current and (x) is the distance in (cm) from the high current density edge of the panel.

Primary current densities were chosen according to the method published by Watson⁽¹²⁰⁾ to give current density ratios of 25:1; 12:1; 5:1; 3:1 as shown in the diagram below. Thicknesses corresponding to the current densities chosen were read from the graph.

Example of calculation - Method I (Watson)

8.8.1.1 Macrothrowing Power Air Agitated.



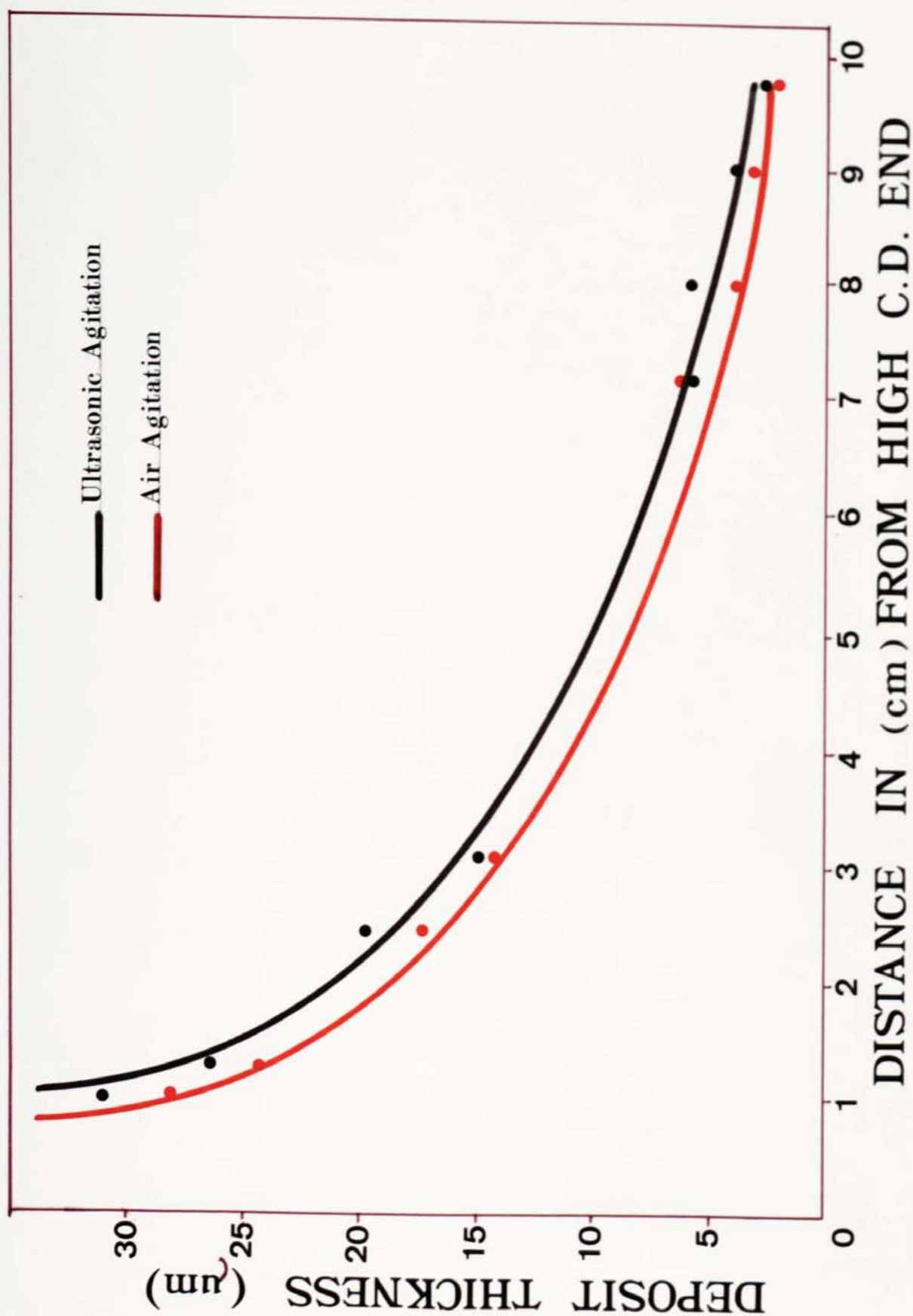


Fig. (90) Average deposits thickness of nickel-cobalt alloy (10 g/l cobaltous sulphate)/ distance in (cm) from high current density end of the cathode panel.

The following primary current ratios correspond to the following metal distribution ratios:-

P	M
3:1	2.26
5:1	3.63
12:1	7.46
25:1	15.22

Then macrothrowing power values for the air agitated panels according to Field's equation is equal to

$$T = \frac{100(P - M)}{P + M - 2} \quad \%$$

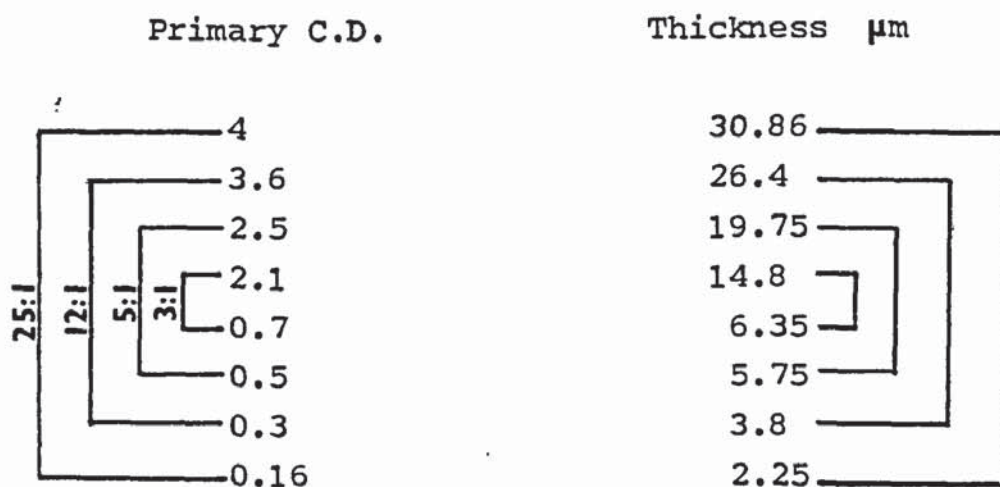
$$\text{M.T.P (3)} = \frac{100(3 - 2.26)}{3 + 2.26 - 2} = \frac{74}{3.26} = 22.7 \%$$

$$\text{M.T.P (5)} = \frac{100(5 - 3.63)}{5 + 3.63 - 2} = \frac{137}{6.63} = 20.66 \%$$

$$\text{M.T.P (12)} = \frac{100(12 - 7.46)}{12 + 7.46 - 2} = \frac{454}{17.46} = 26.0 \%$$

$$\text{M.T.P (25)} = \frac{100(25 - 15.22)}{25 + 15.22 - 2} = \frac{978}{38.22} = 25.6 \%$$

8.8.1.2 Macrothrowing Power Using Ultrasonic Agitation Power 350 Watts.



The following primary current ratios correspond to the following metal distribution ratios.

P	M
3:1	2.3
5:1	3.43
12:1	6.94
25:1	13.715

The macrothrowing power values for the panel were as follows:

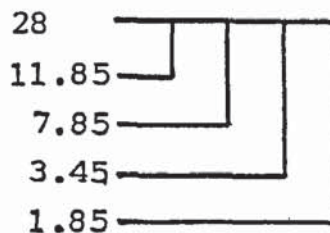
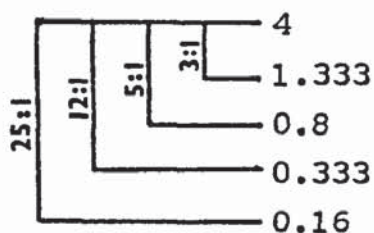
$$\begin{aligned}
 \text{M.T.P (3)} &= \frac{100(3 - 2.3)}{3 + 2.3 - 2} = \frac{70}{3.3} = 21.2 \% \\
 \text{M.T.P (5)} &= \frac{100(5 - 3.43)}{5 + 3.43 - 2} = \frac{157}{6.43} = 24.4 \% \\
 \text{M.T.P (12)} &= \frac{100(12 - 6.94)}{12 + 6.94 - 2} = \frac{506}{16.94} = 30.8 \% \\
 \text{M.T.P (25)} &= \frac{100(25 - 13.715)}{25 + 13.715 - 2} = \frac{1128.5}{36.715} = 30.75 \%
 \end{aligned}$$

Method II

Throwing power was recalculated from the same panels by obtaining the primary current ratios by the method shown below, for an air agitated panel.

Primary C.D.

Thickness (μm)



The following primary current ratios correspond to the following metal distribution ratios.

<u>P</u>	<u>M</u>
3:1	2.36
5:1	3.57
12:1	8.1
25:1	15.135

Macrothrowing power values for the air agitated panels

$$\text{M.T.P (3)} = \frac{100(3 - 2.36)}{3 + 2.36 - 2} = \frac{64}{3.36} = 19.05 \%$$

$$\text{M.T.P (5)} = \frac{100(5 - 3.57)}{5 + 3.57 - 2} = \frac{143}{6.57} = 21.8 \%$$

$$\text{M.T.P (12)} = \frac{100(12 - 8.1)}{12 + 8.1 - 2} = \frac{390}{18.1} = 21.55 \%$$

$$\text{M.T.P (25)} = \frac{100(25 - 15.135)}{25 + 15.135 - 2} = \frac{986.5}{38.135} = 25.9 \%$$

The same method was applied on an ultrasonically agitated panel. The following primary current ratio correspond to the following metal distribution ratios were obtained.

<u>P</u>	<u>M</u>
3:1	2.28
5:1	3.44
12:1	6.34
25:1	11.93

Macrothrowing power values for the ultrasonic agitation 350 watts were as follows.

$$\text{M.T.P (3)} = \frac{100(3 - 2.28)}{3 + 2.28 - 2} = \frac{72}{3.28} = 22 \quad \%$$

$$\text{M.T.P (5)} = \frac{100(5 - 3.44)}{5 + 3.44 - 2} = \frac{156}{6.44} = 24.2 \quad \%$$

$$\text{M.T.P (12)} = \frac{100(12 - 6.34)}{12 + 6.34 - 2} = \frac{566}{16.34} = 34.6 \quad \%$$

$$\text{M.T.P (25)} = \frac{100(25 - 11.93)}{25 + 11.93 - 2} = \frac{1307}{34.93} = 37.4 \quad \%$$

It is obvious from the results obtained by these two methods that the macrothrowing power is positive but relatively low, as shown in Table XXXVIII. The macrothrowing power result values obtained using ultrasonic agitation were slightly higher than those obtained by air agitation in both methods. The results given by the two methods of calculation were very similar and so later results will be calculated only by Method I.

The metal distributions on panels plated with air and ultrasonic agitation in a solution containing 110 g/l cobaltous sulphate ($\text{CoSO}_4 \cdot 7\text{H}_2\text{O}$) are shown in Fig.(91). The macrothrowing power values are listed in Table XXXIX; they are positive but relatively low.

The macrothrowing power of the ultrasonically agitated solution is slightly higher than the air agitated one as shown in Table XXXIX.

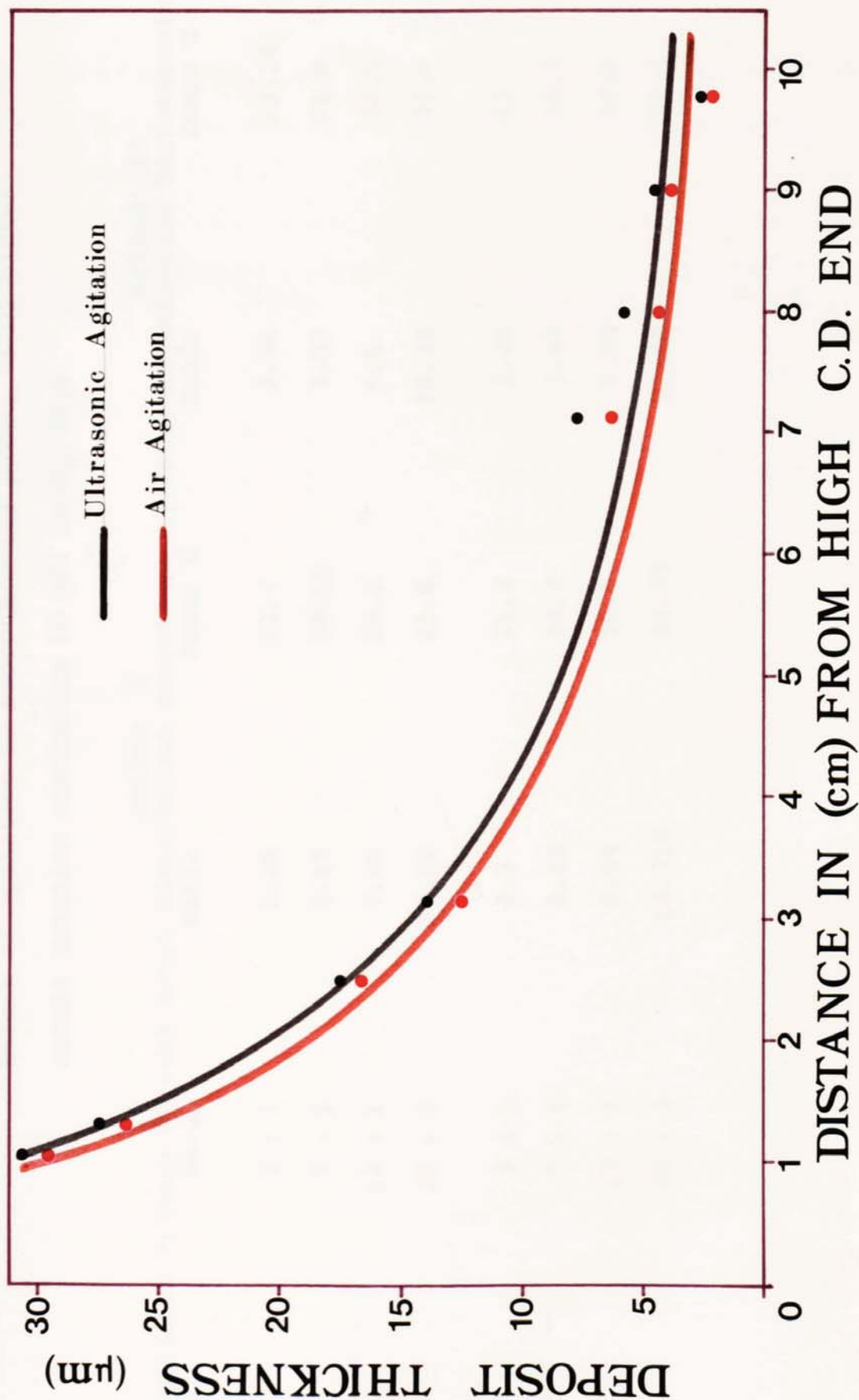


Fig.(91) Average deposits thickness of nickel-cobalt alloy (110 g/l cobaltous sulphate)/ Distance in (cm) from high current density end of the cathode panel.

Table XXXVIII

Effect of agitation on macrothrowing power, using nickel-cobalt solution containing 10 g/l $\text{CoSO}_4 \cdot 7\text{H}_2\text{O}$

Type of agitation	Primary Current Ratio	Method I		Method II	
		Metal Distribution Ratio	Macrothrowing Power %	Metal Distribution Ratio	Macrothrowing Power %
Air	3 : 1	2.26	22.7	2.38	18.34
	5 : 1	3.63	20.66	3.57	21.8
	12 : 1	7.46	26.0	6.6	32.5
	25 : 1	15.22	25.6	13.33	32.0
Ultrasonic 350 Watts	3 : 1	2.3	21.2	2.28	22
	5 : 1	3.43	24.4	3.44	24.2
	12 : 1	6.94	30.8	6.34	34.6
	25 : 1	13.715	30.75	11.93	37.4

Table XXXIX

Effect of agitation on macrothrowing power, using nickel-cobalt solution containing 110 g/l cobaltous sulphate ($\text{CoSO}_4 \cdot 7\text{H}_2\text{O}$).

Type of Agitation	Primary Current Ratio	Metal Distribution	Macrothrowing Power %
Air	3 : 1	2	33.33
	5 : 1	3.7	19.4
	12 : 1	7.14	28.35
	25 : 1	13.24	32.45
Ultrasonic 350 Watts	3 : 1	1.8	42.85
	5 : 1	3	33.33
	12 : 1	6	37.5
	25 : 1	12	37.14

8.8.2 Nickel-Iron Deposits.

Table XXXX

Effect of agitation on macrothrowing power
using nickel-iron solution.

Type of Agitation	Primary Current Ratio	Metal Distribution	Macrothrowing Power %
Air	3 : 1	1.93	36.5
	5 : 1	3.25	28
	12 : 1	6.14	36.3
	25 : 1	11.92	37.5
Ultrasonic 350 Watts	3 : 1	1.89	38
	5 : 1	2.83	37
	12 : 1	4.87	47.9
	25 : 1	8.69	51.5

The metal distributions on panels plated with air and ultrasonic agitation are shown in Fig.(92).

It is clear from these results in Table XXXX that the macrothrowing power obtained using ultrasonic agitation 350 is slightly higher than those obtained using air agitation and these results are relatively higher than the Ni-Co ones.

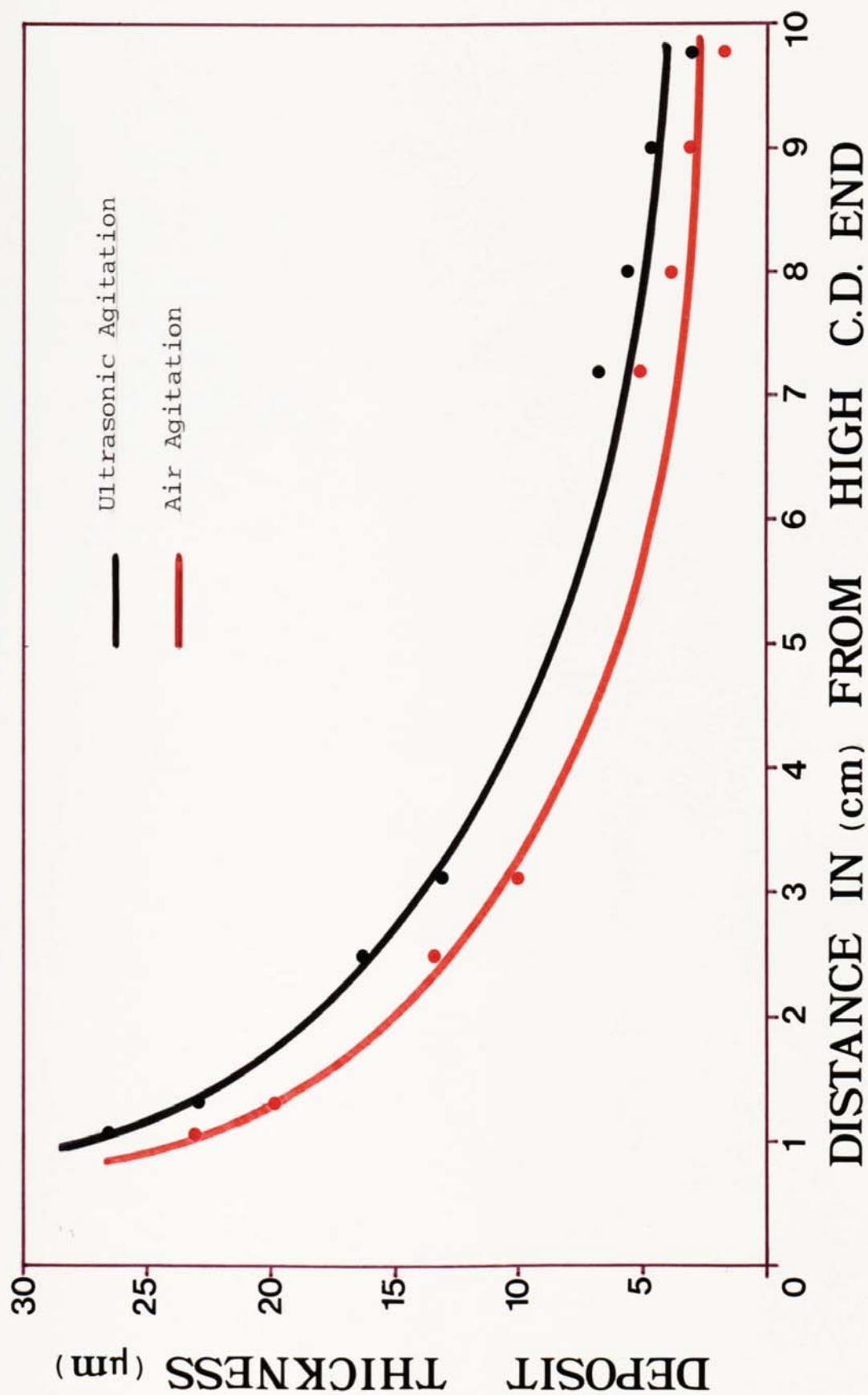


Fig.(92) Average deposits thickness of nickel-iron alloy / Distance in (cm) from high current density end of the cathode panel.

CHAPTER NINE

9. DISCUSSION.

9.1. Electrolyte Agitation.

No matter how turbulent the motion, there is always in close contact with the surface a thin layer of liquid that is moving with viscous flow. Although agitating techniques, e.g. conventional stirring, can reduce its thickness to approximately 10 μm , this barrier layer cannot be completely eradicated. Such films are always thinner at points and edges than on the bulk of a plane surface. An increase in the concentration of active ions in the immediate vicinity of the electrodes (i.e. an increase in the diffusion driving force) allows the reaction rate and also the current density to be increased. To increase the current density (i.e. the rate of electron transfer to or from the electrode surface) without stimulating a compensatory build-up of the reactive ions causes the diffusion rate across the boundary layer to fall.

Consideration of Fick's law and the Nernst model shows that, as an alternative to increasing the mass transfer driving force, the rate of diffusion of the reacting species to the electrode can be improved by reducing the boundary layer thickness. Various techniques have been developed in the hope of achieving this reduction of

layer thickness.

The most obvious technique is to increase the velocity of the solution flowing over the electrode face. Electro-writers have adopted high cell flowrates in conventional cells at several installations, however, studies suggest that velocities at the cathode face of 0.3 m/s are necessary before any significant thinning of the boundary layer occurs. To achieve such velocities in conventional cells is almost impossible due to the amount of by-passing that occurs. The use of turbulent solution flow achieved with a minimum flow rate of 1.25 m/s or an equivalent rapid rate of cathode movement sustains high current densities above 100 A/dm^2 to provide rates for metal deposition above $20 \text{ }\mu\text{m/min}$. Fast rate electro-deposition facilities can be engineered to reduce plant investment and labour and conserve materials and energy.⁽¹³²⁾

Mechanical agitation by propellers within electrolytic cells has generally been ineffective. The extent of turbulence in the electrolyte varies with the distance from the impeller with the result that different turbulent velocities are experienced across the cathodes.

Cathode rotation has been quite successful on a small scale with current densities of up to 32.5 A/dm^2 reported. The technique is limited by the eventual rotation of the catholyte with the boundary layer as the speed increases thereby decreasing the relative motion between electrolyte and boundary layer.

Another procedure which promotes reduction of the boundary layer is air agitation. Attempts involving air agitation techniques to achieve very high turbulence in the electrolyte surrounding the cathodes have been carried out using specially designed cells. These have enabled current densities up to 21.6 A/dm^2 to be reached and copper deposits of excellent quality have been obtained.⁽¹³³⁾

9.2 Ultrasonic Agitation.

Ultrasonic agitation can be used to achieve a reduction in the boundary layer. It is considerably more effective than conventional agitating techniques, since unlike bulk mixing, ultrasonic agitation concentrates the intense mixing effect and energy dissipation at either the solid-liquid surface interface or at a boundary layer. The effects of polarization at the electrodes are therefore considerably reduced and in addition, the activity over the surface of the cathode is equalised producing a more even deposit.

9.2.1 Introduction of Ultrasonic Energy to the Cell.

To achieve maximum efficiency from ultrasonic agitation, intimate contact is preferred between the probe and the item requiring agitation.

Although less efficient, the most satisfactory technique for introducing the energy into the system is to locate the probes directly into either the floor or walls of the cell.

9.2.2 Operating Cell Voltage and Possible Power Saving.

At conventional electroplating current densities the cathode polarisation contributes little to the overall cell voltage and mainly results from the slowness with

which ions diffuse up to the electrode to replace those discharged. It is associated therefore with a decrease in concentration of the electrolyte in the immediate vicinity of the electrode. Any agitation therefore should be beneficial in reducing this contribution and consequently a slight reduction in the overall cell voltage may be achieved. At higher current densities the contribution due to concentration polarisation will increase and therefore the benefits from agitation will be greater.

When ultrasonic waves strike either a surface or a concentration gradient, the violent agitation encountered readily ensures the virtual destruction of the barrier layer existing in the immediate vicinity of a cathode. A similar effect will be observed at the anode where the agitation should assist the liberation of oxygen as well as ensuring a supply of hydroxyl ions available for discharge. Thus any effects due to concentration polarisation will be almost totally eliminated.

9.3 Efficiency of Ultrasonic Equipment.

After consultation with the manufacturers of the ultrasonic equipment it was ascertained that the efficiency of ultrasonic power in the plating tank during electrodeposition is reduced by a total of about 15%, due to the damping effect of the water film (5%) and plastic tank (10%).

The actual power received by the plating tank from two transducers is shown in Table XXXXI. The values given in all graphs and tables relate to the nominal output from one transducer. However they give a comparative measure of ultrasonic intensity.

The total power generated by two transducers at 100% efficiency and total power received into the tank at 85% at different power intensities is shown.

Table XXXXI

The relations between total power (watts) generated by two transducers at 100% efficiency and total power received (watts) into the bath.

Total power generated (watts) at 100% efficiency	Total power received (watts) at 85% efficiency
40	34
80	68
200	170
400	340
700	595

9.4 Hardness.

9.4.1 Statistical Analysis of Hardness Results.

To obtain information on the accuracy of hardness measurements an Analysis of Variance was performed on two separate lots of hardness data. Variance is the mean of the squares of variations from the arithmetic mean. The (F) ratio or variance ratio is used for comparing two variances. In each case 10 hardness measurements were made on each of 10 hardness indentations, i.e. a total of 100 hardness measurements were made.

In both cases the hardnesses were measured on electro-deposits obtained from a nickel-cobalt solution pH 4; C.D. 4 A/dm^2 using air agitation. To simplify the arithmetic 260 was subtracted from the first lot of measurements and the resultant data laid out in the following matrix Table XXXXII. The Analysis of Variance is shown in Table XXXXIII. The calculated F ratio < 1 clearly showed that there was no error in the hardness measurements. A similar calculation was done on the second batch of hardness results. In this case 254 was subtracted for ease of calculation. Details are given in the matrix Table XXXXIV and the Analysis of Variance Table laid out in XXXXV. Again the calculated F ratio < 1 showing lack of error in the hardness measurements. The experimental errors in hardness testing can be ignored and averages taken on the same specimen give accurate hardness results.

Table XXXXII

Hardness measurements with 260 subtracted from all results of case I

Hardness Measurements Readings	A	B	C	D	E	F	G	H	I	J
1	7	1.5	-7	1	-2	6.5	0.5	-4.5	6	10
2	10	-6	10	6	-1	11	10	5	-4	4
3	6	0.5	13	4	6	-2	-7	6	6	-7
4	0.5	2	6	5	-7	-8	0	4.5	1	10
5	6	-0.5	-2	5	-0.5	-2	0.5	1.5	-2	10
6	-2	6	-3.5	1.5	2	-3.5	-1.5	-2	4	-6
7	1	4	-3.5	-0.5	1.5	-5	-4	-3.5	5	-1
8	-6	0	-2	-6	10	1	-8	1	-6	0
9	-7	-1	-2	2	12	2.5	-10	-1	-8.5	1
10	0	1	0	-2	2	-2	-6	0	2	-6
Total	15.5	7.5	9	16	23	-1.5	-25.5	7	3.5	15
ΣX^2	311.25	97	390.5	149.5	344.5	238.75	367.75	122	246.3	439

$$\begin{aligned}\text{Grand total, } G &= 15.5 + 7.5 + 9 + 16 + 23 - 1.5 - 25.5 \\ &\quad + 7 + 3.5 + 15 = 69.5\end{aligned}$$

$$\text{Correction factor C.F.} = \frac{(69.5)^2}{100} = 48.3$$

$$\begin{aligned}\text{Total sum of squares} &= (7^2 + 10^2 + \dots + (-6)^2 - \text{C.F.}) \\ &= 2751.25 - 48.30 = 2702.95\end{aligned}$$

$$\begin{aligned}\text{Sums of squares S.S. between methods} &= \frac{1}{10} (15.5^2 + \dots + 15^2) - \text{C.F.} \\ &= 210.125 - 48.3 \\ &= 161.825\end{aligned}$$

Table XXXXIII

Analysis of Variance (case I)

Source of variation	D.F.	S.S.	M.S. (Variance)
Between	9	161.825	17.98
Within (error)	90	2541.125	28.28
Total	99	2702.95	

$$F \text{ ratio} = \frac{17.98}{28.23} < 1 \text{ which is not significant}$$

There is no difference between readings and hardness measurements as shown in Analysis of Variance Table XXXXIII

D.F. Degrees of Freedom

M.S. Mean Square.

Table XXXIV

Hardness measurements with 254 subtracted from all results of case II

Hardness Measurements Readings	A	B	C	D	E	F	G	H	I	J
1	-8	0	6.5	-10	8.5	-6	-2	1	-4	-4
2	6	6	2	-2.5	1	-6	-4.5	0	0.5	2
3	10	8	4	7	-10	-12	6	-2	-6	8.5
4	-10	6	7	6.5	2	8	7.5	6	0	-8
5	-6	6.5	2	-6	0	-2	-4	-4	-2.5	-5
6	-8	-10	8.5	-6	-4	2	-6	-2	-3.5	6
7	0	1	-6	7	0	-2	6	7.5	-3.5	0
8	-4	-8	-4.5	6	-0.5	6.5	4.5	0	-4	2
9	1	-4.5	-1.5	0	8	4	-3	-4	2	4
10	2	0	6.5	8	7	0	7	10	8	6
Total	-17	5	24.5	10	12	-7.5	11.5	12.5	-13	11.5
χ^2	421	363.5	288.25	418.5	306.5	350.25	282.75	233.25	167	273.25

$$G = 50.4$$

$$C.F. = \frac{(50.4)^2}{100} = 25.4$$

$$\text{Total S.S.} = 3104.25 - 25.4 = 3078.85$$

$$\begin{aligned} \text{S.S. Between methods} &= \frac{1}{10} (289 + 25 + 600.25 + 100 \\ &\quad + 144 + 56.25 + 132.25 + 156.25 \\ &\quad + 169 + 156.25 - C.F.) \\ &= \frac{1}{10} (1828.25) - 25.40 \end{aligned}$$

$$\text{Sum of squares} = 157.425$$

Table XXXV

Analysis of Variance (case II)

Source of variation	D.F.	S.S.	M.S.
Between methods	9	157.425	17.49
Within methods (error)	90	2921.425	32.46
Total	99	3078.85	

$$F \text{ ratio} = \frac{17.49}{32.46} < 1 \text{ not significant.}$$

There is no difference between readings and hardness measurements.

The statistical analysis of hardness results has emphasised that significant increases in hardness are achieved by the use of ultrasonic agitation instead of air agitation.

Since average hardness measurements are very accurate any average hardness values differing by more than about 10 can be said to come from different statistical populations. At an intensity of 350 watts, the increase in average hardness for deposits studied ranged between 65 to 97 HV. The average results are shown in Table XXXXVI.

Table XXXXVI

Increase in average hardness using 350 watts ultrasonic agitation instead of air agitation, plating conditions pH4, C.D. 4 A/dm² and temp. 55°C for all solution except 68°C for Ni-Fe.

Plating solution		Increase in hardness HV
Ni-Co	10 g/l CoSO ₄ ·7H ₂ O	80
	35	92
	60	97
	85	90
	110	75
Ni		65
Co		78
Ni-Fe		90

9.4.2 Effect of Cobalt Content on Hardness of Nickel-Cobalt Alloys.

Harder deposits are advantageous in many applications and there is potential merit in using cobalt as the hardening agent.

Endicott and Knapp⁽⁵⁰⁾ examined the influence of operating variables on alloy deposits produced from conventional nickel sulphamate solutions containing cobalt, and Ericson⁽⁹⁵⁾ reported an increase in hardness due to cobalt addition to a concentrated nickel sulphamate solution. Belt et al⁽⁴¹⁾ recently reported the effects of cobalt additions on the composition, hardness and ductility of deposits from the concentrated sulphamate electrolyte. This study showed that sound nickel-cobalt alloys could be deposited with values of hardness up to 525 HV, but the deposits always contained at least some tensile stress, by appropriate reduction in current density and cobalt concentration in the solution, it is possible to produce low stress nickel-cobalt alloy deposits with a hardness in excess of 400 HV.

Belt et al⁽⁸⁸⁾ reported that the relation between cobalt-concentration in the solution, cobalt content of the deposit and hardness is not a direct and simple one. Deposits of relatively high cobalt content may be softer than those containing a smaller proportion of cobalt, and in the presence of small amounts of cobalt in solution, hardness and cobalt content vary substantially with change in current density. In the absence of cobalt, or when the cobalt-ion concentration in solution is in the range 5 to 10 g/l, the effect of current density on hardness is relatively slight.

Table XXXXVII shows that the cobalt content in the

deposit obtained from sulphate-chloride solutions with the following concentration of cobalt sulphate of 10, 35, 60, 85 and 110 g/l has a clear effect on hardness using air agitation. By increasing the cobalt content in the alloy deposit from 23.3% to 81.8% the average hardness increased from 265.6 to 308 HV. This can be related to the hardening effect of cobalt content in the deposit as reported by Endicott⁽⁵⁰⁾. The small percentage of cobalt present in the bath resulted in a high percentage of cobalt in the deposit. This effect is to be expected due to the anomalous nature of co-deposition (i.e. the less noble cobalt deposits preferentially). By applying ultrasonic agitation, 350 watts to the nickel-cobalt solutions with different cobalt contents using the same plating conditions the cobalt content decreased from 23.3% to 18.4% and the deposit is 80 HV harder using the solution with 10 g/l cobalt sulphate.

Results of cobalt content and hardness obtained from solutions of 35, 60, 85, and 110 g/l cobalt sulphate are given in Table XXXXVII. For the same cobalt concentration in solution, it can be seen clearly that the hardness obtained using ultrasonic agitation is greater than that obtained using air although the cobalt content in the deposit is less. Consequently ultrasonic agitation had a greater effect on hardening than cobalt content. The probable explanation for the change in composition of the nickel-cobalt deposits is the effects of ultrasonics

on the relative rates of transport of metal and cobalt ions into the cathode film.

Table XXXXVII

Variation in hardness and cobalt content using either air or ultrasonic agitation in nickel-cobalt solutions containing different cobalt sulphate contents (Plating conditions pH 4, current density 4 A/dm², 55°C)

Plating solution (CoSO ₄ ·7H ₂ O)g/l	Agitation	Cobalt content in deposit %	Hardness HV
10	Air	23.3	265.6
35	Air	51	280
60	Air	66.4	289
85	Air	71.7	300
110	Air	81.8	308
10	Ultrasonic 350 W	18.4	345
35	Ultrasonic 350 W	42	372
60	Ultrasonic 350 W	58.4	386
85	Ultrasonic 350 W	63.8	390
110	Ultrasonic 350 W	68.3	383

9.4.3 Dependence of Hardness on Grain Size.

Kenahan et al⁽¹²¹⁾ indicated that ultrasonic agitation produced a significant increase in hardness in both copper-zinc and copper-tin alloy deposits, the hardness of copper-zinc increased from 216 HV without, to 250 HV

with ultrasonic agitation and the copper-tin alloy deposit increased from 247 HV to 315 HV with ultrasonic agitation. He related the increase in hardness to fine grain size which resulted by applying ultrasonic agitation.

Similarly Kochergin and Vyaseleva⁽⁴⁾ reported that the hardness of nickel deposits formed in an ultrasonic field were 60% harder than those produced by air agitation.

The transmission electron micrographs shown in Figs. 23 to 27, of deposits obtained from nickel-cobalt solution containing 10 g/l cobalt sulphate, showed that the grain size was larger using ultrasonic agitation than with air. Ultrasonic agitation also produced a significant increase in grain size in nickel-cobalt alloy deposits obtained from solution containing 110 g/l cobalt sulphate as shown in Figs. 28 to 33. Ultrasonic agitation also appears to increase the grain size of cobalt deposits as shown in Figs. 34 to 38.

Ultrasonic agitation does not appear to have much effect on the grain size of the bright nickel-iron electrodeposits. Changes could hardly be detected even when using a very high magnification of X 500000 as shown in Figs. 39 to 45. The very fine grain size of this alloy deposit was caused mainly by the organic addition agents in the solution.

Kochergin et al⁽⁴⁾ showed that with ultrasonic agitation below the cavitation threshold, the variable sound pressure of the ultrasonic field became the controlling factor in any property change. Under these conditions the cathode became passivated, a smaller grain size results in the deposit, which gave an increase in hardness. When the ultrasonic agitation is accompanied by cavitation, the cathode is depassivated. In the present work cavitation was taking place.

Walker⁽¹⁸⁾ showed that the microhardness of copper deposits obtained from an acid sulphate solution increased with current density and decreased with bath temperature. Both these factors affect the grain size, fine structures being obtained with a high current density and low temperature. Ultrasonically agitated plating baths gave a harder deposit with a finer grain size than those from a magnetically stirred one.

Macnaughton and Hothersall⁽¹²²⁾ suggested that the hardness was connected with grain size and, for a given grain size, differences in the hardness could be due to different packing within the crystal lattice. Kozan⁽¹⁶⁾ reported that the ultrasonic agitation promotes a generally larger grain structure throughout the thickness of deposit obtained from Watts nickel solution. The hardness of nickel deposits obtained from Watts nickel solution varied from 245 HV using conventional agitation to 350 HV using ultrasonic agitation. These values are

in fairly close agreement with results obtained in the present work for Watts nickel deposits. The values given in Table XI are 247 HV for air agitation and 312 HV for ultrasonic at 350 watts. Kozan did not report the cobalt content of his deposits but in the present study the deposits contained some cobalt although extensive solution purification was carried out. However, both deposits had almost the same cobalt content, 5.88% for air and 5.7% for ultrasonic agitation. It seems that hardness is affected by factors other than cobalt content and fine grain size as reported by many investigators.

Table XII shows that the average hardness of cobalt deposits produced using ultrasonic agitation is 78 HV greater than for ones produced using air agitation. There was no effect on hardness due to reduced grain size because deposits obtained by air agitation were finer grained than those obtained by ultrasonic agitation as shown in Figs. 34 to 38.

Table XIII shows the average hardness of nickel iron deposits increased from 523.2 HV with air to 635 HV using ultrasonic agitation and the average iron content decreased from 24.78% with air to 22.8% using ultrasonic agitation, 350 watts. It is apparent that the cobalt content of deposits is reduced more than the iron content when ultrasonic agitation is used.

9.4.3.1 Conflicting Factors Involved in Grain Size.

In general, the change depends upon the metal being deposited, the experimental conditions such as current density, and the frequency and intensity of the ultrasonic field. There is considerable support for the argument that ultrasonic agitation causes an increase in grain size since it reduces concentration polarization. However, passivation favours the formation of nuclei and consequently fine grained deposits, whereas a decrease in concentration polarization at the cathode surface reduces nucleation and gives large grained deposits.

9.4.4 Dependence of Hardness on Work Hardening Effect

Recently Vrobel⁽⁸⁾ and Walker⁽¹²³⁾ related the hardness of electrodeposits to the cavitation phenomena, which can lead to surface work hardening by shock waves generated by the collapse of vapour bubbles which can cause severe erosion of the electrode surface. Walker⁽¹²³⁾ reported that the hardness of annealed nickel increased from 110 to 225 HV after ultrasonic bombardment for 1500 minutes and then softened to 190 HV when stored at room temperature. He explained that the decrease in hardness at room temperature was due to recovery of point defects in the work hardened surface layer. The increase in hardness of the nickel electrodeposited using ultrasonic agitation however, is permanent and no softening was

observed during storage. This permanency is probably due to the fact that metal is constantly being plated onto the work hardened cathode and the whole deposit is affected in this manner. In this form the point defects are not considered able to diffuse through the deposit to the surface and result in softening.

The hardness of nickel-cobalt deposits of varying composition plated using ultrasonic agitation were re-determined after two years storage at room temperature. The results showed no softening during storage. This supports Walker's theory about the probable permanency of hardness due to work hardening.

9.4.5 Dependence of Hardness on Dislocation Density.

Hofer et al⁽¹²⁴⁾ found that three factors seemed to influence the hardness of copper deposits: the fineness of the grains, the dislocation density and the pinning of the dislocation by impurities. Deposits with the smallest grain size and the highest strain had the highest hardness value. Strengthening is brought about by obstructing the movement of dislocations, hence the obstacle causes a stress concentration factor.

It is most probable that ultrasonic agitation causes an increase in dislocation density due to different growth mechanisms during deposition.

9.4.6 Dependence of Hardness on Internal Stress.

The stress may be tensile or compressive and is important because it has a marked effect on many properties. A high tensile stress is normally detrimental to the properties of the plated article. One cause of internal stress in electrodeposits is the incorporation of atomic hydrogen in the deposit. This hydrogen is produced during the deposition of metals with a current efficiency of less than 100% and the presence of hydrogen has been shown to produce a stress of up to 7 kg/mm^2 ($68 \times 10^{-3} \text{ kN/mm}^2$) for copper deposits obtained from a pyrophosphate bath as reported by Smalowska⁽¹²⁵⁾.

Walker⁽²³⁾ reported that in copper deposits plated at different current densities, the stress in the deposit produced in an ultrasonic bath was lower than that in a stirred solution, the reduction in some cases was as high as 50%. The stress at a given deposit thickness increased with the current density. Typical stress values for deposits of thickness about one micron are given below.

Current density A/dm^2	Stress kN/mm^2	
	Stirred bath	Ultrasonic bath
3.13	4.9×10^{-3}	3.7×10^{-3}
6.26	7.8×10^{-3}	4.3×10^{-3}
7.78	8×10^{-3}	5.6×10^{-3}
9.28	10×10^{-3}	7.1×10^{-3}

Results of cathode current efficiencies for nickel-cobalt and nickel-iron obtained during the current research programme were generally very close to 100% (96 - 98%) using ultrasonic agitation, 350 watts. Due to the high efficiency only a small amount of atomic hydrogen was produced. In addition the production of gaseous hydrogen from atomic hydrogen at the cathodic surface is assisted by ultrasonic agitation. This decreases the tendency for atomic hydrogen to be incorporated in the metal and reduces the internal stress of the deposit. The structure of cobalt electrodeposit plated by means of air agitation as shown in Fig.34 seemed to be stressed as indicated by the streaky diffraction pattern shown in Fig. 34D. The deposits produced using ultrasonic agitation were less stressed than those produced using air as shown in Figs. 36D, 37D and 38D.

9.4.7 Significance of Factors Affecting Hardness.

On consideration of the results obtained for nickel-cobalt and nickel-iron deposits, it seems that fine grain size, composition and internal stress do not make a major contribution to increased hardness when using ultrasonic agitation. It is more likely that it is due to a combination of an increase in dislocation density and the work hardening effect of cavitation. It is of interest to note that the harder nickel-iron alloy exhibited a greater increase in hardness than nickel-cobalt. A similar large increase of 100% in hardness has

been observed by Petrov⁽¹³¹⁾ for chromium obtained from a chromate electrolyte.

9.5 Composition

Kenahan et al⁽¹²¹⁾ reported that the composition of the brass deposits obtained from cyanide solutions remained relatively constant (83 to 86% copper) using air agitation at a current density of 0.5 to 4 A/dm². Ultrasonic agitation with high-frequency 18.5 kHz increased the zinc content of the deposit by 23%, and decreased the copper content.

The composition of copper-tin alloys decreased in tin content from about 10% at a current density of 0.33 to about 4% at 10 A/dm². Ultrasonic agitation at a frequency 18.5 kHz also decreased the tin content of the deposits at each current density. Much larger changes in the composition of copper-cadmium alloys were obtained using ultrasonic agitation. At current densities of 0.33 A/dm², ultrasonics decreased the amount of copper in the deposit by as much as 70%. As the current density was increased above 0.33 A/dm², the percentage of copper in the deposits was higher, but even at 1.2 A/dm², ultrasonics decreased the copper and increased the cadmium content of the alloys by about 18%.

Ultrasonic agitation has also been shown to have an effect on the composition of electroless deposits. Mallory⁽¹²⁶⁾ reported on the effect of ultrasonic agitation on electroless nickel-phosphorous solution and found that the deposition rates of electroless nickel

plating baths are increased by ultrasonic agitation with a decrease in the phosphorus content of the resultant deposits.

In the current research programme the results showed that the intensity of the ultrasonic power has a significant affect on the composition of the alloy electrodeposits. Using ultrasonic agitation of 100, 200 and 350 watts and nickel-cobalt solution containing 10 g/l cobalt sulphate the average cobalt contents were 20%, 19.2% and 18.4% respectively. Cobalt concentration in deposits from the solution containing 110 g/l cobalt sulphate, using the same intensities of ultrasonic agitation, were 71.5%, 69.5% and 68.3% respectively. Similar trends were obtained for solutions containing 35, 60 and 85 g/l cobalt sulphate as shown in Table IX. In the case of ultrasonically agitated nickel-iron solution the iron content in the deposit increased slightly as the intensity of the ultrasonic agitation increased, as shown in Table XIII.

The results obtained by different researchers showed that ultrasonic agitation affects the composition of the alloy electrodeposits but this affect is different from one alloy to another.

9.6 Tensile Strength and Ductility.

McFarlen⁽⁵⁶⁾ reported that as the cobalt concentration in the deposit increases, the hardness and tensile strength increases as well, using sulphamate solution.

Muller and Kuss⁽²⁾ have found an increase in the tensile strength of copper obtained from acid sulphate solution using ultrasonic agitation.

Mee⁽¹²⁷⁾ reported that the use of ultrasonics resulted in reduction in the hydrogen embrittlement as demonstrated by an increase in ductility, using acid pickling baths and a cadmium cyanide bath for the plating of high tensile steel wire and strip.

Ultrasonic agitation resulted in 20% higher ductility than that obtained on specimens plated conventionally. When ultrasonic plating followed a normal pickle in 5% HCl, there was an increase in ductility suggesting that hydrogen absorbed during pickling was removed by ultrasonic agitation during subsequent plating.

Although, in the present work, the ductilities of nickel-cobalt and nickel-iron deposits increased significantly when using ultrasonic agitation, their tensile strengths did not decrease.

The improvement in ductility was probably mainly due to

the reduction in the atomic hydrogen embrittlement, reduction in internal stresses of the deposit, and decrease in the microdistortion and dislocation content in the coating. The cathode efficiency of the solutions was in the range 97.5 to 99%.

Levy et al⁽⁷⁴⁾ reported that the elongation of iron foils increased as the tensile strength decreased. A summary of tensile strength and elongation of iron foils produced from ferrous fluoborate-ferrous chloride baths is given in Table XXXVIII.

Table XXXVIII

The effect of plating variation on tensile strength and ductility using ferrous fluoborate-ferrous chloride solution.

Plating Condition			Average Tensile strength kN/mm ²	Average Elongation %
C.D. A/dm ²	Temp. °C	pH		
5	60	3.2	0.78	0.8
10	70	3.2	0.74	1.1
20	80	3.2	0.70	1.4

Levy⁽¹¹⁶⁾ reported that the nickel-iron alloy deposits obtained from sulphate chloride electrolytes containing 7.5 g/l sodium 1,3,5-naphthalene trisulphonate as a stress reducer, exhibited higher values of tensile strength, 1.37 - 1.76 kN/mm² compared to those obtained from fluoborate-chloride solution, but low ductility of 2 - 3% was obtained.

Brook⁽¹¹⁹⁾ reported on the nickel electrodeposit obtained from standard Watts solution containing 300 g/l nickel sulphate, 60 g/l nickel chloride using plating conditions of pH 4 and current density 4.3 A/dm^2 .

Results of measurements of the tensile strength showed that the average value for 24 readings was 0.74 kN/mm^2 without referring to the ductility of the deposit.

Bailey et al⁽¹²⁸⁾ reported that the nickel electrodeposits obtained from Watts solution was matt and had a tensile strength of approximately 0.41 kN/mm^2 ; their elongation was about 30%.

Deposits from conventional sulphamate solution (300 g/l $\text{Ni}(\text{NH}_2\text{SO}_3)_2 \cdot 4\text{H}_2\text{O}$) had a tensile strength of approximately 0.41 kN/mm^2 , the elongation was about 18%.

Belt et al⁽⁸⁸⁾ reported that nickel-cobalt alloy electrodeposits from concentrated sulphamate electrolyte with plating conditions of pH 4, 60°C showed that values of U.T.S. and elongation obtained at the annealing temperature were lower than corresponding values measured at room temperature after annealing. U.T.S. decreased rapidly with increase in heat treatment temperature and declined to a value of 0.099 kN/mm^2 during 17 hours at 600°C . Ductility values were also lower, but this time elongation reached a maximum at 400°C (1 hour and 17 hours) before falling sharply at 500°C and 600°C , reaching 3% and 2% after 1 hour and 17 hours respectively at 600°C .

Table XXXXIX shows the ultimate tensile strength and elongation of test pieces after heat treatment.

Table XXXXIX

The effect of heat treatment variation on tensile strength and ductility. Obtained from concentrated sulphamate solution pH 4, Temp. 60°C.

Heat treatment °C		Ultimate tensile strength kN/mm ²	Elongation %
1 hour	200	0.94	10
	300	0.89	10
	400	0.64	18
	500	0.47	37
	600	0.45	43
17 hours	200	0.76	14
	300	0.72	15
	400	0.53	35
	500	0.45	25
	600	0.40	37

Results obtained by Belt et al show clearly that when the ultimate tensile strength increases the ductility decreases and vice versa as shown in Table XXXXIX using different time intervals of heat treatments of 1 hour and 17 hours.

McFarlen⁽⁵⁶⁾ reported the behaviour of nickel-cobalt alloy

deposits obtained from sulphamate solution containing organic additives. These additives contain sulphur, however, and sulphur embrittlement of these deposits has been encountered at temperatures as low as 260°C, producing ultimate strength of 1.37 kN/mm².

The highest value for ultimate strength obtained from this solution was 1.96 kN/mm² with a cobalt content of 38.5% at a current density of 5.8 A/dm². The results of the tensile tests and ductilities of samples are shown in Table XXXXX.

Table XXXXX

The effect of current density variation on cobalt content, tensile strength and ductility pH 4 at room temperature.

Current density A/dm ²	Cobalt content %	Ultimate strength kN/mm ²	Elongation %
2.5	22.0	1.68	3
2.5	24.8	1.6	4
5	24.7	1.67	3
5.8	38.5	1.96	-
7.5	17.3	1.47	1.5
7.5	16.2	1.56	2.5
7.5	-	1.38	1.5

Tensile strength and ductility results reported by McFarlen for nickel-cobalt alloy deposits using sulphamate solution ranged from 1.38 to 1.96 kN/mm² and 1.5 to 4%

respectively. The cobalt contents in the deposit were 16.2 and 38.5% obtained using different current densities as shown in Table XXXXX.

Bath variables have a clear effect upon nickel-cobalt alloy composition. By increasing the cobalt concentration in the deposit, the strength increases and the ductility decreases. Brenner et al⁽¹²⁹⁾ showed the effect of plating variables on the properties of electrodeposited nickel obtained from sulphate type, Watts nickel, all chloride nickel, and cobalt bright nickel (cobalt content of 1.08% weight in composition) solutions respectively as reported in Table XXXXXI.

Table XXXXXI

The effect of plating variables on the U.T.S. and ductility.

Type of Solution	Plating condition			Tensile strength kN/mm ²	Elongation %
	pH	C.D. A/dm ²	Temp. °C		
Sulphate	1.5	5	55	0.57	20
	3.0	5	55	0.46	20
	5.0	5	55	0.72	6
	1.5	5	55	0.57	14
Watts nickel	1.5	5	55	0.46	28
	3	5	55	0.39	28
All chloride nickel	5	5	55	0.87	7
	3	5	30	0.61	14
	5	1	55	0.91	4
Cobalt bright nickel	2.3	5	65	0.53	9
	3.7	5	65	0.42	4

Safranek⁽⁹⁸⁾ reported results of tensile strengths and ductility obtained from nickel-cobalt solutions as shown in Table XXXXXII.

Table XXXXXII

The effect of composition variation on tensile strength and ductility obtained from different nickel-cobalt solutions.

Cobalt content %	Tensile strength kN/mm ²	Elongation %	Plating bath
1	1.41	4	Sulphate-chloride
20	1.4	3-6	Sulphamate-bromide
35	1.03-1.3	1-1.5	Watts
40	1.37-1.51	2-4	Sulphamate-bromide
50	1.76-1.88	-	Sulphamate
80	0.55	1	Sulphamate

9.6.1 Nickel-Cobalt.

Table XXXXXIII shows the tensile strength and ductility results of nickel-cobalt (obtained from sulphate-chloride solution containing 10 g/l cobalt sulphate) and nickel-iron alloy coatings using either air or ultrasonic agitation, obtained in the current research work.

Tensile strength and ductility results obtained by Safranek using a similar solution to that used in the current

Table XXXXIII

Average tensile strength and ductility of plated nickel-cobalt and nickel-iron coatings.

Composition	Agitation	Average U.T.S. of coating kN/mm^2		Elongation %	
		At first crack	At failure of test piece	At first crack	At failure of test piece
Nickel-cobalt containing $10 \text{ g/l } \text{CoSO}_4 \cdot 7\text{H}_2\text{O}$	Air Ultrasonic 100 Watts Ultrasonic 200 Watts Ultrasonic 350 Watts	1.22	0.84	11	37.15
		1.13	0.97	20.06	41.22
		1.04	0.9	25	42.56
		1.05	0.84	28.7	45.53
Nickel-Iron	Air Ultrasonic 100 Watts Ultrasonic 200 Watts Ultrasonic 350 Watts	1.37	1	1.67	22
		1.44	1.05	5.7	28.56
		1.23	0.7	6.2	31.1
		1.45	0.95	9.9	34.75

research programme show that the tensile strength of deposits containing 20% cobalt ranged from 1.03 to 1.3 kN/mm² while ductility improved very slightly from 1 to 1.5%. Deposit with 1% cobalt content exhibited a tensile strength of 1.41 kN/mm² and ductility of 4%, obtained from sulphate-chloride solution.

It is difficult to compare results obtained by other researchers with the present work because of the different plating conditions which result in deposits of varying composition. Results obtained by this current work showed clearly that by using ultrasonic agitation the ductility improved significantly but the U.T.S. increased only slightly.

Using air the ductility of the nickel-cobalt coating at the first crack was 11% and at failure increased to 37.15%. Using ultrasonic agitation of 100, 200 and 350 watts the ductility of the coating at the first crack increased to 20.6, 25 and 28.7% respectively and at failure increased to 41.22, 42.56 and 45.53% respectively.

The ductility values using ultrasonics are higher than the air agitated values. The ductility of the uncoated brass was 69.9% at failure which was considerably higher than the ductility of the nickel-cobalt coated brass using air agitation which was only 37.15%. However the ductility was increased to 45.53% using ultrasonic agitation of 350 watts, and only slightly lower for the

lower ultrasonic power. This is because ultrasonic agitation increases the ductility of the coating from 11% using air up to 28.7% using 350 watts ultrasonic agitation as shown in Table XXXXVIII. Detailed results are shown in Tables XV and XVII. For engineering applications it would be advantageous to use ultrasonic agitation when an electrodeposit of nickel-cobalt is required so that any reduction in ductility is reduced to a minimum.

The U.T.S. of the brass substrate had an average of 0.317 kN/mm^2 which was only marginally increased to about 0.33 kN/mm^2 when electrodeposited with nickel-cobalt alloy deposit using both agitation modes (Table XVII).

The U.T.S. of the coatings up to the first cracks are considerably higher than the U.T.S. of the uncoated brass as shown in Fig.22 (Load/Extension). The strength of a plated test piece up to this point is obviously much higher than an unplated one. The load carried by plated brass will therefore be more than the load carried by brass alone.

The U.T.S. at the first cracks using air 1.22 kN/mm^2 is slightly higher than the U.T.S. obtained using ultrasonic agitation, 1.05 to 1.13 kN/mm^2 , Table XXXXVIII. However at failure the U.T.S. values are all about 0.9 kN/mm^2 using either air or ultrasonic agitation. The slight reduction in U.T.S. at the first cracks using ultrasonic agitation is far outweighed by the beneficial use of ultrasonics in considerably increasing the ductility at failure particularly at 350 watts.

The U.T.S. of the coatings at first cracks are somewhat higher than those obtained for the coating at failure. This is to be expected because the load will be carried by a smaller cross-sectional area due to the presence of cracks.

The U.T.S. results obtained in this work, especially for nickel-cobalt, are in reasonable agreement with those obtained by other workers. Ductilities measured at first cracks showed much higher values than those obtained by other workers although the exact methods of measurement were not given in most cases.

9.6.2 Nickel-Iron.

Similar results were found with the nickel-iron coatings. However the U.T.S. of the coatings at the first cracks were higher than those obtained for the nickel-cobalt coatings using either agitation mode. This is probably because the nickel-iron deposits are harder than the nickel-cobalt ones (Table XXII) and finer grained.

The nickel-iron results showed that the ductility at the first crack significantly increased from 1.67% using air to 9.9% using ultrasonic agitation, 350 watts. The ductilities increased with increasing power of ultrasonic agitation but were considerably lower than those for nickel-cobalt, Table XXXXIII. The ductilities at failure again increased with increasing power of ultrasonic agitation but were also considerably lower than

those for nickel-cobalt.

These ductility results obtained in the current work are much higher than those obtained by other researchers. Levy⁽¹¹⁶⁾ reported a ductility of 2 - 3% from a similar type of solution containing a stress reducer. All other workers obtained lower ductility values than Levy and these are all considerably lower than those obtained in the current work.

Generally the ductility of nickel-cobalt and nickel-iron deposits were significantly improved using ultrasonic agitation, 350 watts, compared to results obtained by other workers using either air or other conventional methods of agitation.

The increase in ductility of both nickel alloys is probably due to the decrease in internal stress of the deposit. One cause of internal stress is the incorporation of atomic hydrogen into the deposit. Results of cathode current efficiencies for both nickel-cobalt and nickel-iron obtained during the current research programme were generally very close to 100% (96 - 98%) using ultrasonic agitation and therefore only a small amount of atomic hydrogen was produced.

From the diffraction patterns the deposits produced using ultrasonic agitation were less stressed than those produced using air.

9.7 Surface Topography and Progressive Growth.

Ultrasonic agitation influenced the growth mechanisms of the deposition process and was the overriding factor for nickel-cobalt deposits obtained from solutions containing 35 g/l cobaltous sulphate. The spaghetti like structures, obtained from solutions containing 60, 85 and 110 g/l cobaltous sulphate using air agitation, were different from the spaghetti like structures obtained from the various combinations of cobalt content of solution and ultrasonic agitation. Possible explanations are the interactive effects of agitation and cobalt content of solution which may not be the same for all cobalt concentration agitation combinations.

In the case of nickel iron deposits ultrasonic agitation had a much greater effect than for nickel-cobalt. Possible explanations are the effects of ultrasonic agitation on the concentration gradients of the addition agents in the cathode layers.

Progressive growth of deposits after short plating times showed that they were influenced by both ultrasonic agitation and plating time.

Deposits obtained from a solution containing 110 g/l cobaltous sulphate were very similar after 5, 10 and 15 minutes of plating using air agitation. When ultrasonic agitation was substituted for air the surface topography

was found to be different for the three deposits obtained after 5, 10 and 15 minutes plating time, although there were some similarities. It appears that ultrasonic agitation continuously modifies the deposition mechanism thus giving different effects.

Walker⁽²³⁾⁽¹²³⁾ has shown photographs of nickel deposits plated in still, stirred and ultrasonically agitated baths. In some instances he appears to have confused grain size with surface topographical features. He claimed that shock waves and cavitation inhibit perpendicular growth thus improving smoothness⁽²³⁾. In the present work ultrasonic agitation had an adverse effect on the smoothness and levelling of nickel-iron deposits. Walker also claimed an improvement in the surface finish of Watts nickel deposits due to the elimination of porosity. The craters shown in deposits produced from a stirred solution are indicative of poor plating conditions. It is most misleading to suggest that the deposit shown is typical of a Watts deposit plated from an adequately agitated solution. Nevertheless it is likely that the improvement reported is due to the rapid liberation of gas by the ultrasonic agitation. Gas pitting and porosity did not occur in the case of any of the air agitated deposits produced in the present work.

Penn et al⁽¹¹⁾ observed the occurrence of ripples in copper deposits plated using ultrasonic agitation below the cavitation level. Due to standing waves the zones

of depleted electrolyte at the cathode were found to stratify at the displacement nodes. These stratification effects provide an explanation of the surface ripple produced.

9.7.1 Comparison of Results Obtained using SEM and Replica Techniques.

Surface topography of deposits was studied after 40 minutes plating using the SEM but the replica technique was used to study progressive growth and the longest plating time used was 15 minutes. The later technique gave much better resolution. The results obtained could not be compared directly since larger growth features would be expected after longer plating times. The appearance was similar in many instances but in other cases the two techniques did appear to reveal differences. However, care should be exercised when comparing illustrations since various magnifications were used.

9.8 Cathode Current Efficiency.

In practical electroplating, a metal is hardly ever deposited at 100% current efficiency; some hydrogen nearly always develops. This hydrogen accumulates at the cathode surface in small visible bubbles. These bubbles may adhere for a while to the surface or they may keep growing and finally detach themselves from the surface. Such bubbles are immediately attacked in an ultrasonic field and are driven off by the pressure of the sound waves.

The current efficiency is the percentage of the total current usefully employed in the cathode deposition or anodic dissolution of a metal. If the current efficiency is less than 100% some of the current is used in detrimental secondary reactions such as the co-deposition of hydrogen at the cathode.

Domnikov⁽²⁵⁾ reported that the effect of plating in an ultrasonic field has been found to increase the cathodic current efficiency in the plating of copper and nickel. An increase from 14% to 23% has been found for chromium deposits when using ultrasonic agitation.⁽²⁵⁾ Kenahan⁽¹²¹⁾ reported on the effects of ultrasonic agitation at a frequency of 18.5 kHz on the electrodeposition of copper-zinc (brass) alloys from cyanide electrolytes. He found that the cathode and anode current efficiencies at current densities up to 10.8 A/dm^2 decreased steadily as the current density was increased. Current efficiency dropped

from about 84% at a current density of 0.54 A/dm^2 to about 63% at 3.2 A/dm^2 . Higher current densities were not used because of excessive cell voltage. Ultrasonics at a frequency of 18.5 kHz increased the cathode current efficiency at every current density where comparisons could be obtained. From 0.54 to 3.2 A/dm^2 , the current efficiency was between 85 and 90%. As the current density was increased above 3.2 A/dm^2 , a steady decrease in cathode current efficiency occurred. However, even at a current density of 8.65 A/dm^2 , the cathode current efficiency was slightly higher with ultrasonics than it was at 3.2 A/dm^2 in the absence of ultrasonics.

Without ultrasonics, the anodes corroded at a high rate at cathode current densities of 0.54 to 1.6 A/dm^2 . At a cathode current density of 2.2 A/dm^2 , the anode current efficiency dropped to 76%; at 2.7 and 3.2 A/dm^2 , there were sharp decreases to about 38 and 20% respectively. Above a current density of 3.2 A/dm^2 , the anodes became passive and stopped corroding. When the anodes were ultrasonically agitated, anode current efficiencies were about 90% up to a current density of 8.6 A/dm^2 . At 10.8 A/dm^2 , the anode efficiency dropped sharply to 48%.

Results from the current research work showed that an increase of 3.4% in cathode current efficiency was achieved, averages of 95.4% and 98.8% were obtained using air and ultrasonic agitation respectively. Both results were obtained from sulphate-chloride nickel solution

containing 10 g/l cobalt sulphate pH 4, current density 4 A/dm² and temperature 55°C.

The cathode efficiency of nickel-iron plating solution showed an increase of 3.8%. Air agitated nickel-iron solution showed an average cathode efficiency of 94.5%, the ultrasonically agitated solution exhibited an average current efficiency of 98.03%.

It is apparent that the same general trend occurred for nickel-iron as for nickel-cobalt solution. The efficiency increased slightly as the degree of ultrasonic agitation was increased. Increase in cathode current efficiencies in both alloy systems by the application of ultrasonic agitation, was most probably due to the depolarization effects produced at both electrodes, where ultrasonics reduced the tendency for the anode to become passive. Ultrasonics probably resulted in lower cell voltages for both alloy systems, the limiting current density was increased over a wide range for nickel-cobalt and nickel-iron as shown in Tables XXVII and XXXII. Small increases have been shown because of starting from a base value of 95%.

The calculation shown on the next page for a nickel-cobalt alloy illustrates the method used to determine cathode current efficiencies.

In the present investigation the following assumptions were made when calculating the efficiency:-

- a) The copper bath was 100% efficient.
- b) The total current was used to deposit or liberate the three elements cobalt, nickel and hydrogen, that used to liberate hydrogen represents the wasted energy.
- c) One Faraday (F) which equals 96494 coulombs deposits the gramme equivalent weight of each element which is for example:-

$$\frac{58.93}{2} = 29.46 \text{ (chemical) equivalent of cobalt}$$

$$\frac{58.7}{2} = 29.35 \text{ (chemical) equivalent of nickel}$$

$$\frac{63.546}{2} = 31.77 \text{ (chemical) equivalent of copper}$$

The number of gramme equivalents of Cu

$$\text{deposited} = \frac{\text{The weight of Cu deposited}}{\text{Chemical equivalent of Cu}}$$

The number of gramme equivalents of Ni

$$\text{deposited} = \frac{\text{The weight of Ni deposited}}{\text{Chemical equivalent of Ni}}$$

The number of gramme equivalents of Co

$$\text{deposited} = \frac{\text{The weight of Co deposited}}{\text{Chemical equivalent of Co}}$$

The cathode current efficiency =

$$\frac{(\text{The number of gramme equivalents of Ni+Co}) \times 100}{\text{The number of gramme equivalents of Cu}}$$

9.9 Limiting Current Density.

Endicott et al⁽⁵⁰⁾ reported that a decrease in current density resulted in a decrease in the nickel content of the deposit obtained from a nickel-cobalt sulphamate bath. The data obtained supports the statements of Brenner⁽⁴⁷⁾ that in the nickel-cobalt plating system, anomalous codeposition occurs and cobalt deposits preferentially, although cobalt is less noble than nickel. Bailey et al⁽¹²⁸⁾ showed that, for the cobalt containing Ni Speed* bath, the cobalt content of the deposit increased as the cobalt content of the solution was increased but fell when the current density was raised. As the cobalt content of the solution is increased, deposit hardness rises to a peak value of 525 HV at 5 A/dm² with 6 g/l cobalt, corresponding to a deposit containing 35% cobalt.

The work carried out by Eastham et al⁽¹³⁰⁾ using nickel-iron (Permalloy) solution showed that higher current densities gave lower iron concentration suggesting that changes in hydroxyl ion concentration might be responsible. Kenahan et al⁽¹⁾ have found, during electrodeposition of copper from a cyanide bath using ultrasonic agitation that the anode corroded satisfactorily at current densities up to 1 A/dm² but became passive when the cathode current density was increased to 2 A/dm². When the anodes were ultrasonically agitated, anode current efficiencies were about 100% up to a current density of 6 A/dm². Cell

*Proprietary product.

voltage increased with increasing current density. Without ultrasonic agitation, there was a particularly large increase in cell voltage when the current density was raised from 1 A/dm^2 to 2 A/dm^2 . Ultrasonic agitation lowered the cell voltage at every current density. The decrease in cell voltage arising from the use of ultrasonics was especially large between current densities of 2 and 6.5 A/dm^2 (above one volt). Normally, the cathode polarized (became less noble) rapidly at all current densities and then gradually levelled off to a steady-state potential. The grain size decreased as current density increased, both with and without ultrasonic agitation, but smaller grain size occurred when the cathode was ultrasonically agitated. However, there was rapid evolution of hydrogen and low current efficiencies, especially at the higher current densities.

Wolfe et al⁽²⁰⁾ attributed the rapid initial depolarization at the cathode to disruption of concentration gradients by the ultrasonic waves. These workers related this effect to the micro-agitation action of the ultrasonic waves.

Vrobel⁽⁸⁾ reported that the use of ultrasonic agitation resulted in an increase of permissible current density and higher current efficiency in a bright gold cyanide bath.

Kozan⁽¹⁶⁾ noted that the use of ultrasonic agitation

during nickel plating from Watts nickel solution permits an approximately twofold increase in plating current density and still produces acceptable deposits.

Walker et al⁽²³⁾ reported that ultrasonic agitation has been used in copper plating to increase the limiting current density and the hardness. These vibrations reduce the activation polarization and also the thickness of the cathodic double layer, so increasing the limiting current density.

Table XXVIII shows that the hardnesses of electrodeposits obtained, over a wide range of current densities using air agitation, from nickel-cobalt solution containing 10 g/l cobalt sulphate were increased from 259 to 293 HV by increasing the current density. The cobalt content decreased from 15.1% to 3% using current densities of 10 and 80 A/dm² respectively. For the same solution using ultrasonic agitation of 350 watts it can be seen clearly that the hardness increased from 311 to 370 HV and the cobalt content decreased from 16.9 to 5.3% using the same current densities of 10 and 80 A/dm² as in air agitation.

Satisfactory deposits were obtained using air agitation up to the current density of 18 A/dm² with no trace of edge burn. By using ultrasonic agitation of 350 watts the satisfactory deposits could be obtained even at 28 A/dm² with no edge burn. Table XXXIII shows that the

hardnesses of nickel-iron alloy deposits obtained from limiting current density experiments using air agitation were increased from 562.8 to 614.5 HV and the iron content decreased from 20.1% to 12.2% using current densities of 10 and 80 A/dm² respectively. Using ultrasonic agitation, 350 watts, it can be seen that the hardness became even harder than with air agitation and ranged from 609 to 645.3HV. The iron content decreased from 19.6 to 11.6% using the same current densities of 10 and 80 A/dm² respectively.

Satisfactory bright, sound deposits were obtained between 10 to 16 A/dm² with no trace of edge burn using air agitation as shown in Fig.82.

Bright, sound deposits were obtained using ultrasonic agitation, 350 watts, between 10 and 34 A/dm² as shown in Fig.83.

The surface appearance of nickel-iron deposits from air and ultrasonic agitation show a very marked difference. The deposits from air agitation had a powdery burnt appearance at 18 A/dm², whereas from the ultrasonic agitation the deposit was satisfactory at 34 A/dm². The limiting current density was increased for the nickel-cobalt and nickel-iron systems using ultrasonic agitation. The current efficiencies were increased for both alloys by the application of ultrasonic agitations, probably because depolarization effects were produced at both

electrodes; ultrasonics reduced the tendency for the cathode to become passive.

The increase in cathode efficiency was more probably due to a decrease in cell voltage for both alloys using ultrasonics, and the other factor which affected the increase in current density was probably the reduction in the boundary layer thickness due to the radiation pressure of the ultrasonics which can also influence a diffusion process by exerting a mechanical pressure on the diffusion layer.

Ultrasonics affected the composition of the nickel-cobalt and nickel-iron electrodeposits over a wide range of current densities. The cobalt and iron contents of deposits plated from nickel-cobalt and nickel-iron deposits respectively, decreased using air agitation. This is probably because the cobalt content of nickel-cobalt alloys deposited from simple baths decreases with decreasing current density due to the anomalous nature of this system.

Depletion of cobalt ions in the cathode diffusion layer causes the system to come under diffusion control. Using ultrasonic agitation it has been found that the irradiation of the electrode with sound above the cavitation threshold produced a greater affect on mass transport than air agitation at current densities above 10 A/dm^2 for nickel-cobalt alloys.

At any particular current density the iron content of deposit plated using either air or ultrasonic agitation was similar.

The detailed results are shown in Tables XXVIII, XXIX, XXXIII and XXXIV.

The increase in hardness due to increased current density is probably due to a reduction in grain size; in the case of ultrasonic agitation this would be in addition to the reasons given in section (9.4.7).

9.9.1 Analysis of Results Using Regression Analysis.

To investigate possibilities of quantitative relationships between hardness, current density and either cobalt or iron content of deposit the data from Tables XXVIII, XXIX, XXXIII and XXXV were analysed. For each of the 4 lots of data the following equations were calculated.

$$H = \%Co \times k_1 + k_2$$

$$H = C.D. \times k_3 + k_4$$

$$H = (\%Co \times k_5) + (C.D \times k_6) + k_7$$

Similar equations were developed for Fe.

The calculations were done on a Harris computer using the GLIM⁽¹³⁴⁾ (Generalised linear interactive modelling) soft ware package. The results of the analysis were used to:

- i. Construct linear equations that could be used to predict hardness values from current density and either % cobalt or % iron content of deposit.
- ii. Investigate the combined effects of current density and either cobalt or iron content of deposit on hardness.

In all cases hardness was made the dependent variable because hardness is easily measured and is obviously dependent on current density and metal content of deposit. The effect of ultrasonic agitation on hardness was obtained from data in Tables XXIX and XXXV.

To obtain information on the goodness of fit of the experimental data to the regression equations the following information was examined for each calculated equation.

A) Deviance, the sum of squares of the residuals (the differences between the observed and estimated results). A small value means a good fit and vice versa.

B) Variance, the averaged value of (A) obtained by dividing the sum of squares of the residuals by the degrees of freedom. The degrees of freedom being the number of units - the number of parameters fitted.

e.g. 8 hardness units - (hardness + C.D.)

$$= 8 - 2$$

$$= 6 \text{ D.F.}$$

or e.g. 8 hardness units - (hardness + C.D. + %Co)

$$= 8 - 3$$

$$= 5 \text{ D.F.}$$

The smaller the number calculated in (B) the better the fit.

C) The GLIM package also calculated residuals, that is the hardness number was calculated from the equation and compared with the experimental one. The difference between them being the residual, the smaller the residual the better the fit.

Regression Analysis on Data from Table XXVIII

Nickel-cobalt alloy deposits with changes in current density using air agitation, pH 4; 55°C.

$$H = 254.4 + 0.4424 \times \text{C.D.}$$

$$\text{Deviance} = 97.17$$

$$\text{D.F.} = 6$$

$$\begin{aligned} \text{Variance} &= 97.17/6 \\ &= 16.19 \end{aligned}$$

<u>Observed</u>	<u>Fitted</u>	<u>Residual</u>
259	258.8	0.2
263	263.2	-0.2
271	267.6	3.4
274	272.1	1.4
269	277.4	-8.4
280	280.9	-0.9
287	286.2	0.8
293	289.8	3.2

Changes in cobalt content of deposit

$$H = 294.1 - 2.45 \times \% \text{Co}$$

$$\text{Deviance} = 168.9$$

$$\text{D.F.} = 6$$

$$\begin{aligned} \text{Variance} &= 168.9/6 \\ &= 28.16 \end{aligned}$$

<u>Observed</u>	<u>Fitted</u>	<u>Residual</u>
259	257.1	1.9
263	264.7	-1.7
271	268.1	2.9
274	273.3	0.7
269	279.2	-10.2
280	282.3	-2.3
287	284.5	2.5
293	286.8	6.2

Changes in cobalt content of deposit and current density

$$H = 210.6 + (0.9156 \times \text{C.D.}) + (2.777 \times \% \text{Co})$$

$$\text{Deviance} = 70.01$$

$$\text{D.F.} = 5$$

$$\begin{aligned} \text{Variance} &= 70.01 / 5 \\ &= 14.00 \end{aligned}$$

<u>Observed</u>	<u>Fitted</u>	<u>Residual</u>
259	261.7	-2.7
263	262.3	0.7
271	267.5	3.5
274	270.9	3.1
269	275.2	-6.2
280	278.9	1.1
287	287.4	-0.4
293	292.2	0.8

Regression Analysis on Data from Table XXIX

Nickel-cobalt alloy deposits with changes in current density using ultrasonic agitation, 350 watts, pH 4, 55°C.

$$H = 303.3 + 0.8391 \times \text{C.D.}$$

$$\text{Deviance} = 140.0$$

$$\text{D.F.} = 6$$

$$\begin{aligned}\text{Variance} &= 140.0 / 6 \\ &= 23.34\end{aligned}$$

<u>Observed</u>	<u>Fitted</u>	<u>Residual</u>
311	311.7	-0.7
318	320.1	-2.1
329	328.5	0.5
345	336.9	8.1
339	347.0	-8.0
356	353.7	2.3
364	363.7	0.3
370	370.4	-0.4

Changes in cobalt content of deposit

$$H = 402.1 - 5.437 \times \% \text{Co}$$

$$\text{Deviance} = 135.8$$

$$\text{D.F.} = 6$$

$$\begin{aligned}\text{Variance} &= 135.8/6 \\ &= 22.63\end{aligned}$$

<u>Observed</u>	<u>Fitted</u>	<u>Residual</u>
311	310.2	0.8
318	318.9	-0.9
329	332.0	-3.0
345	339.6	5.4
339	346.1	-7.1
356	352.6	3.4
364	359.2	4.8
370	373.3	-3.3

Changes in cobalt content of deposit and current density

$$H = 356.6 + (0.3885 + C.D) - (2.943 \times \%Co)$$

$$\text{Deviance} = 124.3$$

$$D.F = 5$$

$$\text{Variance} = 124.3 / 5$$

$$= 24.86$$

<u>Observed</u>	<u>Fitted</u>	<u>Residual</u>
311	310.8	0.2
318	319.4	-1.4
329	330.3	-1.3
345	338.3	6.7
339	346.5	-7.5
356	353.2	2.8
364	361.4	2.6
370	372.1	-2.1

Regression Analysis on Data from Table XXXIII

Nickel-iron alloy deposits with changes in current density using air agitation pH 4, 68°C.

$$H = 559.4 + 0.7555 \times \text{C.D.}$$

$$\text{Deviance} = 274.8$$

$$\text{D.F.} = 6$$

$$\text{Variance} = 274.8 / 6$$

$$= 45.79$$

<u>Observed</u>	<u>Fitted</u>	<u>Residual</u>
562.8	567.0	-4.2
574.4	574.5	-0.1
579.4	582.1	-2.7
591.8	589.6	2.2
605.5	598.7	6.8
615.5	604.7	10.8
606.4	613.8	-7.4
614.5	619.9	-5.4

Changes in iron content of deposit

$$H = 702.1 - 6.941 \times \% \text{Fe}$$

$$\text{Deviance} = 123.9$$

$$\text{D.F.} = 6$$

$$\text{Variance} = 123.9 / 6$$

$$= 20.65$$

<u>Observed</u>	<u>Fitted</u>	<u>Residual</u>
562.8	562.6	0.2
574.4	573.7	0.7
579.4	583.4	-4.0
591.8	591.7	0.1
605.5	603.5	2.0
615.5	607.0	8.5
606.4	611.1	-4.7
614.5	617.4	-2.9

Changes in iron content of deposit and current density

$$H = 793.5 - (0.5003 \times C.D) - (11.35 \times \%Fe)$$

$$\text{Deviance} = 96.27$$

$$\text{D.F.} = 5$$

$$\text{Variance} = 19.25$$

<u>Observed</u>	<u>Fitted</u>	<u>Residual</u>
562.8	560.5	2.3
574.4	573.6	0.8
579.4	584.5	-5.1
591.8	593.1	-1.3
605.5	606.4	-0.9
615.5	608.1	7.4
606.4	608.9	-2.5
614.5	615.1	-0.6

Regression Analysis on Data from Table XXXV

Nickel-iron alloy deposits with changes in current density using ultrasonic agitation, 350 watts, pH 4, 68°C.

$$H = 628.0 + 0.4093 \times \text{C.D.}$$

$$\text{Deviance} = 86.25$$

$$\text{D.F.} = 6$$

$$\text{Variance} = 86.25 / 6$$

$$= 14.38$$

Observed	Fitted	Residual
631	632.1	-1.1
634	636.2	-2.2
642	640.3	1.7
651	644.4	6.6
647	649.3	-2.3
649.7	652.5	-2.8
654.3	657.5	-3.2
663.9	660.7	3.2

Changes in iron content of deposit

$$H = 698.1 - 3.370 \times \% \text{Fe}$$

$$\text{Deviance} = 46.05$$

$$\text{D.F.} = 6$$

$$\text{Variance} = 46.05 / 6$$

$$= 7.675$$

<u>Observed</u>	<u>Fitted</u>	<u>Residual</u>
631	629.7	1.3
634	636.8	-2.8
642	641.2	0.8
651	646.6	4.4
647	648.9	-1.9
649.7	651.6	-1.9
654.3	656.3	-2.0
663.9	661.7	2.2

Changes in iron content of deposit and current density

$$H = 760.3 - (0.373 \times \text{C.D.}) - (6.33 \times \% \text{Fe})$$

$$\text{Deviance} = 34.51$$

$$\text{D.F.} = 5$$

$$\text{Variance} = 34.51 / 5$$

$$= 6.9$$

<u>Observed</u>	<u>Fitted</u>	<u>Residual</u>
631	628.1	2.9
634	637.7	-3.7
642	642.2	-0.2
651	648.6	2.4
647	648.5	-1.5
649.7	650.6	-0.9
654.3	655.0	-0.7
663.9	662.1	1.8

Conclusions from Regression Analysis

Reasonably quantitative linear relationships existed in all cases. In a few instances the residuals were high, the highest being 10.8 but this was well within the numerical difference between the highest and lowest observed hardness $(614.5 - 562.8) = 51.7$

It is important that the equations are only used within the experimental values of current density. Clearly no metal will be deposited at 0 A/dm^2 and above 80 A/dm^2 practical plating conditions may no longer apply.

To allow direct comparison of the goodness of fit of all the equations their Variances are given (rounded to the nearest whole number) in the following table.

For air agitated solutions improved fit resulted when all 3 variables were in the equations i.e. hardness, current density and either %Co or %Fe in the deposit. This indicated the possible dependence of hardness on both current density and either %Co or %Fe in the deposit and not on either current density or percent metal in the deposit alone. Ultrasonic agitation did not seem to influence the combined effects of current density and % cobalt on hardness of deposit. The fact that ultrasonic agitation gave higher hardnesses than air clearly demonstrated the effect of this type of agitation.

Table XXXXXIV

Variance of regression equations

Agitation	Parameter	Variance
Air	C.D.	16
	% Co	28
	C.D. + % Co	14
Ultrasonic	C.D.	23
	% Co	23
	C.D. + % Co	25
Air	C.D.	46
	% Fe	21
	C.D. + % Fe	19
Ultrasonic	C.D.	14
	% Fe	8
	C.D. + % Fe	7

Nickel-iron solution with ultrasonic agitation gave a much better fit than when using air, particularly when 3 variables were used i.e. hardness, current density and % iron in the deposit. This suggested that hardness was effected by the interaction of current density with % iron in the deposit and was further influenced by ultrasonic agitation.

It is not advisable to state with great confidence that the above discussion is completely valid because the data

was based on only a few degrees of freedom. However it did show possible trends and indicated in which direction further work could be guided.

9.10 Macrothrowing Power.

Acidic plating baths (Sulphates, Chlorides, Sulphamates of Cu, Zn, Sn and Ni) generally possess poor macrothrowing power, because current efficiencies are near 100% at high as well as low current densities. Alkaline baths (Cyanides of Cu, Zn, Cd, Ag, Au and Sn) have better macrothrowing power. In an alkaline bath, metals to be deposited must be incorporated in complex ions, and these generally incur high concentration polarization.

Walker et al⁽²³⁾ and Domnikov⁽²⁵⁾ reported that plating in an ultrasonic field produced a more uniform concentration of electrolyte at the cathode surface and improved the throwing power of copper and nickel respectively. Kozan⁽¹⁶⁾ reported that the macrothrowing power of a Watts nickel with low pH 1.5 decreased with an increase in current density, being +4.8% at 5.4 A/dm^2 and 3% at 10.8 A/dm^2 , when using air agitation. The macrothrowing power was reduced to -14.9% when deposited with the aid of ultrasonic agitation at 10.8 A/dm^2 . However, there was no further decrease in macrothrowing power when the current density was raised to 21.5 A/dm^2 , remaining at -14.9%. He found that the macrothrowing power of the conventional hard chromium increased with an increase in current density, other conditions remaining the same, being -143.1% at 23.25 A/dm^2 , and increasing to -130.4% at 46.5 A/dm^2 . The macrothrowing power of this bath increased from -143.1% to -132.7% when the chromium was

deposited at 23.25 A/dm^2 with the aid of ultrasonic agitation. However, with the ultrasonic agitation the macrothrowing power decreased to -139.2% at a current density of 58.13 A/dm^2 . An increase in the temperature of the bath resulted in a decrease in macrothrowing power.

Watson⁽¹²⁰⁾ reported that the efficiency of Watts solution, on which many proprietary bright nickel solutions are based, falls increasingly rapidly as current density is progressively lowered, and this effect partially nullifies its favourable polarization characteristics, resulting in low macrothrowing power.

The conductivity of most nickel plating solutions is high, and although some improvement can be achieved by raising the salt concentration or by lowering pH, these changes produce deleterious side effects: the former modification increases drag-out, the latter reduces efficiency.

The macrothrowing power of nickel-cobalt solution containing 10 g/l cobalt sulphate was increased, using ultrasonic agitation, 350 watts, about 3% from that obtained using air, details are shown in Table XXXVIII. Macrothrowing power of the same solution but containing 110 g/l cobalt sulphate was increased from 28.4% using air agitation to 37.7% using ultrasonics. Macrothrowing power of nickel-iron was increased slightly by an average of 3.2% using ultrasonics instead of air agitation; the

results are shown in Table XXXX. Plating conditions remained unchanged for all alloy solutions during electroplating. Macrothrowing power was increased by using ultrasonic agitation as shown in the current research work. Improvement in concentration polarization characteristics appears to be the method of increasing macrothrowing power.

Increasing macrothrowing power was probably due to the improvement of conductivity of the electrolyte (mass transfer of ions) using ultrasonic agitation, a high conductivity will minimise the IR drop in the bath which cause differences in potential over a complex cathode surface and therefore causes the rate of deposition to be uniform. The throwing power can be enhanced by the occurrence of other reactions, e.g. hydrogen evolution, at the same time as metal deposition. Since hydrogen evolution will occur at points on the surface where the potential is high; the current for hydrogen evolution will then contribute to the IR drop without leading to metal deposition. Hence it causes a reduction in the local overpotential, and leads to a more even deposit.

It can be seen also that the main process parameters which affect the macrothrowing power are the composition of the plating bath (i.e. total electrolyte concentration, complexing agent, pH, additives), temperature and current density.

Ultrasonic agitation decreases the concentration polarization as reported by many researchers, but in the mean time increases the ion mass transport in bulk solution which results in improvement of throwing power.

10 CONCLUSIONS

(i) Although there was some absorbtion of ultrasonic energy at various interfaces it was estimated that about 85% entered the plating solution.

All plating solutions were used at their optimum conditions using either air or ultrasonic agitation. Hardnesses of nickel-cobalt, nickel-iron, nickel and cobalt all increased with increasing ultrasonic agitation.

(ii) The strength of plated tensile test pieces remained unchanged when using ultrasonic agitation but the ductility was improved significantly.

(iii) The cobalt content of deposits decreased with increasing power of ultrasonic agitation at constant current density but the iron content of the nickel iron deposits remained unchanged with increasing ultrasonic power.

(iv) The surface topography was influenced by both the cobalt content of the plating solution and the ultrasonic agitation. In the case of nickel iron deposits the surface changed from very smooth to regular smooth directionally orientated nodular deposits (cobble stone appearance).

Early growth studies showed differences between the

effects of air and ultrasonic agitation on the deposit.

(v) Ultrasonic agitation slightly improved the cathode efficiencies of the plating solutions which were already near 100%.

(vi) The use of ultrasonic agitation allowed the use of much higher current densities when compared with air agitation. With increasing current density the cobalt content decreased as the hardness increased using air agitation. Similar results were obtained for nickel iron deposits. The use of ultrasonics gave similar reductions in cobalt and iron for both alloys but the hardnesses were substantially increased.

(vii) Regression analysis showed that both current density and cobalt or iron content affected the hardness of both alloys using either air or ultrasonic agitation.

(viii) The use of ultrasonic agitation in place of air gives increased ductility and higher hardness with no loss of tensile strength and so should be of interest for engineering applications.

11 SUGGESTIONS FOR FUTURE WORK

The equipment used to generate the ultrasonic radiation was fixed at 13 kHz frequency, therefore the project was confined to a particular frequency. Consequently further work is needed to be conducted with variable frequency equipment to investigate the effect of this variable on electrodeposition.

Measurement of electrode potentials in the working cell would be useful to help in the explanation of diffusion layer phenomena, such as thickness and ion concentration gradient. Mass transport in the bulk electrolyte (conductivity, salt concentration) can also be investigated using cell voltage measurements.

Since only an approximate estimate of the efficiency of conversion of electrical to ultrasonic energy was possible, it would be preferable to devise an accurate method of determining the energy loss. This could be achieved by using a calorimetric method, although there are many experimental problems to be overcome.

By use of a focusing transducer a high intensity of ultrasonics could be applied to the deposition area to improve the plating speed and maintain the quality of the deposit with a low overall power consumption.

12 ACKNOWLEDGEMENTS

The author wishes to thank the State Organisation for Technical Industries in Baghdad (Al-Yarmouk State Establishment) for providing the grant and financial support for the work carried out. The author also wishes to thank the academic and technical staff of the Metallurgy and Materials Engineering Department at the University of Aston in Birmingham for their continuous support throughout the research.

In particular the author wishes to thank his supervisor Dr.J.K.Dennis for his considerable guidance throughout the work, and Mr.P.L.Barrett. My thanks also to Mr.B.Cox, Mr.S.Fuggle, Mr.R.Howell, Mr.J.Foden and Mr.K.Smith of the technical staff.

References.

- 1) C.B.Kenahan and D.Schlain, Effects of Ultrasonic on Brass Plating, Bureau of Mines Reports of Investigations, January 1961.
- 2) F.Muller and H.Kuss, Helv.Chem.Acta, 33, (1950), 217-228, C.A.44 (1950), 4804-6.
- 3) T.F.Heuter and R.H.Bolt, in (Sonics), J.Wiley and Sons, 1955.
- 4) S.M.Kochegin and G.Y.Vyaseleva, In Electrodeposition of Metals in Ultrasonic Fields, Consultants Bureau, New York, 1966.
- 5) C.T.Walker and R.Walker, Electrodeposition, Surface Treatment, 1, 1972/73.
- 6) D.Ensminger (Ultrasonics, The low and high intensity applications), Marcel Dekker, New York, 1973.
- 7) S.R.Rich, Plating, 1955, 42, 1407.
- 8) L.Vrobel, Trans. Inst. Met. Finish, 1975, 53, 40.
- 9) R.Walker and C.T.Walker, Ultrasonics, 1975, 13, (2), 1979.
- 10) A.Roll, Metal Finishing, 55, (1975) 55.
- 11) R.Penn, E.Yeager and F.Hovorka, J. Acoust. Soc. Amer., 1959, 31, (10), 1372.

- 12) R.W.Wood and A.L.Loomis, Phil. Mag., 4, 1927, 417.
- 13) M.J.Ashley, Chemical Engineering, 1974, 368.
- 14) M.P.Drake, Trans. Inst. Met. Finish. 1981, 58, 67.
- 15) Eggett, Garlick, Hopkins and Ashley, I. Chem. E. Sympos. Series No.42.
- 16) T.G.Kozan, Plating, 49, 1962, 495.
- 17) R.Walker and R.C.Benn, Plating, 58, 1971, 476.
- 18) R.Walker and R.C.Benn, Electrochem. Acta., 16, 1971, 1081.
- 19) L.Vrobel, Trans. Inst. Met. Finish., 44, 1966, 161.
- 20) W.R.Wolfe, H.Chessin, E.Yeager and F.Hovorka, Journal of Electrochemical Society, 1954, 101, 590.
- 21) G.Kurtze, Nachr Akad Wiss, Goettingen, 1958, 11a Nr.1.
- 22) R.J.Lanyi, D.H.Lane, C.A.Forbes and H.E.Ricks, S.A.E. Trans., 71, (1963), 520.
- 23) R.Walker and J.F.Clements, Metal Finishing J. (London), 16, (1970), 100.
- 24) R.Walker, Proc. 12th Seminar on Electrochemistry, Karaikudi, India, March 1972, p.385.
- 25) L.Domnikov, Metal Finishing, July 1966, 68.
- 26) C.B.Kenahan and D.Schlain, 1960, US Bur. Mines Rep. Invest. Number 5890. pp.53.

- 27) W.H.Safranek, F.B.Dahle and C.L.Faust, Plating, 35, 39 (1948); "Applications of Nickel", Materials Advisory Board, National Research Council Publ. MAB-248, Washington D.C., Dec 1968, reprinted March 1969.
- 28) F.A.Lowenheim "Electroplating", McGraw-Hill, Inc. New York 1978, pp.211-224, and pp.314-315.
- 29) W.A.Wesley, U.S. Patent 2,331,751 (1943).
- 30) W.A.Wesley and E.J.Roehl, Trans. Electrochem. Soc. 82, 37 (1942).
- 31) B.B.Knapp and D.S.Carr, U.S. Patent 2,594,933 (1952).
- 32) W.Blum and C.Kasper, Trans. Faraday Soc., 31, 1203, (1935).
- 33) W.A.Wesley and J.W.Carey, Trans. Electrochem. Soc., 72, 209, (1939).
- 34) R.J.Kendrick, Trans. Inst. Met. Finish. 44, 78, (1966); J.A.Crossley, R.J.Kendrick and W.J.Mitchell, *ibid.*, 45, 58 (1967).
- 35) W.L.Pinner and R.B.Kinnaman, Mon. Rev. Am. Electroplat. Soc., 32, 227 (1945).
- 36) G.B.Hogaboom, U.S. Patent, 2,351,966 (1944); P.J.Lalonde Electrotyper's and Stereotyper's Bull., 32, 3, (1946).

- 37) C.Struyke and A.E.Carlson, Plating, 37, 1242, (1950).
- 38) H.L.Koessler and R.R.Sloan, Electrotyper's and Stereotyper's Bull., 36, 33, (1950).
- 39) L.Cambi and R.Piontelli, Italian Patent 368,824 (1939).
- 40) R.C.Barrett, Electrotyper's and Stereotyper's Bull., 36, 55 (1950).
- 41) R.J.Kendrick, Trans. Inst. Met. Finish., Proc. 6th Intl. Met. Finish. Conf., 42, 235 (1964);
K.C.Belt, J.A.Crossley and R.J.Kendrick, 7th Intl. Met. Finish. Conf. (Hanover), May 1968, pp.222
"Interfinish 68".
- 42) O.J.Klingenmaier, Plating, 52, 1138, (1965).
- 43) J.K.Dennis, F.A.Still "The use of electrodeposited cobalt alloy coatings to enhance the wear resistance of hot forging dies. Cobalt 1975. 1. pp.17-28.
- 44) S.Nakahara and S.Mahajan, J. Electrochemical Society 1980, 127, No.2, 283.
- 45) N.S.Cassel and G.H.Montillon, Acidity of Cobalt and Nickel Plating Baths. Use of the Oxygen Electrode, Trans. Electrochem. Soc., 45, 1924, pp.259-272.
- 46) F.K.Shelton, J.C.Stahl and R.E.Churchward, Electrodeposit of Cobalt from Cobaltite Concentrates, U.S. Bur. Mines, Rep. Invest. 4172, January 1948, pp.98, Chem. Abstr. 42, p.2181d.

- 47) A.Brenner, Electrodeposition of Alloys Vol.II, Academic Press, New York, 1962, pp.76.
- 48) Modern Electroplating, ed F.A.Lowenheim, 3rd Edition. John Wiley and Sons, Inc., New York, 1974.
- 49) J.H.Lindsay and H.J.Read, "Some Properties of Electrodeposited Cobalt", Plating, 57, 497-503, (1970).
- 50) D.W.Endicott and J.R.Knapp Jnr., Electrodeposition of Nickel-Cobalt alloy;"Operating Variables and Physical Properties of the Deposits", Plating 53, 43-60, (1966).
- 51) A.A.Brenner, "Microhardness Tester for Metals at Elevated Temperatures, Plating, 38, 1951, pp.363-366.
- 52) F.R.Morral, C.T.Sims and E.F.Adkins, "A Comparison of Zone-Refined and Sintered Cobalt", paper presented at Amer. Inst. Min. Metal. Eng. 1958, Annual Meeting, New York, and published in part in J. Metals, 10 (10), 1958, pp.662-664.
- 53) M.G.Losinsky and S.G.Fedotov, "The Correlation between Indentation Hardness and the Modulus of Normal Elasticity of Pure Metals at High Temperatures", Izvest. Akad. Nauk. SSSR., Tekhn.3, 1956, pp.59-67
- 54) R.C.Barrett, "Plating of Nickel, Cobalt, Iron and Cadmium from Sulphamate Solutions", Tech. Proceedings Am. Electroplaters' Soc., 47, 170-175 (1960).

- 55) R.D.Fisher "The Influence of Residual Stress on the Magnetic Characteristics of Electrodeposited Nickel and Cobalt", Journal Electrochem. Soc., 109, 479-485, (1962).
- 56) W.T.McFarlen, Plating, 1970, 57, 46-50.
- 57) K.I.Gaigalas, A.I.Bodnevas, Yu. Yu. Matulis, "Phase Transformations in Electrodeposits of Cobalt in Relation to Condition of Electrolysis Composition", Trudy Akademii Nauk Litovskoi SSSR., Seria B, 4 (55), 59-68 (1968).
- 58) G.Okund, "Crystal Structure of Electrodeposited Cobalt. I, II", Bulletin of the University of the Osaka Prefecture, Series A, 4, 89-100, 101-110, (1956).
- 59) R.Sard, C.D.Schwartz and R.Weil, "Deposition Modes of Cobalt from Sulphate-Chloride Solutions", Journal Electrochem. Soc., 113 (5), 424-428, (1966).
- 60) W.Chubb, "Contribution of Crystal Structure to the Hardness of Metals", Journal of Metals, AIME Transactions, 203, 189-192, (1955).
- 61) H.Connor and V.A.Lamb, Plating, 48, 388 (1961).
- 62) V.A.Lamb and W.Blum, Proc. Am. Electroplat. Soc., 1942, 106.
- 63) U.S. Patent: 992,951 (1911).

- 64) C.T.Thomas and W.Blum, Trans. Am. Electrochem. Soc., 57, 59 (1930).
- 65) J.D.Thomas, O.J.Klingenmaier and D.W.Hardesty, Trans. Inst. Met. Finish., 47, 209 (1969).
- 66) S.H.Lai and J.M.McGeough, J. Mech. Eng. Scie., 18, 19, 1976.
- 67) W.B.Stoddard, J. Trans. Electrochem. Soc., 84, 305, 1943.
- 68) C.Kasper, "Notes on the Rapid Electrodeposition of Iron", Monthly Review, Am. Electroplaters' Soc., 23 (10), 34-36 (1936)., "Rapid Electrodeposition of Iron from Ferrous Chloride Baths", Research paper RP 991, Journal of Research, National Bureau of Standards. 18, 535-541, (1937)..
- 69) R.M.Schaffert, Trans. Electrochem. Soc., 84, 316, 1943.
- 70) M.Mukai and M.Ootake, "Electrolytic Refining of Iron. XV. Effect of PR Process Applied to Iron Electrodeposition", Journal of the Metal Finishing Society of Japan, 7, 54-58 (1956).
- 71) R.M.Schaffert and B.W.Gonser, "A Sulphate-Chloride Solution for Iron Electroplating and Electroforming", Trans. Electrochem. Soc., 84, (1943); 15pp (preprint).
- 72) D.J.MacNaughton, J.Trans. Steel Inst., 109, 409, (1924).

- 73) M.B.Diggin, "Modern Electroforming Solutions and their Applications", Symposium on Electroforming Applications, Uses and Properties of Electroformed Metals, ASTM Special Technical Publication No.318, 10-31 (1962).
- 74) E.M.Levy and G.I.Hutton, Plating, 55, 138, 1968.
- 75) A.C.Hart, W.R.Wearmouth and A.C.Warner, Trans. Inst. Metal Finish., 54, 56, 1976.
- 76) J.K.Dennis and T.E.Such, "Nickel and Chrom. Plating", 1972, Pub. Newnes-Butterworth, pp.10, 11.
- 77) H.H.Uhlig, Corrosion and Corrosion Control, Published J.Wiley and Sons, New York, 1963, 41.
- 78) F.A.Still, Ph.D. Thesis, 1974, "Electrodeposited Cobalt Alloy Coatings and their Use on Hot Forging Dies".
- 79) J.Z.Tafel, Physik Chem., 1904, 50, 641.
- 80) J.K.Dennis and T.E.Such, "Nickel and Chrome Plating", 1972, Pub. Newnes-Butterworth, 16.
- 81) O.Hinricksen, British Patent 461,126 (1937).
- 82) L.Weisberg and W.B.Stoddard Jnr., U.S.Patent 2,026,718 (1936), British Patent 464,814 (1937).
- 83) R.T.Mathieson and M.Sedghi. Trans. Inst. Met. Finish., 1972, 50, 152.

- 84) C.B.F.Young and C.Struyk, Trans. Electrochem. Soc., 1946, 89, 383.
- 85) S.Glasstone and J.C.Speakman, Trans. Faraday Soc., 1931, 27, 29; also J.Electrodepositors, Tech. Soc. 1930, 6-57.
- 86) W.M.Fassell Jnr., and J.P.Baur, Reported in Electrodeposition of Alloys by A.Brenner, Academic Press Inc. New York, 1963.
- 87) R.Piontelli and G.F.Patuzzi, Metal. Ital., 1942, 34, 245-249.
- 88) K.C.Belt, J.A.Crossley and S.A.Watson, "Nickel-Cobalt Alloy Deposits from a Concentrated Sulphamate Electrolyte", Trans. Inst. Metal Finish. 48, 133-137, (1970).
- 89) W.R.Wearmouth and K.C.Belt, Annual Tech. Conf. Inst. Met. Finish. June 1974.
- 90) R.Piontelli and L.Caronica. Proc. 3rd Intern. Conf. on Electrodeposition (Electrodepositors' Tech. Soc.), 1948 pp.121-125.
- 91) S.Glasstone and J.C.Speakman, Trans. Faraday Soc. 1930, 26, 565; also J. Electrodepositors' Tech. Soc. 1930, 6, 49.
- 92) C.G.Fink and K.H.Lah, Trans. Am. Electrochem. Soc. 1930, 58, 373-381.

- 93) V.Sree and T.L.Rama Char, J. Electrochem. Soc. 1961, 108, 64.
- 94) W.R.Wearmouth, Trans. Inst. Met. Finish. 1982, 60, 68.
- 95) H.Ericson, Galvanotechnik, 1966, 57, 85.
- 96) F.A.Lowenheim, Electroplating Fundamental of Surface Finishing pp.523, 1978. McGraw-Hill, New York.
- 97) L.Weisberg, Levelling in Cobalt-Nickel Plating Solutions, Proc. Am. Electroplaters Soc., 37, 1950 pp.185-191.
- 98) W.H.Safranek, "The Properties of Electrodeposited Metals and Alloys", 63-64, (1973).
- 99) R.Weil and H.J.Read, "The Structure of Electrodeposited Metals, Parts 1-11, Metal Finishing, 53, (11), 1955, pp.60-65, 53 (12), 1955 pp.60-64.
- 100) B.R.Wilding, Trans. Inst. Met. Finish., 1968, 46, 101.
- 101) I.W.Wolf "Electrodeposition of Magnetic Meterials", Journal Applied Physics, Supplement, 33(3), 1152-1159 (1962).
- 102) V.V.Bondar, M.M.Melnikova and Yu.M.Polukarov "Electrodeposition of Magnetically Hard Alloys I. Electrodeposition of Cobalt-Phosphorus Alloys" Inform. Sistemy, Moscow, 117-127 (1964).

- 103) G.Bate, J.R.Morrison and D.E.Speliotis, "Static Magnetization Reversal in Thin Films of Cobalt-Nickel-Phosphorus", Journal Applied Physics, 35 (3), 972-973 (1964).
- 104) C.B.F.Young and C.Egerman, Trans Electrochem Soc., 72, 447, 1937.
- 105) R.J.Clauss, Trans. Inst. Met. Finish. 53, 22, 1975.
- 106) A.Du-Rose, Steel, 1944, 114, No.24, 124, P.Pine.
- 107) H.Brown, E.Hoover, Plating, 1953, 40, 874.
- 108) H.Chessin, Plating and Surface Finishing 1976, 63, No.12, 32.
- 109) Nickel-Iron Advertisement, Metal Finishing, 1978, 76, Nos. 6 and 5.
- 110) Nickel-Iron Advertisement, Plating and Surface Finishing, 1978, 65, No.5.
- 111) R.A.Tremmel, U.S. Patent 3,974,044 Aug.10, 1976.
- 112) R.A.Tremmel, Plating 60, 803, 1973.
- 113) R.A.Tremmel, Plating and Surface Finishing, 68, 22, 1981.
- 114) A.M.Ginberg, Yu.V.Granovskii, Yu.E.Titov, Yu.A.Klyachko, "Choosing Optimum Electrodeposition Conditions by the Box-Wilson Method", Zashchita Metallov, 1 (6), 716-718, (1965).

- 115) Nickel-Iron Products Finishing, 1977, 41, No.8, 64
- 116) E.M.Levy, "Nickel-Iron Alloys Electrodeposited from Sulphate-Chloride Electrolyte: Effects on Mechanical Properties and Microstructure of Stress-Reducing Agent, Heat Treatment, pH, and Chemical Compositions", Plating, 56, 903-908 (1969).
- 117) N.S.Fedorova, "X-ray Diffraction Structure Investigation of Electrodeposited Nickel-Iron Alloys", Zh. Fiz. Khimii, 32, 1211-1213, (1958).
- 118) H.V.Venkatasetty, J.Electrochem. Soc., 117, 403, (1970).
- 119) P.A.Brook, Plating 47, 1269, (1960).
- 120) S.A.Watson, Trans. Inst. Metal Finishings, 37, 28, (1960).
- 121) C.B.Kenahan and D.Schlain, and E.Chin, Effects of Ultrasonics on Electrodeposition of Copper Alloys from Cyanide Electrolytes, Bureau of Mines report of investigation 6938, April 1967.
- 122) D.J.Macnaughton and A.W.Hothersall, Trans. Faraday Soc., 24, 387 (1928); 31; 1168 (1935).
- 123) R.Walker "Effect of Ultrasonics on Nickel Electrodeposits" Trans. Inst. Metal Finishing 1975, 53, 40-42.
- 124) E.M.Hofer and H.E.Hintermann, J. Electrochem. Soc., 112, 167 (1963).

- 125) Z.Szlaraska-Smalowska and M.Smalowski, Bull. Acad. Polska. Sci. Ser. Sci-Chem. 1958, 6, 427.
- 126) G.O.Mallory "The effects of ultrasonic irradiation on electroless nickel plating" Annual Technical Conference, Torquay, 4 May 1978.
Trans. Inst. Metal Finishing. 1978, 56, 81-85.
- 127) J.W.Mee "The application of ultrasonics to electroplating with a view to reducing hydrogen embrittlement". Trans. Inst. Metal Finishing. 1963, 40, 242-248.
- 128) G.L.J.Bailey, S.A.Watson, L.Winkler "Electroforming with concentrated nickel sulphamate solution in Europe". Paper presented to first annual conference of the Australasian Institute of Metal Finishing held in Melbourne, October 1969. pp.21-38.
- 129) A.Brenner, V.Zentner, C.W.Jennings "Physical properties of electrodeposited metals". Plating August 1952 Project No.9.
- 130) D.R.Eastham, P.J.Boden and M.E.Henstock, Factors Affecting the Composition Gradient in Electrodeposited Permalloy Films.
Trans. Inst. Metal Finishing, 1968, 46, 37-43.
- 131) Yu.N.Petrov. Appl. Elec. Phenom., (1965) 21.
- 132) W.H.Safranek and C.H.Layer, Trans. Inst. Metal Finishing. 1975, 53, 121.

- 133) W.W.Harvey, M.R.Randlett and K.I.Bangerskis,
"Elevated Current Density Electrowinning".
Kennecott Copper Corporation, Lexington, Mass.
Technical Note 105. 1973.
- 134) R.J.Baker and J.A.Nelder "Generalised Linear
Interactive Modelling" 1978. Distributed by the
numerical Algorithms Group, 7 Banbury Rd., Oxford,
England.